

2022 | Faculty of Engineering Technology

KNOWLEDGE IN ACTION

Doctoral dissertation submitted to obtain the degree of Doctor of Engineering Technology, to be defended by

Bram Bamps

DOCTORAL DISSERTATION

Study of optimal heat seal performance of flexible food packaging, using material properties, machine and processing parameters in a design of experiments approach.

www.uhasselt.be

Hasselt University Martelarenlaan 42 | BE-3500 Hasselt

KNOWLEDGE IN ACTION

Promoter: Co-promoters: Prof. Dr ir. Mieke Buntinx | UHasselt

Prof. Dr Roos Peeters | UHasselt

Prof. Dr ir. Wim Deferme | UHasselt

2022 | Faculty of Engineering Technology



KNOWLEDGE IN ACTION

Doctoral dissertation submitted to obtain the degree of Doctor of Engineering Technology, to be defended by

Bram Bamps

DOCTORAL DISSERTATION

Study of optimal heat seal performance of flexible food packaging, using material properties, machine and processing parameters in a design of experiments approach.



Promoter: Prof. Dr Roos Peeters | UHasselt

Co-promoters: Prof. Dr ir. Mieke Buntinx | UHasselt

Prof. Dr ir. Wim Deferme | UHasselt

D/2022/2451/92

Preface

A doctoral study is the result of individual efforts, embedded in a stimulating environment. It would take many pages to mention everyone so I list up the most influential persons for this doctoral study.

My partner, Leen Swerts, complements me in our relationship. Accepting differences in personality enriches life. Our relationship increased my understanding in well-being of others, which is essential to socially navigate through life.

My parents, Anne-Marie Poosen and Erik Bamps, assisted me in becoming educated and morally aware. The relation with both of my parents has matured from parent-child to equal. Because of this, at the age of 37, I still consider my parents as important life consultants. Especially the support I received in bad health made it possible for me to commit fully to academic research in better health.

My brother, Mandes Bamps, feels like a second me because of the background and many experiences we shared. Unlike my partner and parents, we are not seeing each other that frequently anymore, but the distance in location is secondary to our strong emotional bond.

The love I feel for these people gives meaning to life, of which my work as an academic researcher played a big role in the last years.

From a mainly professional point of view, other persons played essential roles.

Dr. Ing. Stan Claes initiated seal research at MPR&S and shared knowledge in a very transparent way in the beginning of my academic career, back in 2012.

Prof. Dr. Roos Peeters provided the framework to do seal research, she assisted me thoroughly in the first months, after Stan made the switch to industry. Because of this, I was able to perform research more autonomously. We collaborated successfully in many applied research projects on heat sealing and packaging in general of the last decade. These projects contributed to this doctoral study.

Dr. Ir. Karlien D'Huys and Dr. Ir. Bart De Ketelaere were external project colleagues (KU Leuven). Also, Dipl.-Ing. Benjamin Stephan, Dipl.-Ing. Ina Schreib and Dipl.-Ing. Johanna Wolf were external project colleagues (Fraunhofer-IVV). Karlien and Bart mainly provided statistical knowledge, while Benjamin, Ina and Johanna added knowledge on heat sealing. The collaboration of both institutes was crucial in achieving high quality research and thus obtaining funding to be able to do research.

Prof. Dr. Ir. Mieke Buntinx contributed in the peer-reviewed study on bioplastics. Prof. Dr. Ir. Peter Ragaert (Pack4Food) coordinated the first national project on heat sealing, back in 2012. Roos, Mieke, Prof. Dr. Ir. Wim Deferme, Prof. Dr. Ir. Naveen Reddy and Prof. Dr. Wouter Marchal provided many important comments to increase the quality of the dissertation during the last 2 years. These thorough reviews were supplemented by some final valuable comments of Bart, Peter and Prof. Dr. Rudinei Fiorio (Maastricht University).

Finally, I want to thank all mentioned and non-mentioned family, friends and colleagues for being there and supporting me. It's this stimulating network of many different people that enabled me, as initiator, to do this study.

Table of Contents

Pre	етасе			1
Tal	ole of	Cont	rents	ii
Lis	t of A	bbrev	viations	vi
Lis	t of Ta	ables		viii
Lis	t of Fi	gure	s	×
Sy	nopsis	s (EN)	xv
Sy	nopsis	s (NL)	xvii
1.	Intr	oduc	tion	1
	1.1	Bor	nd formation	2
	1.2	Sea	l technologies	4
	1.3	Sea	ıl materials	4
	1.3	.1	Thermal properties of thermoplastics	4
	1.3	.2	Multilayer structures	5
	1.4	Sea	l performance	6
	1.5	Fac	tors that impact seal performance	6
	1.6	A b	roader framework	7
	1.6	.1	A design of experiments (DOE) approach	8
	1.6	.2	General aim and structure of the dissertation	9
	1.7	Ref	erences	11
2.	Hea	it sea	aling: technology, materials and performance evaluation	13
	2.1	Hea	at seal technology	13
	2.1	.1	Heat conductive sealing	13
	2.1	.2	Ultrasonic sealing	16
	2.1	.3	Other heat seal technologies in food industry	21
	2.2	Hea	at seal materials	25
	2.2	.1	Poly(ethylene)	25
	2.2	.2	Poly(propylene)	29
	2.2	.3	Isotactic poly(1-butene)	31
	2.2		Ethylene copolymers	31
	2.2	.5	Poly(ethylene terephthalate)	35
	2.2	.6	Biobased and biodegradable plastics	36

	2.2.	7	Coated paper	41		
	2.2.	8	Additives	43		
	2.2.	9	Comparison of seal, mechanical and economic data	44		
2	.3	Seal	performance evaluation	48		
	2.3.	1	Seal Strength	48		
	2.3.	2	Hot tack	53		
	2.3.	3	Seal interface temperature	54		
	2.3.	4	Seal integrity	55		
	2.3.	5	Gas permeation through seals	56		
	2.3.	6	On-site evaluation	57		
	2.3.	7	Leak seal prevention	59		
	2.3.	8	Additional characterization	61		
	.4 pproa		strial sealing processes and the need for a design of experiment	:s 62		
_	.5 xperii	-	acting factors of heat-sealed food packages in a design of sapproach	65		
	2.5.	1	Grouping of factors	65		
	2.5. indu		A design of experiments approach to evaluate and optimize the sealing process	67		
	2.5. mat	3 erials	Previous doctoral studies on heat sealing of packaging	72		
2	.6	Refe	erences	73		
3. perf			ria evaluation and optimization of the ultrasonic sealing pased on design of experiments and response surface			
	hodo			85		
3	.1	Intro	oduction	85		
3	.2	Mate	erials and methods	87		
	3.2.	1	Film material	87		
	3.2.	2	Ultrasonic sealing and seal performance tests	87		
	3.2.	3	Experimental design and seal optimization	88		
	3.2.	4	Seal window calculation	90		
3	.3	Resu	ults and discussion	90		
	3.3.	1	Design space and experimental design	90		
	3.3.	2	Response surface model	91		
	3.3.3		3.3.3 Optimization procedure			

	3.3.	4 Single response	93
	3.3.	5 Multiple responses	93
	3.3.	6 Optimized seal settings and experimental validation	96
	3.3.	7 Seal window	96
3	3.4	Conclusions	97
3	3.5	References	98
4. con		uation and optimization of seal behaviour through solid nation of heat-sealed films	101
4	1.1	Introduction	102
4	1.2	Objectives	102
2	1.3	Materials & methods	103
	4.3.	1 Materials	103
	4.3.	2 Methods	103
4	1.4	Results and Discussion	107
	4.4.	1 Film characterization	107
	4.4.	2 Evaluation and optimization of contaminated seal strength	109
4	1.5	Conclusions	116
2	1.6	References	117
5. top		uation and optimization of the peel performance of a heat sealed nd bottomweb undergoing cold storage	119
5	5.1	Introduction	119
5	5.2	Objectives	120
5	5.3	Materials & methods	120
	5.3.	1 Materials	120
	5.3.	2 Methods	120
5	5.4	Results and Discussion	123
	5.4.	1 Influence of cool time	123
	5.4.	2 Seal optimization	124
	5.4.	3 Film characterization	130
	5.4.	4 Evaluation of peel performance during cold storage	133
5	5.5	Conclusions	139
5	5.6	References	140
6. bio	Characterizing mechanical, heat seal and gas barrier performance of iodegradable films to determine food packaging applications		

6.1	Intr	oduction	144	
6.2	6.2 Materials & methods			
6.2.	1	Materials	145	
6.2.	2	Methods	146	
6.3	Res	ults and Discussion	149	
6.3.	1	Mechanical performance	149	
6.3.	2	Gas permeability	153	
6.3.	.3	Seal performance	155	
6.3.	4	Additional characterization	160	
6.4	Con	clusions	162	
6.5	Refe	erences	162	
7. Con	clusio	ons and recommendations	167	
7.1	Gen	eral conclusions	167	
7.2	Rec	ommendations	171	
Scientific	outp	put	173	

List of Abbreviations

ACR Acid copolymer resin
AFM Atomic force microscopy

APET Amorphous poly(ethylene terephthalate)
ASTM American Society for Testing and Materials

bioPE Biobased polyethylene

bioPET Biobased poly(ethylene terephthalate)

BMWi Federal Ministry for Economic Affairs and Industry

C4 Butane
C6 Hexane
C8 Octane
CH4 Methane

CHDM Cyclohexane dimethanol

CNMR Carbon Nuclear Magnetic Resonance

CO2 Carbon dioxide COF Coefficient of friction

CORNET COllective Research NETwork

CPET Crystalline poly(ethylene terephthalate)
CRYSTAF Crystallization analysis fractionation
DMA Dynamic mechanical analysis

DMT Dimethyl terephthalate
DMTA Dynamic mechanical them
DOE Design of experiments

DSC Differential scanning calorimetry EEA Poly(ethylene-co-acrylic acid)

EG Ethylene glycol

EMA Poly(ethylene-co-methacrylic acid)
EVA Poly(ethylene co-vinylacetate)
EVOH Poly(vinylalcohol-co-ethylene)

FTIR Fourier-transform infrared spectroscopy

H₂O Water

HDPE High-density polyethylene
HFFS Horizontal form-fill-sealing
IGF Industrial Community Research

IMO-IMOMEC Institute for Materials Research - Institute for Materials Research

in MicroElectronics

IPA Isophtalic acid

ISO International Organization for Standardization

IVLV Industry Association for Food Technology and Packaging

LDPE Low-density poly(ethylene)
LLDPE Linear low-density poly(ethylene)
MAP Modified atmosphere packaging

MDO-PE Machine-direction oriented polyethylene MeBioS Mechatronics, Biostatistics and Sensors

mLLDPE Metallocene catalysed linear low-density polyethylene

MPR&S Materials and Packaging Research & Services

N2 Nitrogen Na Sodium O2 Oxygen OFAT One-factor-at-a-time
OTR Oxygen transmission rate
oPA Oriented poly(amide)
PA Poly(hexano-6-lactam)
PB Isotactic poly(1-butene)

PBAT Poly(butylene adipate terephthalate)

PBS Poly(butylene succinate)

PBSA Poly(butylene succinate-co-butylene adipate)

PCL Poly(caprolactone)
PE Poly(ethylene)

PEF Poly(ethylene furanoate)
PET Poly(ethylene terephthalate)

PETG Poly(ethylene glycol-co-1,4-cyclohexanedimethanol

terephthalate)

PHA Poly(hydroxyalkanoate)
PHB Poly(hydroxybutyrate)

PHBHHx Poly(3-hydroxybutyrate-co-3-hydroxyhexanoate)

PHHx Poly(hydroxyhexanoate)

PHBV Poly(3-hydroxybutyrate-co-3-hydroxyvalerate)

PHV Poly(hydroxyvalerate)
PLA Poly(lactic acid)
PP Poly(propylene)
PS Poly(styrene)
PVC Poly(vinylchloride)

RSM Response surface methodology
SEM Scanning electron microscopy
TEM Transmission electron microscopy

TETRA TEchnology TRAnsfer

Tg Glass transition temperature

Tm Melting point
TPA Terephtalic acid
TPS Thermoplastic starch

TREF Temperature rising elution fractionation

VFFS Vertical form-fill-sealing

VLAIO Flanders Innovation & Entrepreneurship

WVTR Water vapour transmission rate

List of Tables

Table 1: Glass transition temperatures (Tg) and melting points (Tm) of materials used in heat sealable films ¹⁰ .	5
Table 2: Advantages and disadvantages of seal technologies ² .	24
Table 3: Properties of commercial LLDPE-grades ^{29, 31} .	29
Table 4: Chemical composition of polyhydroxyalkanoates considered in food packaging.	39
Table 5: Qualitative comparison of seal performance (* or \diamond), underlying causes ($\stackrel{\wedge}{\cong}$ or $\mathop{\heartsuit}$), mechanical performance and economic data of plastics.	45
Table 6: Online inspection of seal/package integrity ¹³² .	58
Table 7: Experimental runs and input parameters of the Box-Behnken design and seal strength [N/mm], horn displacement [µm] and energy consumption [J] responses for the PET/LLDPE-C4 film material.	91
Table 8: Significant coefficients, terms, regression significance and equation of the seal strength model for the PET/LLDPE-C4 film.	91
Table 9: Significant coefficients, terms, regression significance and equation of the horn displacement model for the PET/LLDPE-C4 film.	91
Table 10: Significant coefficients, terms, regression significance and equation of the seal energy model for the PET/LLDPE-C4 film.	92
Table 11: Experimental validation of predicted optimum. The predicted optimum and confirmation runs were tested for being significantly different ($a = 0.05$ and $a = 0.1$) using the confidence interval approach	96
Table 12: Multilayer structure of the 3 packaging films.	103
Table 13: Melting onset and melting peak temperatures of films and granulates, tested with DSC.	107
Table 14: Experimental design with parameters (seal temperature (T), time (t) and pressure (p)) and responses (clean and contaminated seal strength) of films 1, 2 and 3 (F1, F2 and F3).	110
Table 15: Significant coefficients, terms and regression significance of the seal strength model for clean seals of film 1, 2 and 3.	111
Table 16: Significant coefficients, terms and regression significance of the seal strength model for coffee contaminated seals of film 1, 2 and 3.	112
Table 17: Significant coefficients, terms and regression significance of the seal strength model for blood powder contaminated seals of film 1, 2 and 3.	112
Table 18: Validation of statistical optimum $(n=10)$ + optimal settings.	113

Table 19: Experimental design with parameters (seal temperature, seal time, seal pressure and processing temperature) and responses (average peel strength, maximum peel strength, peel energy) during and after cold	
storage (n=2).	125
Table 20: Significant terms with parameter estimates (V) and corresponding p-values (p-V) of average peel strength, maximum peel strength and peel energy during and after cold storage.	127
Table 21: Validation of statistical optimum at various processing temperatures during and after cold storage $(n=5)$.	130
Table 22: Sample description.	146
Table 23: Results of mechanical characterization.	151
Table 24: Results of gas barrier characterization (orientation samples: transmission rates are measured from outside to inside, inside = seal side).	155
Table 25: Results of seal characterization.	157
Table 26: Maximized seal strengths of clean and contaminated seals.	160
Table 27: Average opacities Y (in %) and standard deviations $(n=4)$.	161
Table 28: Average water contact angles (WCA) (in $^{\circ}$) and standard deviations (n=15).	161
Table 29: Scientific output: published papers.	173
Table 30: Scientific output: posters and oral presentations.	174

List of Figures

Figure 1: Adhesion mechanisms: chain entanglement with mechanical interlocking of polymer chains at both sides of the interface; intermolecular bond with chemical forces, that attract polymer chains with other chains or with a non-polymeric substrate; mechanical bond with	
mechanical interlocking of polymer flow in a porous substrate.	3
Figure 2: Glass transition and melting in a DSC curve.	4
Figure 3: Factors that impact seal performance, adapted from Ilhan et al^4 ; bold: all factors and seal performance indicators of interest in this dissertation.	10
Figure 4: Temperature profile in the cross section of a sealed multilayered packaging film when both sides come into contact by closing heated tools (dark grey: outer layer, light grey: seal layer).	14
Figure 5: Hot knife sealer.	14
Figure 6: Band sealer.	15
Figure 7: Impulse sealer (black: outer layer, grey: seal layer).	15
Figure 8: Ultrasonic sealing tool set up.	16
Figure 9: Amplitude and frequency of sound waves to ultrasonically seal thin packaging films ($< 100 \mu m$). The upper figure shows waves of 20 kHz (20.000 waves/second) and 35 kHz. The lower figure shows two 35 kHz waves of 18 and 36 μm amplitude.	17
Figure 10: Amplitude amplification at the tip of the horn by decreasing the ratio mass end – mass begin.	18
Figure 11: Temperature profile of the joining films (black: outer layer, grey: seal layer) for heated tool sealing (left) and ultrasonic sealing (right).	19
Figure 12: Equilibrium state - horn distance vs. seal time with 60 μm random copolymer PP.	20
Figure 13: Fracture mechanisms along the border unmolten material - flown material (black: outer layer, grey: seal layer (light grey: molten material, dark grey: unmolten material)).	20
Figure 14: Cap sealer with induction heating.	22
Figure 15: Layer distribution of topfilm for induction cap sealing.	22
Figure 16: Poly(ethylene) structure.	25
Figure 17: Branched morphology of LDPE and HDPE.	26
Figure 18: Branching morphology of LLDPE with Philips, Ziegler-Natta and Kaminsky catalysts.	28
Figure 19: Poly(propylene) structure.	29

Figure 20: Tacticity of methyl heads of PP.	30
Figure 21: Sequence of monomers in homopolymer, random copolymer and block copolymer PP.	30
Figure 22: Poly(1-butene) structure.	31
Figure 23: Poly(ethylene-co-vinyl acetate) structure.	32
Figure 24: Poly(ethylene-co-acrylic acid) and poly(ethylene-co-methacrylic acid) structures.	33
Figure 25: Ionomer.	34
Figure 26: Schematic structure of regions in ionomers.	34
Figure 27: Poly(ethylene terephthalate) structure.	35
Figure 28: Poly(lactic acid) structure.	37
Figure 29: Amylose and amylopectin structures.	38
Figure 30: Polyhydroxyalkanoate structure.	39
Figure 31: Poly(butylene succinate) structure.	40
Figure 32: Tail holding methods ¹⁰⁸ .	49
Figure 33: Opening of different packaging concepts by end consumer (left: pouch, right: topfilm and tray).	49
Figure 34: Influence of bar temperature and seal layer composition on the maximum seal strength of two PET/PE 12/50 flowpack films, sealed at 1.0 s and 1.0 N.mm $^{-1}$, n=3.	50
Figure 35: Seal separation modes (black: outer layer topfilm, light grey: seal layer topfilm, dark grey: bottomweb).	51
Figure 36: Cohesive peel failure during seal strength test.	51
Figure 37: Interference by material break (black: outer layer topfilm, light grey: seal layer topfilm, dark grey: bottomweb).	51
Figure 38: Peel test of round cup and top lid at constant peel angle.	52
Figure 39: Inflated sealed pouch and restraining plate.	52
Figure 40: Examples of why hot tack is important. (A) Internal pressure from the weight of the product or air in a vertical form fill seal operation. (B) Holding shut wrinkles and folds in a horizontal form fill seal operation ⁴⁹ .	53
Figure 41: Seal interface temperature measurement setup.	54
Figure 42: Influence of seal time on seal interface temperature of an oPA/PE 15/40 flowpack film, sealed at 120 °C and 1 N.mm ⁻² .	54
Figure 43: Bubble leak test.	55
Figure 44: Hot bar with resilient counterpart.	60

Figure 45: Horizontal serrations in a seal bar and the different factors of a serrated pattern.	60
Figure 46: Flowpack process.	62
Figure 47: Fin (I) and lap (II) seal.	63
Figure 48: Cross seal with laminated material (black: outer layer, grey: seal layer, red cross: high risk area for channel leaks).	63
Figure 49: Tray sealer.	64
Figure 50: Vertical form-fill-sealing unit.	64
Figure 51: Factors affecting heat seal quality; The amount of research that is already performed for each of the factors correlates with the darkness in coloration; Arrows visualise the interaction between factors ¹⁴¹ .	66
Figure 52: Comparison of 'one factor at a time' (OFAT) and factorial design spaces in a seal experiment example that considers bar temperature and seal time as input factors.	68
Figure 53: Maximum ultrasonic seal strength results of 60 µm LLDPE-C4 monolayer, presented in a 3D-design space (Box-Behnken -15 runs with inclusion of 3 center points).	70
Figure 54: Seal strength of a flowpack film with sodium ionomer seal layer, sealed at a seal time (ts) of 0.7s, a seal pressure (p) of 2 N.mm ⁻¹ , $n=3$.	71
Figure 55: Contour graph of predicted seal strength (light grey: <1.0 $N.mm^{-1}$;1.0 < dark grey < 1.8: black > 1.8) of a flowpack with sodium ionomer seal layer in a seal temperature and time operating window.	71
Figure 56: Response surface model for seal strength, horn displacement and seal energy as a function of force and amplitude (seal time = 0.2 s) for the PET/LLDPE-C4 film.	92
Figure 57: Profiler and desirability plot for the optimization towards seal strength only. The optimum and the optimal settings for force and amplitude are highlighted in red.	93
Figure 58: Profiler and desirability plot for the combined optimization towards seal strength and horn displacement. The optimum and the optimal settings for force and amplitude are highlighted in red.	94
Figure 59: Profiler and desirability plot for the combined optimization towards seal strength, horn displacement and seal energy. The optimum and the optimal settings for force and amplitude are highlighted in red.	95
Figure 60: Seal window of the PET/LLDPE-C4 film. The light grey area indicates all combinations of the input parameters force and amplitude within the considered design space that result in a seal strength value of at least 90% of the option the seal strength. The seal time was shown to	07
have no significant effect on the seal strength for this film.	97

sample; II: Fixation of seal sample on cardboard tool, prior to heat conductive sealing; III: Cleaning of sealed sample with brush.	104
Figure 62: Dye penetration test; I: Sealed edges (grey) of sealed contaminated sample (grey + black dots, representing coffee powder); II: Visual inspection after applying dye solution at contaminated seal.	105
Figure 63: Hot tack graph with variation in seal temperature, seal parameters: 1.0 s seal time – 0.3 N.mm ⁻² seal pressure – 0.1 s cool time $(n=3)$ for three packaging films.	108
Figure 64: A: Raw images of coffee (left) and blood powder (right) contaminated samples of film 2, sealed at 181.5 °C, 0.7 s and 1.0 N.mm-2 with a high-resolution digital imaging set up with LED backlight illumination for high contrast. These raw images are converted to binary images (B) where clean areas are black.	114
Figure 65: Temperature vs. time process windows for clean, coffee and blood powder contaminated samples. The process windows indicate those combinations of temperature and time that result in a seal strength of at least 90% of the optimum value. Pressure was kept constant at 2.5 N.mm ⁻² .	115
Figure 66: Influence of cool time on maximum peel strength $(n=3)$.	124
Figure 67: Prediction profilers of models of average peel strength, maximum peel strength, peel energy, during and after cold storage, optimized by matching 0.5 N.mm ⁻¹ for average and maximum peel strength and maximizing peel energy at 23 °C processing temperature.	129
Figure 68: Influence of ambient temperature on flexural stress-strain curves of a PET/PE bottomweb $(n=5)$.	131
Figure 69: Influence of processing temperature on tensile stress-strain curves of a PET/PE-EVOH-PE topfilm $(n=5)$.	132
Figure 70: Influence of ambient temperature on tensile stress-strain curves of a 60 μ m thick blown extruded monolayer LDPE (LDPE FE8000, Total) film, tested at 300 mm.min ⁻¹ . on 15 mm wide rectangular shaped samples (n=5).	133
Figure 71: Bending of sealed bottomweb during a peel test. A, B and C represent respectively start situation, peel initiation and peel end (black: outer layer, grey: seal layer).	134
Figure 72: Influence of cold storage on peel performance of regular and reinforced samples, sealed at 170 °C, 1.0 s, 2.0 N.mm ⁻² , during (A, B and C) and after (D and E) cold storage at -18, 4 and 23 °C ($n=5$).	136
Figure 73: Pictures and cross sections of sealed and peeled samples, that are tested in a peel test at 23 °C.	138
Figure 74: Pictures and cross sections of peeled samples, that are tested in a peel test during cold storage at 4 and -18 °C.	139
Figure 75: Digital photos of samples on white paper.	146

Figure 76: Set-up to contaminate the seal area.	148
Figure 77: Stress-strain curves.	151
Figure 78: Impact of ambient temperature on average values of peak stress of biodegradable films \pm standard deviations(n=5).	152
Figure 79: Impact of ambient temperature on average values of total strain of biodegradable films \pm standard deviations (n=5).	153
Figure 80: Permeation of gas and/or vapor, from atmosphere to headspace, through coated low barrier substrates.	155
Figure 81: Prediction profilers of models of clean and contaminated seal strengths of coated papers, optimized by maximizing.	158
Figure 82: Prediction profilers of models of clean and cheese contaminated seal strengths of cellulose films, optimized by maximizing.	159

Synopsis (EN)

Most of the food packaging needs to be closed and protected from the external environment to guarantee food safety and quality. **Heat sealing** is a cost-effective technology to close packaging. Heat is applied to mobilize thermoplastic polymer chains in the seal area. Several heating principles can be used, such as **conduction** with hot tools and **ultrasonic** friction. When hot surfaces are brought into contact, a bond can be formed. Heat seal formation depends on material properties, process parameters, presence of contamination and further processing, such as cooling. A well performing seal has a desired opening strength and seal failure mechanism, such as peeling or tearing, and is leak tight. These performance indicators can be measured with appropriate experiments.

There is a low number of available studies to gain understanding of the heat sealing process of food packages. Moreover, these studies are often executed with a one-factor-a-time approach which only gives information on the influence of one factor, while other factors are fixed. This dissertation presents a study of multiple factors that are relevant to the food packaging industry to optimize and to evaluate seal performance in an efficient way.

A **design of experiments** (DOE) approach is developed, validated and applied for ultrasonic sealing. Besides seal performance optimization, a seal window is developed that defines the region of the design space where 90% of the optimum seal strength can be achieved. This approach is flexible to new materials and seal technologies. It is the foundation of described DOE-methods in this dissertation. Heat conductive seal-through-contamination performance of three PET/PE films with different seal materials is studied. Films with metallocene catalyzed LLDPE, plastomer and ionomer-based seal layers are compared. The plastomer based seal layer achieved the best **seal-through-contamination performance**, based on a high seal strength and a high amount of leak tight seals. The study also evaluated hot tack results to predict the seal-through-contamination performance but did not find a one-on-one relation.

Heat conductive **peel performance**, during and after cold storage is studied of a packaging concept with topfilm and bottomweb. Seal strength increased at lower processing temperatures during processing. A minor impact of ambient temperature on the bending of the bottomweb is suggested as a first cause of this increase. A second cause of the increase in seal strength, with higher impact, is clearly related with a different seal failure mechanism. Both causes can be explained by a restricted chain mobility at low temperatures.

A special emphasis is given to **biodegradable materials**, because of the good fit of composting such materials in a vision of a circular economy to minimize plastic waste accumulation. The scope is broadened to gas permeation and mechanical performance to define application areas in food industry. Seal performance indicators are related to application areas for each of the materials: low seal initiation temperatures with high-speed applications, good hot tack performance with vertical-form-fill sealing, high seal strength with heavy-load packaging and low seal strength with easy opening.

The presented methods in this dissertation are flexible to multiple industrial contexts, with different factors, limitations of the design space, seal performance indicators and types of desirability functions. These methods are crucial to study

the heat sealing maintains food qu	more	efficiently	and	thus	support	safe	packaging	that

Synopsis (NL)

Om voedselveiligheid en -kwaliteit te garanderen, is het sluiten van voedingsverpakkingen essentieel. Sealen door opwarming is een veelgebruikte techniek met lage kostprijs. Hierbij moeten geen materialen zoals lijmen toegevoegd worden tijdens het sealproces. Warmte wordt gebruikt om thermoplastische polymeerketens in het sealgebied mobiel te maken. Verschillende principes kunnen toegepast worden om de seal op te warmen. Het **geleiden** van de warmte via warme balken of **ultrasone** wrijving zijn hiervan twee voorbeelden. Als warme oppervlakken in contact worden gebracht, kan er een binding gevormd worden. Het vormen van seals is afhankelijk van materiaaleigenschappen, procesparameters, de aanwezigheid van contaminatie en verdere verwerking zoals koelen. Een performante seal heeft een gewenste openingssterkte en is lekdicht. Daarnaast faalt deze seal ook op de gewenste manier tijdens het openen. Peelen en scheuren zijn twee voorbeelden van sealfaalmechanismen. Al deze performantie-indicatoren kunnen gemeten worden door geschikte experimenten uit te voeren.

Er is een laag aantal peerreview-artikels beschikbaar over het sealproces. Deze artikels beperken zich meestal tot de invloed van één factor. Om de sealperformantie te optimaliseren voor verschillende relevante industriële contexten, wordt in deze dissertatie een studie en methodologie gepresenteerd om meerdere invloedsfactoren te variëren en hun impacten te bestuderen.

In deze studie worden **experimentele ontwerpen** ontwikkeld, gevalideerd en toegepast voor ultrasoon sealen. Naast het optimaliseren van de sealperformantie worden er sealvensters ontwikkeld waar 90% van de optimale sterkte bereikt kan worden. De gepresenteerde aanpak is flexibel voor nieuwe materialen en sealtechnologieën en vormt hiermee de basis voor de beschreven methodes van deze dissertatie.

De performantie om te sealen via warmtegeleiding door vaste voedingsdeeltjes is het onderwerp van een studie bij 3 PET/PE folies. Folies met seallagen die gebaseerd zijn op plastomeer, metallocene PE en ionomeer worden onderling vergeleken. De folie op basis van plastomeer is het meest **performant met contaminatie** omwille van de hoge sealsterkte en het hoge aantal lekdichte seals. Deze studie evalueerde ook de voorspellende waarde van hot tack resultaten voor de gecontamineerde sealperformantie maar vond geen een-op-een relatie.

De **peelperformantie** van een verpakkingsconcept met een topfolie en bodemlaag is het onderwerp van een volgende studie in deze dissertatie. Tijdens en na koude bewaring worden sealsterktes bepaald. Sealsterkte stijgt tijdens bewaring. Voor een klein deel is dit mogelijk het gevolg van het rigidere buiggedrag van de bodemlaag bij lage temperatuur. Het gewijzigde sealfaalmechanisme speelt een grotere rol in de hogere sterkte. Beide oorzaken kunnen verklaard worden door een verminderde ketenmobiliteit bij lage temperatuur.

Biodegradeerbare materialen krijgen speciale aandacht omdat composteren van deze materialen goed past in een circulaire economie om plastic afval te minimaliseren. De studie is uitgebreid naar gasdoorlaatbaarheid en mechanische eigenschappen om toepassingen te bepalen in de voedingsindustrie. Indicatoren van sealperformantie ziin in verband gebracht met toepassingsgebieden: lage sealinitiatietemperaturen met hoge

snelheidstoepassingen, goede hot tack performantie met verticale vorm-vulsluitmachines, hoge sealsterkte met het verpakken van zware ladingen en lage sealsterkte met peelbare toepassingen.

De ontwikkelde en gevalideerde methodes van deze dissertatie kunnen aangepast worden voor verschillende industriële contexten. Zo kunnen factoren, limietwaarden van de ontwerpruimte, sealperformantie-indicatoren en types wenselijkheidsfuncties aangepast worden. Deze methodes zijn noodzakelijk om op efficiënte wijze meer inzicht te krijgen in het sealen door opwarming. Op deze manier draagt deze dissertatie bij aan veilige verpakkingen die voedselkwaliteit waarborgen.

1. Introduction

This chapter introduces the topic of heat sealing by giving a brief history of food packaging, explaining how heat seal bonds are formed, and listing up relevant seal technologies, seal materials, seal performance indicators and factors that impact seal performance. At the end of this chapter, objectives and structure of the dissertation are described.

Brief history of food preservation and transportation: Role of food packaging

Hunter-gatherer societies only used rudimental packaging, such as animal skins and other textiles, to transport and store foods. With agricultural innovations and the resultant accumulation of foods, transportation and storage became more important. Basket weaving, which is the predecessor of pottery, dates back to the beginning of that era, at 10000 BC. Glass packaging, which is offshoot of pottery, dates back to 7000 BC¹. Storage technologies, of which acidification, drying and salting are examples, were developed for an increasingly differentiating processed food supply. The role of packaging in society became increasingly important because of strict requirements to maintain food safety and quality.

Rigid packaging became increasingly popular over 200 years ago, because of the invention of the canned process. Tin materials were used but later replaced with aluminium and steel. Glass packaging became popular at the end of the 19th century, with the invention of the automated glass bottle process. Flexible packaging also has an early history, going back to the use of paper wraps around food in ancient China in 100-200 BC. More recently, in the beginning of the 20th century, aluminium film emerged. In the consumer culture of the 20th century, people eat more processed food and go to supermarkets to obtain foods. Before, food was purchased in small open markets. With the rise of supermarkets, and the resulting emphasis of self-service over customization, transparency was crucial. Consumers did not have to wait for clerks to serve them, when transparent film is used. Cellophane film emerged in the beginning of the 20th century, and was later that century replaced by fossil-based alternatives, such poly(vinylchloride), polyester and polyolefins. Besides preservation and transparency, food packaging has many functions, such as giving information, branding, portioning, convenience and circularity¹.

Lightweight materials such as paper, plastic and composites are most relevant for flexible food packaging². Because of the light weight, less energy is consumed during transportation. The global market share of flexible packaging ranges around 30%, the majority of flexible packaging has food packaging as primary end use. Flexibility facilitates production of packages in different shapes¹.

Need for closure systems

Food needs to be protected from the environment, such as microorganisms, light and external gases, to prevent and/or inhibit microbial and biochemical degradation. Additionally, the aromatic gases need to be kept inside the package to maintain the flavour during the life span of the packed product. Therefore, packages should remain tight until the consumer opens it for consumption. Sealing is defined as the process to close something, packaging in this particular case,

securely. With heat sealing, temperature is increased when two sides of packaging materials are coming into contact. In an optimal seal performance, a leak tight seal with a desired tensile strength is achieved. Other closure technologies, such as gluing, stitching and stapling require the addition of materials that can negatively impact food safety and food quality, and are not always suited to generate leak tight seals. The seal should have sufficient strength to withstand relevant processes (f.e. in-company processing, transportation, storage) in relevant environments (f.e. freezing, cooling, microwave, etc.). In many applications, the seal strength should also be low enough to allow easy opening.

Thermoplastics to heat seal packages

Thermoplastics become pliable at elevated temperature and solidify when cooled down. Films with a thermoplastic material at the seal side of packaging materials are used to heat seal³. Besides ensuring a good seal performance, these seal materials can also add mechanical and barrier properties to the overall film performance. There are several options in materials and technologies to produce heat seals. A first sum up is given in 1.2. As thermoplastics need to be heated to seal, thermal properties are of high importance, in particular glass transition (T_g) and melting temperature (T_m). At glass transition temperature the material changes from a glassy state into a rubbery state. At melting temperature all crystals melt and the material changes from a solid to a liquid state, the material flows. Depending on the material, glass transition and melting are gradual processes over a specific temperature range. Amorphous polymers have no crystalline regions, for these polymers melting temperature is not relevant. For semi-crystalline polymers both thermal properties are relevant.

1.1 Bond formation

Four different stages can be differentiated during a heat sealing process:

- melting/softening and wetting
- diffusion
- adhesion
- entanglement and recrystallization⁴

During wetting, small gaps between the interfaces are filled in the first milliseconds of heat sealing. After wetting, polymers can diffuse through the interface and/or create a bond by several adhesion mechanisms. In a final step, polymers can entangle and recrystallize.

During heat sealing, different adhesion mechanisms can occur³. Figure 1 shows three common mechanisms: chain entanglement, intermolecular bond and mechanical bond.

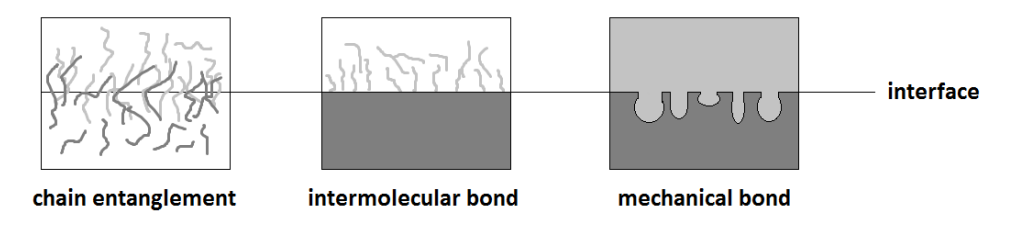


Figure 1: Adhesion mechanisms: chain entanglement with mechanical interlocking of polymer chains at both sides of the interface; intermolecular bond with chemical forces, that attract polymer chains with other chains or with a non-polymeric substrate; mechanical bond with mechanical interlocking of polymer flow in a porous substrate.

The main bond mechanism is **chain entanglement**⁵. With rising temperature, well above glass transition, chains become more mobile and when they are brought into close contact chains diffuse through the interface if the materials at both sides are miscible⁶. After diffusion, entangling can occur. The density of interfacial entanglements increases with rising time and temperature until a plateau is reached⁷. With amorphous polymers a seal with sufficient strength can be made by this bond principle, referred to as autohesion⁶. PET films are sealed this way.

Semi-crystalline polymers have a slightly different bond mechanism because these polymers need to be heated up to or over the melting point to melt the crystals before the majority of chains can participate in the diffusion process prior to entanglement. After diffusion and entangling, the seal cools down and forms new crystalline structures over the interface which can further increase the bond strength⁸. Polyolefin films are sealed this way. Strong seals are obtained when a high amount of linear long chains is released at the seal interface by the heating process, followed by diffusion, entanglement and crystallization after cooling down. The length of the chains and the branching morphology are important factors that impact the strength of the seal⁹.

Intermolecular bonds are a result of intermolecular forces such as hydrogen bonding, van der Waals forces, ionic bonding and other dipole interactions. These bonds can even take place without intermingling on non-porous substrates such as aluminium. This can be observed on cups with aluminium lids with an acrylate seal layer for easy-opening⁵.

There is some confusion in heat seal literature on the terminology of intermolecular bonds. Chain entanglement can be referred to as an intermolecular bond as well^{3, 4}.

With a **mechanical bond**, or wedge bond, the polymer is heated and flows in a porous substrate such as uncoated paper or Tyvek®. When the polymer cools down it solidifies in the voids of the substrate⁵.

1.2 Seal technologies

There are several technologies that can be used to increase heat in packaging materials.

A first group of technologies uses a heat source. Hot tools are pressed to the outer side of packaging films to **conduct** the heat through the material to reach the seal interface, tools can be heated constantly or with an impulse. Heat can also be transferred by **convection** in hot air sealers. Another seal technology within this group uses infrared **radiation** to heat packaging materials.

In **ultrasonic** sealing mechanical vibrations in the ultrasonic range are applied to generate heat in packaging materials.

A last group of technologies uses electromagnetic energy. In **induction** sealing, heat is generated when packages with metal layers, such as aluminium, approach a rapidly changing magnetic field. In **dielectric** sealing, heat is generated when packages with polar polymers, such as PVC, approach a rapidly changing electric field.

All of these technologies share the heat seal principle: a seal is produced after increasing temperature for a specific time while two or more sides of packaging are pressurized to make contact. But depending on the technology, different parameters are used. This dissertation studies heat conductive sealing, which is the most used seal technology in food industry, and ultrasonic sealing, which is an alternative technology with some interesting features in some applications where the use of hot tools is not the most suitable solution. Both technologies are discussed in detail in 2.1.

1.3 Seal materials

1.3.1 Thermal properties of thermoplastics

Thermal properties can be determined with differential scanning calorimetry (DSC). DSC shows thermal transitions by heating and cooling a polymer while heat flow is compared to a reference without polymer. Changes in heat flow indicate a thermal transition. When crystal structures are melted during heating, heat flow becomes negative because of the energy needed to dissolve the energetic stable crystal structures. In Figure 2 glass transition and melting are shown in a DSC curve. Next to these transitions, also crystallization, crosslinking and oxidation or decomposition can occur during heating.

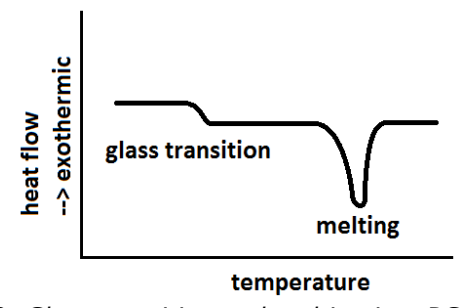


Figure 2: Glass transition and melting in a DSC curve.

Table 1 lists glass transition and melting temperatures of materials that are commonly used in seal layers of heat sealable commercial packages. The list contains predominantly polyolefins, a group of polymers from unsaturated and light hydrocarbon polymers, such as poly(ethylene), poly(propylene) and poly(1-butene) These polyolefins and other seal materials are discussed in detail in 2.2. The data in this table is derived from the CES Edupack software ¹⁰.

Table 1: Glass transition temperatures (Tg) and melting points (Tm) of materials used in heat sealable films¹⁰.

	Polymer	T _g (°C)	T _m (°C)
Semi-crystalline	Low-density poly(ethylene) (LDPE)	-125 → -90	98 → 115
	Conventional Linear LDPE (LLDPE)	-125 → -90	122 → 124
	Metallocene LLDPE (mLLDPE) f.e. Lumicene® M1810	Not provided	110
	EP		
	Sodium ionomer	43 → 57	82 → 94
	Zinc ionomer	55 → 73	70 → 96
	Polyolefin plastomer (POP) f.e. Affinity™ PL 1880G	Not provided	99
	= polyolefins with rubber-like properties		
	Poly(ethylene-co-vinyl acetate) (EVA), 25% VA	-90 → -82	47 → 52
	Poly(vinylalcohol-co-ethylene) (EVOH)	49 → 72	142 → 191
	Poly(ethylene-co-methyl acrylate) (EMA), 17-25%	-96 → -88	74 → 95
	MA		
	Random copolymer PP	-24 → -16	140 → 150
	Homopolymer poly(propylene) (PP)	-14 → -6	161 → 170
	Poly(1-butene) (PB) adhesive resin	-38 → -24	83 → 97
	Poly(lactic acid) (PLA)	52 → 60	145 → 175
	Poly(hexano-6-lactam) (PA6)	44 → 56	210 → 220
	Semi-crystalline poly(ethylene terephthalate) (PET)	68 → 80	255 → 265
Amorpho us	Amorphous PET (APET)	60 → 84	/
	Poly(ethylene glycol-co-1,4-cyclohexanedimethanol	81 → 91	/
	terephthalate) (PETG)		
	Poly(styrene) (PS)	90 → 100	/
	Poly(styrene-co-methyl methacrylate) (SMMA)	101 → 110	/

1.3.2 Multilayer structures

In the food packaging industry, different materials are combined in a multilayer structure to obtain cost-effective films with suited functionality (barrier, seal, mechanical properties, etc.) for the desired application. The widespread use of multilayers in industry, of which heat sealing is one of the main causes, compels an introduction in this dissertation.

In heat conductive sealers, heat is applied at the outer sides and conducted through the material to produce a seal at the inner side. Multilayer structures with materials with high and low melting temperatures are respectively used in the outer and seal layers to prevent degradation and/or sticking against tools. Poly(ethylene terephthalate) (PET) and polyamide (PA) are examples of materials with high melting temperature. These materials start melting at respectively 250 and 210 °C and are often used as outer layers.

Poly(propylene) (PP) and high-density poly(ethylene) (HDPE) are alternative thermoplastics that can be used in outer layers to improve the heat resistance and mechanical properties of the overall film. PP and HDPE have respective melting temperatures around 160 and 130 °C. (Linear) low density poly(ethylene) ((L)LDPE) are often used in seal layers, these materials have a melting range between 100–125 °C.

Also, non-plastic components can be included in multilayer structures, such as aluminium and paper in the example of beverage carton. The influence of these materials on seal performance is mainly related with heat conduction.

1.4 Seal performance

In this dissertation, heat seal performance, shortened to seal performance, is used as an umbrella term, covering seal properties and environmental relations.

Seal properties are the properties of the sealed material, from which the **opening strength or energy** in a tensile test and leak tightness are the most described properties in literature because of their direct relation with maintaining food safety and quality, which is the main requirement of food packages.

The strength of seals can be measured immediately after heating¹¹, which is referred to as 'hot tack strength', a relevant property in automatic production. Strength can also be measured after a cool down period of several hours or days, which is referred to as 'seal strength'¹², which is more relevant for transportation, storage and opening by consumers.

Leak tightness, also referred to as '**seal integrity'**, can be evaluated with different methods, depending on the desired outcome, of which leak size, leak location, pinhole sensitivity are examples. Inflating the package or putting it in a vacuum chamber while measuring pressure difference, and using a penetrating dye solution, are examples of evaluation methods.

Other seal properties, such as thickness, crystallinity, gas permeability and opacity are less or not discussed in literature compared to strength and integrity.

Besides seal properties, also the impacts in the **relation of sealing and the seal's environment** can be considered as performance indicators. One example is food deterioration, e.g. molten chocolate because of the proximity of hot bars to heat sensitive chocolate. Other examples are energy consumption, package permeability and package aesthetics.

1.5 Factors that impact seal performance

A recent review of Ilhan⁴, which is the only available review of heat seal science in open literature, on the understanding of factors that impact seal performance, groups 4 main categories to guide future research of leak formation in flexible food packaging:

- material properties
- process parameters
- contamination
- and further processing.

Previously indicated properties, such as chain length and branching morphology, and properties, such as seal layer thickness, rheology and orientation, are amongst other, examples of material properties that can impact seal performance. The review showed that the impact of **material properties**, related with rheology, crystallinity and molecular weight received more attention in seal

literature than those related with surface characteristics, thickness, orientation and other film layers.

Machine parameters, that can be set on the seal machine are considered as **process parameters.** Examples are temperature for heat conductive sealing and seal amplitude for ultrasonic sealing. Besides these set up parameters of seal machines, seal tool design, cooling rate, film tension during sealing and packaging design are other examples of process parameters. Seal literature often covers the three machine parameters of heat conductive sealing, which are temperature, time and pressure. Mutual interactions of these machine parameters, and interactions with other factors, such as seal layer thickness or the presence of other layers are described in a lesser extent.

Because of the contact, that is required in formation of a bond, **contamination** of the seal area is not desired. 4 contamination types are differentiated: liquids, solid particles, gases, and complex food matrices. Most of these contaminations are caused by spoilage of food on the seal area. Liquids can cause a heat sink effect; air bells can be produced after evaporation with the risk of opening the seal. Solid particles can cause microchannels in the seal area with the risk of leakage. Even gas, such as water vapor, can impact the seal performance. Food is however often composed of many different molecules in different states. Carbonated beverages, raw meat and ready meals are some examples of complex food matrices. Besides food, also non-food contamination of the seal area is possible. Examples of non-food contaminations are condensation of water and dust.

Packed food is characterized with a specific shelf life, which is the time that a food product will be unfit for consumption. In order to achieve sufficient shelf life, a match is made with the food product and packaging concept with desired properties. The desirability of these properties is highly dependent of the food product. **Further processing**, such as freezing, cooling, pasteurization and sterilization is often applied to increase shelf life. Besides food preservation technologies, also storage time and transportation are processes with a potential impact on seal performance. The review of Ilhan underlines the lack of studies on the impact of contamination and/or further processing in seal performance in seal literature. The interactions of these groups with material properties and process parameters remain unknown in open literature.

1.6 A broader framework

The covid era is characterized by accelerating social changes, such as teleworking and home delivery of food, because of the new viruses and changing insights on how to minimize their negative impact on society. The pandemic emphasized vulnerabilities in global logistic chains, such as the supply of resources and the shipping of packed goods. It resulted in increasing costs, delays and shortages, effects that are magnified with the war between Russia and Ukraine. In the same period climate awareness is growing amongst governments, companies and citizens, because of increasingly common natural disasters, as a result of climate change. This awareness results in accelerated restrictions in the use of fossil resources because of the negative impact of CO_2 and CH_4 on the greenhouse

effect. In the current global economy, that uses fossil resources as main component to produce energy and also as main structural component to produce widely used material groups such as plastics and rubbers, social and technological changes are key ingredients of the climate revolution of the next decades. With the application of climate friendly solutions to replace current technologies and materials in a similar food supply system, it is very probable that food packaging and seal research are becoming increasingly important in order to guarantee food safety and quality in a sustainable global market. Governments and industry commit to ambitious goals and legislation, such as the European directive (EU) 2018/852¹³, that fits in a vision of a circular economy of plastics.

With roughly 10 publications each year, from 1994 until now, the scientific knowledge of sealing of food packages is at an early stage⁴. Because of the multiple factors and their potential interactions, rapidly changing materials and seal and processing technologies, it is not sufficient to progress in knowledge development with a one-factor-a-time approach in the next years in an industrial relevant context. **This could lead to postponing decisions or making decisions without scientific substantiation**. A framework with broad applicability towards material properties, process parameters, contamination and further processing is needed to pace up knowledge development to make it more feasible to respond quickly to changes in the sealing process of flexible food packaging.

1.6.1 A design of experiments (DOE) approach

There are, however, statistical tools to study the relation of multiple factors and one or more results, also referred to as responses or performance indicators. In a **design of experiments** (DOE) approach, a design space is set with several experimental runs. Runs are combinations of specified factor levels, that are evaluated to study the impact of these levels on one or more specific responses, such as seal strength. Sufficient variations and replications of runs are necessary to estimate accurately the impact of individual factors and their interactions on the response(s). Experimental results are matched with predictive models. These models are experimentally validated by comparing predicted and experimental values.

The goal is to evaluate the impact of each factor and/or interaction and to optimize seal performance within the limitations of a set design space in a quick and cheap way. For optimization in an industrial context this approach is valuable. It is also valuable as an evaluation and screening tool in open science. Seal performance can be screened efficiently with a DOE approach in a first step. In a second step, relations, of individual factors, interactions and responses, of interest can be studied with well targeted experiments, such as additional mechanical or chemical characterization. The gain in efficiency of the DOE approach also increases efficiency of other experiments that are needed to acquire more knowledge of the sealing process of flexible food packaging.

1.6.2 General aim and structure of the dissertation

The main objective of the dissertation is to **study** and to **optimise heat seal performance** of flexible food packaging by developing and validating innovative **design of experiments** approaches, including **material properties, process parameters, contamination and further processing**, for different industrial contexts.

Specific objectives are designated to achieve the main objective:

- Developing and validating DOE-methods to study the important industrial contexts: ultrasonic sealing; heat conductive sealing; seal-throughcontamination; and peeling during and after cold storage.
- Study the relation of process parameters and seal performance by including ultrasonic and heat conductive process parameters as factors in a DOE.
- Study the relation of contamination and seal performance by evaluating different solid and liquid contaminations.
- Study the relation of further processing and seal performance by adding ambient temperature as factor in a DOE.

This dissertation has the following structure:

- **Chapter 2** gives a literature review of seal technologies, materials and characterization methods of seal performance of food packaging. It also further describes the relevance of a DOE-approach in seal studies.
- **Chapter 3** sets up the DOE-approach for ultrasonic sealing. This chapter gives a detailed description of this approach on a film and technology with respect to its broader application.
- Chapter 4 makes adaptations to the approach of chapter 3 to study seal-through-contamination. Besides optimization and evaluation, the DOE is also used as a first screening tool, supplemented with additional experiment to address issues with solid contamination of the seal surface of flexible food packaging.
- **Chapter 5** follows a similar framework as chapter 4, by making adaptations to the DOE and by supplementing the DOE results with additional experiments to study the seal performance of flexible peelable food packaging during and after cold storage.
- Chapter 6 evaluates packaging functionality, broadly defined as a combination of gas barrier, seal and mechanical performance, of biodegradable films. The framework of chapters 4 and 5 is supplemented with gas permeation and mechanical experiments to determine application areas in food packaging.
- **Chapter 7** positions the study in a broader perspective by giving conclusions and recommendations for future seal research.

To summarize, all factors and seal performance indicators of interest in this dissertation, are shown in bold in Figure 3.

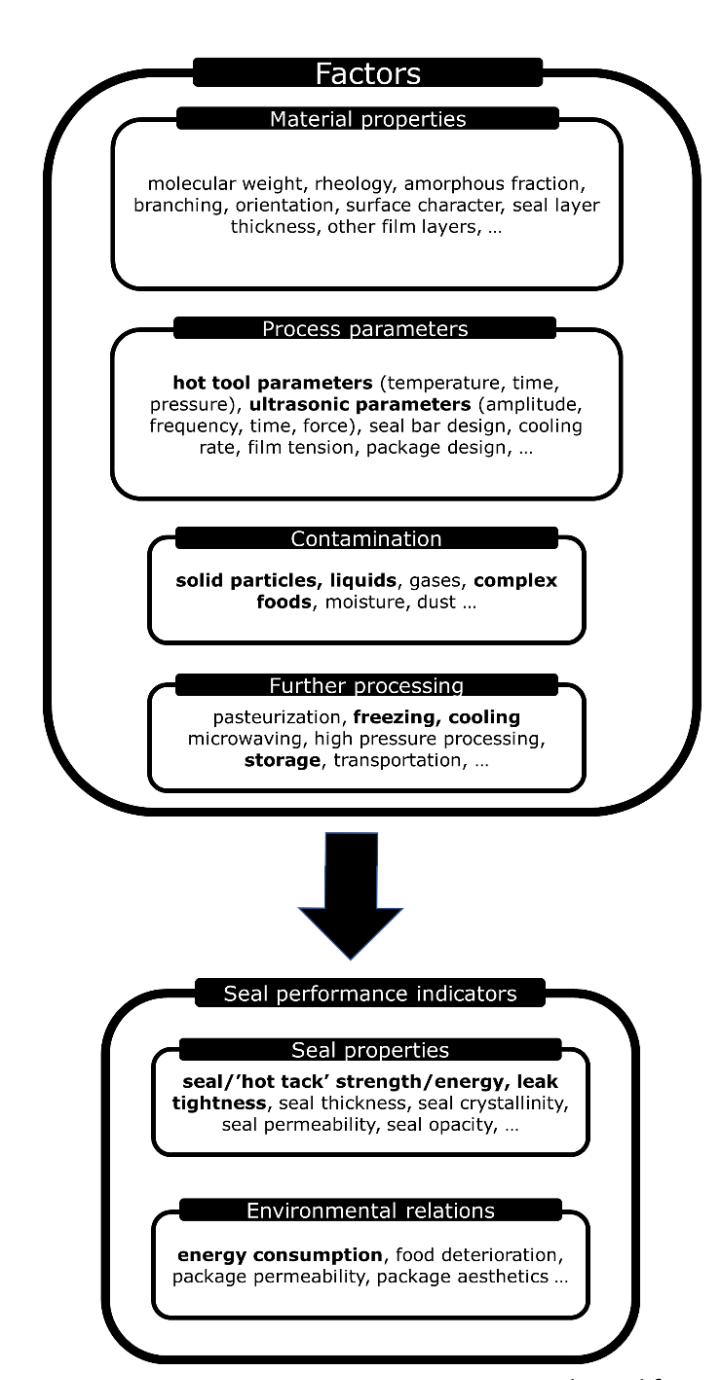


Figure 3: Factors that impact seal performance, adapted from Ilhan et al⁴; bold: all factors and seal performance indicators of interest in this dissertation.

1.7 References

- [1] Morris B. 2017. The science and technology of flexible packaging multilayer films from resin and process to end use. *Elsevier inc* **2016**, Amsterdam, pp. 3-19, 249-250. ISBN: 978-0-323-24273-8.
- [2] Piergiovanni L, Limbo S. Food packaging materials. *Springer international publishing* **2016**, Switzerland, pp. 1-3. ISBN: 978-3-319-24730-4.
- [3] Hishinuma K. Heat sealing technology and engineering for packaging: Principles and applications. *DEStech Publications inc* **2009**, Lancaster, pp. 1-4. ISBN: 978-1-932078-85-5.
- [4] Ilhan I, Turan D, Gibson I, ten Klooster R. Understanding the factors affecting the seal integrity in heat sealed flexible food packages: a review. *Packaging technology and science* **2021**; 34; pp. 321-337; DOI: 10.1002/pts.2564.
- [5] Darby D. Sealing Seminar: exploiting polymer properties for sealing. *IPI International Packaging Institute* **2011**; conference proceedings; Schaffhausen.
- [6] Awaja F. Autohesion of polymers. *Polymer* **2016**; 97(5); pp.387-407, DOI: http://dx.doi.org/10.1016/j.polymer2016.05.043.
- [7] Ge T, Robbins M, Perahia D, Grest G, Robbins M. Molecular Dynamics Simulations of Polymer Welding: Strength from Interfacial Entanglements. *Physical review letters* **2013**; 110(9): 098301, DOI: 10.1103/PhysRevLett.110.098301.
- [8] Mueller C, Capaccio G, Hiltner A, Baer E. Heat Sealing of LLDPE: Relationships to Melting and Interdiffusion. *Journal of Applied Polymer Science* **1998**; 70, pp. 2021–2030, DOI: <a href="https://doi.org/10.1002/(SICI)1097-4628(19981205)70:10<2021::AID-APP18>3.0.CO;2-A."
- [9] Sadhegi F, Ajji A. Application of Single Site Catalyst Metallocene Polyethylenes in Extruded Films: Effect of Molecular Structure on Sealability, Flexural Cracking and Mechanical Properties. *The Canadian journal of chemical engineering* **2014**; 92(7); pp1181-1188, DOI: 10.1002/cjce.21964.
- [10] CES EduPack[™] **2017** version 17.2.0 [computer software]. *Granta design limited*.
- [11] American Society for Testing and Materials **2015**. Standard Test Methods for Hot Seal Strength (Hot Tack) of Thermoplastic Polymers and Blends Comprising the Sealing Surfaces of Flexible Webs (ASTM F1921 / F1921M 12). Retrieved from https://www.astm.org/Standards/F1921.htm.
- [12] American Society for Testing and Materials **2015**. Standard Test Method for Seal Strength of Flexible Barrier Materials (ASTM F88/F88M-15). Retrieved from https://www.astm.org/Standards/F88.htm.
- [13] Eur-Lex. Directive (EU) 2018/852 of the European Parliament and of the Council of 30 May 2018 amending Directive 94/62/EC on packaging and packaging waste (Text with EEA relevance). Retrieved January 28 2022 from https://eur-lex.europa.eu/legal-content/EN/ALL/?uri=CELEX:32018L0852.

2. Heat sealing: technology, materials and performance evaluation

This chapter describes the state of the art and relevant background information for specific heat seal technologies, heat seal materials and seal performance evaluation. The relevance of parameter interactions and the resulting need for a design of experiments-approach are explained to introduce the statistical methodology that is used to evaluate and optimize seal performance.

2.1 Heat seal technology

The main focus of this section is heat conductive sealing and ultrasonic sealing because of their high relevance for food packaging and present as seal technologies in the later chapters 3, 4, 5, and 6. Other seal technologies will be briefly explained in 2.1.3.

2.1.1 Heat conductive sealing

Heat is conducted from **hot tools** (bar/jaw or plate) to the packaging material. The temperature of the tool is material specific and kept constant during sealing. Bar temperature is regulated by a thermocouple. The location of that thermocouple and the conductivity of the tool material influence the temperature at the contact area and thus at the seal interface¹.

As discussed in 1.3.2 it is important that the outer part of a packaging film does not stick to the heated tool. An important property of packaging films to prevent this is ΔT . ΔT can be defined as the difference between the melting temperature of the outer surface and the seal temperature of the inner surface of packaging films, as described in Equation 1.

$$\Delta T = T_{melt\ outer\ surface} - T_{seal\ inner\ surface}$$
Equation 1.

Figure 4 shows the temperature profile of a sealed multilayer film between two heated tools. Sealing occurs at the minimum value (T_1) of the temperature profile. The contact surface of the outer layer and the heated tool has the maximum value (T_2) of the temperature profile².

PE is often used as sealing medium in packaging films. It melts around 120 $^{\circ}$ C and should be combined with outer layer with higher melting temperatures to prevent the film from sticking against the bars³.

PET/PE films have a ΔT between 70-140 °C, based on the difference of melting temperature, the temperature window in which strong seals can be made is rather wide.

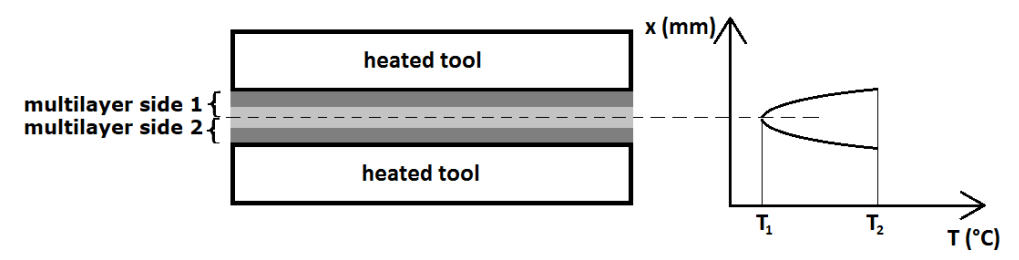


Figure 4: Temperature profile in the cross section of a sealed multilayered packaging film when both sides come into contact by closing heated tools (dark grey: outer layer, light grey: seal layer).

When $\Delta T \leq 0$ °C there is high risk of sticking against the tools. This is the case with monolayer films and with laminated or coextruded film structures with an outer layer with low melting temperature and/or inner layer with high seal temperature. Besides sticking effects these films can lose visual aesthetic properties (f.e. wrinkles can occur because of shrink at high temperature). To seal films with a $\Delta T \leq 0$ °C other conductive systems can be used such asband and impulse sealing, these systems are later explained in this section⁴.

In **hot wire/hot knife sealing**, heat is conducted from the heated tool to the packaging material. Because of the small surface of the knife or wire, as shown in Figure 5, seal pressure is high. The combination of high seal temperature and pressure makes this technology suitable for applications that demand sealing and cutting at the same time. Monomaterials can be sealed and cutted with this technology. This seal technology is not well suited to cut and seal multimaterials as each material has its own melting temperature, the value of seal temperature should be well above the highest melting peak temperature with high risk of burning the other materials.⁴

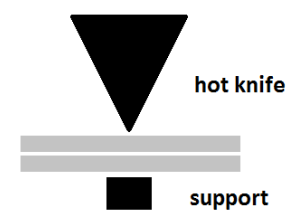


Figure 5: Hot knife sealer.

In a continuous system, materials can be sealed by heated tools in a **band seal** system, as shown in Figure 6. It can include cool bars to add a cooling under pressure feature and overcome a disadvantage of hot bar sealing⁴.

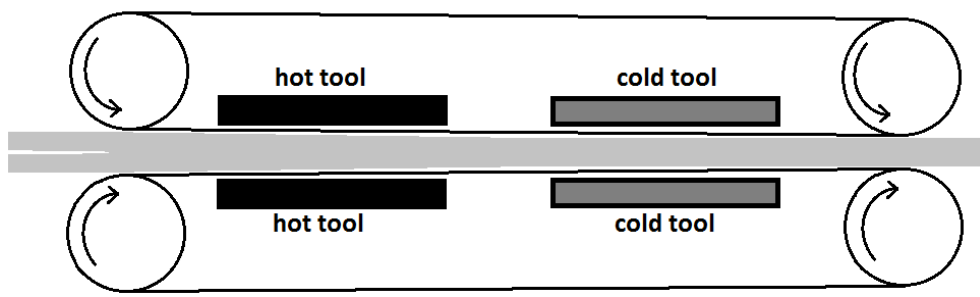


Figure 6: Band sealer.

With **impulse sealing** the heat is generated by an electric current passing a nichrome wire for a limited amount of time. Heat increases with time until the current is switched off. It is possible to make temperature constant at a certain value by using electronic temperature control. To prevent packaging material from sticking against one or more wires a non-sticking sheet is applied on the wires, typically Teflon®. The nichrome wire is often laid over a resilient surface to improve contact between hot bar and packaging material. All parts are shown in the figure of the impulse sealer. There are also systems available with one heating bar and one counterpart^{5,6}.

Compared to constant heating, less energy is used, because energy consumption only occurs during sealing and there is no need for heat-up or cool-down time. Nichrome wires and Teflon® sheets degrade over time. Because of the need of wires to heat up bars this technology is less versatile and it is more difficult to seal circular or rectangular shapes⁴.

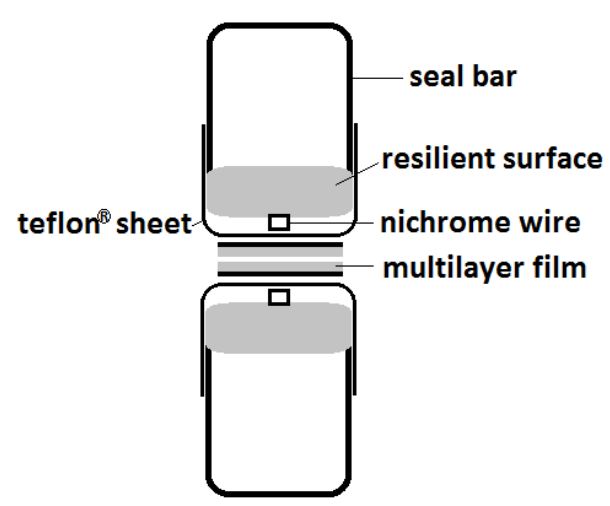


Figure 7: Impulse sealer (black: outer layer, grey: seal layer).

Advantages of conductive heating technology are the simplicity of the technology and assembly of seal system. There is a wide range of systems available as this is the most common used seal technology in the food industry. Investment costs are low and process control is simple. Constant heating is not ideal for heat

sensitive products, such as chocolate bars or frozen food. It is not suited for thick materials because the temperature is conducted from the outside to the seal interface. Cooling under pressure is only possible with impulse and band sealers.²

2.1.2 Ultrasonic sealing

Ultrasonic sealing is also characterized by melting/softening, wetting, diffusion, adhesion, entanglement and recrystallization, similar to conductive sealing. The difference is the principle of heating. With ultrasonic sealing, packaging is heated with ultrasonic vibrations⁷.

A particular tool set up is needed to **transfer** these **vibrations**. Figure 8 shows the tools that are required. Vibrations are conducted from converter to the lower surface of the horn where it's transferred on the material between horn and anvil.

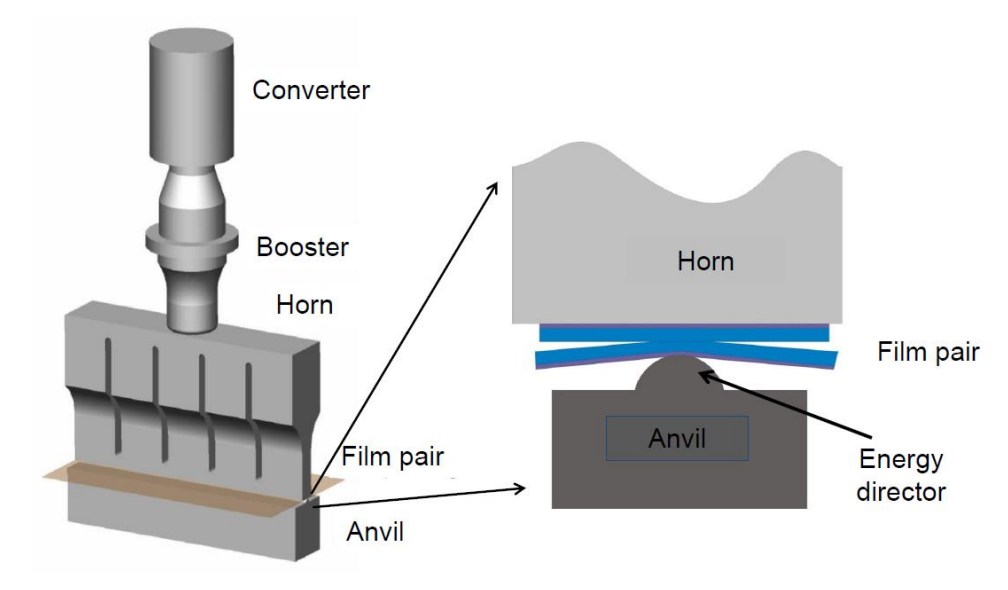


Figure 8: Ultrasonic sealing tool set up.8

Ultrasound frequencies are sound frequencies that cannot be heard by the human ear. Humans can hear sound vibrations within the frequency range of 16 Hz to 16 kHz. The lowest ultrasound frequency of 15 kHz is still audible for the human ear. The frequency range of ultrasonic sealing is between the range of 20 and 50 kHz 9 , 10

Figure 9 shows two ultrasonic amplitudes and frequencies. These values can be used to seal thin packaging films (< $100~\mu m$). The choice of these numbers depends on ultrasonic tool set up and packaging material properties. ¹¹ The upper figure shows a low frequency wave of 20 kHz (20.000 waves/second) and a high frequency wave of 35 kHz. The lower figure shows a low and a high amplitude wave of 35 kHz.

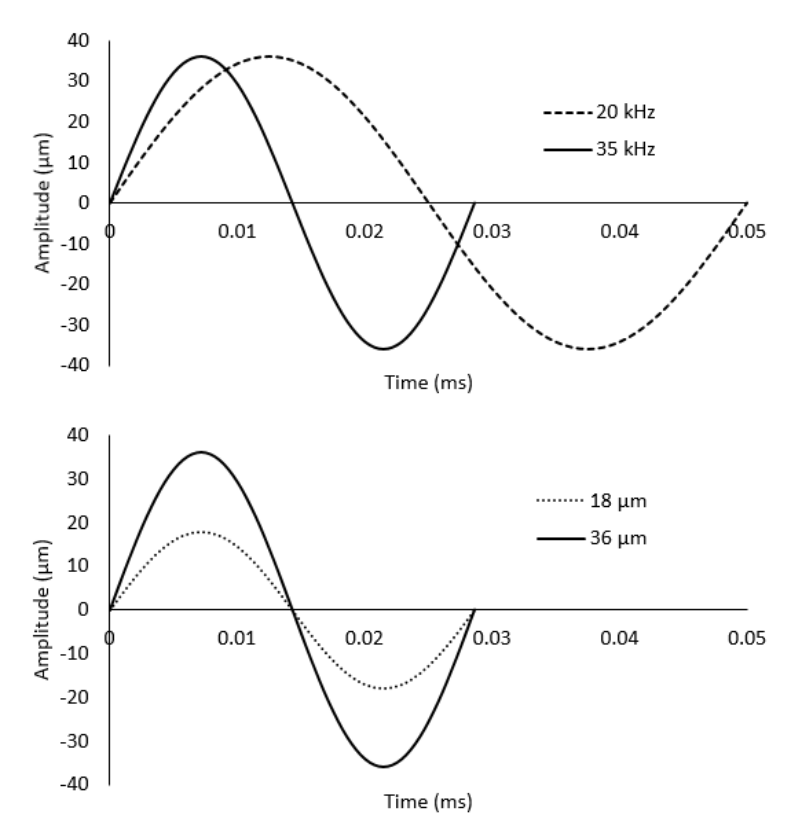


Figure 9: Amplitude and frequency of sound waves to ultrasonically seal thin packaging films (< 100 μ m). The upper figure shows waves of 20 kHz (20.000 waves/second) and 35 kHz. The lower figure shows two 35 kHz waves of 18 and 36 μ m amplitude.

The generator produces a high voltage signal at a fixed ultrasonic frequency. The electrical frequency is converted by the converter or transducer, which contains piezoelectric ceramic discs that can expand and contract, in mechanical vibrations. These vibrations pass a booster and a (profiled/flat) horn (=sonotrode) to reach the surface of the packaging film. Booster and horn can amplify or minify the amplitude of vibration at the tip of the converter⁹.

This amplitude is proportional with the ratio mass begin – mass end of booster and horn $^{12,\,13.}$ For a rectangular shaped horn, as illustrated in Figure 8, the relation of amplitude A (µm) and width W (mm) of begin and end can be described by Equation 2.

$$\frac{A_{begin}}{A_{end}} = \frac{W_{end}}{W_{begin}}$$
Equation 2.

Figure 10 shows this effect for two different rectangular horn designs over the full length of the horn.

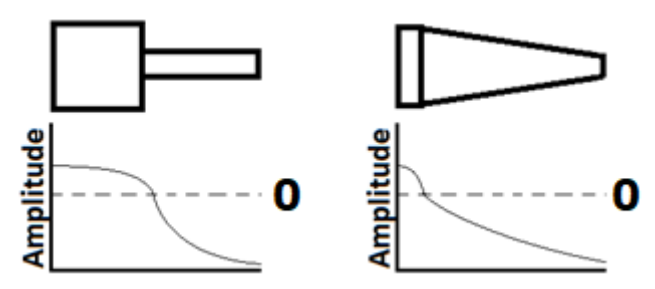


Figure 10: Amplitude amplification at the tip of the horn by decreasing the ratio mass end – mass begin.

The end of the horn is lower in mass than the upper part, which leads to an amplification of the amplitude at the tip of the horn. In a reverse design (higher mass end – lower mass begin) the amplitude would decrease. The horn can be made in high strength aluminium alloy, titanium or hardened steel depending on its application. Often horns are coated to improve the performance (f.e. carbide coating on titanium horns, chrome coating on high strength aluminium alloy, etc.) $^{9, 13}$.

Packaging materials are sealed between horn and anvil. One or both of these components contain an energy director. Energy directors are necessary to concentrate the ultrasonic energy and create a high strain at a particular area so well-defined heating and melting at that place is facilitated¹¹.

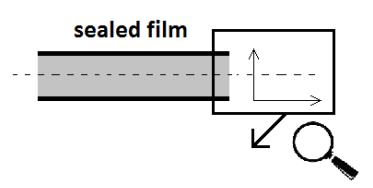
Thermoplasts can be **ultrasonically heated** by interfacial and/or intermolecular friction. Interfacial friction is the friction of joining surfaces. This mechanism only occurs in the first milliseconds with stiff seal layers, containing materials with an elastic modulus above 1000 MPa such as HDPE, because of the rougher surface, compared to soft polymers such as LDPE. Interfacial friction, however, does not speed up the heating process. Intermolecular friction is the dominant heating mechanism and refers to the friction between molecules. The average energy dissipated per unit time Q (J.m⁻³.s⁻¹) through intermolecular friction can be described with the formula:

$$Q = \pi \times f \times \varepsilon_0^2 \times (E'')$$
Equation 3.

in which f is the frequency (s⁻¹) of the horn; ε_0 is the strain (ratio), which can be influenced by seal amplitude, seal force, material properties and the profile of the energy director; and E" the loss modulus (N.m⁻²) of the material, depending on the ultrasonic direction^{8, 11}.

Heat is transferred from the hot seal interface, towards the colder outer area of the films. These outer areas are surrounded with a cold horn and anvil. The seal interface is, opposite to heat conductive sealing, hotter than the outer area of the films^{2, 11}.

The temperature profile of the joining films is illustrated in Figure 11 for heat conductive sealing (left) and ultrasonic sealing (right).



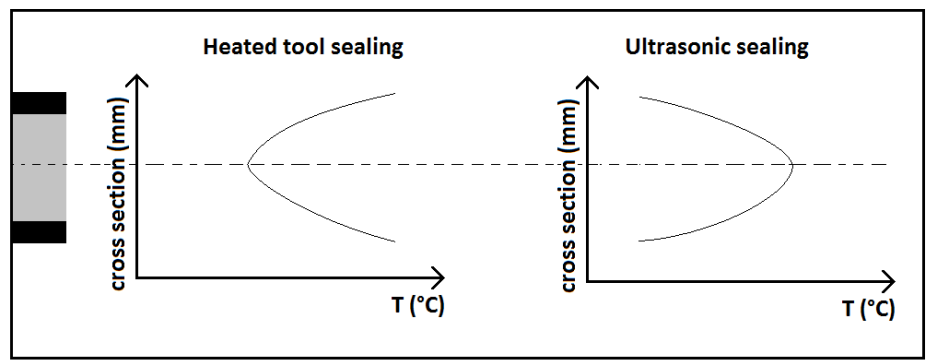


Figure 11: Temperature profile of the joining films (black: outer layer, grey: seal layer) for heated tool sealing (left) and ultrasonic sealing (right).

Melted polymer **flows** very quickly from the central area of the seal. Seal layers at both sides of the interface repeatedly encounter incompletely molten material. The hotspots are moving to the edges of the seal because of the dispelled melt. At the edges, the melt solidifies. As a result of this solidification the melt can no longer flow to the edge area and the horn 'swims' on the melt. At this stage, an equilibrium is reached. The materials melt but are not dispelled. ¹⁴

This effect can be visualised by monitoring the horn travel during a seal experiment. Figure 12 visualises the progress of horn distance that results in a decline of the gap between horn and anvil. Two 60 μm random copolymer PP films are ultrasonically sealed at appropriate settings for this material. A cylindrical energy director and respective seal amplitude, time and force of 27 μm , 200 ms and 4 N.mm $^{-1}$ are chosen, based on a previous study 11 . The horn distance is shown at the y-axis. The horn starts at zero distance when the ultrasonic vibrations start. The horn travels deeper into the material as temperature rises. Ultrasonic vibrations after 120 ms do not result in a further increase of horn distance, it reaches a stationary plateau. This is a desirable property as it is possible to apply several seal times to achieve a similar horn distance.

60 μm random copolymer PP sealed at 27 μm - 200 ms - 4 N.mm $^{-1}$

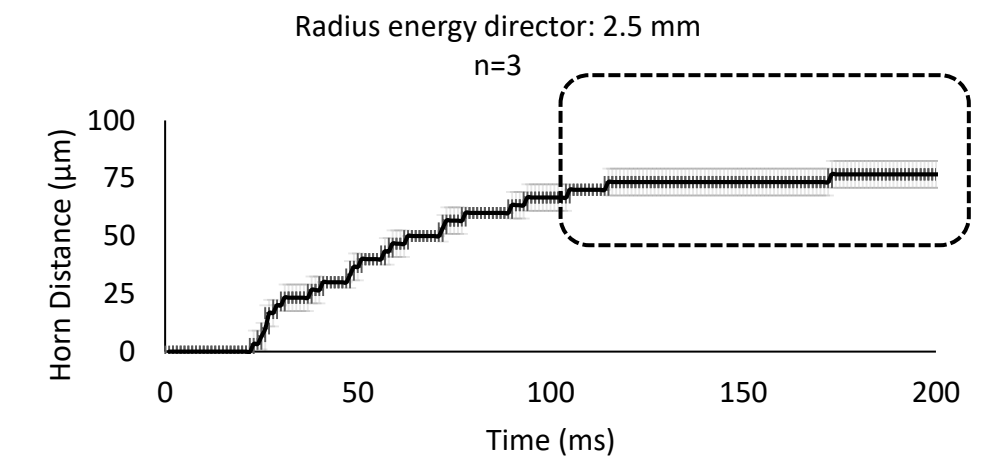


Figure 12: Equilibrium state - horn distance vs. seal time with 60 μm random copolymer PP.

There is a clear border between two different crystalline areas if sufficient ultrasonic vibrations are transferred to packaging, resulting in a strong seal: the unmolten and flown material of the seal layer. The dispelled melt, at the edges of the seal, is not well attached to the unmolten material. Figure 13 shows a seal strength test, where the border is a crack initiator that eases tearing of the seal. This often results in a lower seal strength. This behaviour is typical with ultrasonic sealing, caused by inner heating. With conductive sealing, the melt bead has a more concave shape because the film is heated from the outside ¹⁵

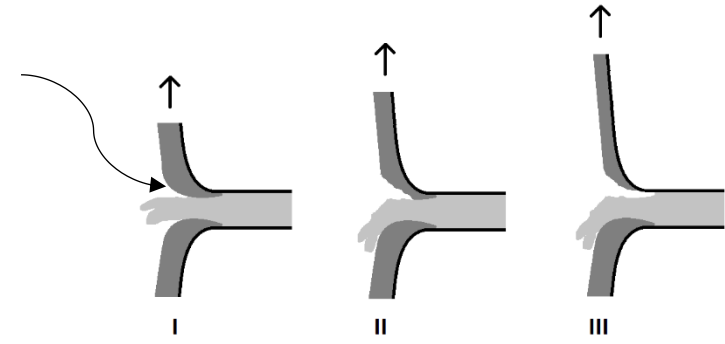


Figure 13: Fracture mechanisms along the border unmolten material - flown material (black: outer layer, grey: seal layer (light grey: molten material, dark grey: unmolten material)).

With semi-crystalline polymers, **diffusion** occurs very quickly once the melting point is exceeded. From that point, there are no crystalline structures to limit diffusion. Estimates of the time of intermolecular diffusion are on the order of 10⁻¹

⁷s for semi-crystalline polymers. This very short time has no influence on the sealing process. Diffusion of chains with amorphous polymers occurs even faster once glass transition temperature is exceeded⁷.

Ultrasonic sealing has several advantages over heated tool sealing. It has a good seal-through-contamination performance, especially with powders. There is less heat exposure for heat sensitive products, such as chocolate bars, because of the use of cold tools. Monomaterials, sticky and thick materials can be sealed more easily and/or faster because the heat is generated at the seal interface. The investment cost is high because of the use of more complex tools. With these complex tools it can be difficult to integrate the ultrasonic system in an automatic packaging line. The seal width is limited to approximate 40 cm which makes this technology undesirable for many packaging applications, such as plate sealing of many cups in a single movement. Handling is less intuitive as with heated tool sealing, extra training of operators is recommended².

Ultrasonic sealing can be applied in horizontal and vertical form-fill-sealers to increase the seal-through-contamination performance and/or to seal thick materials or monomaterials as an alternative to heat conductive technology.

2.1.3 Other heat seal technologies in food industry

Inductive sealing

If a conductive material, such as aluminium, is close to a rapidly changing magnetic field, which can be generated by passing alternating current through a working coil, joule or resistive heating occurs because of the eddy currents, which are closed loop currents, that are generated perpendicular to the magnetic field in the conductive material. Heat is transferred to an adjacent seal layer and heat sealing can occur when this layer is in contact with another seal layer¹⁶.

This technology is suitable for beverage cartons, cap seals and tubes. In cap sealers the pressure remains after completion of the heat seal operation, it is controlled by torque, which is the rotational force that is applied on the cap. Process variables are power, time, cool time, pressure and distance.

Any heat sealable polymer can be melted with this technology if a conducting material is present 17 .

Besides process and seal material variables, the thickness and the diameter of the aluminium foil can vary as well, this will impact heat generation. In the periphery of the aluminium film the current is strong, this is referred to as the skin effect. For cap sealing applications a hot periphery is essential to bond to the lip of the container¹⁸.

This principle is illustrated in Figure 14.

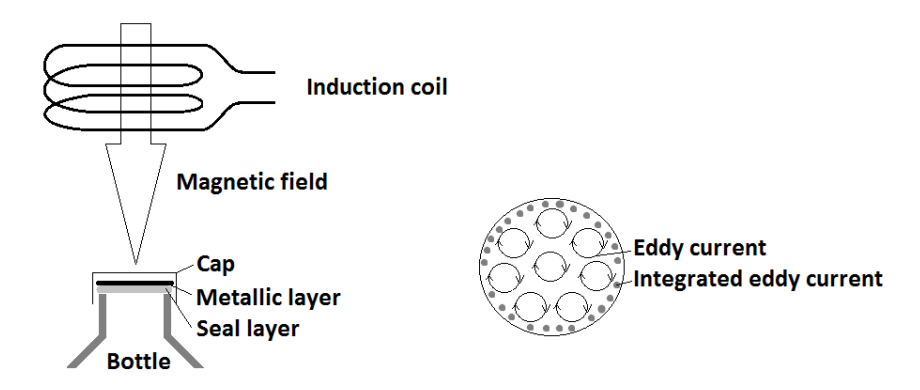


Figure 14: Cap sealer with induction heating.

The top of the thin aluminium foil is pasted to cardboard to achieve mechanical rigidity. Aluminium and cardboard are connected with a wax layer that melts during the heat seal operation. After melting the cardboard can be easily detached from the aluminium layer¹⁸.

The layer distribution of a topfilm for induction cap sealing is illustrated in Figure 15.

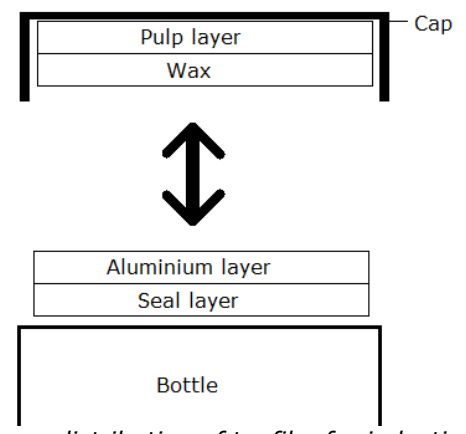


Figure 15: Layer distribution of topfilm for induction cap sealing.

Beverage cartons are thick laminates that can be sealed in short seal times with induction sealing. The simple set up and process control, the relative low investment costs are other advantages of this technology. The need of a conductive layer, typically aluminium, and the lack in versatility, as it is only suitable for some applications, are disadvantages of this technology².

Heat convection sealing

In heat convection sealing hot air, between 250 and 400 °C, is used to heat thermoplastic materials. This technology can be used to seal tubes and open mouth pouches, it can also be used to make the longitudinal seal in vertical formfill-sealers. Hot air can be directed at the interface before pressing, which can

decrease the seal time of thick materials. The simplicity of the process, low investment costs and the possibility to heat without contact are other advantages of this technology. The need for pressurized air, heat treatment of surrounding parts and difficulties to control the seal temperature are disadvantages^{2, 3}.

Heat radiation sealing

In heat radiation sealing an electromagnetic source, typically an infrared laser, radiates waves to a packaging material that absorbs the energy and is converted into heat. In an efficient process peak power wavelength of the electromagnetic source is close to peak absorption wavelength of the packaging material. After melting of the surfaces, pressure is applied to bring the seal layers in contact¹⁶. Energy can be introduced by slow/high speed scanning and continuous illumination, where multiple laser sources can be used to seal complex geometries without shadow effects¹⁹.

Because of local heat input, less heat is transferred to the packed food. The high investment costs, the sensitivity to colour changes and the need for moving sources are disadvantages of this technology².

Dielectric sealing

In dielectric sealing heat is generated internally by dielectric hysteresis losses in thermoplastic materials with polar groups. These groups try to orient themselves in a rapidly changing electrical field, which can result in intermolecular friction and heat generation. Only materials with high dielectric constant and high dielectric loss are good candidates to seal with this technology. This technology is used to seal poly(vinylchloride) (PVC) sheets¹⁹.

The ability to cool under pressure and the decrease of radiative heat in the package are advantages of this technology. However, common seal layers of packaging films, such as PE and PP, are not suited for this technology because of the dielectric properties. Another disadvantage is the risk of heating polar packed food².

Advantages and disadvantages

Advantages and disadvantages of above described seal technologies are summarized in Table 2.

Table 2: Advantages and disadvantages of seal technologies².

Table 2: Advantages and disadvantages of seal technologies ² .							
Seal technology	Advantages	Disadvantages					
Heat conductive	 Simple technology Low investment cost 95% market share Simple process control 	Heat treatment of food products, e.g. chocolate, frozen meal Limits for thick materials, seal time depends on thickness and conductivity of packaging material Cooling under pressure is only possible for impulse and band sealing					
Ultrasonic	Less heat treatment of food product, because of local heating Short seal times for thick packaging materials, e.g. paper/board Energy efficient, in particular for thick materials Possible to cut and seal without a knife Seal-through-contamination Possible to cool under pressure	High investment cost, compared to conductive sealing Requires high accuracy of the mechanical construction Requires process know-how					
Inductive	Less heat treatment of food product, because of local heating Short seal time for thick packaging materials, e.g. beverage carton with aluminium layer Simple process control Low investment cost Possible to cool under pressure	Requires aluminium or other metal components for heating Less versatile, only suited for few applications					
Heat convection	Simple technology Low investment cost Heating without contact Short seal time for thick packaging materials, e.g. tube sealing Possible to cool under pressure	Heat treatment of food products No precise control of temperature at seal area Expensive because many applications use pressurized air					
Heat radiation (laser)	Less heat treatment of food product, because of local heating Possible to cool under pressure	 High investment cost, compared to conductive sealing Requires optics and/or motion to seal lines Sensitive to color changes, e.g. printed information 					
Dielectric	 Possible to cool under pressure Less radiative heat in packaging because of local heating 	Requires polarity in polymers Heat treatment of polar food products					

2.2 Heat seal materials

This section describes the main polymers used in seal materials for food packaging materials. This section provides background information for chapters 3, 4 and 5. In 2.2.6 special emphasis is given to less used, but emerging polymers that are biobased and biodegradable materials as detailed in chapter 6.

2.2.1 Poly(ethylene)

Introduction

PE is a polyolefin that is produced by the polymerisation of ethylene. The structure is shown in Figure 16.

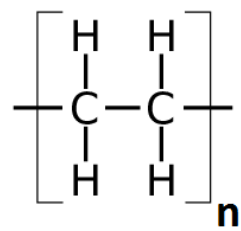


Figure 16: Poly(ethylene) structure.

It is the most common plastic in general and an important seal material in packaging material²⁰.

A first differentiation in PE is made by the difference in density, this is mentioned in the name of PE. Very low, low, medium, and high-density PE are commercially available PE subtypes. LDPE was developed during the 1930's, HDPE during the 1950's, and linear low-density was developed during the 1970's⁴. As a seal material LDPE and LLDPE are important types of PE. These materials are flexible and can be sealed at a relative low temperature (> T_m) compared to PP. Melting temperatures of LDPE, LLDPE and homopolymer PP have respective ranges of 98-115, 122-124 and 161-170 °C. Recent studies have shown that there are several molecular parameters that influence the thermo-rheological and processing properties such as the amount, length and distribution of branches, the molecular weight and the distribution of molecular weight^{21, 22, 23, 24,25, 26, 27}.

For commercial purposes, different grades of PE are blended to have a material with the desired properties. At this time there is a staggering number of grades available with specific characteristics (seal temperature, clarity, puncture resistance, ...) and costs. Besides sealability, PE can also bring optical (clarity, gloss), barrier (good water vapor barrier) and mechanical performance (toughness, puncture resistance, tear resistance, ...) to the packaging material.

General seal characteristics

Seal initiation of PE can occur when the amorphous fraction increases by heating as crystalline regions dissolve and polymer chains become more mobile. In the study of Meka et al., seal initiation of untreated LDPE and LLDPE films, occurred

when the amorphous fraction increased to 77%. With rising temperature, entanglement is facilitated and there is a fast increase in seal strength, which is measured over 24h after sealing at room temperature, until the melting point is reached²⁸. Following the same study, a plateau seal strength is achieved after this point. The plateau strength value is related with the yield stress, a tensile characteristic that marks a transition between elastic and plastic behaviour. Yield stress is a function of the amorphous fraction of PE. A lower fraction of the amorphous content at room temperature leads to higher seal strength.

In recent studies some details are discussed about the influence of the molecular structure on the seal performance.

Following Moreira's study, the presence of long chain branches interferes with the forming of crystalline structures but once after all crystals are melted the diffusion of the long-branched chains make a strong network because of the contribution of the long chain branches to entanglement. However, this stronger entanglement at the interface is not represented in high seal performance because of the interference of crystal formation by the long chain branches.²⁶

Following Sadeghi's study the distribution of small chain branches is an important factor for the seal performance. If more small chain branches are present on medium to long molecular weight chains the melt point will be decreased and crystals with longer chains are created. These longer chains can be released in the interface around the melting temperature so diffusion can take place and seal performance is increased. With larger crystal size yield strength is also increased²⁹.

This corresponds with the finding of Meka that relates high yield strength with high plateau seal strength. These studies are performed on several PE-grades and indicate the complexity of the sealing process.

LDPE

LDPE has a density of 0.915-0.940 g.cm⁻³. Figure 17 shows that polymer chains can't be packed as dense as with HDPE (0.94-0.97 g.cm⁻³). This is because of the high number of branches.



Figure 17: Branched morphology of LDPE and HDPE.

With decreasing density, the material becomes less crystalline and more flexible. LDPE has small and long chain branches and has molecules of low and high molecular weight and this has positive and negative consequences.

A positive consequence is the ease in processability, because of the shear thinning and the bubble stability.

Shear thinning is the decrease of viscosity under shear strain, this is an important property for extrusion where plastics are molten by a combination of shear heating

and external heating. High molecular weight plastics are more viscous than lower molecular weights. The distribution of molecular weight influences the dependence of viscosity on shear rate. LDPE has a wide molecular weight distribution compared to LLDPE, at similar molecular weights LDPE shows a higher degree of shear thinning than LLDPE making it better processable for extrusion²¹.

In Wong's study, LDPE and LLDPE have molecular weight distributions, measured by gel permeation chromatography, of respectively 5.03 and 3.90. Bubble stability is of high importance for blown extrusion. It depends on properties, such as melt strength, which can be calculated after measuring the extensional load of molten polymer, and process parameters, such as the blow-up ratio³⁰.

LDPE has a good bubble stability because strain hardening occurs under stress. This is less the case for LLDPE which has a low melt elasticity and polymers relax rapidly when they undergo stress in a molten state²¹.

Negative consequences of the molecular structure are the mechanical properties. Low molecular weight molecules in LDPE decrease the mechanical properties such as strength and toughness compared to the higher molecular weight molecules in LLDPE^{24, 31}.

LDPE is not the best option to increase speed of the sealing process. Seal temperature is approximately 110 °C. There are materials with a higher seal temperature (f.e. PP), but there are also materials with a lower seal temperature (f.e. polyolefin plastomers, these polyolefins have rubber-like properties) and more appropriate for high speed packaging lines³². The hot tack performance, discussed more in detail in 2.3.2, of LDPE is relatively bad, this is probably because of the interference of crystal formation by the small- and long-chain branched structure, making it a weak seal when it is still hot.

LDPE is a weak subtype of PE for seal strength, mainly because of the presence of low molecular weight molecules and the highly branched structure that disrupts the crystalline structure. However, this is not a limitation for applications where a low seal strength is sufficient or desirable (f.e. in peel films where peel component is added to decrease seal strength).

LDPE is a common seal material as it combines good processing properties with mediocre seal (and mechanical) properties at low cost. The seal (and mechanical) properties can be increased by blending LDPE with other PE subtypes to achieve the desired performance³³.

LLDPE

LLDPE has a density of 0.915 – 0.926 g.cm⁻³. This material has a similar density and more linear structure as LDPE. Both materials are in competition and also often blended to combine properties⁴.

With LLDPE short chain branches are distributed over linear main chains. Side branching and molecular weight are affected by comonomer content and process settings during production. The length of the branches is dependent on the comonomer which is used during production. Commercial LLDPE has branches of 4, 6 or 8 carbon atoms for each branch (abbreviated as LLDPE-C4, -C6 or -C8). In general, three different catalysts are used to produce commercial PE: Philips catalyst (chromium-based, 1950's), Ziegler-Natta catalysts (titanium-based, 1950's) and Kaminsky catalysts (metallocene-based, 1970's; metallocenes are chemical structures with positively charged metal ions, such as Zirconium (Zr),

Hafnium (Hf) or Titanium (Ti), sandwiched between two cyclopentadienyl deratives)³⁴. The choice of catalyst influences the structure of LLDPE as shown in Figure 18.

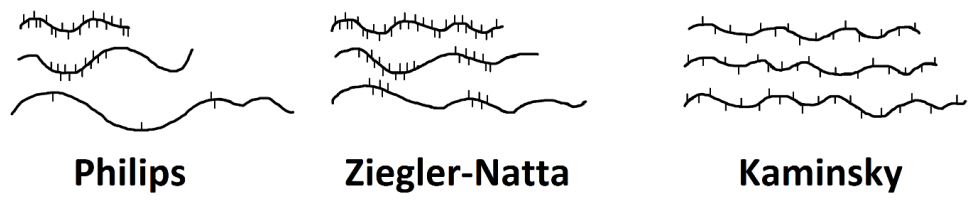


Figure 18: Branching morphology of LLDPE with Philips, Ziegler-Natta and Kaminsky catalysts.

Conventional catalysts produce LLDPE with a broad molecular weight distribution leading to good processability, but less mechanical strength. Metallocene-based LLDPE (mLLDPE) is less processable but has better mechanical properties.

Another point of difference is the comonomer distribution, with conventional catalysts the small chain branches are mainly concentrated on the smaller main chains while the long main chains are less branched and linear. With mLLDPE more short chains are distributed on long main chains. As described in the previous part, seal performance (low melt point, high seal strength) is improved by placing more short chain on medium to long main PE chains. Because of this mLLDPE is regarded as a better seal material as conventional LLDPE^{25, 26, 29}.

The crystal size with mLLDPE is more regular distributed compared to conventional LLDPE. The lack of large crystals in mLLDPE makes it more transparent as conventional LLDPE because less light is reflected by large crystals. mLLDPE is also glossier as conventional LLDPE or LDPE^{4, 35}.

The first generation of mLLDPE in the 1990's had limited market success because of the lack in processability, during the 2000's processability is improved by adding long chain branches to the molecular structure (f.e. Affinity $^{\text{TM}}$) which decreases the viscosity and increases the bubble stability $^{29, 35}$.

Many metallocene catalysed PE grades with a high amount of comonomer are named as VLDPE (Very low-density PE) because of the low-density ($0.880-0.915~\rm g.cm^{-3}$) and/or polyolefin plastomers (POP) as they combine rubbery with thermoplastic properties. These materials have a low viscous behaviour when heated and can fill in gaps in pouches or flow around contamination, thus preventing leakers. This ability is called caulkability and is discussed in $2.3.7~\rm in$ relation with the seal-through-contamination performance.

There are many variations possible in the production process of LLDPE (process parameters, comonomer length/content, catalyst) that affect the molecular structure (length and distribution of small and long chain branches, molecular weight, molecular weight distribution, crystallinity) and this has an impact on the properties of the film (seal performance indicators such as seal- and hot tack strength, optical and mechanical properties, processability). Concluding for LLDPE, there are many grades on the market with different properties, some of these are shown in Table 3. The values of three properties show the difference between these commercial LLDPE grades.: Melt flow index, which is a measure of the ease of flow through a capillary, density and molecular weight. LLDPE's are

high performing heat seal polymers for packaging films because of good sealing (low seal initiation, high seal strength, high hot tack, seal-through-contamination) properties, good optical properties (transparency and gloss) and good processability. Examples of such differences in seal performance of LLDPE films can be found in Sadhegi's study. For seal initiation temperature e.g., they reported a low value, below 80 °C, for Dow's resin Affinity™ 1140, a mLLDPE-C8 of medium molecular weight with sparse long chain branching. Seal initiation temperature values of other mLLDPE's (Affinity™ 1450 of Dow: mLLDPE C8 of low molecular weight with sparse long chain branching; Exact™3132 of ExxonMobil: mLLDPE-C6 of medium molecular weight) are between 80 and 100 °C and the seal initiation temperature of LLDPE (TF-Y534-IP of Nova Chemicals: LLDPE-C6 of medium molecular weight) occurs above 100 °C ²⁹.

Table 3: Properties of commercial LLDPE-grades^{29, 31}.

Resin (code)	Description	Supplier	Melt flow index (MFI) (190 °C. 2.16 kg ⁻¹)	Density (g.cm ⁻³)	Mw (kg. mol ⁻¹)
Affinity 1450	mLLDPE-C8	Dow Chemical	7.5	0.902	NA
Affinity 1140	mLLDPE-C8	Dow Chemical	1	0.895	105
Dowlex 2045	LLDPE-C8	Dow Chemical	1	0.920	102
Exact 3132	mLLDPE-C6	ExxonMobil	1.2	0.900	NA
(TF-Y534-IP)	LLDPE-C6	Nova Chemicals	0.75	0.934	118
(FPI 20)	LLDPE-C8	Nova Chemicals	1	0.920	105

2.2.2 Poly(propylene)

PP is a polyolefin that is produced by the polymerisation of propylene. The structure is shown in Figure 19. For packaging it is the second most used polymer, after PE. It was first developed in the 1950's⁴.

Figure 19: Poly(propylene) structure.

A first differentiation of PP is made by the location of the methyl heads (CH $_3$ branches) in the polymer chain. With isotactic PP all heads stick out at the same side as shown in Figure 20. Isotactic PP is a rather stiff material that can crystallize, it has a good chemical and heat resistance 36 . With syndiotactic PP the heads repeatingly stick out at both sides. Syndiotactic PP can also crystallize 37 . With atactic PP all heads stick out randomly, the resulting polymer will not crystallize and is amorphous. Standard commercial PP used in packaging is over 90% isotactic and has a small amount of atactic polymer. Commercial PP has a narrow density range of 0.898 – 0.908 g.cm $^{-3}$ and no extensive differentiation based on density is made, unlike PE.



Figure 20: Tacticity of methyl heads of PP.

A second differentiation of PP is made between homopolymers with a repeating sequence of propylene units, and copolymers where small amounts of comonomer, usually ethylene and/or butene, are added to the PP main chain. Addition of comonomers to the PP chain can give the material more transparency, higher impact strength, higher flexibility and/or a lower and broader melting point. The randomness and the amount of incorporation of comonomer are determining factors. There is a wide range of copolymer grades commercially available. Within the copolymers block and random can be differentiated, based on the distribution of comonomers as shown in Figure 21⁴.

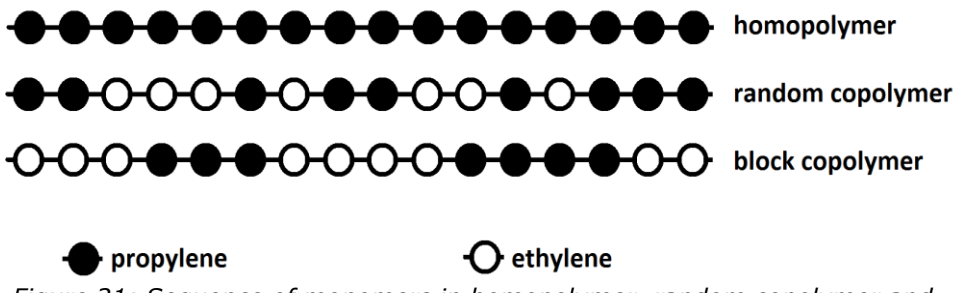


Figure 21: Sequence of monomers in homopolymer, random copolymer and block copolymer PP.

All three types can be used in packaging applications. PP is commonly used for its rigidity as a tray or cup, and as a seal material in topfilm for sealing these trays or cups. The high T_m , with ranges of 140-150 °C for random copolymer and 161-170 for homopolymer PP, can be beneficial if the package needs to be heat treated after sealing. If a lower seal temperature³⁸, higher transparency and flexibility is needed, random and terpolymer (copolymer with three different monomers) can be used. If high impact resistance and high flexibility at freezing conditions is desired block copolymers can be used, this is used in more complex heterophasic copolymers, often called impact copolymers. These impact copolymers have a

decreased T_g^{39} . Blends and multilayer structures can be made of homopolymer and copolymer(s) to combine properties to get a suitable material for the desired application.

A third differentiation is made between cast and oriented PP. Cast PP can be used as seal material while oriented PP is only used as substrate in flexible packaging, typically for snack packages⁴⁰.

2.2.3 Isotactic poly(1-butene)

PB is a polyolefin that is produced by the polymerisation of 1-butene. The structure is shown in Figure 22.

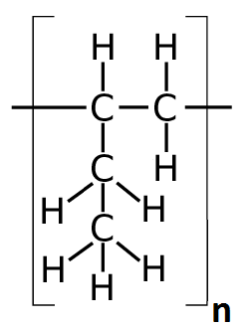


Figure 22: Poly(1-butene) structure.

PB is available as homopolymer and copolymer with ethylene or propylene. PB is well known as a peel component in easy-opening packages that peel cohesive^{41,, 42, 43}. It can be blended as peel component with PE, PP and ethylene comonomers such as poly(ethylene-co-vinylacetate) (EVA), poly(ethylene-co-methacrylic acid) (EMA) and ionomers^{44, 45}. By adding PB as small component to the PP seal matrix the seal initiation temperature can be decreased⁴³. The most common peel system in practice is the blend of PE and PB, both polymers are immiscible and PB is dispersed in low amounts (f.e. 15%) in a PE matrix. The amount of PB, the chemical composition of the used PB and PE grades, and the dispersion determine the peel performance of the overall film. PB is present as small islands in the PE matrix. These islands behave like small microperforations after sealing as PE and PB. This seal however is still hermetic and safe⁴⁶. Because of the weak spots a smooth cohesive peel failure is obtained during opening of the seal. The smoothly peeled white area is tamper evident.

2.2.4 Ethylene copolymers

Poly(ethylene-co-vinylacetate) (EVA)

EVA is produced by copolymerizing ethylene and vinylacetate. The structure is shown in Figure 23.

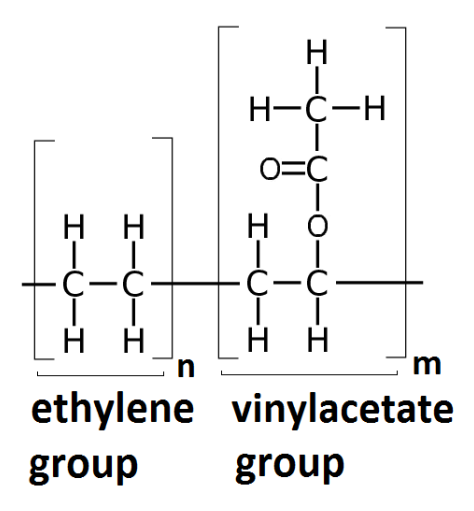


Figure 23: Poly(ethylene-co-vinyl acetate) structure.

This polymer can be differentiated by the amount of vinyl acetate. Polymers with low vinyl acetate level are referred to as vinyl acetate modified PE. With higher vinyl acetate levels (4 - 40%) the polymers are referred to as thermoplastic EVA. EVA can be used in seal layers, often it is added in seal layer blends with PE. In these blends, addition of EVA changes the seal (decreases the seal initiation temperature, broaden the seal plateau temperature range), mechanical (increase toughness), and/or optical (increase clarity and gloss) performance^{47, 48}. Besides the chain like entanglements that are characteristic for PE, EVA shows polar interactions that increases its strength properties slightly⁴⁹.

By blending EVA in PE, yield strength decreases gradually which has a negative impact on the seal strength. The high mobility of EVA in the blend leads to higher diffusion and better surface adhesion which can increase the seal strength. These counteracting phenomena are more or less pronounced, depending on the amount of EVA in the PE/EVA blend. Following Narjadeh's study, interdiffusion was more pronounced with 20 and 40% EVA which increases the seal strength. At 60% or higher the yield strength decreases significantly and this decreases the seal strength. Differences in seal strength of the tested PE/EVA blends with variating EVA content during the study were small, between 0.5 and 0.7 N.mm⁻¹. Differences in seal initiation and plateau temperature range were big. For seal initiation temperature for example, the values ranged between 75 and 110 °C for⁵⁰. EVA can also be blended with other polyolefins such as PP and PB.

Acrylic acid copolymers

Two common acrylic acid copolymers are poly(ethylene-co-acrylic acid) and poly(ethylene-co-methacrylic acid) (EAA and EMA). EEA is the copolymer of ethylene and acrylic acid. EMA is the copolymer of ethylene and methacrylic acid. In literature, this group of polymers is often referred to as acid copolymer resin (ACR). Both structures are shown in Figure 24.

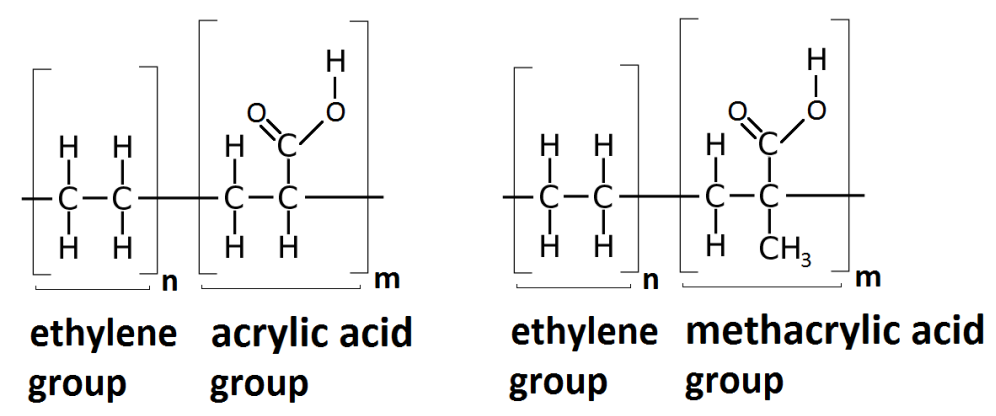


Figure 24: Poly(ethylene-co-acrylic acid) and poly(ethylene-co-methacrylic acid) structures.

Both copolymers are next to their uses in seal layers widely used as an adhesive in laminated structures such as pouches and tray/cup and topfilms because of the superior adhesion to polar substrates such as PET, aluminium, paper, etc.⁵¹ A differentiation with these types of polymers can be made by acrylic acid content and composition. EMA is the starting substance in the production process of ionomers, a material group that will be discussed in the next section. EAA and EMA have the ability to make hydrogen bonds which can enhance its strength properties⁴⁹.

Next to ethylene, styrene can be used as a copolymer in acrylic resins. This combination is often used in water soluble dispersions such as Joncryl® of BASF. It is commonly used as a heat seal lacquer in flexible packages $^{52,\ 53,\ 54.}$ Sealable lacquers can be an alternative to extruded seal layers. Heat seal lacquers are very thin, from 1-10 μm , this feature could be beneficial to improve recyclability of multimaterial structures. The peel seals of acrylic heat seal lacquers with aluminium substrates are typical examples of adhesive peeling, f.e. yoghurt cups with topfilm.

Ionomer

Ionomers are produced by adding metal ions to the poly(ethylene-co-methacrylic acid) structure. Sodium (Na) and Zinc (Zn) ions are used for packaging and industrial grades. The structure is shown in Figure 25. In industrial grades Magnesium (Mg), Lithium (Li) and Potassium (K) can be used as metal ions.

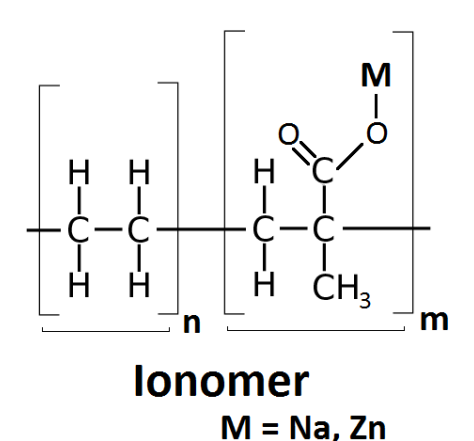


Figure 25: Ionomer.

The presence of positive ions partially neutralizes the acid groups in the polymer. Next to crystalline and amorphous regions this polymer also has ionic clusters as shown in Figure 26⁴⁰. The possibility to make ionic interactions adds up to its strength potential, besides hydrogen bonding and chain entanglement⁴⁹.

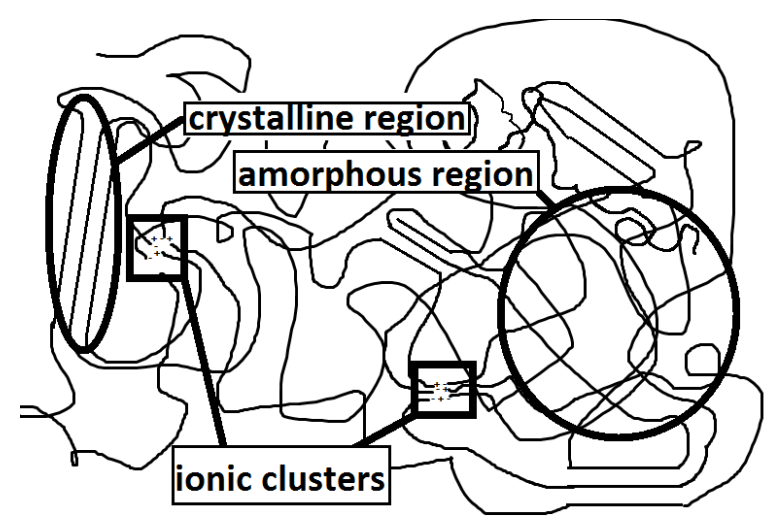


Figure 26: Schematic structure of regions in ionomers.

The crosslinks in these cluster are thermal reversible so it is still a thermoplastic polymer. The crosslinks restrict the chain mobility⁵⁵. The melt strength, which can be calculated after measuring the elongational load of molten polymer, is improved and the melt flow index is decreased as more ions are added. The high melt strength is related with the hot tack strength. Relative to other polyolefins, high hot tack strength values can be reached because of the high melt strength⁴⁰. A differentiation between ionomers can be made in acid content similar as with acrylic acid copolymers, in the amount of neutralization and in the type of metal ions. Ionomers can be blended with other polymers to reach the desired

functionality, for example in a blend with PB peelable ionomeric seal layers are obtained 42 . In technical papers, the seal performance (hot tack strength, seal-through-contamination), the oil and grease resistance, the puncture and abrasion resistance of ionomers are described as interesting features to implement ionomers in packaging 56 , 57 .

2.2.5 Poly(ethylene terephthalate)

PET is a polyester, it has a repeated sequence of a terephthalate and an ethylene group as shown in Figure 27. It is made in a polymerization process of dimethyl terephthalate (DMT) or terephtalic acid (TPA) for the terephthalate group and ethylene glycol (EG) for the ethylene group. For packaging it is a popular polymer because of its light weight, low cost, good appearance, mechanical and gas barrier properties. It was first developed in the 1940's. It is most famous as bottle material for carbonated drinks. PET is also used in sealable packaging concepts such as trays, cups and films⁴.

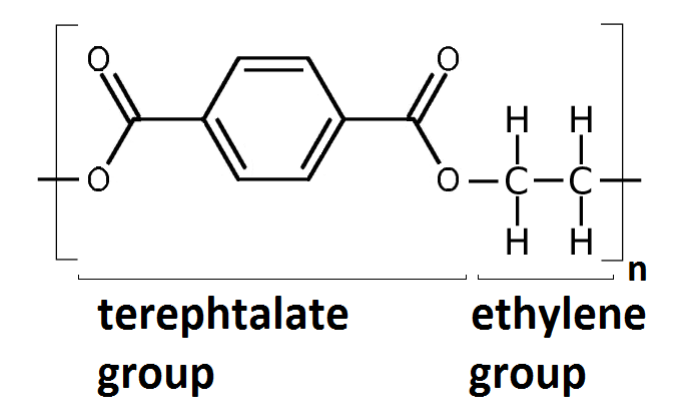


Figure 27: Poly(ethylene terephthalate) structure.

A differentiation is made between amorphous and crystalline PET (APET and CPET). The crystallization is influenced by structural factors such as molecular weight distribution, molecular weight, linearity of chain structure. A narrow molecular weight distribution, high molecular weight and linear chains are ideal to obtain high crystalline PET⁵⁸. Crystallinity is however also influenced by extrinsic factors such as temperature profile and stretching during production. The crystal growth rate decreases with increasing molecular weight⁵⁹. At equal extrinsic crystallization conditions high molecular weight samples can reach lower levels of (incomplete) crystals if crystallization time would not be sufficient because of the decreased growth rate.

Amorphous PET is more soft, flexible, high transparency, gloss and has higher impact strength, while CPET has more rigidity, higher temperature and solvent resistance, higher strength and hardness. They differ in T_g (approx. 67 °C for APET and 81 °C for CPET). APET is a material that is still ductile, at temperatures below its T_g , such as room temperature. This is a result of the production process. PET

sheets are directly after cast extrusion quenched against a cold roll to limit the crystallization process⁴⁰. APET is more often used in packaging concepts, such as bottles, films and trays. In films, APET is in competition with oriented polyamide, oriented poly(propylene) and machine-direction oriented poly(ethylene) as outer layer material⁶⁰. APET has poor heat sealability and is often laminated or coated with a seal material⁴⁰. As previously described, crystallinity is not desired during heat sealing because crystal structures prevent chains to participate in the diffusion and entangling process. It is not feasible to melt PET, allowing a polyolefin-like chain entanglement because of resulting brittleness and coloration. CPET is not able to seal because of its crystallinity. It is used for trays when a high temperature resistance is needed, such as in ovenable trays. Because of the crystal structure, CPET has no good transparency, it is opaque which is not desired by consumers. CPET can be coloured with pigments, in combination with the high gloss it can be made visually attractive⁴.

A second differentiation of PET can be made between homopolymers and copolymers or copolyesters. The homopolymer is made of one dibasic acid (DMT or TPA) and glycol component while the copolymers are made of more than on dibasic acid (DMT, TPA and/or isophtalic acid, ...) and/or glycol (EG, neopentyl glycol and/or cyclohexane dimethanol, ...) component. Isophtalic acid (IPA) f.e. can be used to lower the crystallinity and melting temperature which is important to increase the seal performance. IPA can also make the whole composition radiofrequency (RF) sealable (Radiofrequency sealing is previously discussed in detail in 2.1.3)⁶¹. When some of the ethylene glycol part is replaced by 1,4-cyclohexane dimethanol (CHDM) the resulting polymer is referred to as poly(ethylene glycol-co-1,4-cyclohexanedimethanol terephthalate) (PETG). CHDM inhibits crystallization. PETG is an amorphous copolyester and is not likely to become brittle by heating which makes it interesting in heating processes such as heat sealing. It is much softer and has excellent oil resistance⁴⁰.

As previously mentioned PET is not melted when sealed. It is sealed by the principle of autohesion 62 . PET has to be heated above glass transition temperature to diffuse and to entangle the polymer chains at the interface. Because sealing occurs well below T_m PET does not behave low viscous like polyolefins during sealing. PET seal layers are less caulkable as polyolefins, making it less suited for pouches because it is not possible to fill up any gaps close to folded areas. The stiff PET behaviour during sealing is also undesirable to seal-through-contamination. However, soft amorphous seal layers (f.e. PETG) can be used to increase caulkability.

PET is often in competition with PP for tray and topfilm packaging concepts. Several properties (mechanical properties, thermal resistance, migration, cost, visual appearance, seal performance, recyclability, weight, etc.) have to be evaluated in relation with the application to choose the optimal material.

2.2.6 Biobased and biodegradable plastics

Bioplastics can be biobased and/or biodegradable (f.e. composting, anaerobic digestion). Biobased plastics are made from renewable resources. Biodegradable plastics can be degraded into environmentally acceptable products. In this section some biodegradable plastics are discussed. Biobased plastics that can't

biodegrade, such as bioPE, bioPET and poly(ethylene furanoate) (PEF), are not mentioned because these materials have mostly equal properties as their petrochemical counterparts, that were discussed earlier in this dissertation or because of the lack of relevance for heat sealing applications in the food industry. Biodegradable plastics that are not biobased, such as poly(caprolactone) (PCL) and poly(butylene-adipate-co-terephthalate) (PBAT), will only briefly be mentioned as minor components in biodegradable food packaging for heat seal applications.

The amount of studies on the sealability of biobased and biodegradable plastics is rather limited. In this section four commercially available biobased polymer types are discussed with focus on heat sealability: poly(lactic acid) (PLA), starch, polyhydroxyalkanoates (PHA) and poly(butylene succinate) (PBS).

PLA

Polylactic acid is a semicrystalline biodegradable polyester that can be produced from renewable resources. It can be produced by condensation of lactic acid and lactide. The structure is shown in Figure 28.

Figure 28: Poly(lactic acid) structure.

PLA is a transparent material with a T_m of 170 °C and a T_g of 60 °C. It is a strong and stiff material. PLA has a low melt strength because of its highly linear structure, which makes it not suited for blow extrusion. Without modification PLA is a very brittle material. These weaknesses can be overcome by blending with other polymers (such as PBAT) and/or adding additives.

In recent studies the influence of composition of PLA-PBAT blended film with and without chain extenders on the heat conductive seal strength was evaluated. The highest seal strength was reached with a blend of PLA-PBAT and chain extender in a 40-60-0.15 proportion 63 . In another study seal strengths of 8-10N/15mm at a broad range of interfacial seal temperatures between 76 and 105 °C and low haze (<4%) were reached with PLA-PBAT blended film in a proportion of 80-20 64 . The ultrasonic seal performance of plasticized PLA films was evaluated in another study 65 . In that study high molecular weight poly(ethylene glycol-co-1,4-cyclohexanedimethanol terephthalate) (PETG) was used as plasticizer to decrease the overall brittleness. The films were produced by cast extrusion to a thickness of 50 μ m. All films, with and without plasticizer, were sealable with ultrasonic technology. The addition of plasticizer improved the seal performance because the process windows of seal parameter was broader. In a last study the impulse and ultrasonic seal performance of PLA films was evaluated 66 .

It can be concluded that with the limited available research on the seal performance of PLA, films weaknesses can be overcome by blending with other

materials. Peel and non-peel seals can be produced and several technologies (heat conduction, ultrasonic, impulse) can be used to heat seal this material. PLA is currently used as an emerging seal material in many applications, the trend is positive as there is a growing demand for flexible bioplastic packaging⁶⁷.

Starch

Starch is a semicrystalline biodegradable polymer that can be produced from renewable sources. Starch-based films have an amylose and amylopectin fraction. Increasing amylose content improves the crystallinity and the mechanical and barrier properties. This is because of the morphology and interchain bonds between the molecules. Amylose is a linear long chain with interchain hydrogen bonds, this results in a more dense and stronger structure. Films with higher content of amylopectin are less crystalline because of the branched structure, caused by additional a-1,6-glycosidic bonds, and the smaller amylopectin chains⁶⁸. Both structures are shown in Figure 29.

Figure 29: Amylose and amylopectin structures.

In a recent study mung bean starch is used as film material along with plasticizer (glycerol or sorbitol). Seal strengths around 0.4 N.mm⁻¹ can be reached⁶⁹. In the discussion of the seal strengths this result is higher than recorded in previous seal studies with starch^{70, 71}. This seal strength is sufficient for handling and storage during practical applications. With an amylose/amylopectin ration of 41:59 mung bean starch is considered as rich in amylose compared to other starch sources. The tensile strength of the evaluated films was of a similar order as LDPE, HDPE, PP and PS. In another study seal strength of edible films with corn starch and functional polysaccharides (amylose or hydroxypropylmethylcellullose) were evaluated. In this study seal strengths around 0.4 N.mm⁻¹ can be reached⁷². In another study several types of starch with and without nanoparticles (nanoclay, nano-silicon dioxide) and plasticizer (sorbitol and glycerol) are compared. Addition of nanoparticles can increase the seal strength, but this was not the case for every type of starch. Without nanoparticles maximum seal strengths around 0.5 N.mm⁻¹ were reached with sago and potato starch. In this study the films with mungbean starch had very low seal strengths⁷³. These studies show the potential of the use of starch as emerging seal layer. With the high amount of potential renewable starch sources and possibilities to optimize films by blending, the addition of nanoparticles, plasticizers and others, high performing films can be obtained depending the purpose of use, such as heat sealability.

Polyhydroxyalkanoates (PHA)

Polyhydroxyalkanoates are a family of thermoplastic polyesters that can be produced and degraded by a wide range of microorganism species. The properties of PHA's range from brittle wax-like to plastic behaviour, and are related with the chemical structure. Figure 30 shows the general structure of PHA's. Table 4 shows the chemical composition, based on Figure 30, of the PHA's considered in food packaging. Poly(hydroxybutyrate) (PHB) for example is a highly crystalline (up to 70%) and stiff, but brittle, polymer with high melting temperature (175 °C). Copolymerisation and the presence of long side chains can disrupt the crystal structure and decrease melting temperature and Young's modulus. Poly(3-hydroxybutyrate-co-3-hydroxyvalerate) (PHBH) and poly(3-hydroxybutyrate-co-3-hydroxyhexanoate) (PHBHHx) are promising copolymers with lower melt temperatures, down to 97 °C in the case of PHBH, and Young's moduli⁷⁴.

$$\begin{bmatrix} R_1 & H & O & R_2 & H & O \\ I & I & II & O & I \\ ---O & C & C & C & C & C & C \\ H & H & H & X & H & H & X \end{bmatrix}_{x}$$

Figure 30: Polyhydroxyalkanoate structure.

Table 4: Chemical composition of polyhydroxyalkanoates considered in food packaging.

	R1	R2	X
PHB	-CH3	-CH3	1
PHV	-CH2-CH3	-CH2-CH3	1
PHBV	-CH3	-CH2-CH3	1
PHHx	-CH2-CH2-CH3	-CH2-CH2-CH3	1
PHBHHx	-CH3	- CH2-CH2-CH3	1

Seal research on PHA's is very rare. One study of Kuusipalo showed that the seal initiation temperature of extrusion coated paper with 3-hydroxybutyrate/ 3-hydroxyvalerate copolymer was 40 to 50 °C higher, compared to polyolefins. This corresponds closely with the difference in melting temperatures. Heat sealing can be achieved in a temperature window between 190 °C and 230 °C, at a seal pressure of 275 kPa and a seal time between $1-2~\rm s^{75}$.

Poly(butylene succinate) (PBS)

PBS is a synthetic and biodegradable polyester. Depending on the resources of monomers it can be fossil and/or biobased. The structure is shown in Figure 31.

Figure 31: Poly(butylene succinate) structure.

Because of the long alkyl chains PBS is rather soft. It has a melting temperature around 110-115 °C and a tensile strength of 30-35 MPa. These properties are comparable with polyolefins and thus this material can be seen as a biobased and biodegradable alternative^{76,77}. The same machinery can be considered for monofilament extrusion, blown extrusion and injection molding as for conventional thermoplasts⁷⁸. Because of food contact approval and good sealability this material could be used as seal material at the inner side of food packaging. However, at this moment there are no studies available on the seal performance of PBS packaging films. Properties can be modified by blending, adding fillers and copolymerization, among others ^{79,80,81} and ⁸².

Cellulose

Cellulose is the main polymer that can be found in the cell wall of plants. So, it is a natural occurring polymer which is abundantly present on earth. It can be obtained by extraction processes of plants, food waste, micro-organisms, etc. It is used in food packaging as a structural component because of its low cost, thermal resistance, mechanical potential and biodegradability83. Cellulose is however very brittle, not sealable and moisture sensitive in its natural state. It is modified to use in food packaging, to increase processability and mechanical, gas/liquid/microbial barrier and/or optical properties. Cellophane is the most commonly used cellulose-based packaging film. It was invented in 1900. 84 It is produced by a complex process, dissolving pulp in alkali and disulphide, forming a viscose solution. This is followed by extrusion in a bath of chemicals to reconvert viscose back to cellulose, with the aim of producing flexible film. Before the rise of fossil thermoplastics, cellophane was the first plastic-like film that was allowed for mass-production for food packaging⁴⁰. Cellulose acetate, cellulose sulphate. cellulose nitrate, carboxymethyl cellulose, ethyl cellulose, methyl cellulose and nanocellulose are cellulose derivatives that are subjects of new studies for food packaging applications⁸³.

Composed materials

Increasing the seal performance is one of many motivations (e.g. barrier performance, packaging line compliance) to combine different materials. Two processes can be differentiated: blending and multilayering.

The option to blend thermoplastic materials to tailor the performance is already mentioned in 2.2 for most of the materials. Also, biodegradable thermoplastic materials can be combined in a blend. In recent reviews and studies on optimizing this process for compostable materials, blends of poly(lactic acid) (PLA) and PHB⁸⁵, PLA and PBS⁷⁹, PLA and polycaprolactone (PCL)⁵⁰, PLA and/or PCL and/or thermoplastic starch (TPS)⁸⁶, starch and vinyl alcohol polymers⁸⁷, among others are hot topics, relevant for food packaging. Information in literature on seal performance of biodegradable blends is rare. A 2014 study showed that the hot

tack strength of blends of PLA and PCL increases slightly, up to a value around 0.45 N.mm $^{-1}$, compared to pure PLA, which reaches a value around 0.3 N.mm $^{-1}$. Seal initiation temperatures of blends with PLA and PCL decreases, with values between 65-75 °C, compared to pure PLA, with a value of 85 °C. Both results underline the relevance of blending to increase the seal performance of biodegradable polymers. When the seal is cooled down, differences in seal strength are close to 0^{50} .

If blending of materials is not feasible and/or if the process demands multilayered films, e.g. to prevent the film from sticking to hot tools or to add a heat sealable feature to emerging substrates that are not heat sealable, lamination and/or coating of films can be a solution to combine properties. Common examples of biodegradable substrates are cellulose and paper. Coating and/or laminating cellulose or paper with compostable materials can maintain the compostable feature of packaging. In a recent review, polysaccharides (from wood and lignocellulosic plants: cellulose, hemicellulose, starch; from marine biomass: chitosan, alginates) are subject as coating for paper packaging⁸⁸.

2.2.7 Coated paper

Adding a thin thermoplastic layer in general can maintain the recyclability in the paper waste stream while the packaging performance is increased⁸⁹. Heat seal performance is only one of many motivations, besides barrier and mechanical performance among others, to add thermoplastic material to substrates. There are few studies available, reporting specifically about the heat seal performance of coated paper.

In Andersson's study, seal performance of dispersion-coated papers is evaluated with seal stength experiments to check the influence of calendering, neutralizing solvents and drying intensity. Calendering is evaluated as treatment, NH_3 and NaOH are evaluated as neutralizing solvents, and 10 and 45% are two infrared powers that are evaluated for drying intensity. Fibre tear is regarded as optimal seal failure mechanism. Seals of materials that are neutralized with NH_3 are stronger than those neutralized with NaOH. There is no clear effect of calendering and drying intensity on the strain energy. The amount of exposed fibre is used to assess the seal quality, where 100~% fibre is regarded as optimal seal failure mechanism. NH_3 -treated samples show a higher degree of exposed fibre. There is no clear effect of infrared drying. Calendering increases the area of exposed fibres only when NaOH is used to neutralize the material. These effects are related with rigid salt shell formations, impairing adhesion⁹⁰.

Hauptman et al. studied the heat seal performance of papers that are dispersion coated with a thin acrylic copolymer seal layer to comply with automatic seal machines. The increase of seal time and seal pressure improves the hot tack performance because of an improvement in heat transfer. Higher moisture content improves the seal performance by reduced seal initiation temperatures and increased strength values. In real production environments, where seal time is kept as low as possible to achieve high production rates, seal pressure and humidity are the most important factors to be adjusted towards each other. A thorough control of climate conditions is required in a reliable heat-sealing process⁹¹.

Merabtene et al. studied the compliance of PE coated papers for automatic seal machines. Papers turn brown at temperatures higher than the end of the plateau region (200-220 °C). Seal pressure is varied between 3 and 5.5 bar to check the influence on seal strength, but seal strength does not change within this range. High grammage paper (120 g.m⁻²) achieves higher seal strength than low grammage paper (85 g.m⁻²). This was attributed by the authors to more interdiffusion at the thicker PE seal layer. Several issues are described on the runnability of the papers on automatic seal machines, such as buckling of the film, caused by misalignment and web tensioning, undesired cutting by the forming shoulder, wrinkling of the bag surface, heat generation by frictional force in the forming tube. Further studies are needed to gain more understanding and develop solutions for these issues⁹².

Tuominen et al. studied the influence of flame treatment, a surface treatment to increase wettability and thus to improve printing and coating properties, on seal and hot tack performance. The coated paper is produced by extrusion coating of LDPE on an 83 g.m⁻² paper. Equivalence ratio, which is the air-propane ratio, and line speed are varied for flame treatment, and temperature is varied for sealing. High equivalence ratios, with relative high propane content, decreased hot and cold tack performance by increasing initiation temperatures and thus narrowing hot and cold tack temperature windows. Cross-linking of top molecule layers, caused by high surface temperatures and the lack of oxygen, is suggested as cause of the decreased performance. Seal performance is increased, with lower seal initiation temperatures and thus wider hot and cold tack windows, if lower equivalence ratios are used. A decrease of surface temperature and the increase of oxygen causes a decrease of surface molecular weight, leading to increased chain mobility and interdiffusion across the seal interface⁹³.

Kuusipalo et al. studied hot tack performance of several paper grades with different grammages $(70 \rightarrow 275 \text{ g/m}^2)$, extrusion coated with 3-hydroxybutyrate/3-hydroxyvalerate copolymer and compared with LDPE and ionomer coated papers. Initiation temperatures of PHB/V coated papers are higher, compared to reference films. Longer cool times increase hot tack forces, at fixed values for seal temperature of 135 °C, seal pressure of 0.6-0.8 N/m² and seal time of 0.5 s. For seal time, hot tack forces increase with higher seal times, at fixed values for seal temperature of 135 °C, seal pressure of 0.6-0.8 N/m² and cool time of 1.0 – 1.6 s. The trend for seal pressure is unclear: in some cases, seal pressure increases hot tack forces, in other cases hot tack forces remain constant 94 .

Rhim evaluated seal strength of PLA-coated papers, produced with solution coating and thermocompression and used PE-coated paper as a reference. There is no significant difference in the seal strength of the two PLA-coated papers. The seal strengths of both PLA-coated papers were 2.3 times higher than the PE-coated paper⁹⁵. In a similar study of the same author, the influence of different PLA concentrations on sealstrength strength is compared with solution casted coated papers. Seal strength increases linearly at higher PLA concentration until a plateau value is reached. This can be explained with the increasing coating thickness that is measured during that study at increasing PLA concentrations. Coating thickness also increases linearly with PLA concentration up to a PLA concentration of 4 %. This dependence of coating weight and thickness on the concentration of coating solution is also found in previous studies⁹⁶.

The heat seal performance of PLA coated paper was also the subject of publications of other authors around that time. Lahtinen et al. studied the influence of post-production heat-treatment on the heat seal performance of PLA extrusion coated paper. This is relevant because heat treatment between 100 and 150 °C can alter the polymer matrix to form a better water vapor barrier. Heat treatments between 100-130 °C with long duration times increase crystallinity, thus higher seal temperatures are needed to produce an optimal seal. The PLA remains amorphous after heat-treatments of 140-150 °C but reorder in a less permeable form. At these treatment temperatures, seal temperatures are only slightly elevated, compared to untreated PLA. Heat treatment between 140-150 °C is better suited for high-speed operations because of the decreased water vapor transmission rate and the reduced impact on the seal temperature, compared to heat treatments between 100-130 °C⁹⁷.

Tai et al. evaluated heat sealability of PLA solvent coated papers. Nine different coating solutions are used, with chloroform as main solvent. Ethanol, N-propanol, PEG and PCL are added in some solutions. All solvents are varied while PLA is present in a fixed amount. There is no big difference in load values between samples. Further research is needed for a better understanding of these results⁹⁸.

In a study of edible coated paper of Shao et al., heat seal performance is evaluated. A 140-190 μ m thick paper of celery fibres is made and spray coated with soy protein. The optimal seal strength is achieved at seal temperatures of 110-130 °C and a seal time of 5-7 s. The strength increases from 0.114 to 0.161 N.mm⁻¹ with the increase of soy protein concentration from 10 to 13.75%. The sealing properties were attributed to the viscoelastic features of soy protein⁹⁹.

2.2.8 Additives

Small amounts of organic or inorganic molecules are added to the polymer matrix to tailor the properties of polymers. Stabilizers, modifiers, such as pigments, opacifiers, slip agents, antiblock, chill roll release, lubricants, plasticizers, antistats, process aids, nucleating agents, clarifying agents, antifog, tackifiers and tougheners, and fillers can be differentiated⁴⁰.

Tackifiers can change the viscoelasticity of the seal polymer and thus impact seal performance. Plasticizers, can aid diffusion by increasing the mobility of rigid polymer chains, but can also act as lubricants by increasing intermolecular slippage and thus decrease adhesion. Slip agents, like fatty acid amides, bloom to the surface, where sealing occurs, and can interfere sealing if too much is used. Lubricants and processing aids, like silicon oils, can interfere as well by contaminating the seal interface⁴⁹.

There are few studies available on the influence of additives on seal performance with quantitative date.

The impact of plasticizers is previously described to increase the ultrasonic seal performance of PLA by broadening the process window. The minimum amplitude to seal decreased from 18 to 13 μ m by adding PETG plasticizer, compared to pure PLA, while the maximum amplitude is 32 μ m for plasticized and pure PLA ⁶⁵. Sancaktar's study evaluated the influence of different fillers, such as calcium carbonate, talc, mica and glass fibre, on the ultrasonic weld performance of PP. Samples are injection moulded through a screw of 24 mm. This deviates from the

thin packaging, described above, but gives a first indication on the influence of fillers on seal performance. Weld strength, expressed in N.mm⁻², and elongation decreased by adding filler and by increasing the filler concentration. This is attributed to the prevention of PP bonding. At extreme filler concentrations of 40%, maximum weld strength decreased to 18, 10 and 6 N.mm⁻² for calcium carbonate, mica and talc, while unfilled PP achieve 23 N.mm⁻²¹⁰⁰.

With the potential impact on surface chemistry, crystallinity, among other aspects, additives can impact seal performance. This is uncharted territory in open literature.

2.2.9 Comparison of seal, mechanical and economic data

Seal, mechanical and economic data of most of the above described polymer types are summarized in Table 5. Seal data of common fossil-based and biodegradable seal materials are compared qualitatively with *- and \$\infty\$-symbols, because of the lack of comparable data with absolute numbers. With the use of different multi-layered structures, thicknesses, peel and non-peel films, a quantitative comparison, reduced to the influence of seal materials is not possible, especially in relation with different seal technologies, where multilayer film design is crucial for technology compatibility. Only materials with identical symbols can be compared on seal performance. Below the quality score, a brief explanation is given. More details can be found in the description of these polymers in the beginning of the chapter. Some of the results of chapter 6 are already added to complete the table. No explanation is given on the seal performance of PLA and PBS because of the lack of supporting background information, such as melting temperatures, melt strength, crystallinity of the specific films that were used in chapter 6.

Besides seal performance, mechanical performance and economic data is given to highlight differences in polymers that were previously described. Density is of economic importance because of the increased cost, expressed in €.kg⁻¹, of heavy weight packaging materials. Production volume indicators are given by fractions of the global virgin plastic production for non-biodegradable plastics and by production capacities for biodegradable plastics. The numbers for non-biodegradable plastics are underestimations of real production volumes because of the exclusion of recycled plastics. The numbers for biodegradable plastics are overestimations of real production volumes because of the use of production capacity. However, with few available numbers on production volumes, the values in this table give an indication of production volumes, taking in mind the above described bias.

Cells are empty if relevant comparable data is missing in literature.

Table 5: Qualitative comparison of seal performance (* or \diamond), underlying causes ($\stackrel{\triangle}{\oplus}$ or $\stackrel{\Box}{\heartsuit}$), mechanical performance and economic data of plastics.

		PI	<u> </u>		
		LDPE	LLDPE	mLLDPE	HDPE
Function (Seal and/or		Both	Both	Primarily seal	Structural
structural component)				,	
Relative seal performance (a higher number of symbols indicates a better performance for that attribute)	Low seal initiation temperature	*** T _m ≈ 110 °C	* T _m > 120 °C	***** T _m ≤ 110 °C	
	Ultimate seal strength	*** ¶ Small and long chains + high crystallinity	***** Long linear chains, high crystallinity **	***** Long linear chains, high crystallinity *****	
	Peak hot tack strength	♥ Small chains at surface, ♥ long chain branches ♥ Low melt strength △ high crystallization	♥ Small chains at surface, ♣ no long ♥ Low melt strength chain branches ♣ high crystallization	△ Long linear chains at surface, △ no long chain branches ♥ Low melt strength △ high crystallization	
	Hot tack temperature window Seal-through- contamination	* \$\varthit{\textstrength}\$ ** \$\varthit{\textstrength}\$ Low hot tack performance	** \$\varphi\$ Low melt strength ** \$\varphi\$ Low hot tack performance \$\varphi\$ High seal initiation temperature	* Use the strength to tack performance Low seal initiation temperature	
Mechanical	Tensile strength at break (MD) ASTM D882 (N.mm ⁻²)	26	50	53	80
performance	Elongation at break (MD) ASTM D882 (%)	130	570	500	420
Density - ASTM D792 (g.cm ⁻³)		0.92-0.93	0.91-0.93	0.91-0.93	0.96
Price in Europe mid-2022		1.91 (film)	1.72		1.82 (film)
(€.kg ⁻¹) Production volume indicator (million tonnes)		(standard) 64 (all low dense PE grades) (% Converters plastic demand EU27+3 *Global production virgin plastics '20)			47 (% Converters plastic demand EU27+3 *Global production virgin plastics '20)
References		40, 49, 101, 102.	40, 49, 101, 102.	40, 49, 102.	40, 101, 102.

Other polyolefins						
		cPP	oPP	EVA	ACR	Ionomer
Function (Seal and/or structural component)		Both	Both	Both	Only seal	Only seal
	Low seal			****	****	****
	initiation temperature			T _m ≤ 60 °C	T _m ≤ 100 °C	T _m ≤ 100 °C
	Ultimate seal			***	***	***
Relative seal performance (a higher number of symbols indicates a better	strength			□ Low crystallinity, △ polar interactions	□ Low crystallinity ↑ hydrogen bonding	□ Low crystallinity △ hydrogen bonding, △ ionic interactions
	Peak hot tack strength			*	*** long chain branches High melt strength Chain entanglement low crystallization	**** long chain branches High melt strength Chain entanglement low crystallization
performance for that attribute)	Hot tack temperature window			* Use Low melt strength	**** ## High melt strength	***** High melt strength
attribute)	Seal-through- contamination			** \$\varphi\$ Low hot tack performance \$\triangle \text{Low seal initiation} temperature	**** Good hot tack performance Low seal initiation temperature	***** Good hot tack performance Low seal initiation temperature High oil and grease resistance
Mechanical	Tensile strength at break (MD) ASTM D882 (N.mm ⁻²)	45	140	31		24-37
performance	Elongation at break (MD) ASTM D882 (%)	650	180	530		300-500
ASTN	Density ASTM D792 (g.cm ⁻³)		0.9	0.94	0.93 (EAA)	0.95
Price in Europe mid-2022 (€.kg ⁻¹)		1.87 (PP	homo)	5.4		
Production volume indicator (million tonnes)		(% Complex Com	P grades) onverters demand *Global on virgin (20)			
References		40, 101, 102.	40, 101, 102.	40, 49, 103.	49, 104.	40, 49.

		Ot	her plasti	cs		
		PET	PA 6	PLA	PBS	Cellulose
Function (Seal and/or structural component)		Primarily structure	Only structure	Both	Both	Only structure
Relative seal	Low seal initiation temperature			****	***	
performanc e	Ultimate seal strength			*	\\\\	
(a higher number of	Peak hot tack strength			♦ ♦	**	
symbols indicates a better	Hot tack temperature window			***	♦ ♦	
performanc e for that attribute)	Seal- through- contaminatio n					
Mechanical performanc e	Tensile strength at break (MD) (N.mm ⁻²)	200 (ASTM D882)	90-120 (ASTM D882)	69 (ISO 4593)	57 (ISO 4593)	125 (ISO 4593)
	Elongation at break (MD) ASTM D882 (%)	1116	300-900	147 (ISO 4593)	443 (ISO 4593)	21 (ISO 4593)
Density ASTM D792 (g.cm ⁻³)		1.39	1.15	1.24	1.23-1.26	1.6 (nanocellulose)
	ope mid-2022 kg ⁻¹)	1.78 (bottle)	3.84			
Production volume indicator (million tonnes)		31 (% Converter s plastic demand EU27+3 *Global production virgin plastics '20)	6 (% Converter s plastic demand EU27+3 *Global production virgin plastics '20)	0.46 (Global productio n capacity '21)	0.08 (Global productio n capacity '21)	0.08 (Global production capacity '21)
References		40, 101, 102.	40, 101, 102.	40, 105, 106.	105, 106, 107.	83 , 105, 106.

2.3 Seal performance evaluation

Before describing the need of a design-of experiments approach it is important to give more details on the different options to evaluate seal performance, previously introduced in 1.4. This section focusses on these tests and describes on-site methods and process controls to give the main current options to evaluate seal performance.

2.3.1 Seal Strength

Seal strength is defined as the force per unit width of seal, required to separate flexible material from rigid material or flexible material, under the conditions of the test. It can be expressed in different units, such as N.m⁻¹, N.mm⁻¹, lbf.in.⁻¹, Gmf.in.-1. The seal strength test is carried out on samples with specified width, 15, 25 or 25.4 mm¹⁰⁸. Samples that need to be compared on other aspects as orientation must be cut in one orientation. ASTM F2029 describes how samples can be prepared in the lab¹⁰⁹. For seal strength, often wide samples are sealed. After sealing, a strip is cut for strength testing. Seal parameters, such as bar temperature, seal time and seal pressure, can be varied to test the influence of each of these parameters on the seal strength. Seal parameters can be tested in ranges that are relevant for the studied industrial process. Bar temperature is set at the same value for both bars unless only one bar is heated in the industrial process that is studied, f.e. topfilm-tray seals. The making of heat seals in ASTM F2029 is described as an appropriate method for quality control in manufacturing sealed films. Seal strength, described in ASTM F88, is a quantitative measure for use in process, validation, process control, and capability.

Besides lab made seals, seals can be cut in industrial sealed packages as well. Once the seal is made, in a lab (ASTM F2029) or industrial environment, it can be tested with a universal testing machine. The seal strength test evaluates seals after cooling down and storage for a specified time. When seals are tested shortly (milliseconds, seconds) after sealing hot tack strength is tested instead of seal strength. A storage time of 40 h or higher must be used if information on the stability of heat seal strength is absent. Shorter and longer cool times, that could be relevant to evaluate ageing of the seal, are possible but must be reported 108. Tests are carried out in a standard atmosphere of 23 °C and 50 %, as described in ISO 291¹¹⁰. Test conditions can be varied for specific test objectives. Each leg of the sealed sample is clamped, the ASTM standard recommends a clamp distance of 10 or 25 mm for respectively high and less extendable materials. The tail of the legs can be supported or unsupported. In many cases, a T-peel test is carried out to determine the seal strength. In this test, samples are tested in a 180° angle. Figure 32 shows the different tail holding methods of the ASTM F88 standard.

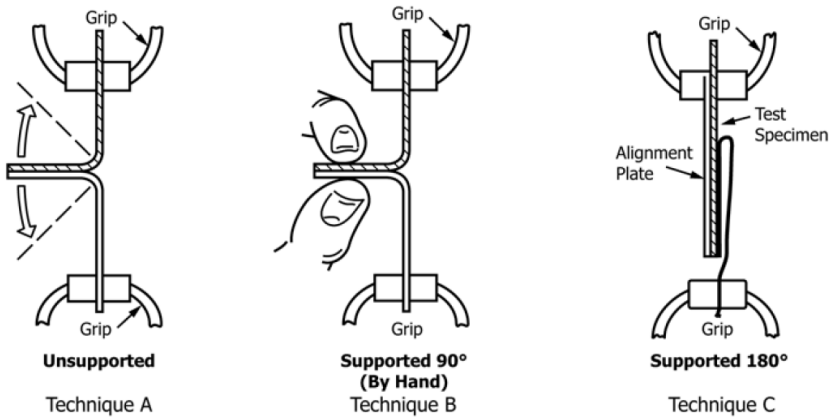


Figure 32: Tail holding methods 108.

It is also possible to change the angle f.e. to simulate the opening process by the end consumer. The opening of a sealed pouch and tray is illustrated in Figure 33.

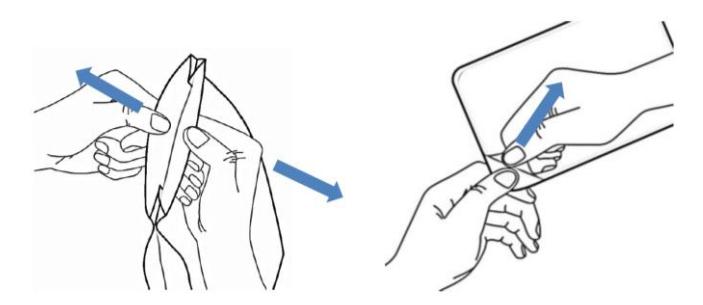


Figure 33: Opening of different packaging concepts by end consumer (left: pouch, right: topfilm and tray) 111 .

Lower test angles tend to increase seal strength of peelable samples 112 . The speed of testing is set at 200 or 300 mm/min. High test speeds tend to increase seal strength of peelable samples 113 . Force and displacement are registered during the test; seal strength is calculated by dividing force with seal width.

To compare the results of several samples to check the influence of one or more factors there are several numerical values that can be used from the seal strength-displacement curve. Maximum seal strength is most often used to compare samples, there is no further interpretation needed in determining a maximum value. Specific peak values, such as the begin and end peaks in a seal strength test of burst peel concepts, can be reported. Average seal strength, which is the average value of a specified region in the seal strength-displacement curve, can be reported for peelable concepts. It describes the average strength which is needed to peel a seal after the opening peak and before the ending peak. Seal energy, which is the work that is needed to open the seal and which is represented by the area under the seal strength-displacement curve, can be reported as well. Seal strength results are expressed in N.mm⁻¹, in some reports and papers the

width of the sample is shown in the unit, f.e. N/15mm. It is necessary to report the width of the sample when only forces are shown. Seal energy can be expressed in J or in J/mm, J/15mm, etc...

Seal strength results of samples with a variation in one seal parameter and/or in one material parameter can be easily compared in a two-dimensional graph. These graphs types are most often shown in seal research papers. An example is given in Figure 34, the average values and standard deviations of the maximum seal strength are shown. The material composition of the thin layer at the seal surface and bar temperature are varied to study their influence on the maximum seal strength. With both materials, maximum seal strength starts to rise quickly from the baseline at a certain temperature. This temperature is referred to as **seal initiation temperature**. The threshold value of 0.05 N.mm⁻¹ indicates seal initiation¹¹⁴. After the seal initiation temperature, there is a steep slope until a plateau value is reached. There is also an end of the plateau, this is not visible at the figure below because bar temperature must be increased to higher values to visualize the end of the plateau region.

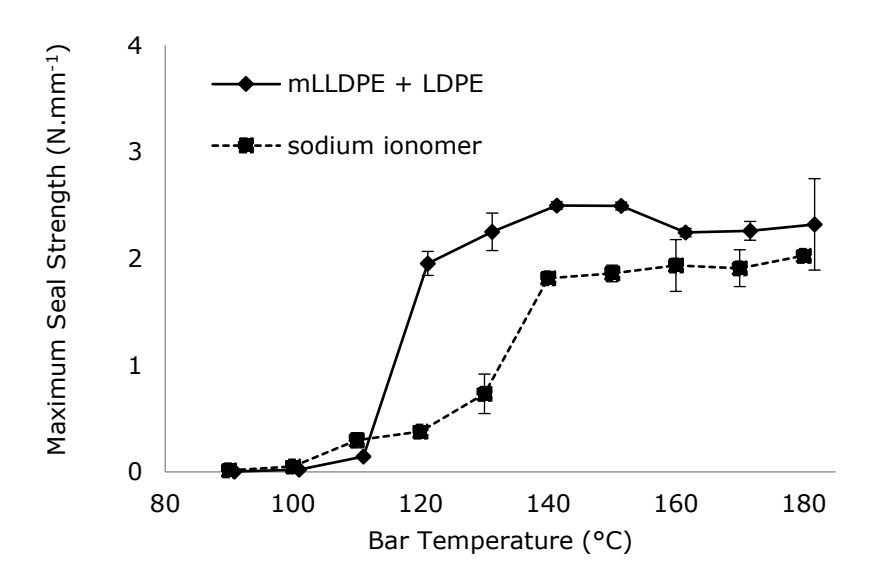


Figure 34: Influence of bar temperature and seal layer composition on the maximum seal strength of two PET/PE 12/50 flowpack films, sealed at 1.0 s and 1.0 N.mm^{-1} , n=3.

Besides calculating seal strength, different failure modes can be observed. The ASTM F88F88M-15 standard¹⁰⁸ suggests a classification of failure modes in two categories: seal separation modes and interferences. The seal can be separated by adhesive peel, cohesive peel and delamination as show in Figure 35.

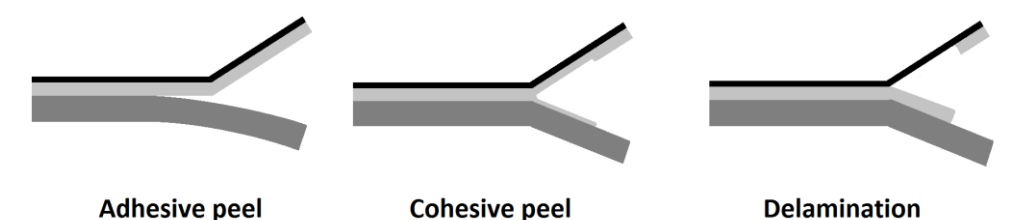


Figure 35: Seal separation modes (black: outer layer topfilm, light grey: seal layer topfilm, dark grey: bottomweb).

An example of cohesive peel failure, as a result of blending PB and PP, as previously described, is shown in Figure 36.

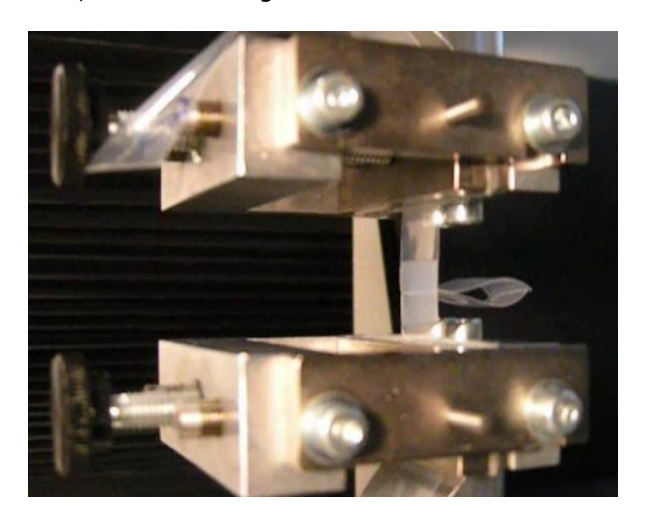


Figure 36: Cohesive peel failure during seal strength test.

One or both films can be interfered by material break at the seal or at remote material as shown in Figure 37.



Figure 37: Interference by material break (black: outer layer topfilm, light grey: seal layer topfilm, dark grey: bottomweb).

Elongation of material and peel with elongation are included in the standard as interfering mechanisms. These seal failure mechanisms are visually determined.

There are other standards available to evaluate seal strength.

ASTM F2824 describes a test method to evaluate the seal strength of round cups with flexible topfilm¹¹⁵. The whole seal area is examined. The test can also be used on rectangular trays and is suitable to test the following packed products: ready meals, creamers, coffee, yoghurt, etc. A constant peel angle can be maintained by a movable sled, as shown in Figure 38.

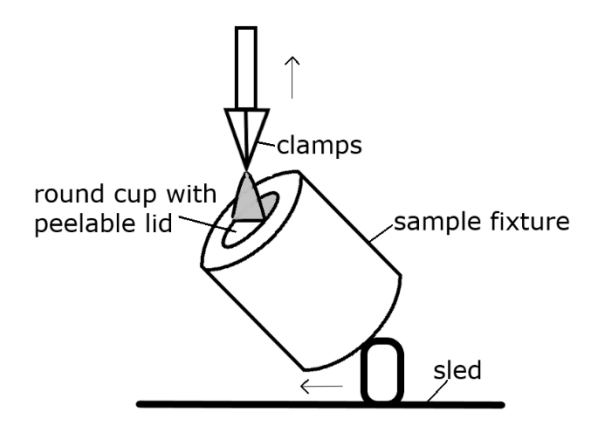


Figure 38: Peel test of round cup and top lid at constant peel angle.

ASTM F1140 describes a test method to evaluate the burst pressure of a package¹¹⁶. In a burst test, the pressure increases until the package fails. The package will fail at the weak spot which is the seal area in many cases.

ASTM F2054 describes the burst test with restraining plates¹¹⁷. By using these plates, material stretching and deformations are minimized and the load will apply more directly on the seal area. A higher burst strength will be reached with restraining plates compared to unrestrained tests. The lower the gap between the plates, the higher the burst strength will be. A schematic of the setup is shown in Figure 39.

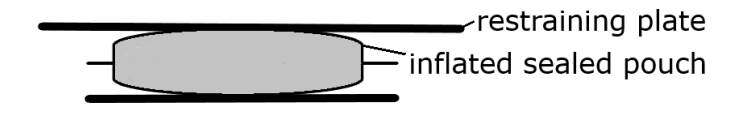


Figure 39: Inflated sealed pouch and restraining plate.

2.3.2 Hot tack

The hot tack performance is measured shortly after heat sealing, at very short cool times, below 1 s. 118 . Besides the very short cool time, hot tack tests differ from seal strength tests with high test speeds. This test gives useful information to rank and evaluate materials for their use in a form-fill-seal process. During this process the seal undergoes disruptive forces. These forces can be caused by food products, spring back behaviour in multi-layered areas and solid contamination. Directly after sealing, the seal is still hot and the seal strength is not a relevant property to evaluate materials and/or optimize the sealing process. The relevance of hot tack performance is illustrated in Figure 40^{49} .

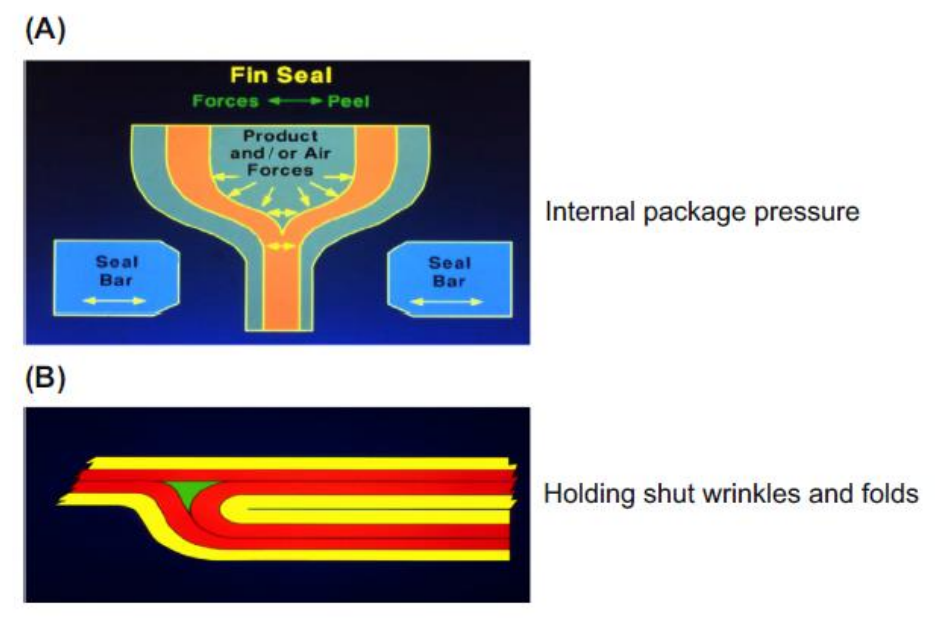


Figure 40: Examples of why hot tack is important. (A) Internal pressure from the weight of the product or air in a vertical form fill seal operation. (B) Holding shut wrinkles and folds in a horizontal form fill seal operation⁴⁹.

The hot tack test is carried out on 15, 25 or 25.4 mm wide strips according to **ASTM F1921**. ¹¹⁹ A hot tack tester has two heated bars and tensile tools to perform the hot tack test. Seal parameters (temperature, time and pressure) must be controlled and seals are tested at a constant test speed. Hot tack strength increases at high test speed. This increase can be explained by the increase of fracture energy, that is added to bending and elongation energy to calculate the work to open a peelable seal. The fracture energy increases at higher testing speeds because of the higher local viscoelastic energy dissipation at the crack tip¹¹². At low test speed the effective cool time will be higher than the setpoint value. It is not recommended to use this low test speed. In a comparative study on hot tack tests, 200 mm/s is recommended ¹¹⁸. The hot seal is tested after a specified delay or cool time. The impact of cool time can give relevant information about the strength development of the seal while it is still hot in the packaging

process. Peel failure occurs more often, compared to seal strength tests because of the lack of crystallization at very short cool times, below $1\ s^{118}$. Lab hot tack testers will cool the seal in a passive way. In food industry, seals can be actively cooled by pressurized air, which increases cool speed.

2.3.3 Seal interface temperature

The temperature of the seal interface is critical for seal quality because entanglement of polymers occurs at the interface¹²⁰. It is possible to measure this temperature with a thermocouple. For ease of use and to increase the lifespan of the thermocouple, membrane thermocouples are preferred. With a proper connection and software, temperature is recorded as a function of time. Data acquisition, temperature range, membrane composition and thickness must be considered to allow good interpretation of results. A low seal pressure and flat to flat bar surfaces are advised to avoid damage to the thermocouple and/or the seal bars. Soft seal bars, f.e. Teflon coated bars, can be damaged by the use of thermocouples.

Figure 41 shows a simple setup of a seal interface temperature measurement. Figure 42 shows the curves of seal interface temperature at different seal times. A type K thermocouple of 130 μ m with a polyamide membrane can be used to perform the measurements¹²¹. Membrane thickness needs consideration because of the impact on temperature conduction. Also, data acquisition rate is of interest because important data points, such as peak values, can be absent at low acquisition rates. The relation of seal temperature, seal time and material can be studied to optimize the sealing process.

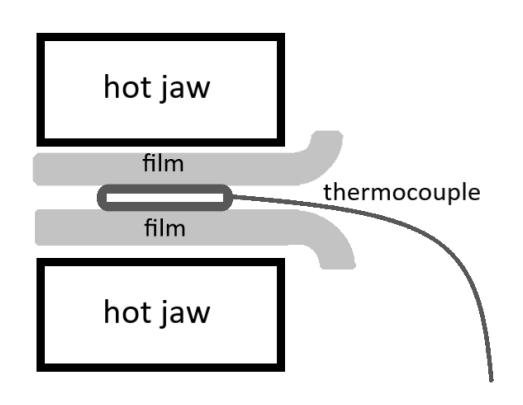


Figure 41: Seal interface temperature measurement setup.

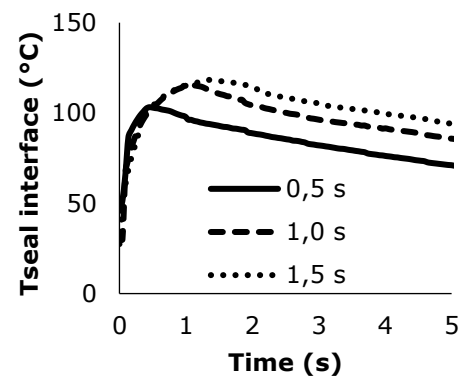


Figure 42: Influence of seal time on seal interface temperature of an oPA/PE 15/40 flowpack film, sealed at 120 °C and 1 N.mm⁻².

2.3.4 Seal integrity

is not clear.

Besides seal strength, seal integrity is crucial for food packages to prevent microbiological or biochemical degradation. Air-leak and dye penetration tests are carried out to evaluate package or seal integrity of food packages. Besides qualitative testing, it is possible to calculate the size of the channel leak with the measured pressure difference with air leak testing¹²².

ASTM F2096 describes a method to detect gross leaks by internal pressurization under water¹²³. In this test, packages are inflated underwater to a predetermined pressure for a certain time, the failure area is visible by the presence of bubbles. This method can be used to check the presence of channel leaks in the seal area. In the annex of the standard a method is described to determine the pressure. A package with a seal with a channel leak is inflated underwater (the seal is approximately 25.4 mm underwater) through one hollow needle and pressure is monitored with another hollow needle. Pressure is increased until bubbles are visible. This pressure can be used as minimum test pressure to evaluate seal integrity. Higher values of pressure can be used to increase the sensitivity of the test but excessive values should be avoided to prevent packages to rupture or creep open. A simple set up of the test is shown in Figure 43.

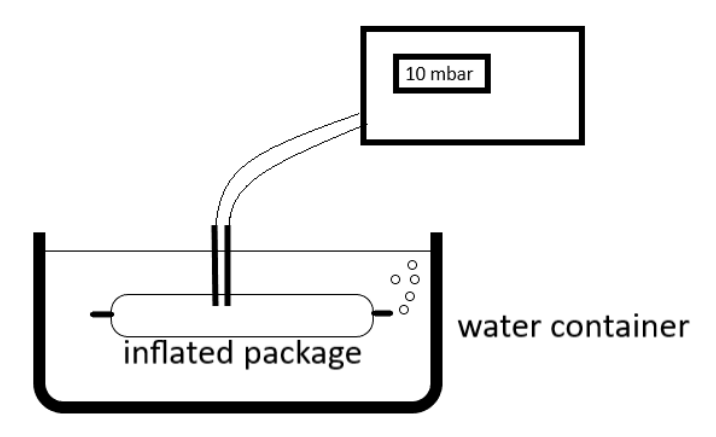


Figure 43: Bubble leak test.

ASTM F2095 describes a similar approach (pressure decay leak test), without the use of water and the option to use restraining plates 124 . Restraining plates can be used to increase the test sensitivity, to avoid extreme deformation and it may reduce the test time if filling time is decreased because of the restrained packaging volumes. Care must be taken to avoid blocking of pinholes with the plates. Test equipment is available today to check seal integrity of packages without destroying the package by inserting hollow needles. Packages are inflated in a vacuum chamber, the escape of tracer gas (CO_2) or pressure difference reveals if there are leaks present. This test is non-destructive but the location of the defect

ASTM F2338 describes this test for leak detection based on pressure difference¹²⁵.

ASTM F3039 describes a method specific to test channel leaks in seal areas. ¹²⁶ An aqueous solution with an indicator dye and a wetting agent is poured or injected on the inner side of the package. The solution is in contact with the seal for five seconds. On the other side the seal is pressed against an absorbing paper, the presence of stains is an indication of a channel leak. The pathway of the leak is coloured by the solution. With transparent packaging films the seal can be studied more into detail by using a light microscope. This method can only give qualitative information. Limited equipment is needed to perform the test. If the solution doesn't weaken the material and seal it can be combined with a seal strength test on the same sample.

2.3.5 Gas permeation through seals

Gas permeation through packaging films consists of three steps:

- adsorption of gas onto the surface,
- diffusion through the film and
- desorption of gas from the other side of the film4.

These three steps also occur through seal materials when the seal is tight. There are no studies available in literature that address this topic. Presumably because the impact of the tight seal permeation on the package is very low because of the relatively small seal surface, and the relatively large pathway gas molecules need to travel, which is in the mm or cm range. The film surface on the other hand is very large, covering almost 100% of the package area. On top of that, the pathway is very small, often below 100 μm .

When seals are not tight, because of the presence of channel leaks, seal permeation can have a big impact on the package permeation. The transport of gasses through channel leaks follow Fick's diffusion and can be calculated with the following formula:

$$N = D * \Delta c / (l + \varepsilon)$$

Equation 4¹²⁷.

N is the massa flux of a particular gas $(g/cm^2/s)$, D is the diffusion coefficient of that gas in air (cm^2/s) , Δc is the difference in concentration (g/cm^3) and $(I+\epsilon)$ is the length of the channel with an end correction term (cm).

ASTM F1307-20 can be followed to detect oxygen molecules with a coulometric sensor through dry packages. Oxygen gas transmission can be calculated after mounting the package to a test fixture and equilibration at the environment. An equal pressure is maintained at both sides of the test sample¹²⁸. This method is suited to test packages when seals are tight. With channel leaks in the seal, oxygen permeability can reach extreme high values. because of the free passage of oxygen molecules, following Equation 4. This can damage the coulometric sensor of oxygen permeation modules, which have an upper detection limit around 200 cc/m².day¹²²². Additionally, it is not possible to maintain the equal pressure with a leaking seal. A fluorescent decay method is better suited for leak measurements and resulting high oxygen ingress. **ASTM F3136-15** can be followed. This standard measures OTR by an accumulation method for plastic

films¹³⁰. To mount a sealed sample on a text fixture, small adjustments can be made, such as the use of a mask to avoid cross leakage at the edges of the seal.

In a 2016 study channel leaks were induced with human hair and pouches with and without defects, containing ham sausage were compared in a food preservation test. The surplus of permeated gases in defect packages did not increase microbiological and biochemical degradation, but there was a discoloration of the ham sausage with defect pouches that can lead to rejection by customers¹³¹.

2.3.6 On-site evaluation

Online inspection of packed food products in companies has many advantages compared to lab research. A first obvious advantage is that every single package can be tested. Another advantage is the speed of identifying the cause of package failure, the cause could be attacked directly after identification. Product recalls can be avoided which results in less product loss, brand protection and maintaining consumer confidence.

There are commercial systems available to perform online inspection of food packages, these are based on several technologies: pressure difference, vacuum decay, tracer gases, camera vision, X-ray inspection, thermal imaging, ultrasound inspection, vibration analysis and high voltage leak detection¹³².

With **pressure difference**, packages are compressed before and after application of a load, movement is measured by a linear encoder. This method is not well suited for sealed trays because of the rigid side walls that partially prevent downwards movement.

The **vacuum decay method** is previously described in 2.3.4, pressure difference is measured of sealed packages in a vacuum chamber. Large leaks will not be detected because there will be no further decay, compared to the room where the test takes place.

It is also possible to **detect tracer gases such as CO_2** with modified atmosphere packaging. CO_2 is a very common tracer gas, it is present in a large amount in modified atmosphere in packages, up to 50%, while in standard atmosphere it is only present in very low amounts, up to $0.5\%^{133}$. The methods with vacuum decay and tracer gas are performed mostly in batch modes and will take several seconds, which makes it hard to achieve high outputs.

High voltage leak detection can be used to detect leaks, specific in containers with liquids by an increase of conductivity.

Vision systems compare seal areas before and after sealing, they are suitable to detect small deviations of the sealed area very quickly. Grey images are made and grey level variance is used with X-ray technology to compare seal areas. **Thermal imaging** uses wavelengths in the infrared spectrum. Areas with slight variations in temperature can be visualized in high contrast. In general, vision systems are suited to identify deviations of the seal area, caused by unsealed parts, contamination in the seal, wrinkles and/or folds, but are not able to identify leaks. **Ultrasonic inspection of seals** and vibration analyses of seal bars are examples of two technologies that can also be used to detect deviations without leak identification.

Upcoming technologies in this area are Terahertz radiation, polarized light stress analysis and laser scatter imaging. Table 6 compares commercially available inspection technologies for seal and package integrity. This table is a result of the comparative literature study on on-site seal evaluation during the VIS project nr.100492 on sustainable and functional packages, funded by VLAIO.

Table 6: Online inspection of seal/package integrity¹³².

	Table 6: Online inspection of seal/package integrity ¹³² .								
Technology	Non-contact	Non-destructive	Package integrity	Seal quality	Shape independent	Speed >60 units/minute	Packaging limitations	Product limitations	Remarks
Pressure difference	-	+	+	1	+	+	Package must contain enough air	No crisp products (e.g. potato chips)	Pinholes down to 3 mm at 200 units/minute
Vacuum decay	-	+	+	-	+	?	Flexible, rigid and semi- rigid packaging	No crisp products	Mostly in batch mode, defect size down to 1.5 µm (liquid filled)
Tracer gases	+	+	+	1	+	1	When CO2 is the tracer gas: only MAP	/	Mostly in batch mode
Camera vision	+	+	ı	+	ı	+	Only transparant packaging material	/	Before or after sealing
X-ray transmission	+	+	ı	+	ı	?	At least one of two films must be transparent	/	Particles down to 0.5 mm ²
Thermal imaging	+	+	1	+	-	+	/	/	Suitable for non- transparant packaging
Ultrasound inspection	+	+	1	+	1	+	/	/	Defect size down to 1 mm
Vibration analysis	+	+	1	+	+	+	/	/	Self-learning algorithm
High Voltage Liquid Detection	-	+	+	-	+	+	Non- conductive packaging material (plastics, glas,)	Liquid-based food products, food product should be in direct contact with packaging material	Pinholes and microcracks down to 1 µm

2.3.7 Leak seal prevention

In a previous study on the seal integrity of food packages in the UK, contamination of the seal area is indicated as main cause for channel leaks¹³⁴. Other causes for channel leaks are inadequate machine settings (bar temperature, seal time, seal pressure, cool time), machine conditions (parallelism of seal tools, profiles of seal tools, tool contamination, temperature distribution of the tool, wear of the tool surface, inappropriate tool materials, gas supply, etc.) and inadequate materials.

To prevent leaks caused by contamination, seal contamination can be prevented and/or seal-through-contamination performance can be improved.

Water from the environment can be avoided by controlling temperature and relative humidity to decrease condensation water. Dust contamination can be minimized by increasing the weight of its particles with high relative humidity so particles are more likely to fall down. Good engineered ventilation systems can blow away contaminated air and bring in new clean air. Housing of the packaging equipment can be considered to avoid environmental contamination¹³⁵. Static electricity can cause dust adhesion at the packaging surface, ionisers can be used to limit this process by firing positive and negative ions¹³⁶.

A similar approach to dust can be used with powdery food products. High-density powders, with small particles, bad cohesion, and low humidity generally cause the biggest dust problems. Dust can be removed directly from the seal area by air wash systems. ¹³⁷ Vibration systems can be installed to remove undesired powder on surfaces. The composition can be changed, f.e. by adding emulsifiers such as soy lecithin, to create more agglomerates and more air in between these surfaces generating a lower powder density ¹³⁸. Filling speed should be optimized, low speeds give rise to getting absorbed in environmental air flows while high speeds generate high air flows. The composition of liquid can be changed to make it more viscous and filling speed can be optimized as well. Dipping filler tubes, dipping nozzles, masking systems and/or pinch bars can be used to avoid contamination on the seal surface ¹³⁴.

In 2.2.1, the ability to encapsulate solid particles by seal materials is mentioned, often referred to as 'caulkability'. In general, soft seal layers and a high thickness of seal layer are preferred to encapsulate solid particles. The seal settings should be optimized to ensure an optimal flow ability of the seal material for the encapsulation process. Other aspects that should be considered are the seal technology and the shape of the seal bars. Ultrasonic sealing gives promising results when sealing through solid particles¹¹. Bar geometry is important for all technologies. Flat to flat seal bars are mostly not optimal because of the possibility of channel leaks when solid particles are present on the seal area. Air acts as insulator at areas without contact and interface temperature drops. Wrinkles and channel leaks can occur at these areas. Insufficient parallelity of seal bars, a feature that can be checked with carbon paper or pressure sensitive film, can also cause areas without contact. Contact between both seal sides can be improved by increasing setpoint pressure and using resilient counterparts (shown in Figure 44) and/or a serrated pattern (shown in Figure 45) that forces the packaging material to stretch when the tools are closed.

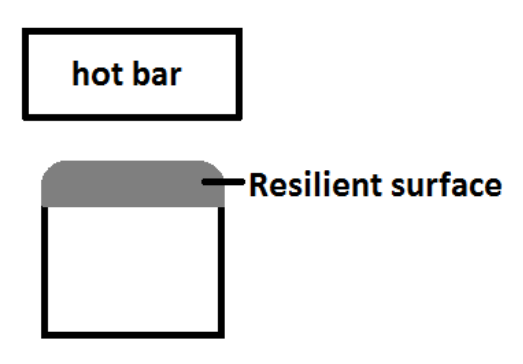


Figure 44: Hot bar with resilient counterpart.

Profiled bars that push more at certain lines, spots are preferred because at these areas, contamination can be pushed away and a tight seal can be made. In a serration pattern, angle, radius, pitch and depth impact the pressure and thus the contact between bar and packaging material, these factors can be adjusted to match films and/or bag types¹. Serrated bars with higher pitch and equal seal length, force, angle, radius and depth will have a lower seal pressure because of an increased surface area and vice-versa. Serrations can occur horizontal, as shown in Figure 45 to ensure tightness of packages. For some applications, such as candy bags, vertical serrations are used to ease the opening of the bags. The vertical lines can serve as easy tear strips³.

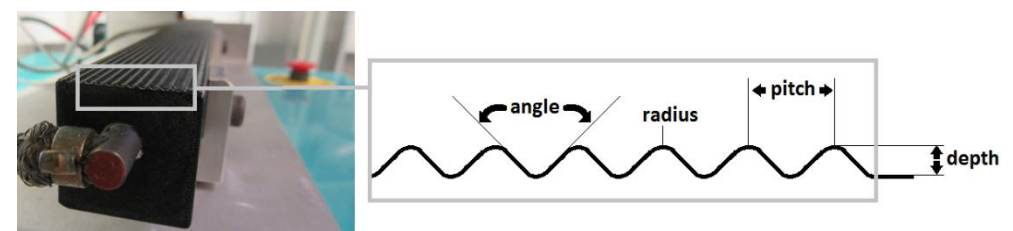


Figure 45: Horizontal serrations in a seal bar and the different factors of a serrated pattern.

The risk of leaks can be decreased by using wider bars and thus increasing seal length.¹³⁹ The hot tack performance increases, because it takes more energy and (cooling) time to open the seal while it is still hot. Higher seal length will however increase the material cost so an optimal balance must be found.

With aqueous solutions as contamination, encapsulation will not improve the seal performance. Seal temperatures are most often over 100 °C with the consequence of boiling water that is still present at the interface. Encapsulated water will be vaporized and large steam bells can open the package. This type of contamination needs to be pushed away at certain areas with the possibility to escape from the seal. An appropriate shape of the seal bar should be selected. The same practice as with aqueous solutions can be used to seal through oil and fat.

In a recent guideline of the IVLV a method is published to optimize the seal-through-contamination performance of applications with a response surface methodology¹⁴⁰.

2.3.8 Additional characterization

Besides the above described methods, researchers of heat seal studies also apply other methods, further from the application, to relate characteristics, such as crystallinity, flow behaviour and molecular structure, with seal performance and thus acquire more knowledge of the sealing process. These other methods are briefly listed below with the objectives and references to seal studies. A generic description of the results, in relation with seal performance, is previously described in 2.2. For further details on these methods and the correlation of the specific results of each of these papers, the reader is referred to these studies.

- Rheology: Dynamic rheological measurements to help obtaining data to estimate the molecular structure^{29, 31, 38}; Viscosity ratio as an important property in the dispersion of polymer blends⁶⁴; Extensional rheology to study the role of molecular structure on melt strength²⁷.; Monitoring the damping factor tan δ to analyse viscoelastic behaviour⁶⁵.
- Gel permeation chromatography to obtain the molecular weight and its distribution ^{25, 26, 29, 31, 38}.
- Temperature rising elution fractionation (TREF) and crystallization analysis fractionation (CRYSTAF): to obtain chemical composition distribution profiles²⁵.
- Fourier-transform infrared spectroscopy (FTIR) to identify polymers and/or to quantify polymers at the surface.^{25, 46}
- Differential Scanning Calorimetry (DSC): to obtain crystallinity and thermal transitions, such as melting and glass transition temperatures^{25,} 26, 27, 28, 29, 38, 46, 65, 66
- Microscopy: Light microscopy to visualize flow behaviour after sealing⁴⁶;
 Transmission and scanning electron microscopy (TEM and SEM): to observe different polymer phases in blends^{46, 64}; Atomic Force Microscopy (AFM) to characterize crystallite structures²⁵.
- Dynamic mechanical (thermal) analysis (DM(T)A): for viscoelastic analysis, such as damping factor tan δ , storage and loss modulus. ^{54, 66}.
- Coefficient of friction (COF): to determine the static and dynamic slip ability⁴⁶.
- Optical properties: gloss and opacity are determined as important characteristics of packaging films^{46, 64}.
- Contact angle measurements to analyse surface-liquid interactions³⁸.
- X-ray diffraction: to study crystallite structures²⁹.
- Carbon Nuclear Magnetic Resonance (CNMR): to quantify long chain branching²⁶.

2.4 Industrial sealing processes and the need for a design of experiments approach

Automatic sealing processes, relevant for the food industry, are described to highlight the complexity of the industrial sealing process.

Automatic heat sealing processing

In packaging lines, sealing is often an automatic process along with the forming and filling process. A differentiation is made between horizontal and vertical form fill sealing.

In **horizontal form-fill-sealing**, packages are formed, filled and sealed in a horizontal line. Pouches that are produced in this way are often referred to as 'flowpacks'. Thermoformed trays with topfilms are also produced in a horizontal line.

A simple scheme of a flowpack process is shown in Figure 46. Three main parts are shown, the infeed chain (I) where the products are moved horizontally, the fin-seal unit (II) where the formation of flowpacks starts and the cross seal unit (III) where the flowpacks are closed and separated with a knife^{141, 142}. In this figure solid products are fed horizontally and a flow is wrapped around each product. It is also possible to fill the pouches vertically so liquids, pastes and creams can be packed. With some machines, cutting is performed between the forming and filling process. In that case the filling is vertically. Several pouch types can be produced with this technology at speed rates up to 1000 packages per minute and more, depending on the machine type⁴.

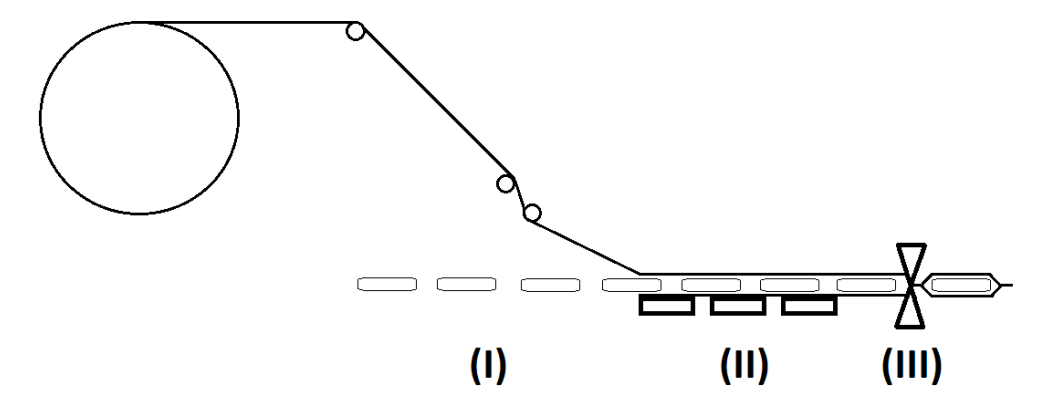


Figure 46: Flowpack process.

In the fin seal unit, seals are made with a rotary sealer. Fin seals are produced when the inner material sides are brought together. Lap seals are produced when the inner side is sealed against the outer side of the film¹⁴¹. This is shown in Figure 47. In section II of Figure 46 it would be possible to produce lap seals as well with the appropriate instruments. Fin seals are possible with all sealable packaging films because it is always possible to produce a seal. With lap seals the packaging material composition has to be considered as it is not always possible to produce

heat seals when different outer and inner sides are brought together. For example, for typical flowpack films with PET outer layer and PE inner layer this would not be possible as these materials can't be sealed together with heat, because of the different melt temperatures and the lack of diffusion. Less material is needed to produce lap seals, compared to fin seals.

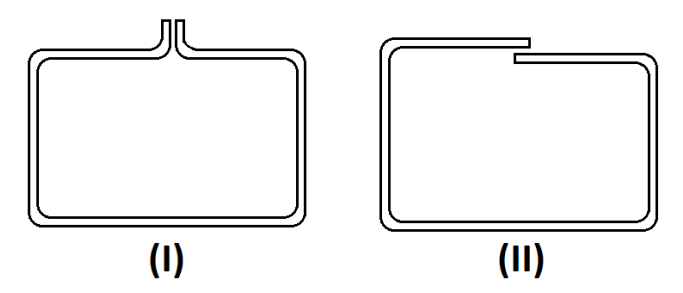


Figure 47: Fin (I) and lap (II) seal.

In a final step (III), shown in Figure 46, the package is closed with a cross seal. During this step a seal can be made while a fold is present, because of the longitudinal seal which is made at the fin seal station⁵⁶. This is shown in Figure 48. As a result, thickness of the package is not equal between the seal bars. The four layered zone will undergo higher pressure than the two layered zone. The fold can create a void at the marked area of Figure 48 if the material flow does not fill up the space that is the result of folding the film. The ability to fill up voids is often referred to as 'caulkability'^{29, 31}. Bar temperature must be high enough over to reach sufficient interfacial temperature over the full width of the package so seal material can flow and fill up voids.

On top of that, the fold can spring back after opening of the seal bars when hot tack strength is insufficient. Both mechanisms can result in a channel leak 56 .



Figure 48: Cross seal with laminated material (black: outer layer, grey: seal layer, red cross: high risk area for channel leaks).

These issues can be resolved by working with appropriate seal materials and parameter settings.

In a **thermoform-fill-seal process** two webs are used in a horizontal line. A thick web is thermoformed into a container (tray, cups, etc.) and filled with food products. A thin web is used as topfilm to close the package. As two separate webs are used it is important to consider the seal materials as only some seal materials are compatible⁴.

Thermorm-fill-sealing, and the sealing of pre-thermoformed and injection moulded trays trays are most often performed with heat conduction. The sealing

process of one tray and topfilm is shown in Figure 49. A hot plate is used at the top, while one or multiple trays are kept in position¹⁴³.

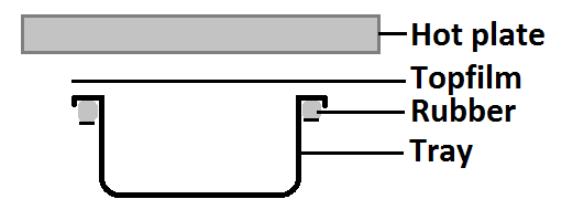


Figure 49: Tray sealer.

When food is filled vertically, the automatic process is referred to as **vertical form fill sealing** (VFFS). Figure 50 shows the VFFS process. In the upper part (I) a pouch-forming collar transforms a web into a pouch. When the pouch is shaped a longitudinal seal is made (II). Similar with the flowpack process this can be a fin or a lap seal. The lower cross seal is made (III) and the pouch is cut into a separate package with a knife that is present in the middle of the cross seal bar. After opening of the seal bars, the product drops down the filling tube (I) into the pouch. At the end the upper cross seal is made to close the package^{3, 4}. Hot tack strength is even more relevant for this application because of the drop of food on the cross seal while it is still hot⁵⁶.

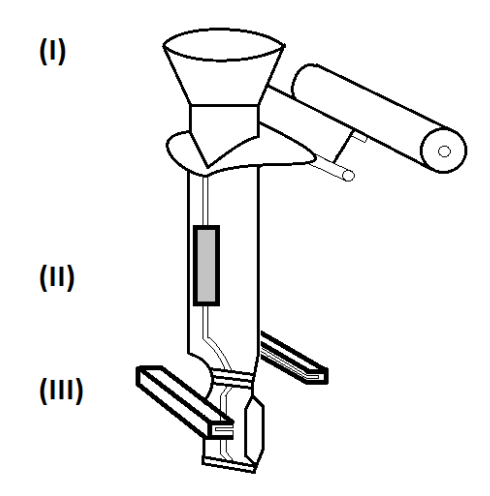


Figure 50: Vertical form-fill-sealing unit.

The choice of an automatic sealing machine is dependent on several aspects such as packed product, available area, packaging speed, packaging concept, etc^{3, 4}.

2.5 Impacting factors of heat-sealed food packages in a design of experiments approach

Factors and interactions that impact heat seal performance and a design of experiment (DOE) approach is described to evaluate and optimize seal performance. This approach is used and explained more specific and detailed in chapters 3, 4, and 5.

2.5.1 Grouping of factors

In a recent review on the factors that affect heat seal quality in flexible food packages, a figure is shown that groups these factors into material properties, process parameters, contaminants and further processes¹⁴¹. Figure 51 is an exact copy. This original figure shows the information by indicating the amount of research that is already performed for each of the factors with the darkness in coloration, and by visualising interacting factors with arrows. The factors in dark areas have been subject of most seal studies, while studies of factors in white areas are absent.

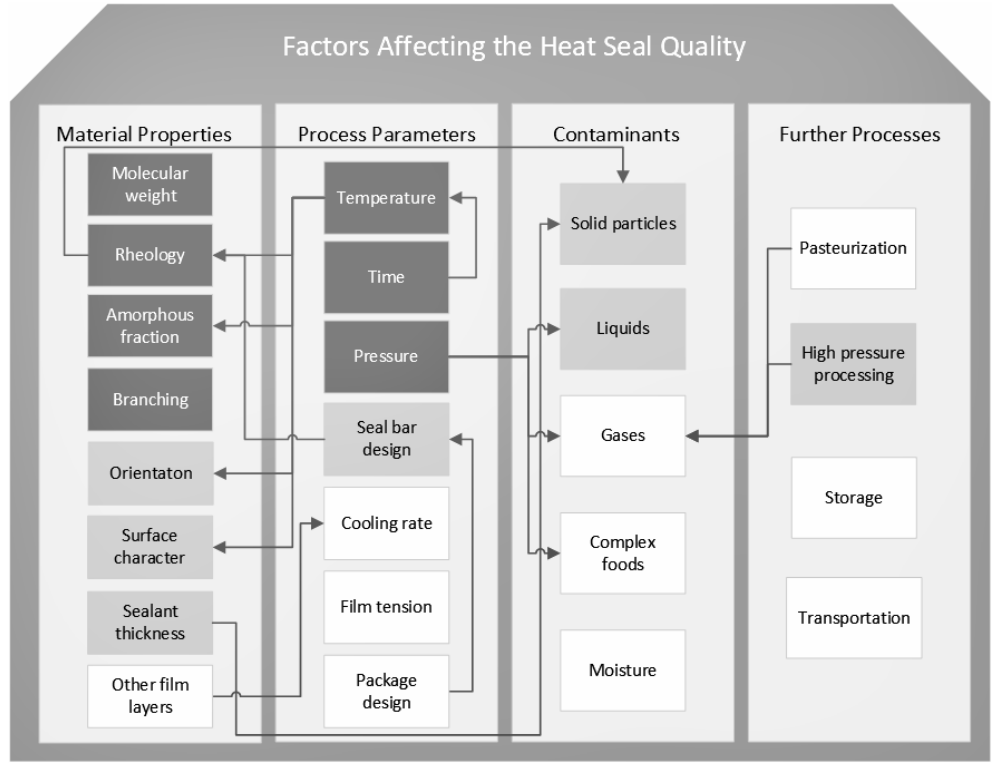


Figure 51: Factors affecting heat seal quality; The amount of research that is already performed for each of the factors correlates with the darkness in coloration; Arrows visualise the interaction between factors¹⁴¹.

When solely focussing on the temperature at the seal interface as crucial factor that affects heat seal quality, previously discussed in 2.3.3, other factors can be grouped slightly different. In a 2011 presentation, Peter Rychiger groups the factors that impact seal temperature of the interface into:

- machine settings (setpoint temperature and machine speed);
- technical machine conditions (position of thermocouple, therma conductivity and tool shape/parallelity);
- packaging material factors (insulation factor, thickness);
- and filling conditions (temperature filling product, headspace)¹⁴⁴.

The process parameters temperature and time are a typical and simple example of interacting factors, indicated with an arrow in Figure 51. The temperature at the seal interface will decrease with higher seal speeds (=lower seal times) while higher tool temperatures will increase the temperature at the seal interface.

Interacting factors are often more complex. In the example of the cross seal in HFFS, described in 0, material flow and hot tack strength are additional factors that affect leak tightness⁵⁷. Interacting temperature and pressure has upper limits to avoid expelling low viscous seal material at the four layered area⁴⁹. Other material properties, such as thickness and conductivity play obvious roles in the heat transfer from contact area to the interface. Thicker materials will need higher

bar temperatures (and/or longer seal times). The presence of a high conducting layer, such as aluminium, can have a beneficial impact in both ways on the heat transfer from contact area to seal interface. Lower bar temperature can be sufficient and the hot tack performance can be increased as heat is better conducted away from the seal interface after opening of the bars¹⁴⁵.

Other factors, amongst contamination presence and environmental factors, will interact and impact seal performance. These interactions are discussed in the following chapters.

2.5.2 A design of experiments approach to evaluate and optimize the industrial sealing process

Introduction

Seal experiments are performed to increase knowledge by increasing the understanding of cause-and-effect relationships. It is a process in which changes are made in levels of input factors, continuous and/or categorical, to observe changes in output, with one or more seal performance indicators. The experiment can have three objectives:

- Exploring by checking which input factor(s) affect performance indicator(s)
- Making a model that describes the effect of input factor(s) on performance indicator(s)
- Optimizing by adjusting level(s) of input factor(s) to produce desired level(s) of performance indicator(s)

Previously, factors that impact the heat seal performance are described. Some of these factors interact with each other. In a common approach to evaluate the impact of factors on a specified performance indicator, also referred to as response, only one factor is varied. This 'one factor at a time' (OFAT) approach is not reliable with processes with interactions because the response will change when other factors are different. The OFAT-approach is inefficient because of the need of many experiments to find out the impact of several factors on seal performance. The major disadvantage is the failure in considering impacts of factor interactions. A factorial experiment, in which factors are varied together, is a better approach that solves the issues of an OFAT approach. A design of experiments is a procedure for planning experiments in an efficient way to obtain valid conclusions. It can be used to explore, characterize and/or optimize the sealing process. The example in Figure 52 shows that the two-factor factorial design with three levels, a minimum, centre and maximum for each factor, is more efficient and effective to cover the design space^{146, 147}.

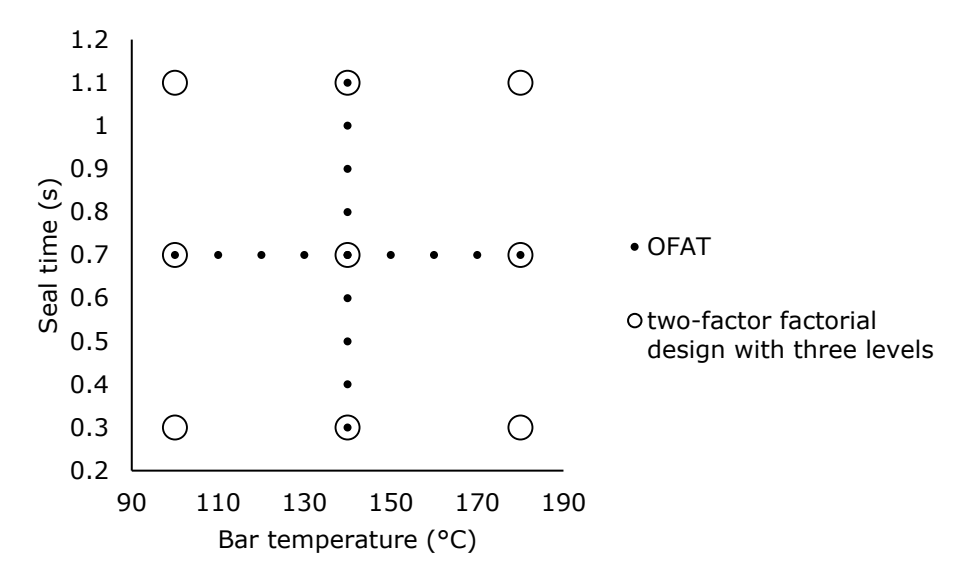


Figure 52: Comparison of 'one factor at a time' (OFAT) and factorial design spaces in a seal experiment example that considers bar temperature and seal time as input factors.

In a DOE, several runs are evaluated. A run is a combination of specified levels. Minimum, centre and maximum are commonly normalized to respectively -1, 0 and +1 for each factor. The impact of these factor levels on a specified response are of interest. These runs are carried out in a random order to average out the impact of noise factors. It is recommended to add replicate runs to the design, these are identical runs that are carried out in a random order. Replicate runs lead to a more accurate estimate of the experimental error, the factor/interaction effect and it can increase precision. Noise effects such as different operators, batch materials can be eliminated by adding blocks and distribute runs to these blocks. Randomisation, replication and blocking are important to minimize experimental bias.

Other important terms related to DOE are 'degrees of freedom' and 'confounding'. The degrees of freedom are the number of fair comparisons that can be made with a data set. For main effects, the degrees of freedom can be calculated by subtracting the amount of levels with one. For interactions it is the product of the degrees of freedom for each factor. Confounding refers to the effect where two or more factor effects are evaluated in one measured effect. For example, the effects of seal temperature, time and their interaction on seal strength cannot be predicted in only two runs with respective low and high levels of seal temperature and time. The calculated effects are caused by seal temperature and/or time. These effects are confounded. Confounding of effects is countered by increasing the resolution of the design. The resolution is a summary characteristic that describes the order of confounding. Typically, more runs and a smart variation in levels of factors within each run should be considered to minimize confounding 148.

The best moment to design an experiment is after finishing the experiment, when the conclusions of that experiment are known. A good practice, specifically if knowledge is limited of a process, is to start with a low number of experimental runs, followed by adding additional runs, based on the conclusion of the first experiments. A 2^k full factorial design is often used to explore the process in a first step. This design uses all combinations of k factors at two levels, minimum (-1) and maximum (+1). In the example in Figure 52 only the four (= 2^2) vertices would remain. It is possible to detect the impact of first order terms (e.g. bar temperature and seal time) and interactions (e.g. bar temperature k seal time). Replications are required to estimate errors. Centre points are added to check the validity of the assumed linear models in a 2^k design. If this assumption is incorrect, second order terms should be considered 2^{149} , 2^{150} .

Response surface methodology

To detect quadratic trends more experimental runs are needed. In the above described example of a 2^2 full factorial design, at least five runs are added to the four original runs (1. $100\,^{\circ}$ C, $0.3\,$ s; $2.\,100\,^{\circ}$ C, $1.1\,$ s; $180\,^{\circ}$ C, $0.3\,$ s; $180\,^{\circ}$ C, $1.1\,$ s): a centre point and four axial points. The two-factor factorial design with three levels (nine runs) in Figure 52 is an example of such as design. This design is referred to as a central composite face-centred design. The methodology that looks for quadratic or higher order trends is referred to as response surface modelling (RSM). Equation 5 shows the resulting model that can be fitted with first order terms, interactions and second order terms, noise effects are excluded. \hat{y} is a seal performance indicator, e.g. seal strength.

$$\hat{y} = \beta_0 + \beta_1$$
 bar temperature + β_2 seal time + β_{12} bar temperature * seal time + β_{11} bar temperature² + β_{22} seal time² Equation 5.

Central composite designs have the advantage that data of a first exploratory full factorial design can be used. This design is efficient because a lower number of runs is needed, compared to a full factorial design with three levels, with the exception if only two factors are considered. The number of runs of a central composite design (Equation 6) is the sum of 2^k , which is the number of the previously described 2^k full factorial design, 2^k axial points and one centre point. The number of runs of a k-factor full factorial design with three levels (Equation 7) is 3^k . n increases if replicates and/or repeats are added in the design.

$$n=2^k+2k+1$$
 $n=3^k$ Equation 6. Equation 7.

Box-Behnken is another example of a design for RSM. One run is put in the centre point, other runs are midpoints of edges of the design space. A Box-Behnken design does not include corner points. It is more efficient than a central composite design but has the disadvantage that no factorial design is embedded. An example of such a design, applied with ultrasonic sealing parameters is shown in Figure 53.151, 152,153.

To highlight the potential of the DOE-approach in seal research, different applications are shown in Figure 53, Figure 54 and Figure 55. In all figures a Box Behnken design space is used with three levels (minimum, centre and maximum)

of three variation factors, thus allowing to fit models that include first order effects, interactions and second order effects.

Figure 53 shows a design space of three ultrasonic factors: amplitude, time and sealing force. The maximum ultrasonic seal strength is visualized by circles with a certain colour and size depending on the value. High strengths are green and big, low strengths are red and small. The main purpose to test seal strength in such a design was not to visualize the impact of several factors in one figure but to evaluate the impact of the factors and interactions on seal strength and to optimize seal strength. By testing at well-defined points, it is possible to fit a model with first order terms, second order effects and interactions. The model can predict seal strength continuously, in between the levels that was tested.

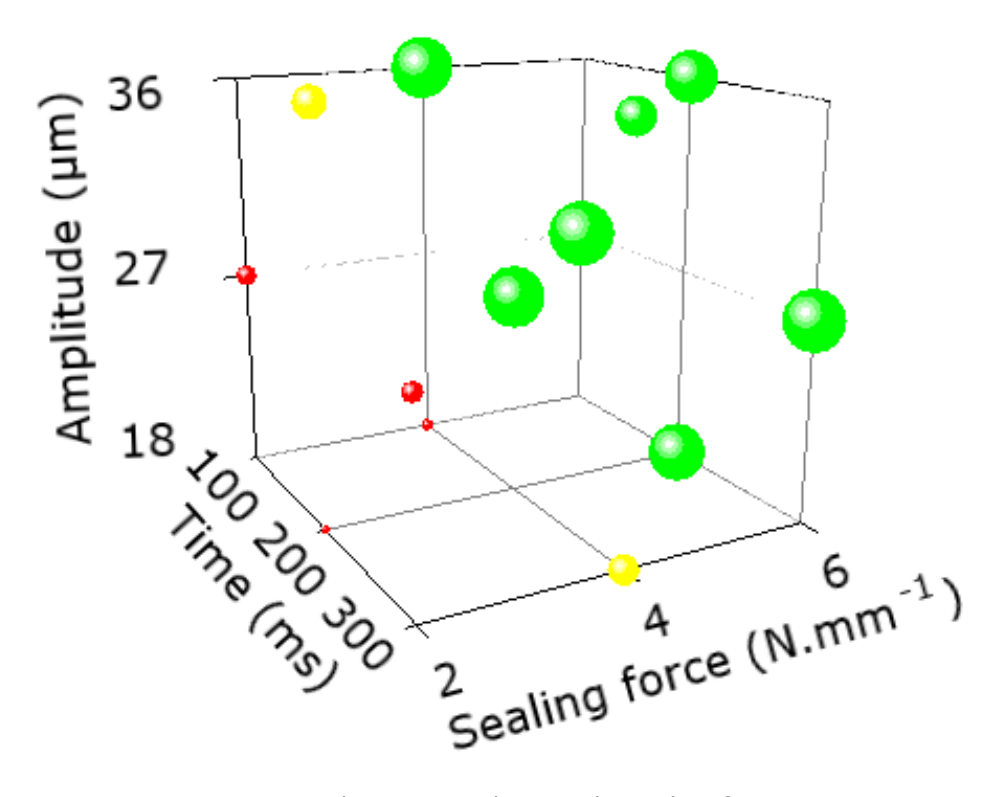


Figure 53: Maximum ultrasonic seal strength results of 60 μ m LLDPE-C4 monolayer, presented in a 3D-design space (Box-Behnken -15 runs with inclusion of 3 center points).

Figure 54 shows a model that was fitted through a set of 15 runs with heat conductive sealing to visualise the ability of a DOE approach. Three hot tool process parameters are varied: seal temperature, time and pressure. In this figure the model is compared with measured values at one fixed seal time and pressure. The model is capable to predict seal strength at settings between the minimum and maximum level of each factor of the design space. The formula includes all significant first and second order terms and interactions. This formula can be used to predict an optimum value, this can be a maximum, a minimum or a target

value. The optimum is validated by checking if this predicted value is within a confidence interval, using c confirmation runs to calculate this interval. This approach is referred to as the CICon approach and is equivalent to a 1-sample t-test¹⁵⁴.

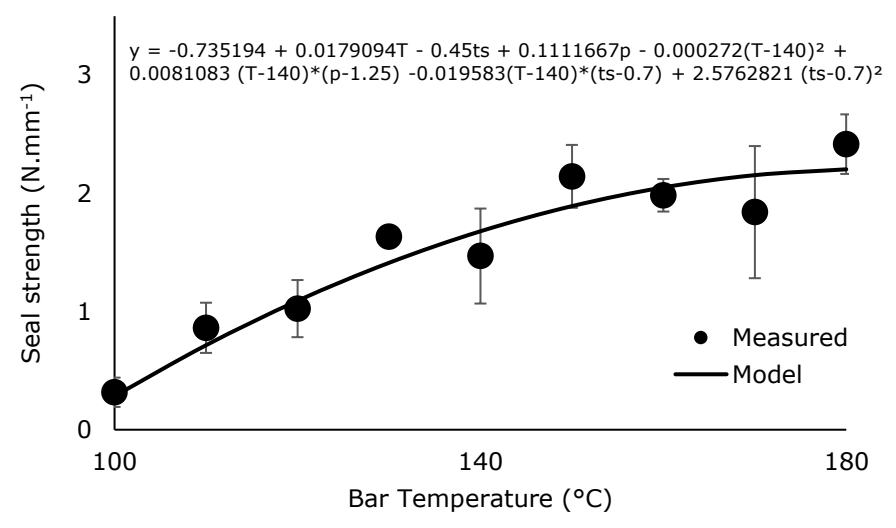


Figure 54: Seal strength of a flowpack film with sodium ionomer seal layer, sealed at a seal time (ts) of 0.7s, a seal pressure (p) of 2 $N.mm^{-1}$, n=3.

The formula in Figure 54 can be used to set up an operating window. Figure 55 shows three areas with different seal strength ranges in a seal temperature – seal time contour graph of the same flowpack film with ionomer seal layer. These graphs can be used to select a material and/or to optimize the performance for an industrial seal application.

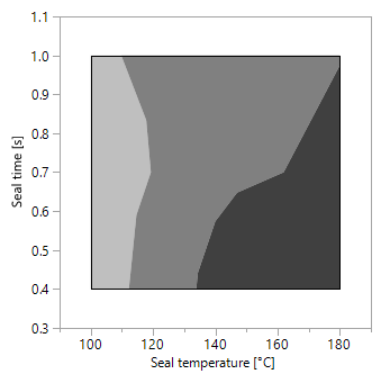


Figure 55: Contour graph of predicted seal strength (light grey: <1.0 N.mm⁻¹;1.0 < dark grey < 1.8: black > 1.8) of a flowpack with sodium ionomer seal layer in a seal temperature and time operating window.

In the following situations, standard designs, such as central composite and Box-Behnken designs, are not the best option:

- The region of interest is not a sphere or a cube because of a constraint in the design variables.
- A nonstandard model is aimed for, based on previous insights on the process that is studied, e.g. a reduced higher order model.
- The number of experiments is not feasible because of high costs and/or time-consuming.

There are many optimization possibilities, depending on which aspect is optimized. An I-optimal design, which is used in chapters 4 and 5, minimizes the average prediction variance over the design space. It is very useful if response prediction is the main objective of the experiment. Another example of an optimal design is a D-optimal design, used in chapter 6. It minimizes the variance of model regression coefficients. Many software packages, such as JMP, Minitab and Design-Expert have algorithms to make such designs, this is useful to customize designs for practical situations¹⁵².

The different options in designs and models emphasize the potential of a DOE-approach, essential to develop knowledge in an appropriate time of the sealing process in a rapidly changing industrial context, with many factors that interact with each other and impact seal performance.

2.5.3 Previous doctoral studies on heat sealing of packaging materials

Besides the scientific papers and handbooks, referred to in this chapter, there are only few doctoral studies available on the topic of heat sealing of packaging materials:

- Bach's study on ultrasonic sealing in 2012 at TU Dresden (title: Untersuchung der Vorgänge und Einflüsse beim Ultraschallfügen flexibler polymerer Packstoffe) ¹⁵⁵.
- Najarzadeh's study on sealing layer in films in 2014 at Polytechnique Montréal (title: control and optimization of sealing layer in films) ³³.
- Thürling's study on process data analysis of ultrasonic sealing at TU Dresden (2016; title: Prozessdatenanalyse zur InlineVerminderung von Störeinflüssen beim Ultraschallsiegeln)¹⁵⁶.
- Ilhan is in the process of obtaining a doctoral degree at UTwente with a topic on heat sealing¹⁴¹.

These authors and their colleagues contributed to heat seal science with a relative high amount of published peer-reviewed studies.

This dissertation aims to add and speed up heat seal knowledge, which is currently at an early stage, in an acceptable timeframe for a rapidly changing industrial context by studying heat seal performance with an innovative DOE-approach. Heat seal technologies, materials and procedures to evaluate and optimize heat seal performance, described in this chapter are subjects of industry-oriented studies in this dissertation.

2.6 References

- [1] Greener corporation. Producing quality packages on vertical form/fill/seal baggers the basics. **2011**. Retrieved August 10 2021 from https://greenercorp.com/wp-content/uploads/wp-vff basics.pdf.
- [2] Bach S. Introduction and overview sealing technologies. *IPI/VVD Symposium* **2013**; conference proceedings; Schaffhausen.
- [3] Bosch. Guide to vertical form-fill-seal baggers. *Bosch packaging technology*® **2014**. Retrieved July 14 2021 from https://toaz.info/docviewer.
- [4] Yam KL. The Wiley Encyclopedia of Packaging Technology, Third Edition. John Wiley & Sons, Inc 2009, New Jersey. Print ISBN: 9780470087046.
- [5] Toss-Gmbh. Thermal impulse sealing. Retrieved July 8 2021 from https://www.toss-gmbh.de/en/industrial-products/general-notes/thermal-impulse-sealing.html.
- [6] Raymond M,Leczynski A, Iovanna J, Tayebi A. Effect of impulse heat sealing process parameters on bond strength of low density polyethylene films. *ANTEC* **2005**; conference proceedings; Boston.
- [7] Benatar A, Gutowski TG. Ultrasonic welding of PEEK graphite APC-2 Composites. *Polymer engineering and science* **1989**; 29(23); pp. 1705-1721, DOI: 10.1002/pen.760292313.
- [8] Van Dun J, Thürling K. Polyolefins for ultrasound sealing. 14th TAPPI European place conference **2013**, conference proceedings, Dresden.
- [9] Zentralverband Elektrotechnik und Elektronikindustrie e. V. Ultrasonic assembly of thermoplastic mouldings and semi-finished products recommendations on methods, construction and applications. Fachverband Electroschweissgeräte 1980; Frankfurt. Retrieved July 14 2021 from https://www.atcp-ndt.com/images/TRZ/Ultrasonic-Assembly-of-Thermoplastic-Moldings-and-semi-finished products-ZVEI.pdf.
- [10] Potente H. Ultrasonic welding principles & theory. *Materials & design* **1984**; 5(5); pp. 228-234; DOI: https://doi.org/10.1016/0261-3069(84)90032-3.
- [11] Bach S, Thürling K, Majschak J-P. Ultrasonic Sealing of Flexible Packaging Films Principle and Characteristics of an Alternative Sealing Method. *Packaging Technology and Science* **2011**, 25 (4), pp. 233–248, DOI: 10.1002/pts.972.
- [12] Marcus M. An approach to determine minimum amplitude required for ultrasonic welding. *EWI* **2017**; Columbus. Retrieved July 15 2021 from https://ewi.org/wp-content/uploads/2018/12/an-approach-to-determine-minimum-amplitude-required-for-ultrasonic-welding.pdf.
- [13] Nad M. Ultrasonic horn design for ultrasonic machining technologies. *Applied and computational mechanics* **2010**, 4(1); pp. 79-88.
- [14] Baudrit B, Stöhr N, Heidemeyer P, Bastian M, Majschak J-P, Stephan B, Thürling K. Insights into the ultrasonic sealing process. *Joining plastics* **2014**;3; pp. 46-51.
- [15] Bach S, Bunk N, Majschak JP. Effect of laminate structure and morphology on fracture mechanics and seam strength of sealed seams. 14th TAPPI European conference **2013**, conference proceedings, Dresden.

- [16] Yeh HJ, Benatar A. Technical evaluation: methods for sealing paper/foil aseptic food packages. *Tappi journal* **1997**; 80(6); pp. 197-203.
- [17] Darby D. Sealing Seminar: seal energy processes. *IPI International Packaging Institute* **2011**; conference proceedings; Schaffhausen.
- [18] Paul AK, Chinoy S. Air-cooled induction heater for efficient sealing of containers using wide range foils. IEEE transactions on industry applications 2016; 52(4); pp. 3398-3407; DOI: 10.1109/TIA.2016.2535112.
- [19] Grewell D, Benatar A. Welding of plastics: fundamentals and new developments. *International polymer processing journal of the polymer processing society* **2007**; 22(1); pp. 43-60; DOI: 10.3139/217.0051.
- [20] Coles R, McDowell D, Kirwan MJ. Food packaging technology. *Blackwell publishing Ltd* **2003**, Oxford, pp. 174-240. ISBN 13: 9780849397882.
- [21] Ajji A, Sammut P, Huneault MA. Elongationale rheology of LLDPE/LDPE Blends. *Journal of applied polymer science* **2003**; 88(14); pp.3070-3077, DOI: https://doi.org/10.1002/app.11931.
- [22] Delgadillo-Velázquez O, Hatzikiriakos SG, Sentmanat M. Thermorheological properties of LLDPE/LDPE blends. *Rheologica Acta* **2008**; 47; pp. 19-31, DOI: <u>10.1007/s00397-007-0193-8</u>
- [23] Field GJ, Micic P, Bhattacharya SN. Melt strength and bubble instability of LLDPE/LDPE blends. *Polymer International* **1999**; 48(6); pp. 461-466, DOI: <a href="https://doi.org/10.1002/(SICI)1097-0126(199906)48:6<461::AID-PI169>3.0.CO;2-7">https://doi.org/10.1002/(SICI)1097-0126(199906)48:6<461::AID-PI169>3.0.CO;2-7.
- Furumiya A, Akana Y, Ushida Y, Masuda T, Nakajima A. Relationship between molecular characteristics and physical properties of linear low density polyethylenes. *Pure and applied chemistry* **1985**; 57(6); pp.823-832; DOI: https://doi.org/10.1351/pac198557060823.
- [25] Simanke AG, De Lemos C, Pires M. Linear low density polyethylene: Microstructure and sealing properties correlation. *Polymer testing* **2013**; 32; pp. 279-290; http://dx.doi.org/10.1016/j.polymertesting.2012.11.010.
- [26] Moreira ACF, Dartora PC, Dos Santos FP. Polyethylenes in blown films: effect of molecular structure on sealability and crystallization kinetics. *Polymer engineering and science* **2017**; 75(1); pp. 51-59; DOI: https://doi.org/10.1002/pen.24384.
- [27] Najarzadeh Z, Ajji A, Bruchet JB. Interfacial self-adhesion of polyethylene blends: the role of long chain branching and extensional rheology. *Rheologica acto* **2015**; 54; pp. 377-389; DOI: <u>10.1007/s00397-015-0843-1</u>.
- [28] Stehling FC and Meka P. Heat sealing of semicrystalline polymer films. II. Effects of melting distribution on heat-sealing behavior of polyolefins. Journal of applied polymer science **1994**; 51(1); pp. 105-119; DOI: https://doi.org/10.1002/app.1994.070510112
- [29] Sadeghi F,Ajji A. Application of single site catalyst metallocene polyethylenes in extruded films: effect of molecular structure on sealability, flexural cracking and mechanical properties. *The Canadian journal of chemical engineering* **2014**, 92 (7), pp 1181-1188 2014. DOI: 10.1002/cjce.21964.

- [30] Wong CM, Shih HH, Huang CJ. Effect of various polyethylene structures on film extrusion. *Journal of reinforced plastics and composites* **1998**; 17(10); pp. 945-954; DOI: https://doi.org/10.1177/073168449801701008.
- [31] Sadeghi F, Ajji A. Effect of molecular structure on seal ability, flex crack and mechanical properties of linear low-density polyethylene films. *Journal of plastic film and sheeting* **2014**; 30(1); pp. 91-111; DOI: 10.1177/8756087913490585.
- [32] CES EduPack[™] **2017** version 17.2.0 [computer software]. Granta design limited.
- [33] Najarzadeh Z. **2014**. Control and optimization of sealing layers in films [doctoral dissertation, Université de Montreal, Department of chemical technology]. Retrieved May 16 2022 from https://publications.polymtl.ca/1406/1/2014 ZahraNajarzadeh.pdf.
- [34] Weckhuysen BM, Schoonheydt RA. Olefin polymerization over supported chromium oxide catalysts. Catalysis today 1999; 51(2); pp. 215-221; DOI: https://doi.org/10.1016/S0920-5861(99)00046-2.
- [35] Dartora PC, Santana RMC, Moreira ACF. The influence of long chain branches of LLDPE on processability and physical properties. *Polimeros* **2015**; 25(6); pp. 531-539; DOI: https://doi.org/10.1590/0104-1428.1732.
- [36] Gahleitner M, Tranninger C, Doshev P. Heterophasic copolymers of polypropylene: development, design, principles, and future challenges. *Journal of applied polymer science* **2013**; 130(5); pp. 3028-3037; DOI: 10.1002/app.39626.
- [37] De Rosa C, Auriemma F. Structure and physical properties of syndiotactic polypropylene: A highly crystalline thermoplastic elastomer. *Progress in polymer science* **2006**; 31; pp. 145-237; DOI: 10.1016/j.progpolymsci.2005.11.002.
- [38] Boutrouka R, Tabatabaei SH, Ajji A. Effect of molecular structure on the heat seal performance of polypropylene films. *ANTEC* **2014**, conference proceeding, society of plastics engineers, Las Vegas.
- [39] Cancelas Sanz A. High impact polypropylene: structure evolution and impact on reaction (doctoral dissertation, *Université de Lyon, Chemical engineering*, France, **2017**). Order number NNT: 2017LYSE1210.
- [40] Morris B. 2017. The science and technology of flexible packaging multilayer films from resin and process to end use. *Elsevier inc* **2016**, Amsterdam, pp. 69-119. ISBN: 978-0-323-24273-8.
- [41] Nase M, Langer B, Grellmann W. Fracture mechanics on polyethylene/polybutene-1 peel films. *Polymer testing* **2008**; 27(8); pp. 1017-1025; DOI: https://doi.org/10.1016/j.polymertesting.2008.09.002.
- [42] Falla D. Peelable seal films with enhanced moisture barrier properties for flexible packaging applications. *TAPPI PLACE Conference* **2016**, conference proceedings, Fort Worth.
- [43] Boutni OM. Polybutene-1: a review of an old polymer produced with a new technology and its application to flexible packaging. *ANTEC* **2007**, conference proceeding, society of plactis engineers, Cincinatti.

- [44] Hahm D. Easing your way to reliable peelable seals (White paper, *DuPont Packaging & Industrial polymers*, **2011**). Retrieved July 8 2021 from https://docplayer.net/21177273-Dupont-packaging-industrial-polymers.html.
- [45] Mohammdi SR, Ajji A, Tabatabaei SH. Peel/seal properties of poly(ethylene methyl acrylate)/polybutene-1 blend films. *AIP conference proceedings* 1664, 080005 **2015**; DOI: 10.1063/1.4918461.
- [46] Nase M, Bach S, Zankel A, Majschak JP, Grellmann. Ultrasonic sealing versus heat conductive sealing of polyethylene/polybutene-1 peel films. Journal of applied polymer science 2013; 130(1); pp. 383-393; DOI: https://doi.org/10.1002/app.39171.
- [47] Poisson C, Hervais V, Lacrampe MF, Krawczak P. Optimization of PE/Binder/PA Extrusion Blow-Molded Films. I. Heat Sealing Ability Improvement Using PE/EVA Blends. *Journal of Applied polymer science* **2006**; 99(3); pp. 974-985; DOI: https://doi.org/10.1002/app.22405.
- [48] Li C, Kong Q, Zhao J, Fan D, Xia Y. Crystallization of partially miscible linear low-density polyethylene/poly(ethylene-co-vinylacetate) blends. *Materials letters* **2004**, 58(27-28); pp. 3613-3617; DOI: https://doi.org/10.1016/j.matlet.2004.06.057.
- [49] Morris B. 2017. The science and technology of flexible packaging multilayer films from resin and process to end use. Elsevier inc **2016**, Amsterdam, pp. 181-257. ISBN: 978-0-323-24273-8.
- [50] Najarzadeh Z, Tabasi RY, Ajji A. Sealability and seal characteristics of PE/EVA and PLA/PCL blends. *International polymer processing* **2014**; 29(1); pp. 95-102; DOI: https://doi.org/10.3139/217.2813.
- [51] Dow®. Nucreal™ acid copolymers. Retrieved July 8 2021 from https://www.dow.com/en-us/brand/nucrel.html.
- [52] Mühlfeld L, Langguth P, Häusler H, Hagels H. Influences of heat seal lacquer thickness on the quality of blister packages. *European Journal of pharmaceutical sciences* **2012**; 45(1-2); pp. 150-157; DOI: https://doi.org/10.1016/j.ejps.2011.11.006.
- [53] Rigney J, Reinhold F. Effect of polymer design and formulation on the performance of water-based acrylic dispersions for heat seal lacquers. *ANTEC* **2017**, Society of plastic engineers, Anaheim.
- [54] Renema J, Van Sluijs C, Metselaar G, Van Meer A. Fast performing seals. *European coatings journal* **2014**; 2; pp. 36-40.
- [55] Eisenberg A, Kim JS. Introduction to ionomers. *Wiley interscience* **1998**, New York, ISBN 0-471-24678-6.
- [56] Morris B. Sure ways to reduce package sealing failure. *Dupont* **2010**. Retrieved November 2018 from http://www2.dupont.com/Packaging Resins/en US/assets/downloads/white-papers/Reduce Package Sealing Failure Barry Morris November 2010.pdf.
- [57] Morris BA. Predicting the seal performance of ionomer films. *Journal of Plastic Film and Sheeting* **2002**; 18; pp. 157–167; https://doi.org/10.1177/8756087902018003002.
- [58] Demirel B, Yaraş A, Elçiçek H. Crystallization Behavior of PET Materials. Bil Enst Dergisi Cilt **2011**, 13, pp. 26-35.

- [59] Baldenegro-Perez LA, Navarro-Rodriguez DN, Medellin-Rodriguez FJ, Hsiao B, Avila-Orta CA, Sics I. Molecular weight and crystallization temperature effects on poly(ethylene terephthalate) (PET) homopolymers, an isothermal crystallization analysis. *Polymers* **2014**; 6(2); pp. 583-600; DOI: https://doi.org/10.3390/polym6020583.
- [60] Chong, S. Mono-material structure a clear trend in circular packaging. *CPRJ Editorial Team* **2019**. Retrieved August 9 2022 from https://www.adsalecprj.com/en/magazine show-10108.html.
- [61] Barhouse PS, inventor; Spartech corporation, assignee. Thermoformable and RF sealable plastic packaging material. US patent 2010/0280152 A1. November 4, **2010**.
- [62] Awaja F. Autohesion of polymers. *Polymer*.**2016**; 97(5); pp. 387-407, DOI: http://dx.doi.org/10.1016/j.polymer.2016.05.043.
- [63] Li X, Ai X, Pan H, Yang J, Gao G, Zhang H, Yang H, Dong L. The morphological, mechanical, rheological, and thermal properties of PLA/PBAT blown films with chain extender. *Polymer advanced technologies* **2018**; 29(6); pp. 1706-1717; DOI: 10.1002/pat.4274.
- [64] Liewchirakorn P, Aht-Ong D, Chinsirikul W. Practical approach in developing desirable peel-seal and clear lidding films based on poly(lactic acid) and poly(butylene adipate-co-terephtalate) blends. *Packaging technology and science* **2018**; 31(5); pp. 296-309; DOI: 10.1002/pts.2321.
- [65] Stoehr N, Baudrit B, Haberstroh E, Nase M, Heidemeyer P, Bastian M. Ultrasonic welding of plasticized PLA films. *Journal of applied polymer science* **2015**; 132(4); pp. 41351-1-41351-8; DOI: 10.1002/app.41351.
- [66] Vogel J, Grewell D, Kessler MR, Drummer D, Menacher M. Ultrasonic welding of polylactic acid films. *Polymer engineering and science* **2011**;51(6); pp. 1059-1067; DOI: 10.1002/pen.
- [67] BIO-POLYLACTIC ACID (PLA) MARKET GROWTH, TRENDS, AND FORECAST (2020 2025). Retrieved July 8 2021 from: https://www.mordorintelligence.com/industry-reports/bio-polylactic-acid-pla-market.
- [68] Zhong Y, Liu S, Li X, Chen L, Zhu J. Effect of amylose/amylopectin ratio of esterified starch-based films on inhibition of plasticizer migration during microwave heating. *Food control* **2017**; 82; pp. 283-290; DOI: 10.1016/j.foodcont.2017.06.038.
- [69] Rompothi O, Pradipasena P, Tananuwong, K, Somwangthanaroj A, Janjarasskul T. Development of non-water soluble, ductile mung bean starch based edible film with oxygen barrier and heat sealability. *Carbohydrate polymers* **2017**; 157(10); pp. 748-756; DOI: 10.1016/j.carbpol.2016.09.007.
- [70] Sadegh-Hassani F, Nafchi AM. Preparation and characterization of bionanocomposite films based on potato starch/halloysite nanoclay. *International Journal of Biological Macromolecules* **2014**; 67; pp. 458–462; DOI: 10.1016/j.ijbiomac.2014.04.009.
- [71] López OV., Lecot CJ., Zaritzky NE, García MA. Biodegradablepackages development from starch based heat sealable films. *Journal of Food Engineering* **2011**; 105(2); pp. 254–263; DOI: 10.1016/j.jfoodeng.2011.02.029.

- [72] Das M, Chowdhury T. Heat sealing property of starch based self-supporting edible films. *Food packaging and shelf life* **2016**; 9; pp.64-68; DOI: 10.1016/j.fpsl.2016.05.002.
- [73] Abdorreza MN, Abd Karim A. Mechanical, barrier, physicochemical, and heat seal properties of starch films filled with nanoparticles. *Journal of nano research* **2013**; 25; pp. 90-100; DOI: 10.4028/www.scientific.net/JNanoR.25.90.
- [74] Ragaert P, Buntinx M, Maes C, Vanheusden C, Peeters R, Wang S, D'hooge DR, Cardon L. Polyhydroxyalkanoates for Food Packaging Applications. *Reference Module in Food Science. Elsevier* **2019**; Amsterdam; pp. 1–9; ISBN: 9780081005965; DOI: http://dx.doi.org/10.1016/B978-0-08-100596-5.22502-X.
- [75] Kuusipalo J. PHB/V in Extrusion Coating of Paper and Paperboard—Study of Functional Properties. Part II. *Journal of Polymers and the Environment* **2000**; 8 (2); pp. 49-57; DOI: https://doi.org/10.1023/A:1011565519440.
- [76] Rafiqah SA, Khalina A, Harmaen AS, Tawakkal IA, Zaman K, Asim M, Nurrazi MN, Lee CH. A review on properties and application of bio-based poly(butylene succinate). *Polymers* **2021**; 13; pp. 1436; DOI: https://doi.org/10.3390/polym13091436.
- [77] Nakajima, H., Dijkstra, P., Loos K. The Recent Developments in Biobased Polymers toward General and Engineering Applications: Polymers that Are Upgraded from Biodegradable Polymers, Analogous to Petroleum-Derived Polymers, and Newly Developed. *Polymers* **2017**, 9(10), pp. 523; doi:10.3390/polym9100523.
- [78] Greene JP. Sustainable plastics: environmental assessments of biobased, biodegradeable, and recycled plastics. *John Wiley & Sons, Inc* **2014**, New Jersey; pp. 96-97; ISBN: 978-1-118-10481-1.
- [79] Su S, Kopitzky R, Tolga S, Kabasci S. Polylactide (PLA) and its blends with poly(butylene succinate) PBS): a brief review. *Polymers* **2019**, 11, pp. 1193, DOI: 10.3390/polym11071193.
- [80] Gowman A, Wang T, Rodriguez-Uribe A, Mohanty AK., Misra M. Biopoly(butylene succinate) and Its Composites with Grape Pomace: Mechanical Performance and Thermal Properties. ACS Omega 2018; 3; pp. 15205-15216; DOI: 10.1021/acsomega.8b01675.
- [81] Ayu RS, Khalina A, Harmaen AS, Zaman K, Jawaid M, Lee CH. Effect of modified tapioca starch on mechanical, thermal, and morphological properties of PBS blends for food packaging. *Polymers* **2018**; 10(11); pp. 1187; DOI: 10.3390/polym10111187.
- [82] Guidotti G, Soccio M, Siracusa V, Gazzano M, Salatelli E, Munari A, Lotti N. Novel random PBS-based copolymers containing aliphatic side chains for sustainable flexible food packaging. *Polymers* **2017**; *9*(12); pp. 724; DOI: https://doi.org/10.3390/polym9120724.
- [83] Liu Y, Ahmed S, Sameen DE, Wang Y, Lu R, Dai J, Li S, Qin W. A review of cellulose and its derivatives in biopolymer-based for food packaging application. *Trends Food Sci. Technol.* **2021**, 112, pp. 532-546, doi: 10.1016/j.tifs.2021.04.016.
- [84] Paunonen S. Strength and barrier enhancements of cellophane and cellulose derivative films: a review. *Bioresources* **2013**; 8(2); pp. 3098-3121.

- [85] Arrieta MP, Samper MD, Aldas M, López J. On the use of PLA-PHB blends for sustainable food packaging applications. *Materials* **2017**; 10; pp. 1008; DOI: :10.3390/ma10091008.
- [86] Bulatović VO, Mandić V, Kučić Grgić D, Ivančić A. Biodegradable polymer blends based on thermoplastic starch. *Journal of polymers and the environment* **2020**, 29, pp. 492-508; DOI: https://doi.org/10.1007/s10924-020-01874-w.
- [87] Li H, Qi Y, Zhao Y, Chi J, Cheng S. Starch and its derivatives for paper coatings: a review. *Progress in organic coatings* 2019; 135; pp. 213-227; DOI: https://doi.org/10.1016/j.porgcoat.2019.05.015.
- [88] Nechita P, Roman M. Review on polysaccharides used in coatings for food packaging papers. *Coatings* **2020**; 10(6); pp. 566; DOI: 10.3390/coatings10060566.
- [89] Lee TJ, Yoon C, Ryu JY. A new potential paper resource; recyclability of paper cups coated with water-soluble polyacrylate-based polymer. *Nordic Pulp & Paper Research Journal* **2017**; 32(1); pp. 155-161; DOI: 10.3183/NPPRJ-2017-32-01-p155-161.
- [90] Andersson C, Erntsson M, Järnström L. Barrier properties and heat sealability/failure mechanisms of dispersion-coated paperboard. *Packaging Technology and Science* **2002**; 15; pp. 209-224. DOI: https://doi.org/10.1002/pts.590.
- [91] Hauptmann M, Bär W, Schmidtchen L, Bunk N, Abegglen D, Vishtal A, Wyser Y. The sealing behavior of new mono-polyolefin and paper-based film laminates in the context of bag form-fill-seal machines. *Packaging Technology and Science* **2020**; 34(2); pp. 2569. DOI: https://doi.org/10.1002/pts.2544.
- [92] Merabtene M, Tanninen P, Varis, J, Leminen V. Heat sealing evaluation and runnability issues of flexible paper materials in a vertical form fill seal packaging machine. *Bioresources* **2022**; 17(1); pp. 223-242; DOI: https://doi.org/10.15376/biores.17.1.223-242.
- [93] Tuominen M, Ek M, Saloranta P, Toivakka M, Kuusipalo J. The effect of flame treatment on surface properties and heat sealability of low-density polyethylene coating. *Packaging Technology and Science* **2013**; 26; pp. 201-214; DOI: https://doi:10.1002/pts.1975.
- [94] Kuusipalo J. PHB/V in extrusion coating of paper and paperboard study of functional properties. Part II. *Journal of Polymers and the Environment* **2000**; 8(2);49-57.
- [95] Rhim JW. Effect of coating methods on the properties of poly(lactide)-coated paperboard: solution coating vs. thermo-compression coating. *Food Science and Biotechnology* **2009**; 18(3); pp. 1155-1160.
- [96] Rhim JW, Kim JH. Properties of poly(lactide)-coated paperboard for the use of 1-way paper cup. *Journal of Food Science* **2009**; 74(2); pp. E105-E111; DOI: https://doi.org/10.1111/j.1750-3841.2009.01073.x.
- [97] Lahtinen K, Kotkamo S, Koskinen T, Auvinen S, Kuusipalo. Charachterization for water vapor barrier and heat sealability properties of heat-treated paperboard/polylactide structure. *Packaging Technology* and Science 2009; 22; pp. 451-460; DOI: https://doi.org/10.1002/pts.869.

- [98] Tai J, Chen G, Chen Q, Tang B. Research on poly lactic acid solvent coated paper. *Applied Mechanics and Materials* **2012**; 200; pp. 380-384; DOI: https://doi.org/10.4028/www.scientific.net/AMM.200.380.
- [99] Shao C, Yang C, Wang X, Luo P. Characterization of soy protein-celery composite paper sheet: rheological behaviour, mechanical, and heat-sealing properties. *Journal of Applied Polymer Science* **2012**; 125; pp. E255-E261; DOI: https://doi.org/10.1002/app.36902.
- [100] Sancaktar E, Walker E. Effects of calcium carbonate, talc, mica, and glass-fiber fillers on the ultrasonic weld strength of polypropylene. *Journal of applied polymer science* **2004**; 94; pp. 1986-1998 DOI: https://doi.org/10.1002/app.21102.
- [101] PlasticPortal. Average polymer prices in Central Europe. *PlasticPortal.eu*, July, **2022**. Retrieved August 9 2022 from: https://www.plasticportal.eu/en/polymer-prices/lm/14/.
- [102] Plastics Europel. Plastics the facts: An analysis of European plastics production, demand and waste data. Retrieved August 9 2022 from https://plasticseurope.org/wp-content/uploads/2021/12/Plastics-the-Facts-2021-web-final.pdf.
- [103] Chemanalyst. Ethylene Vinyl Acetate (EVA) Price Trend and Forecast. Retrieved August 9 2022 from: https://www.chemanalyst.com/Pricing-data/ethylene-vinyl-acetate-74#:~:text=North%20America%20saw%20an%20increase,Texas%20in%20the%20first%20quarter.
- [104] Sigma Aldrich. Properties Poly(ethylene-co-acrylic acid). Retrieved August 9 2022 from: https://www.sigmaaldrich.com/BE/en/product/aldrich/448672.
- [105] Bamps B, Guimaraes RM, Duijsters G, Hermans D, Vanminsel J, Vervoort E, Buntinx M, Peeters R. Characterizing mechanical, heat seal and gas barrier perfor-mance of biodegradable films to determine food packaging ap-plications. *Polymers* **2022**; 14(13); pp. 2569. DOI: https://doi.org/10.3390/polym14132569.
- [106] European bioplastics. Bioplastics market development update **2021**. Retrieved August 9 2022 from: https://docs.european-bioplastics.org/publications/market data/Report Bioplastics Market Dat a 2021 short version.pdf.
- [107] Rafiqah SA, Khalina A, Harmaen AS, Intan, AT, Zaman K. A review on properties and application of bio-based poly(butylene succinate). *Polymers* **2021**, *13*(*9*), pp. 1436, doi: DOI:10.3390/polym13091436.
- [108] American Society for Testing and Materials 2015. Standard Test Method for Seal Strength of Flexible Barrier Materials (ASTM F88/F88M-15). Retrieved from https://www.astm.org/Standards/F88.htm.
- [109] American Society for Testing and Materials **2021**. Standard Practices for Making Laboratory Heat Seals for Determination of Heat Sealability of Flexible Barrier Materials as Measured by Seal Strength (ASTM F2029-16). Retrieved from https://www.astm.org/Standards/F2029.htm.
- [110] International Organization for Standardization **2021**. Plastics Standard atmospheres for conditioning and testing. Retrieved from https://www.iso.org/standard/50572.html.

- [111] Schreib I, Liebmann A. Merkblatt No. 106/2011. Guideline für die Gestaltung von peelbaren Verpackungen unter dem Gesichtspunkt "Easy Opening". Arbeitsgruppe Abfüllen und Verpacken von Lebensmitteln AVL. Fraunhofer Anwendungszentrum für Verarbeitungsmaschinen und Verpackungstechnik, Dresden: Berlin, **2011**.
- [112] Kinloch AJ, Lau CC, Williams JG. The peeling of flexible laminates. *International journal of fracture* **1994**, 66(1), pp. 45-70, DOI: 10.1007/BF00012635.
- [113] Morris B. **2017**. The science and technology of flexible packaging multilayer films from resin and process to end use. *Elsevier inc* **2016**, Amsterdam, pp. 351-400. ISBN: 978-0-323-24273-8.
- [114] Farley JM, Meka P. Heat Sealing of Semicrystalline Polymer films. III. Effect of Corona Discharge Treatment of LLDPE. *Journal of Applied Polymer Science* **1994**, 51, pp. 121-131, DOI: https://doi.org/10.1002/app.1994.070510113.
- [115] American Society for Testing and Materials **2020**. Standard Test Method for Mechanical Seal Strength testing for round cups and bowl containers with flexible peelable lids (ASTM F2824-10). Retrieved from https://www.astm.org/Standards/F2824.htm.
- [116] American Society for Testing and Materials **2020**. Standard Test Methods for Internal Pressurization Failure Resistance of Unrestrained Packages (ASTM F1140-13). Retrieved from https://www.astm.org/Standards/F1140.htm.
- [117] American Society for Testing and Materials (**2020**). Standard Test Method for Burst Testing of Flexible Package Seals Using Internal Air Pressurization Within Restraining Plates (ASTM F2054-F2054M-13). Retrieved from https://www.astm.org/Standards/F2054.htm.
- [118] Falla D, Li M. Reliable hot tack testing of polyolefin film. *ANTEC* **2014**, conference proceeding, society of plastics engineers, Las Vegas.
- [119] American Society for Testing and Materials **2018**. Standard Test Methods for Hot Seal Strength (Hot Tack) of Thermoplastic Polymers and Blends Comprising the Sealing Surfaces of Flexible Webs (ASTM F1921-F1921M-12). Retrieved from https://www.astm.org/Standards/F1921.htm.
- [120] Hishinuma K. Heat sealing technology and engineering for packaging: Principles and applications. *DEStech Publications inc* **2009**, Lancaster, pp. 21-48. ISBN: 978-1-932078-85-5.
- [121] TC Meet- & Regeltechniek BV. Oppervlake thermokoppel (type 10).

 Retrieved April 27 2022 from:

 https://www.tcbv.com/thermokoppels/oppervlakte-thermokoppel.html.
- [122] Dudbridge M. Handbook of seal integrity in the food industry. *Wiley Blackwell* **2016**, Hoboken (USA), pp. 116-132, ISBN: 9781118904602.
- [123] American Society for Testing and Materials **2019**. Standard Test Method for Detecting Gross Leaks in Packaging by Internal Pressurization (Bubble Test) (ASTM F2096-11). Retrieved from https://www.astm.org/Standards/F2096.htm.

- [124] American Society for Testing and Materials (**2021**). Standard Test Methods for Pressure Decay Test for Flexible Packages With and Without Restraining Plates in Packaging by Internal Pressurization (Bubble Test) (ASTM F2095-07). Retrieved from https://www.astm.org/Standards/F2095.htm.
- [125] American Society for Testing and Materials **2020**. Standard Test Method for Nondestructive Detection of Leaks in Packages by Vacuum Decay Method (ASTM F2338-09). Retrieved from https://www.astm.org/Standards/F2338.htm.
- [126] American Society for Testing and Materials **2015**. Standard Test Method for Detecting Leaks in Nonporous Packaging or Flexible Barrier Materials by Dye Penetration (ASTM F3039-15). Retrieved from https://www.astm.org/Standards/ F3039.htm.
- [127] Chung D, Papadakis SE, Yam KL. Simple Models for Evaluating Effects of Small Leaks on the Gas Barrier Properties of Food Packages. *Packaging Technology and Science* **2003**; **16**(2): pp 77-86, DOI: 10,1002/pts.616.
- [128] American Society for Testing and Materials **2020**. Standard Test Method for Oxygen Transmission Rate Through Dry Packages Using a Coulometric Sensor (ASTM F1307-20). Retrieved from https://www.astm.org/f1307-20.html.
- [129] Ametek Mocon. OX-TRAN 2/22 OTR Analyzer. Retrieved May 19 2022 from: https://www.ametekmocon.com/products/permeationanalyzers/otr-permeation-analyzers/ox-tran-2-22-series.
- [130] American Society for Testing and Materials **2015**. Standard Test Method for Oxygen Gas Transmission Rate through Plastic Film and Sheeting using a Dynamic Accumulation Method (ASTM F3136-15). Retrieved from https://www.astm.org/f3136-15.html.
- [131] Bamps B, Peelman N, Ragaert P, De Meulenaer B, De Vlieghere F, Peeters R. Study of food preservation in defective pouches: the effect of oxygen permeation through a channel leak, induced in a seal of a package, on preservation of the food product ham sausage. *ILSI Europe* **2016**, conference proceeding, Barcelona.
- [132] D'huys K. Online inspection of package integrity. VIS-project 100492 **2013**, project proceeding, *Pack4Food*, Gent.
- [133] Coles R, McDowell D, Kirwan MJ. Food packaging technology. *Blackwell publishing Ltd* **2003**, Oxford, pp. 303-331. ISBN 13: 9780849397882.
- [134] Dudbridge M. Handbook of seal integrity in the food industry. *Wiley Blackwell* **2016**, Hoboken (USA), pp. 101-115, ISBN: 9781118904602.
- [135] Airtec solutions. How to prevent airborne dust by increasing air humidity. Retrieved April 27 2022 from: https://airtecsolutions.com/blog/airtec-blog/how-to-prevent-airborne-dust-by-increasing-air-humidity.
- [136] *Panasonic*. Static removers (ionizers). Retrieved April 27 2022 from: https://www3.panasonic.biz/ac/ae/service/tech_support/fasys/tech_guid_e/data/static_e.pdf.
- [137] Fischbein-Saxon. Smart solutions to close open-mouth bags. Retrieved April 29 2022 from: https://www.fischbein.com/wp-content/uploads/2018/06/fischbein-brochure saxon-options.pdf.

- [138] Benković M, Srečec S, Špoljarić I, Mršić G and Bauman I. Flow Properties of Commonly Used Food Powders and Their Mixtures. *Food and Bioprocess Technology* **2013**, 6 (9), pp. 2525-2537; DOI: 10.1007/s11947-012-0925-3.
- [139] Dudbridge M. Handbook of seal integrity in the food industry. *Wiley Blackwell* **2016**, Hoboken (USA), pp. 154-166, ISBN: 9781118904602.
- [140] Bamps B, Peeters R, D'huys K, De Ketelaere B, Schreib I, Stephan B. Method for analyzing the influence of contamination on seal properties of films for packaging applications. Technical bulletin for the testing of packaging systems 114/2019. Industrievereinigung für Lebensmitteltechnologie und Verpackung e.V. (IVLV). Retrieved from https://www.ivlv.org.
- [141] Ilhan I, Turan D, Gibson I, ten Klooster R. Understanding the factors affecting the seal integrity in heat sealed flexible food packages: a review. *Packaging technology and science* **2021**; 34; pp. 321-337; DOI: 10.1002/pts.2564.
- [142] Bosch. Guide to flow wrapping. *Bosch packaging technology*® **2011**. Retrieved August 10 2021 from https://vdocuments.mx/bosch-guide-to-flow-wrapping.html.
- [143] Webomatic. Tray sealer: uncompromised variety for packaging in trays. Retrieved April 29 2022 from: https://webomatic.de/wp-content/uploads/2019/05/traysealer WEBOMATIC.pdf.
- [144] Rychiger P. Typical sealing issues and troubleshooting. *IPI International Packaging Institute* **2011**; conference proceedings; Schaffhausen.
- [145] Schubert G, Plassmann O, Husch S. Hot tack of extrusion coatings on aluminum foil and paper does the process always lead to the same result?. In: *TAPPI PLACE conference* **2010**, conference proceedings, Albequerque.
- [146] Montgomery DC. Design and analysis of experiments, nineth edition. John Wiley & Sons, inc 2017, Hoboken (USA), pp. 1-22. ISBN: 9781119113478.
- [147] Mack C. Lecture64 (Data2Decision) Intro to Design of Experiments. *The university of Texas* **2016**. Retrieved November 16 2022 from: http://www.lithoguru.com/scientist/statistics/Lecture64.pdf.
- [148] Jiju A. Design of experiments for engineers and scientists, second edition. Elsevier Ltd **2014**, Boston (USA), pp. 7-18, DOI: http://dx.doi.org/10.1016/B978-0-08-099417-8.00003-1.
- [149] Mack C. Lecture68 (Data2Decision) Factorial Design of Experiments. *The university of Texas* **2016**. Retrieved November 16 2022 from: http://www.lithoguru.com/scientist/statistics/Lecture68.pdf.
- [150] Montgomery DC. Design and analysis of experiments, nineth edition. John Wiley & Sons, inc 2017, Hoboken (USA), pp. 230-307. ISBN: 9781119113478.
- [151] Mack C. Lecture71 (Data2Decision) Response Surface Modeling. *The university of Texas* **2016**. Retrieved November 16 2022 from: http://www.lithoguru.com/scientist/statistics/Lecture72.pdf.
- [152] Montgomery DC. Design and analysis of experiments, nineth edition. John Wiley & Sons, inc 2017, Hoboken (USA), pp. 489-568. ISBN: 9781119113478.

- [153] Bezerra MA, Santelli RE, Oliveira EP, Villar LS, Escaleira LA. Talanta 2008; 76(5); pp. 965-977; DOI: <u>10.1016/j.talanta.2008.05.019</u>.
- [154] Jensen W. Confirmation runs in design of experiments. *Journal of quality technology* **2016**; 48(2); pp. 162-177; DOI: 10.1080/00224065.2016.11918157.
- [155] Bach S. **2012**. Untersuchung der Vorgänge und Einflüsse beim Ultraschallfügen flexibler polymerer Packstoffe [Doctoral dissertation, Fakultät Maschinenwesen der Technischen Universität Dresden].
- [156] Thürling K. **2016**. Prozessdatenanalyse zur InlineVerminderung von Störeinflüssen beim Ultraschallsiegeln [Doctoral dissertation, Fakultät Maschinenwesen der Technischen Universität Dresden].

3. Multicriteria evaluation and optimization of the ultrasonic sealing performance based on design of experiments and response surface methodology

D'huys, K, Bamps B. Peeters R, De Ketelaere B. Multi-criteria evaluation and optimization of the ultrasonic sealing performance based on design of experiments and response surface methodology. *Packaging Technology and Science* **2019**; 32 (4); pp. 165-174. DOI: https://doi.org/10.1002/pts.2425.

This chapter develops, validates and applies a DOE-method with 3 factors (ultrasonic process parameters: force, amplitude and time) and 3 performance indicators (seal strength; horn displacement, which is closely related to seal thickness; and energy consumption), to evaluate and optimize ultrasonic sealing of a representative flexible packaging film to heat seal, with a thermal resistant poly(ethylene terephthalate) (PET) outer layer and linear low-density poly(ethylene) with C4 comonomers (LLDPE-C4) as a seal layer. The statistical methodology in this chapter is the foundation of the evaluation and optimization methods of chapters 4, 5, and 6. I contributed as second author by defining the research strategy, obtaining a relevant food packaging film, selecting the factors and performance indicators of interest, performing these experiments and reviewing and editing the draft paper. The study was performed within the TETRA project nr. 140313 'ULTRASEAL: The potential of ultrasonic sealing in packages', funded by Agentschap Innoveren & Ondernemen (VLAIO).

3.1 Introduction

Several heating principles can be used to heat seal, such as conduction with hot tools and ultrasonic friction. For heat conductive sealing, the effect of the sealing parameters on the seal quality was the subject of several studies^{1, 2, 3, 4, 5, 6, 7}. In most of these studies, the effect of the sealing parameters (time, temperature and pressure) on the seal/peel strength was evaluated, by varying one of the seal parameters at a time while keeping the others constant. Meka and Stehling (1994) considered the effect of the seal parameters not only on the seal strength of PE films, but also on the seal elongation and energy². The effect of the sealing parameters on the seal quality was also studied for ultrasonic sealing in the past, although much less extensively than for heat conductive sealing^{8, 9, 10, 11}. Bach et al. (2012) stated that the most important parameters influencing the ultrasonic sealing process are the sealing time, force and the amplitude of the horn and the authors studied the individual effect of the sealing time and force on the seal strength of commercial polyamide/poly(ethylene) films⁹. Nase et al. (2013) studied the effect of the seal force on the peel properties of poly(ethylene)/poly(1-

butene) peel films and concluded that the seal force has a strong impact on those properties⁸. Stoehr et al. (2014) performed a parameter study to characterize the effect of amplitude, force and time on the ultrasonic sealing quality of biobased packaging films produced from poly(lactic acid)¹¹. Finally, Van Oordt et al. (2014) studied the effect of ultrasonic sealing time, force and amplitude on the peel strength and behavior of poly(ethylene) composite films. The parameter effects were studied individually, although surface plots of the combined effect of time and amplitude were also shown. The authors provided a practical guideline to identify appropriate sealing parameters, although this did not include a real optimization of the parameter settings¹⁰.

The most commonly applied approach of varying a single seal parameter while keeping the others constant ('one factor at a time' approach) does not allow to study interactions or simultaneous effects of several seal parameters¹². Moreover, it does not result in a complete picture of the effect of all parameters on the seal quality and therefore does not allow for optimization. As an answer to this shortcoming, a few authors introduced the statistical concepts of 'design of experiments' (DOE) and 'response surface modelling' (RSM) in the field of heat conductive sealing 12, 13, 14. These concepts allow for a detailed analysis of the effect of the sealing parameters, provide the capability of predicting a response of interest, and this based on an efficient use of resources (workload, time, film material)¹². The purpose of DOE is to set up an experiment in such a way that insight in the effect of a set of input parameters on a certain response can be gained based on a limited number of carefully selected experimental runs. RSM is based on fitting a polynomial equation to the experimental data collected according to a certain experimental design, and in that way describing the data set and predicting the response within a certain experimental region¹⁵. Dixon et al. (2006) described the use of DOE to define an acceptable window of operating conditions for the heat sealing of medical packaging. The authors set up a central composite design and considered the peel strength as the response of the RSM. No optimization was performed¹². A similar approach was followed by Aiyengar and Divecha (2012) to study the effect of the seal settings on the seal strength of biaxially oriented poly(propylene) film, although they repeated the seal strength test ten times at each of the parameter combinations defined by a central composite design. They stated that an important characteristic of a good heat seal film is a broad seal window14. Finally, Hron and Macák (2013) used a 2k factorial design in which two levels (low and high) of each of the sealing parameters were considered, to perform a screening of the effects of the parameter settings on the seal strength¹³. In all three of these studies, heat conductive sealing was considered, with the seal/peel strength as a single response parameter, and no optimization was performed.

In practice, the seal strength is not the only relevant characteristic of a sealing procedure. Additional aspects may play a crucial role but were barely discussed in previous research. This study considers not only the seal strength, but also the ultrasonic horn displacement and the seal energy consumed by the ultrasonic equipment as measures of the ultrasonic sealing performance.

The goal of this study was to develop an efficient methodology, based on the concepts of DOE and RSM, to evaluate the ultrasonic seal performance of a representative flexible film to heat seal. A laminated film with a thermal resistant

outer PET layer and an LLDPE-C4 seal layer is used in the experiments. Besides for evaluation purposes, the developed methodology was also used for an optimization of the seal parameters towards multiple aspects of the ultrasonic sealing performance, such as the seal strength, the displacement of the ultrasonic horn and the seal energy.

3.2 Materials and methods

3.2.1 Film material

The film material studied in this work was a poly(ethylene terephthalate)-linear low-density poly(ethylene) PET/LLDPE-C4 laminate film. The thicknesses of both layers, as provided by the supplier, were 24 μm (PET) and 40 μm (LLDPE-C4). The measured total thickness of the film was 69 \pm 1 μm . The film was produced by blown extrusion, and subject to a corona pre-treatment and lamination with a solvent based-adhesive Adcote TM 301/350. The film was selected since PE is a sealing medium that is commonly used in commercial packaging films. The PET outer layer is present to improve the mechanical and barrier properties of the film.

3.2.2 Ultrasonic sealing and seal performance tests

The ultrasonic seal samples were prepared with a 35 kHz TSP750E-100-1 ultrasonic sealing device (Telsonic Ultrasonics, Switzerland) equipped with a 75x5 mm rectangular, flat surface sonotrode. An anvil with a semi-cylindrical energy director with a radius of 2.5 mm was used. After sealing, a holding time of 0.5 s and a holding force of 2 N.mm⁻¹ were applied to the seal. The most important parameter settings that have to be selected before sealing are the time, the force and the amplitude.

In this research, three main characteristics of the seal samples were measured in order to evaluate the ultrasonic sealing performance of the packaging films: the seal strength, the displacement of the ultrasonic horn and the energy consumption during sealing.

The **seal strength** [N.mm⁻¹] of all samples was tested using a 10 M universal testing machine (MTS Systems Corporation, USA) equipped with a 2 kN load cell. The measurements were performed after conditioning the samples at 23 °C and 50% relative humidity for 24 hours. A 15 mm wide sample was cut from the center of every 75 mm wide seal. Both ends of this 15 mm wide part were clamped at a distance of 10 mm. Next, a tensile test was performed with a speed of 300 mm.min⁻¹. The maximum strength value encountered in the tensile curve [N] was divided by the width of the seal sample (15 mm) to obtain the seal strength [N.mm⁻¹]. The tensile tests were performed according to ASTM guideline F88/F88M-15¹⁶.

The **horn displacement** [µm] is the maximum travel distance of the ultrasonic horn in the sample. During ultrasonic sealing, the seal material melts and the horn travels deeper into the sample. As a result, the sealed film becomes compacted until a certain maximum value. This maximum value is registered by the ultrasonic

sealing device and can be used to describe the ultrasonic sealing performance of a film material.

Finally, the **energy consumption** [J] is the amount of energy consumed by the ultrasonic sealing device during sealing, and is calculated as the area under the power [W] versus time [s] curve of the sealing process. In the first phase of the sealing process, power builds up. Next, when the seal medium starts to melt, the power decreases. Similar to the horn displacement, the value of the energy consumption is also derived from the output of the ultrasonic sealer.

3.2.3 Experimental design and seal optimization

In this work, an efficient methodology is proposed to evaluate and optimize the ultrasonic seal performance of a PET/LLDPE-C4 film. This methodology consists of five subsequent steps:

Step 1: Firstly, the experimental design space has to be defined. This means that the parameters that have the largest influence on the seal performance must be identified and for each of these parameters the boundaries within which they can be varied should be listed. In the case of ultrasonic sealing, the seal time, seal amplitude and seal force were identified as the most relevant parameters that need to be set when creating a seal. In order to determine the minimum and maximum values to consider for these parameters, preliminary experiments were performed.

Step 2: Next, an experimental design has to be set up that defines at which combinations of the input parameters, i.e. at which locations within the design space, experiments should be performed. The type of experimental design that is most suited depends on several aspects, such as the type of model one expects will provide an adequate description of the data (e.g. only main effects or also quadratic effects, including interactions or not, ...), the number of measurements that is feasible to perform, the number of input parameters, etc. In this study, an experimental design consisting of 15 well-chosen combinations of the seal time, seal force and seal amplitude was set up. These 15 settings were selected according to a Box-Behnken experimental design in order to efficiently obtain as much information as possible on the effect of the sealing parameters based on a limited amount of experiments. Such a Box Behnken design allows to fit a full Response Surface Model (RSM) including interactions and quadratic effects and thus allows for finding the optimal ultrasonic setting¹⁷. The order of the experimental runs was randomized so to minimize the unwanted effect of unknown disturbing factors. At each of the 15 parameter settings, an ultrasonic seal was created and its seal performance was measured as described earlier.

Step 3: Once the seal performance at each of the settings defined by the experimental design is known, a Response Surface Model can be fit to these values. In this study, a quadratic model of the following form was considered:

$$\hat{y} = \beta_0 + \beta_1 x_1 + \beta_2 x_2 + \beta_3 x_3 + \beta_{12} x_1 x_2 + \beta_{23} x_2 x_3 + \beta_{13} x_1 x_3 + \beta_{11} x_1^2 + \beta_{22} x_2^2 + \beta_{33} x_3^2$$
 Equation 8.

with x_1 , x_2 and x_3 the three input parameters seal time, amplitude and force, \hat{y} the response of interest, e.g. the seal strength, and the β 's are the coefficients¹⁸. Besides the main effects, the interaction terms and quadratic terms were also considered in the model. In order to identify significant effects, an all possible subsets procedure was followed and non-significant effects were removed from the prediction model¹⁹. The best subsets approach for variable selection allows to identify the model that fits best from all possible subset models, i.e. from all possible models including a certain combination of the effects described in the formula above. Several criteria can be used for variable selection, such as the Rsquare, the Akaike information criterion (AIC) and the Bayesian information criterion (BIC)²⁰. In general, a model with a high R-square and a low AIC and BIC should be preferred. The R-square provides information on the goodness of fit of the model. The AIC holds information on the quality of the model relative to that of other models and rewards goodness of fit. However, the AIC also includes a penalty for the number of parameters in the model and thus discourages overfitting of the data. The BIC holds information that is similar to the AIC, but overfitting of the data is more severely discouraged by the BIC than by the AIC²¹. Often, these different selection criteria do not hold exactly the same information, i.e. they do not necessarily all point towards exactly the same model. However, they provide an adequate guideline for model selection. In all of the models, the selection of significant terms was based on a significance level a = 0.05.

Step 4: Once the most suited regression model has been selected, this model allows to predict the response (e.g. seal strength) for every possible combination of the input parameters (seal time, amplitude and force). This knowledge can then be used to find the combination of input settings that results in the desired value of the response, based on the use of desirability functions. This desired value can be a maximum, a minimum or a specific target value, each corresponding to a specific shape of the desirability function. Moreover, desirability functions of any arbitrary shape can be defined. If the goal is to maximize the seal strength, for example, the desirability function can be defined as a linear increase between the minimum seal strength (desirability = 0) and the maximum seal strength (desirability = 1). It is not only possible to optimize the input parameters with respect to a single response variable, but also with respect to multiple responses. In this case, an individual desirability function is first defined for each of the responses (e.g. seal strength, horn displacement and seal energy). Next, an overall desirability function is defined as the weighted average of these individual desirability functions and the responses are optimized considering this overall desirability¹⁵.

Step 5: The final step of the efficient optimization procedure involves performing confirmation experiments (10 runs) at the defined optimal settings in order to validate the model obtained. Based on a confidence interval calculation of the confirmation runs (CICon approach) as suggested by Antony (2003), the predicted and measured optima were tested for significant differences^{22, 23}.

All statistical analyses were performed in the software package JMP Pro 12 (The SAS Institute Inc., USA). A significance level a of 0.05 was used in the entire paper, unless indicated otherwise.

3.2.4 Seal window calculation

In practice, it is not only relevant to identify a certain setting at which a packaging film will show high seal performance. Another important aspect is to study how sensitive the seal performance is to slight changes in the seal settings. This aspect was translated into a quantitative measure, which is here defined as the 'seal window'. The seal window was quantitatively expressed as the percentage of the entire design space within which the seal strength reaches a value of 90% of the optimum seal strength, or larger. The larger this percentage, the larger the region of the design space within which a sufficient seal strength is obtained.

3.3 Results and discussion

In Section 3.3.1, the design space and experimental design set up for this study are described. In Sections 3.3.2 and 3.3.3, the response surface modelling and the results of the optimization procedure described above are illustrated. In Sections 3.3.4 and 3.3.5, profilers and desirability plots are given for single and multiple responses. In Section 3.3.6, the optimized seal settings and the experimental validation results are shown. Finally, in Section 3.3.7, the seal window of the PET/LLDPE-C4 film is discussed.

3.3.1 Design space and experimental design

The input parameters considered in the optimization study were the seal time, the force and the amplitude. Based on preliminary experiments, the limits of the design space were selected as follows: the minimum values were set at the parameter combinations at the border of unsealed/peelable seal and the maximum values were set at the parameter combinations at the border of tear seal/cut through. The parameter ranges thus obtained are 0.1 to 0.3 s (seal time), 2 to 6 N.mm $^{-1}$ (seal force) and 18 to 36 µm (amplitude). These ranges show a large overlap with the settings applied in previous research on similar flexible films with polyolefin layers 8 , 9 .

Within these limits of the design space, 15 seal setting combinations were defined according to a three-factor, three-level Box-Behnken experimental design. In Table 7, the 15 design settings together with their output for the seal performance responses (seal strength, horn displacement and seal energy) for the PET/LLDPE-C4 film are listed.

Table 7: Experimental runs and input parameters of the Box-Behnken design and seal strength [N/mm], horn displacement [µm] and energy consumption [J] responses for the PET/LLDPE-C4 film material.

Run	Time [s]	Force [N/mm]	Amplitude [µm]	Strength [N/mm]	Compaction [µm]	Energy consumption [J]
1	0.2	2	36	1.31	10	27.75
2	0.3	4	18	0.30	10	21.93
3	0.1	4	36	1.76	40	17.76
4	0.2	2	18	0.05	10	7.50
5	0.2	4	27	2.90	30	21.05
6	0.2	4	27	2.43	30	20.10
7	0.1	6	27	2.90	80	16.30
8	0.2	4	27	2.09	30	17.65
9	0.3	6	27	2.11	60	47.62
10	0.2	6	18	1.18	40	22.58
11	0.1	2	27	0.96	10	7.55
12	0.2	6	36	3.52	70	59.64
13	0.3	2	27	0.74	10	15.61
14	0.3	4	36	3.22	50	55.86
15	0.1	4	18	0.52	20	5.89

3.3.2 Response surface model

In the next step, a response surface model was fitted for each of the three response parameters (seal strength, horn displacement and seal energy) and a selection of the significant terms was performed as described in Section 3.2.3. The regression equation, significant coefficients, terms and regression significance of the models obtained are shown in Table 8, Table 9 and Table 10 for the seal strength, the horn displacement and the seal energy, respectively.

Table 8: Significant coefficients, terms, regression significance and equation of the seal strength model for the PET/LLDPE-C4 film.

Coefficients	Term	Value	p-value				
$oldsymbol{eta}_0$	Intercept	-2.554	0.004				
$oldsymbol{eta}_2$	Force	0.416	0.001				
β_3	Amplitude	0.108	0.0003				
β_{33}	Amplitude ²	-0.007	0.08				
Regression significance			0.0002				
Seal strength = $\beta_0 + \beta_2 \times \text{Force} + \beta_3 \times \text{Amplitude} + \beta_{33} \times \text{Amplitude}^2$							

Table 9: Significant coefficients, terms, regression significance and equation of the horn displacement model for the PET/LLDPE-C4 film.

Coefficients	Term	Value	p-value						
$oldsymbol{eta_0}$	Intercept	-52.911	0.0005						
$oldsymbol{eta}_2$	Force	13.124	< 0.0001						
β_3	Amplitude	1.250	0.0031						
$oldsymbol{eta}_{23}$	Force × Amplitude	0.417	0.1031						
Regression significance			<0.0001						
Horn displaceme	Horn displacement = $\beta_0 + \beta_2 \times \text{Force} + \beta_3 \times \text{Amplitude} + \beta_{23}$ force \times Amplitude								

Table 10: Significant coefficients, terms, regression significance and equation of the seal energy model for the PET/LLDPE-C4 film.

Coefficients	Term	Value	p-value					
$oldsymbol{eta_0}$	Intercept	-63.138	<0.0001					
β_1	Time	0.117	<0.0001					
β_2	Force	5.483	0.0001					
$oldsymbol{eta}_3$	Amplitude	1.432	<0.0001					
$oldsymbol{eta_{33}}$	Amplitude ²	0.081	0.0243					
$oldsymbol{eta_{12}}$	Time × force	0.029	0.0338					
$oldsymbol{eta_{13}}$	Time × Amplitude	0.006	0.0415					
Regression significance			< 0.0001					
Seal energy = $\beta_0 + \beta_1 \times \text{Time} + \beta_2 \times \text{Force} + \beta_3 \times \text{Amplitude} + \beta_{33} \times \text{Amplitude}^2 + \beta_{12} \times \text{Time} \times$								

Force + β_{13} × Time × Amplitude

In Figure 56, a graphical representation of the response surface models for seal strength, horn displacement and energy as a function of the force and amplitude is shown (seal time = 0.2 s). The seal strength model includes a first order effect of force and amplitude and a quadratic effect of amplitude. Time is not included in the seal strength model. As shown in Figure 56, the seal strength increases with an increasing force. The seal strength increases quadratically with an increasing level of amplitude. The horn displacement model includes first order effects of force and amplitude, and an interaction effect of force and amplitude. As shown in Figure 56, the horn displacement increases towards higher levels of force and amplitude. The seal energy model includes first order effects of time and force, a quadratic effect of amplitude, and interaction effects of time and force and of time and amplitude. As shown in Figure 56, the energy consumed by the sealing process increases when force and amplitude values are higher.

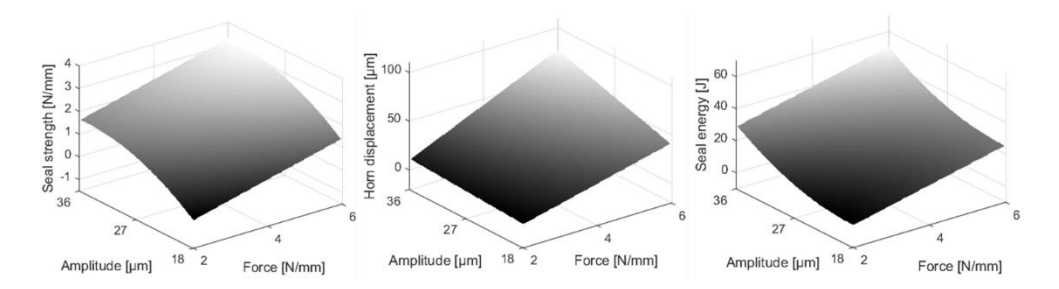


Figure 56: Response surface model for seal strength, horn displacement and seal energy as a function of force and amplitude (seal time = 0.2 s) for the PET/LLDPE-C4 film.

3.3.3 Optimization procedure

The response surface models described in the previous section allow to predict the seal performance responses (seal strength, compaction and energy) for every possible combination of the input parameters (time, force and amplitude) within the limits of the design space. In this section, it is described how the response surface models can be used to optimize the seal settings to obtain an optimum seal performance. In a first case, only a single response (seal strength) is

considered, while in the second case, a multiple response optimization is illustrated.

3.3.4 Single response

In Figure 57, the optimization of force and amplitude settings to obtain a maximum seal strength is illustrated. The two columns on the left-hand side of the graph represent the influence of force and amplitude on the seal strength. The column on the right-hand side shows the desirability function for seal strength. Since the objective in this first case was to maximize the seal strength, the desirability function was defined as a linear increase from the lowest seal strength level (desirability = 0) to the highest seal strength level (desirability = 1). Next, the desirability was maximized, resulting in a seal strength of 3.288 N.mm $^{-1}$ for a seal force of 6 N.mm $^{-1}$ and an amplitude of 35.115 μ m. These optimal settings, together with the predicted value of the optimum, are highlighted in red.

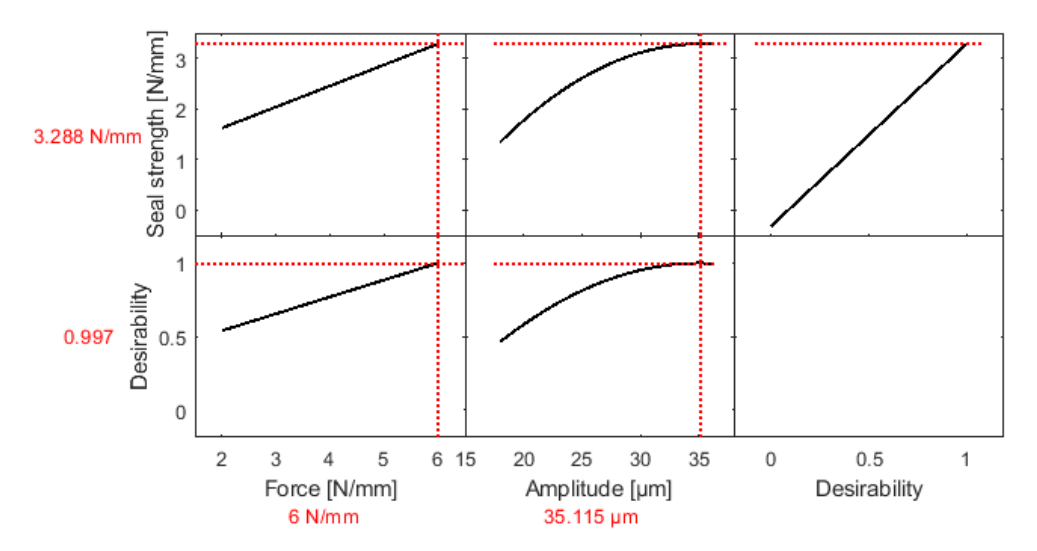


Figure 57: Profiler and desirability plot for the optimization towards seal strength only. The optimum and the optimal settings for force and amplitude are highlighted in red.

3.3.5 Multiple responses

The seal strength is not the only parameter providing relevant information about the seal quality/seal performance. Therefore, in this section the other parameters are also considered in the optimization.

Firstly, a combined optimization considering both **seal strength and horn displacement** was performed. In Figure 58, the desirability plots for this two-response optimization are shown. The desirability plot for seal strength consists of a linear increase from low seal strength to high seal strength, as stated earlier. The desirability function for horn displacement has a different shape. A very large

horn displacement, i.e. almost all of the sealant material has been squeezed out during sealing, is unwanted since there is a risk of completely destroying or cutting through the seal. Therefore, a step-shaped desirability function was defined, assigning a desirability '1' to horn displacement levels ranging from 0 to 40 μm and a desirability '0' to horn displacement levels larger than 40 μm . In this way, it was defined as desirable to have at least 50 % of the original thickness of the seal layer left in the final seal. As described in Section 3.2.3, an overall desirability function was defined as the weighted average of these individual desirability functions and the responses were optimized considering this overall desirability. In this way, an optimized seal strength level of 2.397 N.mm $^{-1}$ and a horn displacement of 40 μm were obtained. The settings at which these optimized responses were achieved are 4.074 N.mm $^{-1}$ (seal force) and 31.446 μm (amplitude). By considering both responses in the optimization, a compromise was calculated that results in desirable results for both.

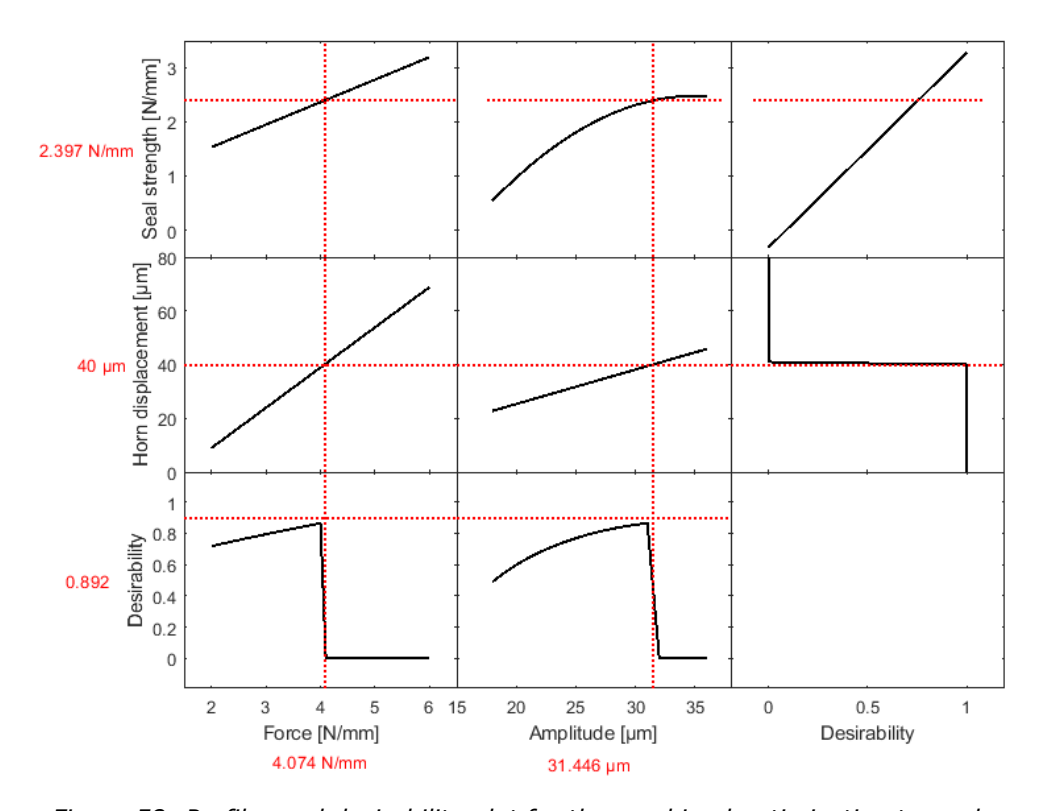


Figure 58: Profiler and desirability plot for the combined optimization towards seal strength and horn displacement. The optimum and the optimal settings for force and amplitude are highlighted in red.

Secondly, a combined optimization considering **seal strength, horn displacement and seal energy** was performed. In Figure 59, the desirability plots for this three-response optimization are shown. The desirability plots for seal strength and horn displacement were identical to the ones used in the two-response optimization. The desirability function for seal energy consists of a linear

decrease from high seal energy levels (desirability = 0) to low seal energy levels (desirability = 1). In this way, an optimal combination of seal settings was identified to achieve a seal strength that is as high as possible, a horn displacement that is limited and a seal energy that is as low as possible. An optimum seal strength of 2.321 N.mm $^{-1}$, an optimum horn displacement of 40 μm and an optimum seal energy of 11.664 J were obtained at a combination of seal settings of 0.1 s (seal time), 4.323 N.mm $^{-1}$ (seal force) and 28.751 μm (seal amplitude). Again, a compromise was calculated that considered a weighted average of all three of the desirability functions.

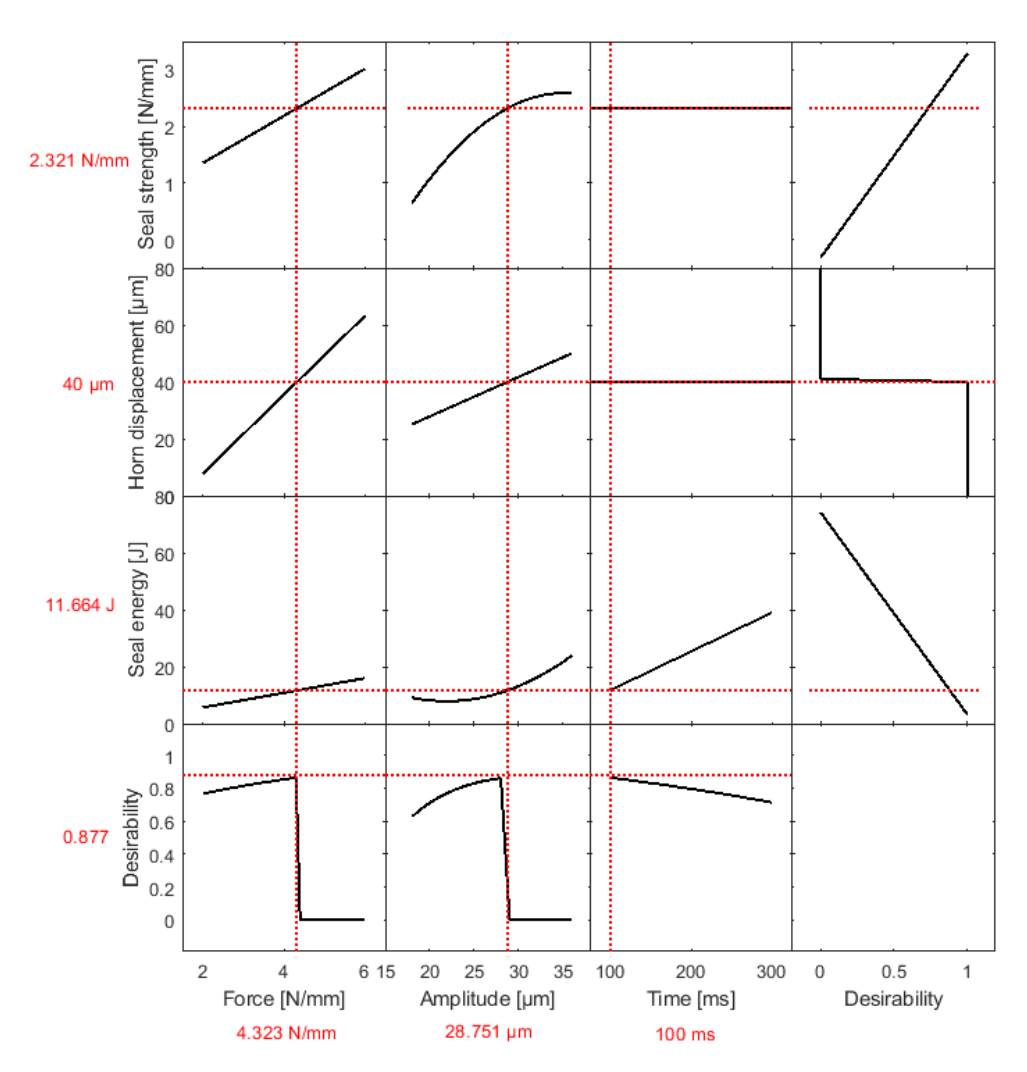


Figure 59: Profiler and desirability plot for the combined optimization towards seal strength, horn displacement and seal energy. The optimum and the optimal settings for force and amplitude are highlighted in red.

3.3.6 Optimized seal settings and experimental validation

Since in addition to the seal strength, in practice both the horn displacement and seal energy are also relevant, the multi-response optimization presented in the previous section was considered as a suitable approach to optimize the seal settings. Validation experiments were performed at the optimum ultrasonic sealing settings. In Table 11, the results of these validation experiments are summarized. The predicted optima and the results of the confirmation runs were tested for significant differences as described in Section 3.2.3. On a significance level of 0.05, predicted and confirmed optima were different for both the seal strength and the seal energy but not for the horn displacement. On a significance level of 0.10, there were no significant differences between predicted and confirmed optima for any of the output parameters considered.

Table 11: Experimental validation of predicted optimum. The predicted optimum and confirmation runs were tested for being significantly different (a = 0.05 and a = 0.1) using the confidence interval approach suggested by Antony^{22, 23}.

Parameter	Predicted optimum	Mean of confirmation runs, n=10	Standard deviation confirmation runs	Significantly different, p < 0.05	Significantly different, p < 0.1
Seal strength (N.mm ⁻¹)	2.32	1.94	0.42	Yes	No
Horn displacement (µm)	40.00	40.00	6.67	No	No
Energy (J)	11.66	13.68	2.13	Yes	No

3.3.7 Seal window

In Figure 60, the seal window for the PET/LLDPE-C4 film is illustrated. As stated in Section 3.2.4, this seal window corresponds to all combinations of input parameters (time, force, amplitude) within the considered design space that result in a seal strength of at least 90% of the optimum seal strength. For this film, the seal window corresponds to all combinations of the input parameters that result in a seal strength of 2.089 N.mm⁻¹ or more. A seal strength of 2.089 N.mm⁻¹ or more is obtained for 39.41% of the input parameter combinations in the considered design space. A broad seal window is in general a desired characteristic of a packaging film, since it ensures sufficient seal strength even in the case of (slightly) deviating seal settings. Since time was shown to have no significant effect on the seal strength, the seal window was shown as a function of force and amplitude only.

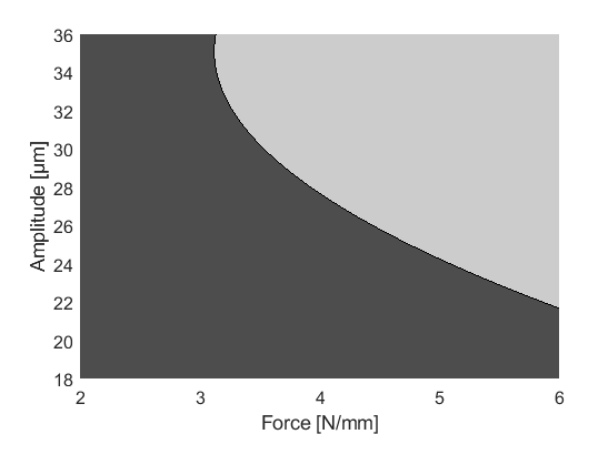


Figure 60: Seal window of the PET/LLDPE-C4 film. The light grey area indicates all combinations of the input parameters force and amplitude within the considered design space that result in a seal strength value of at least 90% of the optimum seal strength. The seal time was shown to have no significant effect on the seal strength for this film.

3.4 Conclusions

In this work, an approach based on the principles of design of experiments and response surface modelling was presented to optimize the ultrasonic sealing performance of a PET/LLDPE-C4 flexible film laminate.

Based on a limited number of experimental runs, defined according to an efficient Box-Behnken experimental design, response surface models of the seal strength, the horn displacement and the seal energy as a function of the seal settings (time, force and amplitude) were built. Next, these models were used to calculate the optimal combinations of seal settings resulting in (1) maximum seal strength, (2) maximum seal strength and a value of the horn displacement below a certain limit and (3) maximum seal strength, a horn displacement below a certain limit and minimum energy use of the sealing process. In the case of the multiple output optimizations, a compromise was obtained by assigning the same weight to each of the different outputs.

Since all three of the outputs are relevant in practice, the combined optimization towards strength, horn displacement and energy was selected as the most relevant and was experimentally validated. The predicted optimum was obtained at a seal time of 0.1 s, a seal force of 4.323 N.mm $^{-1}$ and a seal amplitude of 28.751 µm. The predicted optimum seal strength was 2.321 N.mm $^{-1}$, the horn displacement 40 µm and the seal energy 11.664 J. The confirmation runs performed at this optimum resulted in a horn displacement that was not significantly different (α =0.05) from the predicted value and in a seal strength and seal energy that were not significantly different (α =0.1) from the predicted values. In practice, not only the optimum is of interest, but also the seal window.

The seal window was defined as the region of the considered design space within which the seal strength achieved is at least 90% of the optimum seal strength. For the PET/LLDPE-C4 film, a seal strength of 90% of the optimum or more was obtained for 39% of the input parameter combinations within the design space. A broad seal window is a desired characteristic of a packaging film, since it ensures sufficient seal strength even in the case of (slightly) deviating seal settings.

Although illustrated for a single film and a single sealing process, the approach presented in this paper has a broad applicability towards other film types and sealing processes. It is flexible with respect to the definition of the input parameters and the design space, the considered output parameters and the type of desirability functions. The DOE-approach to evaluate and optimize seal performance is slightly altered in chapters 4, 5 and 6 for the specific cases of seal-through-contamination and peeling during and after cold storage.

3.5 References

- [1] Theller HW. Heat sealability of flexible web materials in hot-bar sealing applications. *J Plast Film Sheeting* **1989**, 5, pp. 66-93, DOI: https://doi.org/10.1177/875608798900500107.
- [2] Stehling FC, Meka P. Heat sealing of semicrystalline polymer films. II. Effect of melting distribution on heat-sealing behavior of polyolefins. *J Appl Polym Sci.* **1994**, 51(1):105-119, DOI: https://doi.org/10.1002/app.1994.070510112.
- [3] Planes E, Flandin L. Optimizing the heat sealing parameters of multilayer polymeric films. *J Mater Sci* **2011**, 46, pp. 5948-5958.
- [4] Najarzadeh Z, Ajji A. A novel approach toward the effect of seal process parameters on final seal strength and microstructure of LLDPE. *J Adhes Sci Technol* **2014**, 28(16):1592-1609, DOI: https://doi.org/10.1080/01694243.2014.907465.
- [5] Matthews J, Hicks B, Mullineux G, et al. An empirical into the influence of sealing crimp geometry and process settings on the seal integrity of traditional and biopolymer packaging materials. *Packag Technol Sci.* **2013**, 26, pp. 355-371, DOI: https://doi.org/10.1002/pts.1991.
- [6] Aithani D, Lockhart H, Auras R, Tansprasert K. Heat sealing measurement by an innovative technique. *Packag Technol Sci.* **2006**, 19, pp.245-257, DOI: https://doi.org/10.1002/pts.728.
- [7] Yuan CS, Hassan A, Ghazali MIH, Ismail AF. Heat sealability of laminated films with LLDPE and LDPE as the sealant materials in bar sealing applications. *J Appl Polym Sci.* **2007**, 104(6), pp. 3736-3745, DOI: https://doi.org/10.1002/app.25863.
- [8] Nase M, Bach S, Zankel JP, Majschak JP, Grellman W. Ultrasonic sealing versus heat conductive sealing of polyethylene/polybutene-1 peel films. *J Appl Polym Sci* **2013**, 130(1), pp. 383-393, DOI: https://doi.org/10.1002/app.39171.
- [9] Bach S, Thürling K, Majschak JP. Ultrasonic sealing of flexible packaging films Principle and characteristics of an alternative sealing method. *Packag Technol Sci* **2012**, 25(4), pp.233-248, DOI: https://doi.org/10.1002/pts.972.

- [10] van Oordt T, Barb Y, Zengerle R, von Stetten F. Lamination of polyethylene composite films by ultrasonic welding: Investigation of peel behavior and identification of optimum welding parameters. *J Appl Polym Sci* **2014**, 131(10), pp. 40291-1-40291-40297, DOI: https://doi.org/10.1002/app.40291.
- [11] Stoehr N, Baudrit B, Haberstroh E, Nase M, Heidemeyer P, Bastian M. Ultrasonic welding of plasticized PLA films. *J Appl Polym Sci* **2014**, 132(4), pp. 41351-1-41351-41358, DOI: https://doi.org/10.1002/app.41351.
- [12] Dixon D, Eatock J, Meenan BJ, Morgan M. Application of Design of Experiments (DOE) techniques to process validation in medical device manufacture. *J Valid Technol* **2006**;12(2), pp. 1-9.
- [13] Hron J, Macák T. Application of design of experiments to welding process of food packaging. *Acta Univ Agric Silvic Mendelianae Brun*. **2013**, LXI(100), pp. 909-915.
- [14] Aiyengar R, Divecha J. Experimental and statistical analysis of the effects of the processing parameters on the seal strength of heat sealed, biaxially oriented polypropylene film for flexible food packaging applications. *J Plast Film Sheeting* **2012**, 28(3), pp. 244-256, DOI: https://doi.org/10.1177/8756087912440000.
- [15] Bezerra MA, Santelli RE, Oliveira EP, Villar LS, Escaleira LA. Response surface methodology (RSM) as a tool for optimization in analytical chemistry. *Talanta*. **2008**, 76, pp. 965-977, DOI: https://doi.org/10.1016/j.talanta.2008.05.019.
- [16] American Society for Testing and Materials **2015**. Standard Test Method for Seal Strength of Flexible Barrier Materials (ASTM F88/F88M-15). Retrieved from https://www.astm.org/Standards/F88.htm.
- [17] Montgomery DC. Design and Analysis of Experiments. 8th ed. New York: *Wiley* **2012**.
- [18] Myers RH, Montgomery DC, Anderson-Cook CM. Response Surface Methodology: Process and Product Optimization Using Designed Experiments. 2nd ed. Hoboken: *John Wiley & Sons, Ltd* **2011**.
- [19] Miller A. Subset Selection in Regression. 2nd ed. New York: *Chapman and Hall/CRC* **2002**.
- Zhang Z. Variable selection with stepwise and best subset approaches. *Ann Transl Med* **2016**; 4(7), pp. 136, DOI: <u>10.21037/atm.2016.03.35</u>.
- [21] Burnham KP, Anderson DR. Multimodal inference: Understanding AIC and BIC in model selection. *Sociol Methods Res* **2004**,33, pp. 261-304, DOI: https://doi.org/10.1177/0049124104268644.
- [22] Antony J. Design of Experiments for Engineers and Scientists. *Burlington*: Butterworth-Heinemann; **2003**.
- [23] Jensen WA. Confirmation runs in design of experiments. *J Qual Technol* **2016**, 48(2), pp. 162-177, DOI: https://doi.org/10.1080/00224065.2016.11918157.

4. Evaluation and optimization of seal behaviour through solid contamination of heat - sealed films

Bamps B, D'huys K, Schreib I, Stephan B, De Ketelaere B, Peeters R. Evaluation and optimization of seal behaviour through solid contamination of heat sealed films. *Packaging Technology and Science* **2019**; 32 (7); pp. 335-344. DOI: https://doi.org/10.1002/pts.2442.

According to a large-scale study in the UK, over one third of sealed food packages have seal integrity problems. Contamination of the seal area is the main cause of defect seals. As a result, a staggering amount of 666.000 tonnes of food and packaging materials could enter landfill for the UK example. Contamination of the seal area causes 65% of seal defects ^{1,2}. There is no standardized method to apply contamination in the seal area. Only few papers in seal literature are available on this topic.

In this chapter I developed and applied a standardized method to apply solid granular contamination in seal areas.

The DOE-methodology, presented in the previous chapter, is adapted and aimed to study seal-through-contamination. A DOE-method with 3 factors (hot tool process parameters: temperature, pressure and time) and 1 performance indicator (seal strength), referred to as response in this publication, is developed, validated and applied to evaluate and maximize clean and contaminated seal strength of 3 flexible packaging films, that differ in the seal layer with metallocene catalysed linear low-density poly(ethylene) (mLLDPE), polyolefin plastomer and/or ionomer. These materials, often used in industry to seal-through-contamination, are evaluated in this chapter. In the broader framework of this study, hot tack and DSC tests are performed and related with the DOE-results, to explain differences in seal performance and thus gain a better understanding of the relation of seal materials and their clean and granular contaminated seal performance. Additional dye penetration experiments are performed on seals that have maximized strengths to evaluate seal integrity. The study was performed within the CORNET-framework (EVOCOSEAL: Evaluation and Optimization of Contaminated Seal Performance for Food Packaging', funded by the Flemish (Agentschap Innoveren & Ondernemen (VLAIO-TETRA nr. 150817)) and German government (German Federal Ministry for Economic Affairs and Energy (BMWi, IGF project no. 172 EBR)).

4.1 Introduction

Only 16 % of the packers perform an inspection of all produced goods. The majority just inspects samples with an interval of 30 minutes².

One way to prevent seal defects as a result of contamination is to work with materials that are able to seal-through-contamination at particular seal settings to decrease the number of defective packages. Several poly(ethylene)-based packaging materials have been developed with a good seal performance through contamination in the last decades. Examples of these materials are metallocene catalysed linear low-density poly(ethylene) (mLLDPE), polyolefin plastomer and ionomer³.

In scientific and technical papers, several tests are performed on packaging films with contaminated seals such as seal strength, leak rate, and degree of particle encapsulation (caulkability)^{4, 5, 6, 7, 8}. This study is focussed on seal strength. Hot tack tests are performed to evaluate the resistance of packaging films against spring back forces^{5, 6, 8, 9}. The relation of seal-through-contamination and hot tack performance is part of this study. In the last decades the influence of seal material composition on the contaminated seal performance was the topic of a limited amount of studies and these studies did not include a well described application method for solid contamination^{4, 5, 7, 8}. Moreover, there are no methods described in these studies to obtain the optimal or maximal seal performance through contamination.

4.2 Objectives

The main objective of this study is to present a method to optimize the granular contaminated seal strength of packaging films. A protocol is described to apply solid contamination in a standardized way, this protocol was missing in previous studies with powder or granulate contamination. An optimization method is presented that is based on our previous study on ultrasonic sealing (chapter 3)¹⁰. In this study, a similar methodology is used in order to receive information on the influence of all relevant seal parameters on the heat conductive sealing process, based on a limited number of carefully selected experiments.

A second objective is to evaluate the influence of variation in seal layer composition (metallocene PE, plastomer and ionomer) on the seal-through-contamination performance (seal strength, width process window, leak tightness) by using the application and optimization methods of this study. Hot tack tests are evaluated as predictive tests for contaminated seal performance.

4.3 Materials & methods

4.3.1 Materials

Commercial multilayer packaging films for flowpack applications

Table 12 shows the multilayer structure of three flowpack films, evaluated and optimized in this study. Each film has a 12 μ m thick poly(ethylene terephthalate) (PET) outer layer. A 3-layer blown film line with three nozzles is used for the production of the seal layers. The upper 35 μ m has the same composition for the three films, containing a blend of low-density poly(ethylene) (LDPE) and metallocene linear low-density poly(ethylene) (mLLDPE). The films differ mainly in the 15 μ m lower seal layer. Film 1 has a blend of LDPE and mLLDPE while film 2 has a blend of LDPE and polyolefin plastomer (mLLDPE with a high amount of comonomer) in that area. Both films have 2% processing aid in the lower seal layer. Film 3 has a 5 μ m layer of acid copolymer resin between the 35 μ m PE and the 10 μ m ionomer layer to ensure the bonding of both layers.

Table 12: Multilayer structure of the 3 packaging films.
Film 1 Film 2 Film 3

PET	12	PET	12	PET	12
	μm		μm		μm
80% LDPE - 20%	15	80% LDPE - 20%	15	80% LDPE - 20%	35
mLLDPE	μm	mLLDPE	μm	mLLDPE	μm
80% LDPE - 20%	20	80% LDPE - 20%	20	acid copolymer resin	5 µm
mLLDPE	μm	mLLDPE	μm		
68% LDPE - 30%	15	68% LDPE - 30%	15	Sodium ionomer	10
mLLDPE	μm	plastomer	μm		μm

Contamination types

Two types of solid contamination are used in this study: sieved ground coffee (Delhaize, Belgium; sieved to obtain a particle size between 500 and 630 μ m using a Fritsch analysette 3 sieve shaker system) and freeze-dried pork blood powder (Solina, Germany; particles with an average size of 100 μ m).

4.3.2 Methods

Sample preparation contaminated seals

Films, sealed samples and solid contamination are stored at a temperature of 23 °C and a relative humidity of 50 %. The precision balance OHAUS Explorer® (Mettler-Toledo International inc, United States of America) with readability of 0.0001 g is used for all weighings.

Figure 61 shows an illustration of the sample preparation. The sample is cut in machine direction (MD) with a width of 50 mm and an appropriate length to perform a seal strength test (in this study the length exceeded 100 mm) (I). An area of 20 mm by 40 mm is then marked on the film sample. It is important that the chosen length has sufficient extra margin compared with the seal length to ensure that the contamination is distributed over the full length of the seal. In this case 20 mm is chosen because the used sealer produces 10 mm length seals. The

required amount of solid contamination is weighed. In order to facilitate the sealing with contamination, a simple cardboard tool is cut out of a cardboard sheet with an inner hole with larger width and length than the seal bar. After one film sample is fixed with plastic tape to this cardboard tool, the contamination is applied with a small spoon in the designated area. In this study 0.020 g is applied in a 20x40 mm² region to achieve a 25 g.m⁻² contamination density. When the contamination is applied and evenly distributed by eye, the second film sample is used to cover the contamination and fixed with plastic tape (II). The cardboard tool with contaminated film samples is manually placed between the seal bars and the seal is formed. Seals are produced with the Labthink HST-H3 heat seal tester (Labthink Instruments Co Ltd, People's Republic of China). This sealer has two flat aluminum bars covered with silicon tape to prevent contamination, pushed or blown out the seal area by seal bar movement, from sticking to the bars. After sealing, the amount of contamination which is not trapped within the seal area is carefully removed using a small brush (III).

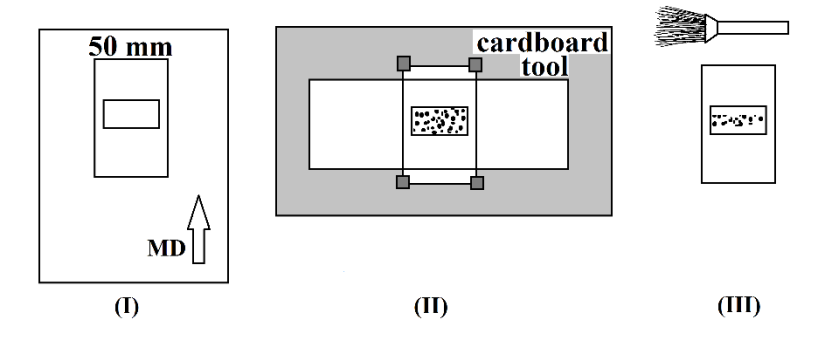


Figure 61: Contaminated seal preparation; I: Width and orientation of seal sample; II: Fixation of seal sample on cardboard tool, prior to heat conductive sealing; III: Cleaning of sealed sample with brush.

Film characterization

<u>Differential scanning calorimetry (DSC):</u> To characterize the thermal behaviour of the packaging material and to relate this to the heat conductive sealing performance, DSC measurements were executed with the instrument 2920 MDSC V.2.6A (TA instruments, United States of America). The three film samples and the main components of the seal layer (granulate form of LDPE, mLLDPE, plastomer, acid copolymer resin and sodium ionomer) were tested in a sequence of two controlled heatings and one cooling down stage within the range of $10^{\circ}\text{C} \rightarrow 200^{\circ}\text{C}$ at a heating/cooling speed of $10^{\circ}\text{C.min}^{-1}$. The heating does not exceed 200°C to prevent the PET layer from melting as this study focusses on the components of the seal layer and the seal layer as its whole. The first heating cycle is performed to delete the thermal history. The second heating cycle is used to obtain the melting peak temperature and the melting onset temperature (intersection of the tangent of the peak and the extrapolated baseline). Both of these temperatures are used to compare the materials.

<u>Hot tack:</u> 25 mm wide samples were tested with a J&B Hot Tack Tester model 5000 MB (Vived-Management, Belgium) according to ASTM F1921 at a tensile speed of 200 mm.s⁻¹. Maximum force is divided by seal width (25 mm) to obtain the hot tack strength. Seal time, seal pressure and cool time were kept constant at respective values of 1.0 s, 0.3 N.mm⁻² and 0.1 s while seal temperature was varied. Samples are tested in threefold, average values and standard deviations are shown.

Seal characterization

Seal strength is tested according to ASTM F88 on 15 mm wide samples. These samples are tested unsupported. Clamp distance is 10 mm and tensile speed is 300 mm.min^{-1} . The seal strength is obtained by dividing maximum force with seal width (15 mm).

The dye penetration test uses an aqueous solution with 0.05% indicator dye (toluidine blue) and 3% wetting agent (poly(ethylene glycol tert-octylphenyl ether)) to determine if there are leaks. It allows to detect and locate channel leaks which are equal to or greater than channels caused by a wire with diameter of 50 µm. The qualitative information (leak or no leak) delivers complementary information to seal strength. It is performed according to ASTM-F3039 on samples as shown in Figure 62. The edges of the (contaminated) seal samples need to be sealed to have a reservoir where 1 ml dye can be poured in (I). After removing the sealed edges at one side of the seal, the seal can be pressed to an absorbing white paper after adding the dye. The package is held in a vertical position for 1 minute so that the dye can penetrate through possible channel leaks by gravity (II). If a stain is visible on the paper the seal is reported as leaker. This test can be performed prior to the seal strength test if the seal strength of a sample is not influenced by the penetrating dye. This was confirmed by preliminary tests (results not shown). Samples that pass this dye penetration test are considered as leak tight.

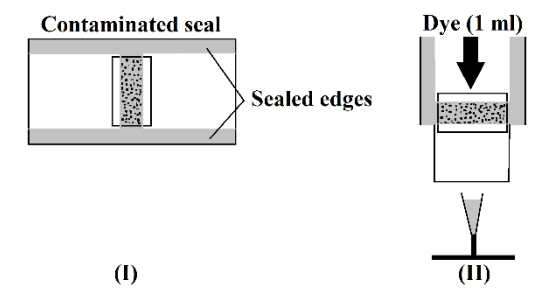


Figure 62: Dye penetration test; I: Sealed edges (grey) of sealed contaminated sample (grey + black dots, representing coffee powder); II: Visual inspection after applying dye solution at contaminated seal.

Maximization of contaminated seal quality

In order to assess the effect of the sealing parameters (temperature, time, pressure) on the seal quality of both clean and contaminated (coffee and blood powder) seals, the approach presented in D'huys et al. (2019) was followed. This approach is based on the concepts of design of experiments (DOE) and response surface modelling. The steps will be briefly described below for the case considered in this study.

First, a design space was defined that includes the three most important seal parameters: bar temperature (°C), seal time (s) and seal pressure (N.mm $^{-2}$). The effect of these parameters is studied within certain limits. There are no strict rules to set these limits. They can be based on film specifications, on the limits of the sealing process, on the relevance for the application and/or on results of preliminary tests. In this study, the limits considered for bar temperature, seal time and pressure are respectively 120 to 180 °C, 0.4 to 1.0 s and 1.0 to 4.0 N.mm $^{-2}$.

Secondly, an experimental design is set up. In this study a 20 point I-optimal design was selected, rather than the Box-Behnken design of a previous study¹⁰. This I-optimal design allows to include corner points of the design space which represent extreme parameter combinations. Moreover, it allows to include a third order effect of seal pressure in the response surface model, which was shown to possibly be of interest, based on preliminary experiments.

The third step involves fitting a response surface model with three input variables (temperature, time and pressure) to the seal strength values obtained at the 20 experimental runs. The following quadratic model with interactions was fitted:

$$y = \beta_0 + \beta_1 x_1 + \beta_2 x_2 + \beta_3 x_3 + \beta_{12} x_1 x_2 + \beta_{23} x_2 x_3 + \beta_{13} x_1 x_3 + \beta_{11} x_1^2 + \beta_{22} x_2^2 + \beta_{33} x_3^2 + \beta_{13} x_1 x_3 + \beta_{11} x_1^2 + \beta_{22} x_2^2 + \beta_{33} x_3^2 + \beta_{13} x_1 x_3 + \beta_{11} x_1^2 + \beta_{22} x_2^2 + \beta_{33} x_3^2 + \beta_{13} x_1 x_3 + \beta_{11} x_1^2 + \beta_{22} x_2^2 + \beta_{33} x_3^2 + \beta_{13} x_1 x_3 + \beta_{11} x_1^2 + \beta_{22} x_2^2 + \beta_{33} x_3^2 + \beta_{13} x_1 x_3 + \beta_{11} x_1^2 + \beta_{22} x_2^2 + \beta_{33} x_3^2 + \beta_{13} x_1 x_3 + \beta_{11} x_1^2 + \beta_{22} x_2^2 + \beta_{33} x_3^2 + \beta_{13} x_1 x_3 + \beta_{11} x_1^2 + \beta_{22} x_2^2 + \beta_{33} x_3^2 + \beta_{13} x_1 x_3 + \beta_{11} x_1^2 + \beta_{22} x_2^2 + \beta_{33} x_3^2 + \beta_{13} x_1 x_3 + \beta_{11} x_1^2 + \beta_{22} x_2^2 + \beta_{33} x_3^2 + \beta_{13} x_1 x_3 + \beta_{11} x_1^2 + \beta_{22} x_2^2 + \beta_{33} x_3^2 + \beta_{13} x_1 x_3 + \beta_{11} x_1^2 + \beta_{22} x_2^2 + \beta_{33} x_3^2 + \beta_{13} x_1 x_3 + \beta_{11} x_1^2 + \beta_{22} x_2^2 + \beta_{33} x_3^2 + \beta_{13} x_1 x_3 + \beta_{11} x_1^2 + \beta_{22} x_2^2 + \beta_{33} x_3^2 + \beta_{13} x_1 x_3 + \beta_{11} x_1^2 + \beta_{12} x_1 x_2 + \beta_{13} x_1 x_3 + \beta_{11} x_1 x_3 + \beta_{12} x_1 x_1 x_3 + \beta_{12} x_1 x$$

with x_1 , x_2 and x_3 the three input parameters seal temperature, time and pressure, y the seal strength, ε the error term and the β 's are the coefficients. Besides the main effects, the interaction terms and quadratic terms were also considered in the model. Moreover, for pressure, a third order effect was also included in the model. Non-significant effects are removed from the model by an all possible subsets procedure. The model with the best fitting subset of effects is selected. The criteria of this selection are R^2 , AIC and BIC. For a more detailed description of the model selection, the reader is referred to the previous study on ultrasonic seals¹⁰.

In a fourth step, the response surface model was utilized for optimizing the input variables towards the response (seal strength). In this study maximum seal strength is defined as an optimal result and was thus assigned a desirability = 1. In addition to determining one optimal parameter setting, a process window can be generated which for example excludes parameter combinations resulting in seal strength below a certain threshold. In this study, process windows were generated containing only those parameter combinations at which at least 90% of the maximum seal strength is reached.

In a fifth and last step, the optimum was experimentally validated by performing repeated measurements (n=10) at the optimal settings to check if the predicted optimum lies within the confidence interval calculated from the measured values. To assess the success of the confirmation, the CICON approach as suggested in previous research was followed^{11, 12}. For details, the reader is referred to the previous study on ultrasonic seals¹⁰.

4.4 Results and Discussion

4.4.1 Film characterization

It is not always possible to compare DSC results of packaging films with blown extruded films with 100 % pure material such as plastomer because of low viscous behaviour of this substance. Because of this, the results of the seal layers of the three packaging films are compared with the individual components in granulate form. This allows to identify similarities and to suggest explanations in differences and similarities of the three packaging films. The melting onset and peak temperatures of the films and granulates in this study are shown in Table 13. The values of film 1 are in between the values of its main components LDPE and mLLDPE in granulate form. In a previous study on blended films of LDPE and mLLDPE it was found that the melting point of the blended monolayer was between the values observed for mLLDPE and LDPE films¹³. The melting onset temperature of film 2 is decreased with 5 degrees compared to film 1. The presence of plastomer instead of metallocene LLDPE in the lower 15 um of the seal layer is suggested as explanation since plastomer has a lower melting point than metallocene LLDPE. This is indicated by melting peak temperatures of the components in granulate form. The melting peak temperature of the seal layer of film 2 is close to the value of film 1. Acid copolymer and sodium ionomer presence, which have lower melting points than LDPE, mLLDPE and plastomer, does not decrease the melting peak and onset temperature of film 3. These components are present in low amount in proportion to LDPE and mLLDPE and their melting temperatures are probably too low to influence the tangent line which is used to obtain the onset temperature.

Table 13: Melting onset and melting peak temperatures of films and granulates, tested with DSC.

		Film		Granulate of film component					
	1	2	3	LDPE	mLLDPE	plastomer	Acid copolymer	Sodium ionomer	
T _{melt}	100	95	98	102	95	87	77	70	
T _{melt peak}	112	113	112	112	111	102	98	90	

The hot tack strength is relevant for sealing through solid particles as these particles can push the seal layers away from each other directly after opening the hot bars when the seal is still hot¹⁴. This spring back effect is similar when wrinkles are present. The effect is discussed in several papers^{5, 6, 8, 9}. Figure 63 shows the hot tack results of all films. The hot tack initiation temperature (temperature where a low but measurable hot tack strength is obtained), peak value and window (temperature range where a relatively high hot tack strength is obtained) are discussed to compare the three packaging films. As there is currently no clear definition of the hot tack initiation temperature, it is defined in this study as the minimum temperature (°C) where a seal with low hot tack strength is produced, a threshold value of 0.03 N. mm⁻¹ must be exceeded. The hot tack window was defined as the temperature range (°C) from minimum to maximum temperature

where seals with medium hot tack strength are produced, a threshold value of 0.1 N. ${\rm mm}^{-1}$ must be exceeded.

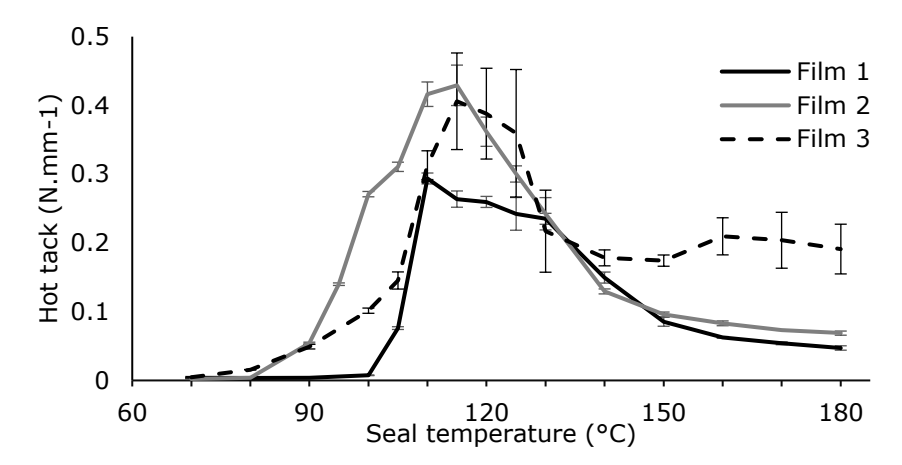


Figure 63: Hot tack graph with variation in seal temperature, seal parameters: 1.0 s seal time -0.3 N.mm^{-2} seal pressure -0.1 s cool time (n=3) for three packaging films.

Film 1 has a relatively high hot tack initiation temperature (105°C) compared to other films. It can be a result of the absence of low melting main components such as plastomer or sodium ionomer in the lower 15 µm of the seal layer. The peak value (0.29 \pm 0.01 N.mm⁻¹) is low compared to other films. The peak value is reached at 110°C, in accordance with the melting peak temperature of film 1 and individual granulates of two main components, LDPE and metallocene LLDPE. The hot tack window is narrow (110-140°C) compared to the other films. Film 2 has a relatively low hot tack initiation temperature (90°C) making it suitable for high speed sealing applications. This can be a result of the presence of plastomer⁵ in the lower 15 μ m of the seal layer. Compared to film 1 the peak value (0.43 \pm 0.03 N.mm⁻¹) is high, suggesting more and/or deeper entanglement, this was previously described in literature⁸. For both films, the hot tack strength decreases strongly in a similar way at elevated temperatures (≥ 150°C). Film 3, with the sodium ionomer seal layer, shows a larger standard deviation compared to the other films. It has a low hot tack initiation temperature (90°C), then the hot tack strength slowly increases until a high peak value (0.41 \pm 0.07 N.mm⁻¹) is reached at 115°C. The hot tack window is very broad (100 - ≥180°C), indicating that this film keeps a large portion of its strength at seal temperatures \geq 150°C, a characteristic that is previously described in literature ¹⁵. Both film 2 and 3 are evaluated as good hot tack performers because of a combination of hot tack properties (low initiation temperature, high peak value and wide window).

4.4.2 Evaluation and optimization of contaminated seal strength

The experimental design of the three films of this study is shown in Table 14. At each of the parameter combinations defined by the design, both clean and contaminated (coffee and blood powder) seals were created and their seal strength was measured. Other responses such as leak tightness, seal energy, optical aspects, seal thickness, etc. are also possible in a single or multi-response model, but were not considered in this study. All clean and contaminated seal strengths of films 1, 2 and 3, produced at the 20 parameter combinations (temperature, time and pressure) defined by the experimental design are also shown in the table. These seal strengths served as an input to build a model that predicts the clean and contaminated seal strength at all possible parameter settings within the defined design space.

Table 14: Experimental design with parameters (seal temperature (T), time (t) and pressure (p)) and responses (clean and contaminated seal strength) of films 1, 2 and 3 (F1, F2 and F3).

						Response: Seal strength (N.mm ⁻¹)								
						Clean			Ground coffee Contamination (25 g.m ⁻²)			Blood powder contamination (25 g.m ⁻²)		
Run	T _{bar} (°C) F1	T _{bar} (°C) F2	T _{bar} (°C) F3	t _{seal} (s)	p _{seal} (N.mm ⁻²)	F1	F2	F3	F1	F2	F3	F1	F2	F3
1	149.3	141.2	143.9	0.7	1.9	2.4	3.0	1.4	1.4	2.3	0.6	0.7	1.4	0.3
2	181.5	181.5	181.5	0.4	3.2	2.3	3.1	1.8	1.9	2.0	0.3	0.3	0.4	0.3
3	119.6	104.1	109.2	0.5	1.6	0.6	1.9	0.1	0.0	0.0	0.0	0.0	0.0	0.0
4	150.5	142.7	145.3	0.7	3.3	2.6	2.8	1.7	1.4	1.9	0.6	0.7	1.7	0.3
5	150.5	142.8	145.4	0.7	3.2	2.5	3.1	1.8	1.5	2.1	0.5	0.7	1.5	0.6
6	162.6	157.8	159.4	1.0	3.4	2.2	2.6	1.3	2.2	2.3	0.8	0.4	0.8	0.5
7	144.1	134.7	137.9	1.0	1.9	2.5	3.0	1.5	1.4	2.6	0.6	1.1	1.4	0.5
8	119.6	104.1	109.2	0.7	3.1	2.3	2.9	0.4	0.6	0.9	0.0	0.5	0.1	0.0
9	181.5	181.5	181.5	0.7	1.0	2.2	2.9	1.8	1.9	2.9	0.5	0.9	0.6	0.2
10	148.8	140.6	143.3	0.7	1.8	2.4	2.9	1.7	2.0	2.9	0.6	0.7	0.9	0.3
11	144.3	135.0	138.1	0.4	4.0	2.3	3.2	0.5	1.2	1.7	0.1	0.7	1.0	0.2
12	119.6	104.1	109.2	1.0	4.0	2.2	2.9	0.4	1.4	1.5	0.1	1.1	0.6	0.3
13	181.5	181.5	181.5	0.4	1.9	2.3	2.9	1.7	1.1	1.4	0.5	0.3	0.3	0.4
14	181.5	181.5	181.5	1.0	1.0	2.2	2.9	1.7	1.3	3.0	0.5	0.6	0.5	0.4
15	150.5	142.8	145.4	0.4	1.0	2.4	3.1	0.7	1.0	2.1	0.3	0.4	1.4	0.2
16	119.6	104.1	109.2	1.0	1.0	2.1	3.0	0.3	1.6	1.1	0.0	0.8	0.3	0.1
17	181.5	181.5	181.5	1.0	2.4	2.2	3.6	1.8	2.0	3.2	0.5	0.4	1.6	0.4
18	181.5	181.5	181.5	0.7	4.0	3.1	2.6	2.2	2.0	2.9	0.7	0.3	0.3	0.4
19	119.6	104.1	109.2	0.4	3.3	0.7	1.1	0.1	0.0	0.0	0.0	0.0	0.0	0.0
20	150.8	143.1	145.6	0.7	1.8	2.3	2.9	1.5	1.2	2.5	0.5	0.6	2.0	0.3

In Table 15, Table 16 and Table 17, the coefficients of the terms included in the models for each film are summarized for clean seals, coffee contaminated and blood powder contaminated seals, respectively. Non-significant terms were not included in the model and therefore no coefficient is shown in the table. Based on these models, the settings of temperature, time and pressure resulting in

maximum seal strength were determined for each film-contaminant combination as described in the Methods section.

Table 15: Significant coefficients, terms and regression significance of the seal strength model for clean seals of film 1, 2 and 3.

	_	Fi	lm 1	Filr	m 2	Film 3	
Coefficient	Term	Value	p-Value	Value	p-Value	Value	p-Value
eta_0	Intercept	-0.2435	0.6765	1.5979	0.0314	-2.0659	0.0001
eta_1	Т	0.0126	0.0012	0.0071	0.0523	0.0219	<0.0001
β_2	Т	0.7350	0.0295	0.6962	0.1144	0.5145	0.0364
β_3	Р	0.0981	0.1577	-0.0479	0.6028	0.0552	0.2711
β_{12}	T*t	-0.0446	0.0029	-0.0328	0.0326	-0.0130	0.1112
β_{23}	t*p	/	/	-0.1641	0.6741	/	/
β_{13}	T*p	/	/	-0.0012	0.7122	/	/
β_{11}	T ²	-0.0005	0.0089	-0.0003	0.0857	-0.0001	0.1203
β_{22}	t²	-2.7627	0.1164	/	/	-4.1615	0.0046
β_{33}	p²	0.1299	0.1344	/	/	-0.1272	0.0535
eta_{333}	p³	/	/	/	/	/	/

Table 16: Significant coefficients, terms and regression significance of the seal strength model for coffee contaminated seals of film 1, 2 and 3.

	_	Fi	lm 1	Fili	m 2	Film 3	
Coefficient	Term	Value	p-Value	Value	p-Value	Value	p-Value
eta_0	Intercept	-1.0186	0.0085	-1.8826	0.0177	-0.7098	0.0111
eta_1	Т	0.0106	<0.0001	0.0250	<0.0001	0.0086	<0.0001
β_2	t	1.2563	<0.0001	1.0453	0.0104	0.0202	0.8879
β_3	р	0.0893	0.0347	-0.0446	0.8187	-0.0254	0.4254
β_{12}	T*t	-0.0459	<0.0001	-0.0207	0.0900	-0.0091	0.0902
β_{23}	t*p	-0.3708	0.0362	/	/	/	/
β_{13}	T*p	/	/	/	/	-0.0029	0.0232
β_{11}	T ²	-0.0006	<0.0001	-0.0006	0.0004	-0.0001	0.1426
β_{22}	t²	/	/	/	/	/	/
β_{33}	p²	/	/	-0.0785	0.4184	-0.0502	0.2118
eta_{333}	p³	/	/	0.1347	0.2000	/	/

Table 17: Significant coefficients, terms and regression significance of the seal strength model for blood powder contaminated seals of film 1, 2 and 3.

		Fi	lm 1	Fili	m 2	Film 3	
Coefficient	Term	Value	p-Value	Value	p-Value	Value	p-Value
eta_0	Intercept	0.4262	0.1593	0.5214	0.3284	-0.5112	0.0049
eta_1	Т	-0.0016	0.3138	0.0030	0.3214	0.0037	0.0004
β_2	t	0.6953	0.0006	0.5969	0.1189	0.3370	0.0025
β_3	р	-0.0194	0.5617	/	/	0.0404	0.0582
β_{12}	T*t	-0.0276	0.0010	/	/	-0.0046	0.1595
β_{23}	t*p	-0.2909	0.0587	/	/	/	/
β_{13}	T*p	-0.0047	0.0059	/	/	/	/
eta_{11}	T ²	-0.0003	0.0013	-0.0007	<0.0001	-0.0001	0.0042
eta_{22}	t²	/	/	/	/	0.4579	0.3619
β_{33}	p²	0.0684	0.1176	/	/	-0.0220	0.3829
eta_{333}	p³	/	/	/	/	/	/

As a validation of the optima of the three films, the predicted optimal parameter settings, predicted maximum seal strengths and limits of the confidence intervals calculated based on the validation experiments (CICON approach) are shown in Table 18.

Table 18: Validation of statistical optimum (n=10) + optimal settings.

		Seal strength (N.mm ⁻¹)										
	Cle	ean	Ground contam		Blood powder contamination (25 g.m ⁻²)							
	predicted	CI measured	Predicted	CI measured	predicted	CI measured						
Film 1	3.0	[2.2;2.7]	2.1	[1.6;2.0]	1.1	[0.6;0.9]						
Film 2	3.3	[3.0;3.2]	3.1	[2.3;2.8]	1.6	[1.4;1.9]						
Film 3	2.2	[1.7;2.0]	0.9	[0.6;0.8]	0.5	[0.3;0.5]						
			Optimal setti	ngs								
Film 1	165 °C_0.7 s	_4.0 N.mm ⁻²	151 °C_1.0 s	_1.0 N.mm ⁻²	150 °C_1.0 s_1.0 N.mm ⁻²							
Film 2	144 °C_1.0 s	_1.0 N.mm ⁻²	161 °C_1.0 s_4.0 N.mm ⁻²		147 °C_1.0 s_2.0 N.mm ⁻²							
Film 3	182 °C_0.7 s	_2.7 N.mm ⁻²	182 °C_0.4 s	_1.2 N.mm ⁻²	157 °C_1.0 s_3.4 N.mm ⁻²							

The predicted values are a good indication of the measured values but the model tends to slightly overestimate the optimized seal strength. A higher accuracy could be reached by adding repetitions to the test or augmenting the experimental design with additional experiments. This can be a subject for further research. Contamination decreases the seal strength, even when optimized. The rate of decrease is dependent on the used seal material (blend LDPE/mLLDPE, blend LDPE/plastomer and sodium ionomer) and the applied contamination (ground coffee, blood powder). For films 1, 2 and 3 the degrees of decrease, based on the measured average values (not shown in table), are respectively 25, 16 and 63 % for ground coffee and 71, 45 and 79% for blood powder contamination compared to the clean seal strength. The samples contaminated with coffee reach a higher optimized seal strength than the samples with blood powder. This can be a result of more binding spots between the seal layers because of the lower amount of coffee particles when a same mass of contamination is applied.

Figure 64 shows that there are more clean areas with contaminated seal samples with coffee particles compared to those with blood powder.

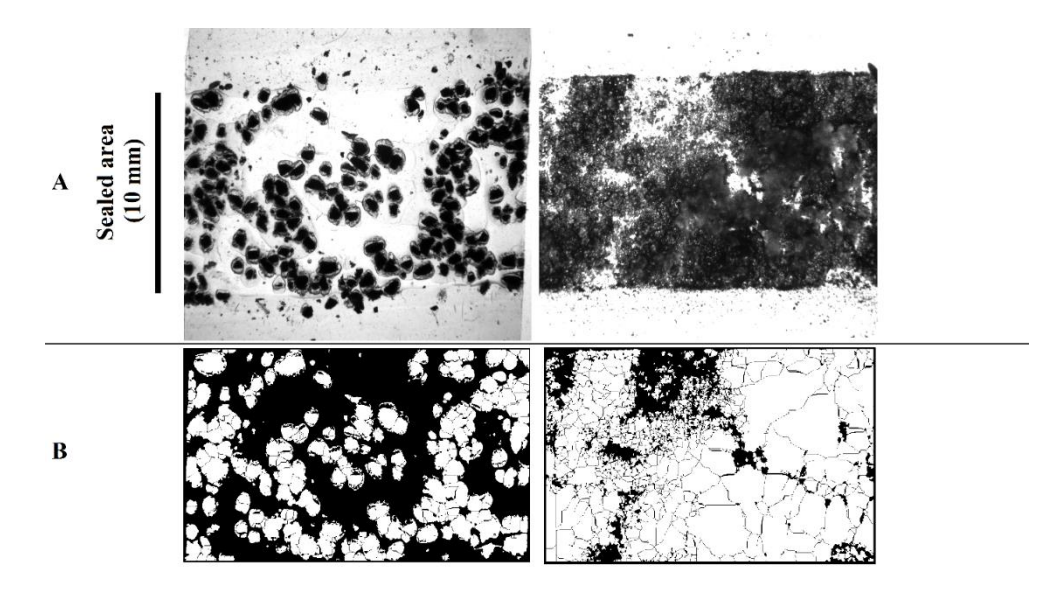


Figure 64: A: Raw images of coffee (left) and blood powder (right) contaminated samples of film 2, sealed at 181.5 °C, 0.7 s and 1.0 N.mm-2 with a high-resolution digital imaging set up with LED backlight illumination for high contrast. These raw images are converted to binary images (B) where clean areas are black.

Seal pressure has a slight or no influence on the seal strength as shown in Table 15, Table 16 and Table 17. There is no significant effect of pressure on seal strength with clean seals. Previous research on clean seals described the very limited influence of seal pressure on seal strength 16,17. With ground coffee contamination, a slight effect of pressure is seen as the first order and t*p term of film 1 and T*p term of film 3 have significant effects. With blood powder contamination there is only a significant effect of the T*p term on seal strength for film 1. Higher significance is observed for temperature and time and the combination of both parameters on clean and contaminated seal strength. This result is in line with previous studies that state that temperature and time are the most important factors influencing seal strength 16, 17. These parameters were used in process windows within which at least 90% of the maximum seal strength is obtained. The process windows for the three films are shown in Figure 65. Film 1 and 2 have the widest process window when seals are clean and process windows become narrow when solid contamination is present. Process windows for clean and coffee contaminated seals are wider for film 2 than for the other films. Even at low seal times of 0.5-0.6 s, it is possible to produce strong seals if the temperature is set at 170°C. In an industrial context, this is an advantageous film property with respect to production speed. Blood powder contaminated seals need higher seal time to produce strong seals. Taken into account the optimal values of Table 18 and the process windows of Figure 65, film 1 (seal layer blend of LDPE and metallocene LLDPE) is less tolerant for solid contamination than film 2 (seal layer blend of LDPE and plastomer) regarding seal strength. The results of this comparison are in line with the comparison of hot tack performance between both films (lower initiation, wider window and higher peak value for film 2). For film 3

all process windows are narrow compared to film 1 and 2. There is almost no overlap between the process windows. Taken into account the seal strengths of Table 18 and the process windows of Figure 65, this film has the worst tolerance for these types of solid contamination regarding seal strength. These results are inconsistent with the good hot tack performance (low seal initiation, high peak value, wide window) of this film. One possible explanation would be that for this film only the lower part of the seal layer participates in the encapsulation of the particles. The lower thickness (5 μm acid copolymer + 10 μm ionomer) of the effective seal layer compared to the particle size could decrease the seal-through-contamination performance. Another possible explanation can lie within the flow behaviour of the seal material. In previous research⁸, flow ability was related to the encapsulation of milk powder particles. These particles can be isolated if the seal material can flow around them. Both topics can be interesting for further research to gain better insight into the clean and contaminated seal performance of packaging films.

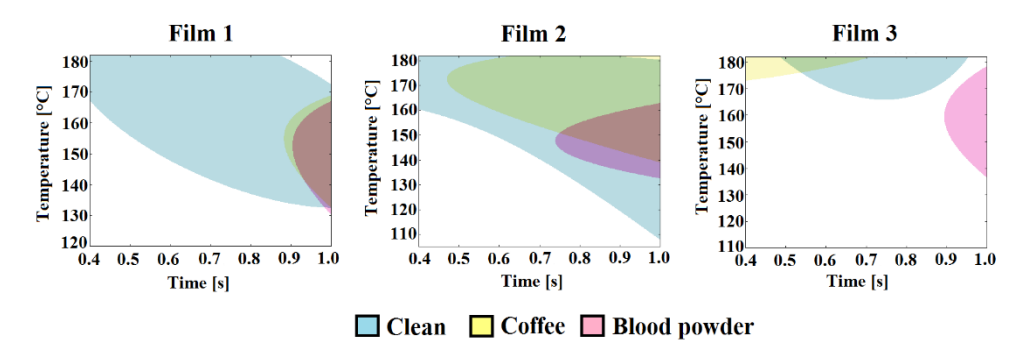


Figure 65: Temperature vs. time process windows for clean, coffee and blood powder contaminated samples. The process windows indicate those combinations of temperature and time that result in a seal strength of at least 90% of the optimum value. Pressure was kept constant at 2.5 N.mm⁻².

All samples that were optimized in seal strength are tested for their leak tightness by a dye penetration test prior to the seal strength test. Samples are tested in tenfold. All clean optimized samples were leak tight. In the case of coffee contamination, films 1 and 3 have respectively 8 and 7 out of 10 leak tight samples. All samples of film 2 were leak tight at optimal settings. In the case of blood powder contamination, film 1 has 9 out of 10 leak tight seals and films 2 and 3 are leak tight at the optimal settings. Comparing the three seal layers, the plastomer-based seal layer in film 2 has the best seal-through-contamination performance regarding leak tightness at optimal settings. A previous study¹⁴ suggests that viscous, hot tack and mechanical properties of seal materials are related with the encapsulation of solid contamination. Low zero shear viscosity, a high hot tack strength window (=area under hot tack curve between hot tack initiation temperature and actual seal bar temperature) and high resistance to elongation under stress were beneficial for preventing leaks¹⁴.

4.5 Conclusions

In this study, a method to optimize the granular contaminated seal strength of packaging films is presented. The optimal values predicted by the response surface method are experimentally validated. Predicted values are a good indication of clean and contaminated seal strength, although there is a tendency of overestimation by the model. Augmenting the initial experimental design or including repetitions in the design could improve this. Besides giving optimal values at one specific parameter setting, process windows for clean and contaminated seals can be obtained by doing a limited number of tests. These process windows are highly relevant for practical use in industry.

To gain understanding on the impact of solid contamination on the seal performance, clean and contaminated seal strengths of films with a metallocene, plastomer or ionomer-based seal layer are maximized and compared on seal strength, process window and leak tightness. Solid contamination causes a decrease in the maximal seal strength and narrows down the parameter region of time and temperature in the process window where 90% of that maximal strength is obtained compared to clean seals. When an equal mass of coffee and blood powder is applied, blood powder has a more negative impact on the maximum strength than coffee powder. The film with the plastomer-based seal layer outperformed the other films with a higher seal strength, wider process windows and a higher degree of leak tightness (evaluated with the dye penetration test). This film also has a better clean seal performance than the other ones.

Hot tack results are compared with clean and contaminated seal performance to evaluate the use of hot tack as a predictive test for the contaminated seal performance. There are similarities in the comparison of films with metallocene and plastomer-based seal layer, such as the hot tack initiation temperature, window and peak value. The hot tack results of the film with sodium ionomer, however, were not predictive for the contaminated seal strength.

The influence of seal technology, bar geometry and effective thickness and flow behaviour of the seal layer on solid granular contaminated seal performance can be subjects of further research. The presented framework of this chapter can be adapted so the above described factors can be studied efficiently, with respect to their mutual interactions. This facilitates further research to pace up knowledge development of seal contamination in open literature and thus contributes to safe and high-quality food packages with minimal losses of food and packaging materials. By adapting the contamination application method, other types of contamination, such as liquids and complex food matrices, can be evaluated as well in relation to seal performance.

4.6 References

- [1] Tauschitz B, Washüttl M, Wepner B, Tacker M. MAP-Verpackungen: ein Drittel nicht optimal. *PACKaktuell* **2003**, 04, pp. 6–8.
- [2] Dudbridge M. Handbook of seal integrity in the food industry. *Wiley Blackwell* **2016**, Hoboken (USA), ISBN: 9781118904602.
- [3] Morris B. 2017. The science and technology of flexible packaging multilayer films from resin and process to end use. *Elsevier inc* **2016**, Amsterdam, pp. 216-218, 249-250. ISBN: 978-0-323-24273-8.
- [4] Simpson MF, Presa JL. A Comparison of AFFINITY Plastomers Produced via INSITE Technology with Ethylene/Acrylic Acid Copolymers, Ionomers, and ULDPE. *Future-Pak* **1996**. Chicago, USA.
- [5] Mesnil P, Rohse N, Arnauts J, Halle RW. Seal Trough Contamination Performance of Metallocene Plastomers. *TAPPI Polymers, Laminations, & Coatings Conference* **2000**, Chicago, USA.
- [6] Morris B. Sure ways to reduce package sealing failure. *Dupont* **2010**. Retrieved November 2018 from http://www2.dupont.com/Packaging Resins/en US/assets/downloads/white-papers/Reduce Package Sealing Failure Barry Morris November 2010.pdf.
- [7] Bach S, Thürling K, Majschak JP. Ultrasonic sealing of flexible packaging films Principle and characteristics of an alternative sealing method. Packag Technol Sci **2012**, 25(4), pp.233-248, DOI: https://doi.org/10.1002/pts.972.
- [8] Sadeghi F,Ajji A. Application of single site catalyst metallocene polyethylenes in extruded films: effect of molecular structure on sealability, flexural cracking and mechanical properties. *The Canadian journal of chemical engineering* **2014**, 92 (7), pp 1181-1188 2014. DOI: 10.1002/cjce.21964.
- [9] Bilgen M, Van Dun J. Hermetic sealing of flexible packages. *International polyolefins conference* **2014**, Houston, USA.
- [10] D'huys, K, Bamps B. Peeters R, De Ketelaere B. Multi-criteria evaluation and optimization of the ultrasonic sealing performance based on design of experiments and response surface methodology. Packaging Technology and Science 2019, 32 (4), pp. 165-174, https://doi.org/10.1002/pts.2425.
- [11] Antony J. Design of Experiments for Engineers and Scientists. *Elsevier* **2003**, Amsterdam. ISBN: 9780750647090.
- [12] Jensen WA. Confirmation runs in design of experiments. *J Qual Technol* **2016**, 48(2), pp. 162-177, DOI: https://doi.org/10.1080/00224065.2016.11918157.
- [13] Sierra JD, Noriega MD, Nicolais V. Effect of metallocene polyethylene on heat sealing properties of low density polyethylene blends. *Journal of plastic film and sheeting* **2000**, 16 (1), pp. 33-42, DOI: <u>10.1106/YYFG-9KH1-R7OU-VK9H</u>.
- [14] Ward M, Li M. Seal-through-contamination and caulkability an evaluation of sealants' ability to encapsulate contaminants in the seal area. *Tappi place conference* **2016**, Fort Worth, USA.

- [15] Suenaga S, Hirasawa E. Connection between Hot Tack Force and Form-Fill-Seal Performance of Packaging Films. *J-stage* **2004**, 16(7), 450-458; DOI: 10.4325/seikeikakou.16.450.
- [16] Theller HW. Heat sealability of flexible web materials in hot-bar sealing applications. *J Plast Film Sheeting* **1989**, 5, pp. 66-93, DOI: https://doi.org/10.1177/875608798900500107.
- [17] Stehling FC and Meka P. Heat sealing of semicrystalline polymer films. I. Calculation and measurement of interfacial temperatures: effect of process variables on seal properties. *Journal of applied polymer science* **1994**, 51(1), pp. 89-103, DOI: 10.1002/app.1994.070510111.

5. Evaluation and optimization of the peel performance of a heat sealed topfilm and bottomweb undergoing cold storage

Bamps B, De Ketelaere B, Wolf J, Peeters R. Evaluation and optimization of the peel performance of a heat sealed topfilm and bottomweb undergoing cool processing. *Packaging Technology and Science* **2021**; 34(7); pp. 401-411. DOI: http://doi.org/10.1002/pts.2562.

In the last decades, flexible food packaging is expected by consumers to open by peeling. For cold storage, which is crucial for food preservation, no study is available on the peel performance (peel strength and peel energy). Test procedures to efficiently evaluate and optimize the peel performance of packaging materials before, during and after cold storage are missing. As a result, insight in this matter is rather limited. With this study, potential issues can be anticipated. The methods of previous chapters are adapted to study peel performance during and after cold storage. A DOE-method with four factors (hot tool process parameters: temperature, pressure and time + ambient temperature) and three performance indicators (average and maximum seal strength, referred to as peel strength in this study, and seal energy, referred to as peel energy in this study), referred to as responses in this publication, is developed, validated and applied to evaluate and optimize seal performance of a representative peelable topfilmbottomweb packaging concept. Additional mechanical and seal experiments are performed to explain the differences in seal performance and thus gaining a better understanding of peel performance during and after cold storage. This study is performed within the CORNET-framework (THERMOPEEL: "Optimal peelable seals in packaging concepts undergoing thermal processing", funded by the Flemish (Agentschap Innoveren & Ondernemen (VLAIO-TETRA nr. 180224)) and German government (Federal Ministry for Economic Affairs and Energy (BMWi, IGF project no. 243 EBR/1)).

5.1 Introduction

Tight packages are crucial to ensure food quality and food safety throughout the process chain. Perishable food products such as meat, cheese, ready meals and others are often packed in a rigid thermoformed tray, heat sealed with a thin flexible topfilm, in vacuum or with modified atmosphere to extend the shelf life. In 90 % of all thermoform fill & seal machines only the bottomweb is formed. Besides heat sealability, materials are selected based on barrier and mechanical properties¹. These properties are determined by the chemical composition, production process and the thickness. The packed product undergoes cold storage

after sealing to extend the shelf life. At the food company, during transportation and storage, at the store and finally at the consumers' place it can be cooled and/or heated. Cold storage can be differentiated in chilling at temperatures from 0 to 5 °C and freezing at temperatures from -24 to -18 °C where the presence of H_2O in a solid state extends the shelf life. Cold storage generally extends the shelf life by decreasing microbial activity and biochemical reactions². To meet the needs of the rapidly growing segment in the population of those aged 65+ with reduced muscle strength, increasingly living in single person households, packaging solutions with easy opening features and smaller size are suggested³. Industrial guidelines⁴ and research⁵ is published to address the suggestion of easy opening of thermoformed trays with peelable seals for this segment of the population. Seal quality must be ensured at all temperatures of the process chain.

5.2 Objectives

The main objective of this study is to present a method to optimize peel performance of packaging concepts undergoing cold storage. This method is based on previous studies with a similar methodology to optimize seal strength with a limited number of tests^{6,7}. A second objective is to evaluate the relation between peel performance and cold storage by applying the proposed method on a commercial packaging concept with poly(ethylene) (PE) seal layer to optimize peel performance at 23 °C and compare this with seals that are produced at equal process parameters during and after cold storage at 4 or -18 °C.

5.3 Materials & methods

5.3.1 Materials

The topfilm is composed of a blown coextruded structure of 45 μm with three layers (PE, ethylene vinyl alcohol (EVOH) and cohesive peelable PE at the seal surface), laminated to a 12 μm thick poly(ethylene terephthalate) (PET) outer layer. The bottomweb is composed of a PE seal layer of 35 μm laminated to an outer PET layer of 250 μm . These materials were provided by Südpack Verpackungen GmbH & Co KG (Germany). The bottomwebs are not thermoformed and characterized as films to eliminate the impact of the thermoform process.

5.3.2 Methods

Previous studies on fracture mechanics have shown that peel energy results of experimental tests are the sum of the energy of creating new interfacial area (N.mm $^{-1}$), which is referred to as the energy of fracture (Ga), the energy to extend the peel arm (Ge) and the energy to bend the peel arm (Gb) $^{8, 9}$. The following equation for peel strength (N/mm) illustrates this sum of impacting components and considers the geometry of the test by including the peel angle θ .

$$Peel\ Strength = \frac{Ga + Ge + Gb}{1 + \epsilon a - cos\theta}$$

Equation 10.

 ε_a represents the inelastic extension (ratio)¹⁰.

Besides presenting an optimization method this study evaluates the relation of cold storage on peel performance by applying the proposed method and performing additional mechanical tests for seal and film characterization.

Seal preparation and characterization

Samples are cut to a width of 30 mm and a length of 100 mm in machine direction of the film. The seal width, this is the width of the bars, is 10 mm. The upper bar is heated at high temperatures while the lower bar is kept at 50 °C to simulate the sealing process in the industry where the lower bar is not actively heated by itself, but only through the frequent touching of the heated upper bar. Seal temperature in this study refers to the temperature of the upper bar. Seal times from 1 to 3 s are used to simulate the sealing process of the topfilm and tray packaging concept in the industry. Seal pressures from 1 to 4 N.mm⁻² are used to cover the full working range of the lab sealer. A peel strength test with a peel angle of 180° is performed within 4 hours after sealing. The bottomweb is clamped at the bottom and the topfilm from above. Clamp distance is set at 20 mm and testing speed is 300 mm.min⁻¹. A preload force of 1 N is used.

Three results characterize the peel performance. The maximum peel strength is calculated by dividing the maximum force measure by the sample width. The average peel strength is calculated by dividing the average force of the central 30 % of the position of the peel curve with the sample width. Peel energy is the energy below the force-elongation curve. Samples are visually analysed afterwards to study the impact of the peel test and temperature processing on peeled multilayer structures. Discussed seal failure mechanisms of ASTM F88 such as cohesive peel and delamination, as shown in Figure 35, are differentiated amongst combinations of these mechanisms by eye. Microscopic cross section of peeled samples with amplifications of 10x20 and 10x50 are made to visualize the layer distribution.

In order to determine the cool time of the experiments to optimize peel performance, the following test is carried out. Samples are sealed with a seal temperature of 150 °C, a seal time of 0.7 s and a seal pressure of 1.0 N.mm⁻². Using these seal settings, samples peeled cohesively in a peel test. Directly after sealing, samples are transferred to temperature chambers of -18, 4 or 23 °C and samples are tested in triplicate after 30 minutes, one hour, two hours, four hours, six hours, one day, two days, four days, eight days, eleven days, one month and two months. Five minutes before testing the samples are kept at 23 °C and the peel test is also carried out at 23 °C to measure the influence of processing time on maximum peel strengths and standard deviations.

Film characterization

All materials are stored in a room with standard environment conditions (23 °C, 50 % relative humidity) 8 days before testing.

A three-point flexural test is performed on bottomweb samples to determine the impact of ambient temperature on bending properties. The bottomweb sample is cut to a width of 30 mm and a length of 50 mm in machine direction. In this direction the sample is naturally slightly bended because of the winding on a roll with 76 mm core diameter. The sample is placed on two supports, with the bend facing upwards, in a temperature chamber of -18, 4 or 23 °C. The length of the

span between these supports is 20 mm. The radii of the supports and loading edge are 5 mm. The position, and thus resulting strain, is zeroed at a preload force of 0.3 N, corresponding closely with a straight parallel sample at considered temperatures. The testing speed is set at 1 mm.min⁻¹ and a comparison is made of the flexural stress σ_f (N.mm⁻²)-strain ε_f (ratio) curves until 2% strain. Flexural stress and strain are calculated according to the ISO 178 standard with Equation 11 and Equation 12.

$$\begin{split} \sigma_f &= \frac{3*F*L}{2*b*h^2} \\ &= \frac{600*s*h}{L^2} \\ &= \frac{600*s*h}{L^2} \end{split}$$
 Equation 11.

F is the applied force in N, L is the span in mm, b is the width in mm, h is the thickness in mm and s is the deflection in mm.

A tensile test on the topfilm is performed to determine its tensile properties. 15 mm wide rectangular topfilm samples are tested in machine direction at 300 mm.min⁻¹ and a clamp distance of 20 mm to match the settings of the peel strength test.

As the topfilm material is a commercial material and the composition of the seal layer remains unknown, additional tensile tests were performed on low-density PE (LDPE) film samples to visualise how cold storage impacts a PE stress-strain diagram at the test temperatures, cool time and test speed in this study.

Seal optimization

To evaluate the impact of the individual parameters seal temperature, seal time, seal pressure, processing temperature and their interactions on the peel performance (peel strength and peel energy) a design of experiment approach was followed according to previous research^{6, 7}.

- In a first step a design space is defined using predefined limits of all individual parameters. The limits are based on preliminary tests, industrial relevance and the working range of the equipment. In this study the minimum and maximum design limits for continuous parameters such as seal temperature, seal time and seal pressure are respectively 130 180 °C, 1.0 3.0 s and 1.0 4.0 N.mm⁻². Processing temperature is considered a categorical parameter because there is no interest in intermediate temperatures.
- In a second step an experimental design is defined within the design space. The combination of continuous and categorical parameters requires a custom design. An I-optimal design with 24 experimental runs is proposed¹¹.
- Each of the runs is tested in duplicate. Additionally, samples <u>during and after</u> cold storage are tested, summing up 4 samples for each run. Each sample generates three results: maximum and average peel strength, and peel energy.
- In a next step a response surface model is fitted to the obtained data.
 Factors were mean centred before calculating interactions or quadratic terms.

- This model is then used to optimize settings to obtain certain target values for peel performance at 23 °C and to predict values at -18, 4 and 23 °C during and after cold storage. The optimized peel performance is based on the capacity of the packaging concept and on target values that can be achieved by 95% of the population⁴.
- In a last step the optimized seals are validated by testing five samples, sealed at optimum settings. For more detail on this methodology the reader is referred to a previous study⁶.

The influence of bending movement of the bottomweb on the peel performance is evaluated by comparing the peel performance of optimized seals at 23 °C with seals that are reinforced by gluing the bottomweb to a 1 mm thick metal plate. The influence of processing temperature on bond strength and elongation is evaluated by testing the optimum seals with a reinforced metal plate during -18, 4 and 23 °C and thus eliminating the difference in bending stiffness of the bottomweb at different temperatures.

Statistical analysis

Results from the higher-mentioned experiment were analysed using a response surface model, considering main effect, interactions as well as quadratic effects. An all-possible subset model selection was performed to define the final model that was used for the optimization. For all analyses, the JMP version 14 software (JMP 14, The SAS institute, Inc, NC, USA).

Apparatus

Sealed samples are prepared with a Labthink HST-H3 heat seal tester (Labthink Instruments Co Ltd, People's Republic of China). Peel and flexural tests are carried out with the Tinius Olsen 5ST universal testing machine (Tinius Olsen Ltd, United Kingdom), the tools and clamps are inside a TH 2700 temperature chamber (Thümler GmbH, Germany). The combination of both instruments is installed by Benelux Scientific BVBA (Belgium). A Nikon Eclipse ME600 microscope and NIS-Elements D4.10.00 software (Nikon, Japan) are used to visualise cross sections.

5.4 Results and Discussion

5.4.1 Influence of cool time

Figure 66 shows the maximum peel strength results at different cool times. There is a very small impact of cool time on maximum peel strength, the average values increase slightly after one day of cool. However, the increase of average values lies within a 95 % confidence interval (shown by the error bars) of the maximum peel strengths at low cool times.

Because of this limited impact and to be able to perform many tests in a short amount of time the following ageing and cool time restrictions are followed in the optimization experiments: Sealed samples are tested in a 4-hour timeframe after sealing in the optimization tests. Samples <u>during</u> sealing are kept in the temperature chamber for 15 minutes prior to the start of the test. Samples <u>after</u> sealing are also kept in the temperature chamber but transferred after 15 minutes to cool down or heat up to 23 °C. These samples are eventually tested at 23 °C in the temperature chamber.

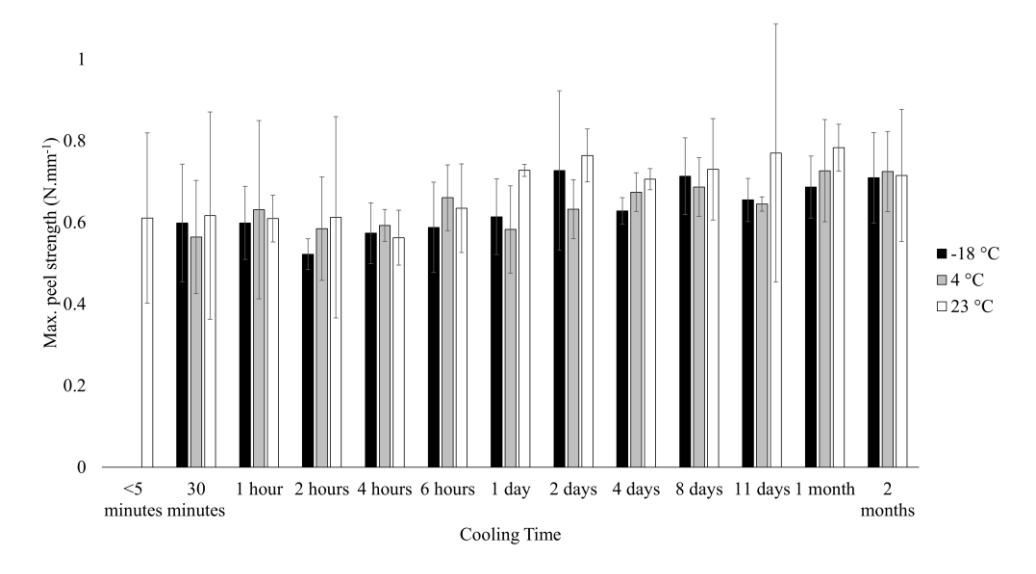


Figure 66: Influence of cool time on maximum peel strength (n=3).

5.4.2 Seal optimization

The experimental design with results is shown in Table 19.

Table 19: Experimental design with parameters (seal temperature, seal time, seal pressure and processing temperature) and responses (average peel strength, maximum peel strength, peel energy) during and after cold storage (n=2).

				During cool processing			After cool processing												
	T _{seal} (°C)	t _{seal}	p _{seal} (N.mm ⁻²)	T _{processing}	Average peel strength (N.mm ⁻¹)	Maximum peel strength (N.mm ⁻¹)	Peel energy	Average peel strength (N.mm ⁻¹)	Maximum peel strength (N.mm ⁻¹)	Peel energy									
					1.1	1.2	0.34	0.8	0.8	0.20									
1	155	2.0	2.5	-18	1.1	1.2	0.33	0.7	0.8	0.18									
					1.0	1.0	0.26	0.7	0.7	0.17									
2	180	1.0	4.0	4	1.0	1.0	0.27	0.8	0.8	0.20									
					0.8	1.0	0.21	0.2	0.3	0.02									
3	155	1.0	1.0	4	0.3	0.7	0.10	0.6	0.7	0.13									
					0.7	1.3	0.23	0.7	1.3	0.23									
4	180	3.0	1.0	23	0.7	0.9	0.21	0.7	0.9	0.21									
_	155 2.0 2.5		2.5	2.5	2.5	2.5	2.5	2.5	2.5	2.5	2.5	2.5	22	0.7	0.8	0.18	0.7	0.8	0.18
5		2.5	23	0.7	0.7	0.19	0.7	0.7	0.19										
6	130	3.0		-18	0.7	1.0	0.21	0.4	0.6	0.08									
0	130	3.0	4.0	-18	0.5	0.7	0.14	0.5	0.6	0.12									
7	180	2.0	1.0	4	0.8	1.0	0.28	0.8	0.8	0.23									
′	100	2.0	1.0	*	1.1	1.1	0.29	0.8	0.9	0.24									
8	180	3.0	2.5	4	2.6	2.7	0.24	2.0	2.1	0.29									
0	100	3.0	2.3		3.1	3.4	0.54	2.3	2.4	0.44									
9	155	3.0	3.0	4.0	23	1.7	1.8	0.14	1.7	1.8	0.14								
9	133	3.0	4.0	23	1.7	2.0	0.11	1.7	2.0	0.11									
10	130	1.0	4.0	23	0.1	0.2	0.02	0.1	0.2	0.02									
10	130	1.0	0	-3	0.0	0.1	0.00	0.0	0.1	0.00									
11	130	3.0	2.5	23	0.5	0.6	0.13	0.5	0.6	0.13									
					0.5	0.6	0.13	0.5	0.6	0.13									
12	130	3.0	1.0	4	1.0	1.0	0.21	0.7	0.7	0.13									
					0.2	0.6	0.06	0.6	0.7	0.10									

130	1.0	1.0	-18	0.0	0.1	0.01	0.0	0.0	0.00
150	1.0	1.0	10	0.0	0.1	0.01	0.0	0.0	0.00
180	1.0	1.0	-18	1.1	1.3	0.42	0.4	0.6	0.10
100	1.0	1.0		0.6	1.1	0.18	0.6	0.7	0.16
130	1.0	2.5	4	0.1	0.3	0.02	0.0	0.0	0.00
130	1.0	2.3		0.2	0.3	0.03	0.0	0.1	0.01
155	3.0	1.0	-18	0.9	1.3	0.39	0.7	0.7	0.17
133	3.0	1.0		1.2	1.3	0.35	0.8	0.8	0.20
155	1.0	4.0	-18	1.0	1.2	0.30	0.5	0.6	0.14
133	1.0	4.0		0.8	1.0	0.21	0.4	0.6	0.12
160	1.0	2.5	23	0.7	0.7	0.19	0.7	0.7	0.19
100	1.0	2.3	23	0.7	0.7	0.17	0.7	0.7	0.17
130	1 3	1.0	23	0.4	0.6	0.07	0.4	0.6	0.07
133	1.5	1.0	23	0.4	0.6	0.09	0.4	0.6	0.09
155	2.0	2.5	-18	1.1	1.3	0.44	0.7	0.7	0.18
133	2.0	2.3		1.2	1.2	0.31	0.7	0.7	0.17
180	2.0	4.0	23	3.3	3.3	0.38	1.3	1.4	0.05
100	2.0			3.3	3.3	0.48	2.2	2.3	0.11
180	3.0	4.0	-18	3.3	3.3	0.38	2.2	2.2	0.33
250	3.0		"	3.3	3.3	0.48	1.8	2.1	0.15
155	3.0	4.0	4	2.5	2.7	0.38	2.1	2.1	0.27
				0.9	0.9	0.25	0.7	1.2	0.21
130	2.0	4.0	4	0.8	0.8	0.12	0.4	0.6	0.08
		""		0.8	0.9	0.13	0.4	0.5	0.09
	130 180 130 155 155 160 139 155 180 180 155	180 1.0 130 1.0 155 3.0 155 1.0 160 1.0 139 1.3 155 2.0 180 2.0 180 3.0	180 1.0 1.0 130 1.0 2.5 155 3.0 1.0 155 1.0 4.0 160 1.0 2.5 139 1.3 1.0 155 2.0 2.5 180 2.0 4.0 180 3.0 4.0 155 3.0 4.0	180 1.0 1.0 -18 130 1.0 2.5 4 155 3.0 1.0 -18 155 1.0 4.0 -18 160 1.0 2.5 23 139 1.3 1.0 23 155 2.0 2.5 -18 180 2.0 4.0 23 180 3.0 4.0 -18 155 3.0 4.0 4	$ \begin{array}{c ccccccccccccccccccccccccccccccccccc$	$ \begin{array}{c ccccccccccccccccccccccccccccccccccc$	$ \begin{array}{c ccccccccccccccccccccccccccccccccccc$	$ \begin{array}{c ccccccccccccccccccccccccccccccccccc$	130

Table 20: Significant terms with parameter estimates (V) and corresponding p-values (p-V) of average peel strength, maximum peel strength and peel energy during and after cold storage.

			During co	ld storage	9				
Term	Averag	je peel	Maximu	ım peel	Peel e	nergy			
	stre		stre	ngth		1)			
	(N.m	nm ⁻¹)	(N.m	nm ⁻¹)					
	V	p-V	V	p-V	V	p-V			
Intercept	-4.7550	<.0001	-4.5976	<.0001	-0.5638	<.0001			
T _{seal}	0.02793	<.0001	0.0278	<.0001	0.0046	<.0001			
t _{seal}	0.45050	<.0001	0.4676	<.0001	0.0531	0.0006			
Pseal	0.28074	<.0001	0.2438	<.0001	/	/			
Tprocessing [-18]	/	/	/	/	0.0674	0.0003			
Tprocessing [4]	/	/	/	/	/	/			
Tprocessing [23]	/	/	/	/	/	/			
T _{seal} *t _{seal}	0.0102	0.0044	0.0094	0.0104	/	/			
t _{seal} *t _{seal}	/	/	/	/	-0.0690	0.0191			
T _{seal} *p _{seal}	0.0103	<.0001	0.0087	0.0010	/	/			
t _{seal} *p _{seal}	0.1246	0.0272	0.1264	0.0315	/	/			
p _{seal} *p _{seal}	/	/	/	/	/	/			
T _{seal} *T _{processing [4 °C]}	/	/	/	/	/	/			
T _{seal} *T _{processing} [23°C]	/	/	/	/	/	/			
t _{seal} *T _{processing [4 °C]}	/	/	/	/	/	/			
p _{seal} *T _{processing [23°C]}	/	/	/	/	/	/			
			After cold	d storage					
Term	Averag	je peel	Maximu	ım peel	Peel e	nergy			
	stre			ngth	(.	Peel energy (J)			
	(N.m		(N.m						
	V	p-V	V	p-V		p-V			
Intercept	-3.0738	<.0001	-3.2361	<.0001	-0.3324	<.0001			
T _{seal}	0.0177	<.0001	0.0186	<.0001	0.0027	<.0001			
t _{seal}	0.3789	<.0001	0.4118	<.0001	0.0493	<.0001			
p _{seal}	0.1485	<.0001	0.1509	<.0001	/	/			
Tprocessing [-18]	/	/	-0.1083	0.0400	/	/			
T _{processing} [4]	/	/	/	/	0.0211	0.0163			
Tprocessing [23]	/	/	/	/	/	/			
T _{seal} *t _{seal}	0.0051	0.0264	0.0059	0.0056	/	/			
t _{seal} *t _{seal}	/	/	/	/	/	/			
T _{seal} *p _{seal}	0.0055	0.0009	0.0049	0.0012	/	/			
t _{seal} *p _{seal}	0.1058	0.0053	0.1212	0.0007	/	/			
p _{seal} *p _{seal}	/	/	/	/	-0.0206	0.0015			
T _{seal} *T _{processing} [4 °C]	/	/	/	/	0.0011	0.0079			
T _{seal} *T _{processing} [23°C]	/	/	/	/	/	/			
t _{seal} *T _{processing} [4 °C]	0.1350	0.0440	0.1465	0.0176	0.0274	0.0083			
p _{seal} *T _{processing} [23°C]	/		/	/	/	/			

Table 20 shows a summary of the coefficients of the terms which are included in the models for each response. Parameters estimates for non-significant terms are not shown in the table because they are not retained in the models. The table shows the complexity of parameters (first order, second order and interactions) that impact the results for peel strength and peel energy. As an example, the polynomial model for maximum peel strength during cold storage is given, factors are mean centred. This complex model is visualised in the prediction profilers of Figure 67.

```
\begin{aligned} & \textit{Maximum peel strength} = -4.598 + 0.028 * \textit{Tseal} + 0.468 * \textit{tseal} + 0.244 * \textit{pseal} + \\ & \textit{Match Tprocessing}[-18 \rightarrow 0.082; 4 \rightarrow 0.042; 23 \rightarrow -0.124] + 0.009 * \textit{Tseal} * \textit{tseal} - 0.212 * \\ & \textit{tseal}^2 + 0.009 * \textit{Tseal} * \textit{pseal} + 0.124 . \textit{tseal}. \textit{pseal} + 0.032 * \textit{pseal}^2 + \textit{Tseal} * \\ & \textit{Match Tprocessing}[-18 \rightarrow 0.008; 4 \rightarrow -0.007; 23 \rightarrow -0.002] + \textit{tseal} * \\ & \textit{Match Tprocessing}[-18 \rightarrow -0.044; 4 \rightarrow 0.118; 23 \rightarrow -0.074] + \textit{pseal} * \\ & \textit{Match Tprocessing}[-18 \rightarrow -0.014; 4 \rightarrow -0.129; 23 \rightarrow 0.143] \\ & \textit{Equation 13}. \end{aligned}
```

Using these models seal settings are optimized. Based on a maximum peel line of 22 mm for a thermoform-fill-seal machine and a minimum opening force that can be achieved by 95 % of elderly female population⁴, and considering the potential peel strength of the packaging concept at 23 °C as shown in Table 19, average and maximum peel strengths of 0.5 N.mm⁻¹ are considered as optimal. Target values of 0.5 N.mm⁻¹ are matched for average and maximum peel strength during and after cold storage, and peel energy is maximized using linear desirability functions to optimize peel performance. It is shown in Table 19 that the target peel strength is achievable with the considered packaging concept. The maximization of peel energy is chosen to generate a peelable seal that maintains this strength over the full length of the sealed surface.

The optimal settings to match the target values at 23 °C during and after cold storage are given by a seal temperature of 170 °C, a seal time of 1.0 s and a seal pressure of 2.0 N.mm⁻². The optimization is shown in the prediction profilers of models in Figure 67. The graphs in the first three column indicate that peel strength and energy increased at high seal temperatures, times and pressures. The graphs in the fourth column indicate that peel strength and energy increased during cold storage, there is no change in peel strength and energy after cold storage. The graphs in the fifth column show the applied desirability functions, with a peak function to match average and maximum peel strength, and a linear function to maximize peel energy.

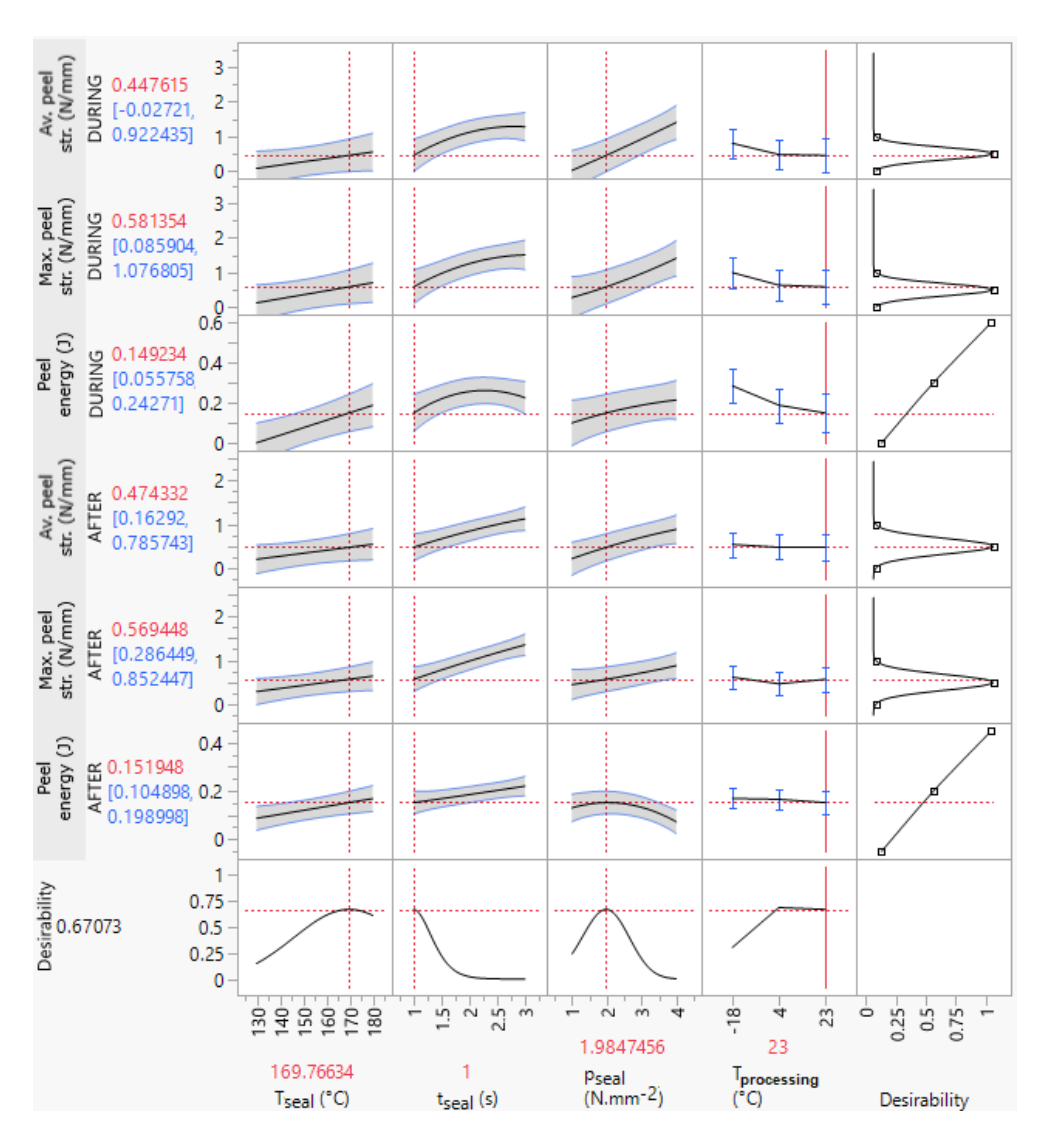


Figure 67: Prediction profilers of models of average peel strength, maximum peel strength, peel energy, during and after cold storage, optimized by matching 0.5 N.mm⁻¹ for average and maximum peel strength and maximizing peel energy at 23 °C processing temperature.

The predicted values for peel strength of the optimal sealed samples, prepared with these settings at processing temperatures of -18, 4 and 23 °C, are compared with confidence intervals based on validation experiments, corresponding with the CICon approach^{12, 13}. The results are shown in Table 21.

Table 21: Validation of statistical optimum at various processing temperatures during and after cold storage (n=5).

	Average peel str	ength (N.mm ⁻¹)	Maximum peel st	trength (N.mm ⁻¹)
Processing temperature	Predicted value	CI measured	Predicted value	CI Measured
-18 °C - during cold storage	0.80	[1.02; 1.24]	0.99	[1.17; 1.25]
-18 °C - after cold storage	0.54	[0.56; 0.67]	0.62	[0.62; 0.68]
4 °C - during cold storage	0.47	[0.94; 1.04]	0.63	[0.97; 1.07]
4 °C - after cold storage	0.48	[0.60; 0.77]	0.47	[0.68; 0.77]
23 °C	0.45	[0.51; 0.62]	0.58	[0.60; 0.66]

The predicted values are a good indication of what can be expected, however these values are slightly underestimated. A higher accuracy can be reached by adding repetitions or by adding extra points to the design. Even when both responses average and maximum peel strength is matched to an equal value of 0.5 the maximum value is slightly higher than the average value, another outcome would not make sense. The calculated confidence intervals follow the trend of the predicted values that during cold storage peel strength increases at -18 °C, however, also at 4 °C increased peel strength is measured. Cold storage has no impact on peel strength when seals are heated up to 23 °C.

5.4.3 Film characterization

The results of film characterization are shown below in Figure 68, Figure 69 and Figure 70. These results are discussed in relation with peel performance in 4.4. Figure 68 shows the flexural stress-strain curves of 5 bottomweb samples for each evaluated ambient temperature. The samples at low temperature (-18 and 4 °C) reach higher stress values when strain increases, compared to samples at standard temperature. The samples at -18 °C tend to have the highest stress, however variation is too high to distinct clearly with the samples at 4 °C. A flexural stress of 70 N.mm⁻² correspond with normalized strength value of 0.2 N.mm⁻¹.

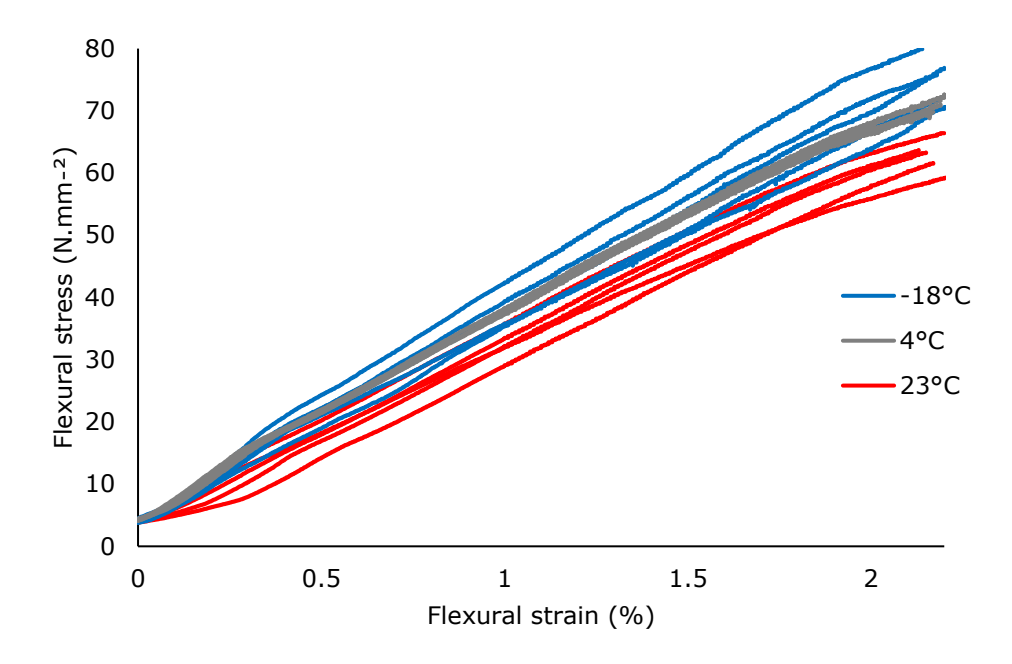


Figure 68: Influence of ambient temperature on flexural stress-strain curves of a PET/PE bottomweb (n=5).

Figure 69 shows tensile stress-strain curves of the topfilm at -18, 4 and 23 °C. At low temperature; the elongation decreases, whereas the yield and peak strength increase. Stress values of 40 and 60 N.mm⁻² correspond respectively to normalized strength values of 2.5 and 3.7 N.mm⁻¹. The average values (not shown) of yield stress at -18, 4 and 23 °C are statistically different at a 95 % confidence level.

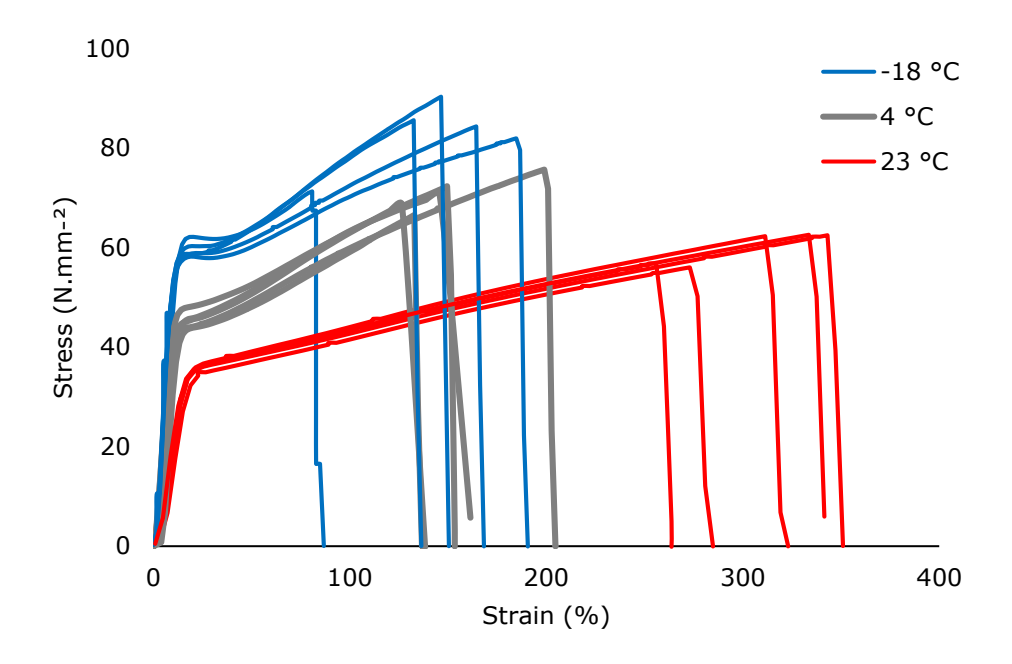


Figure 69: Influence of processing temperature on tensile stress-strain curves of a PET/PE-EVOH-PE topfilm (n=5).

Figure 70 shows stress-strain curves during tensile tests of 60 µm thick standard LDPE blown monolayer film. Increase of yield and peak stresses are observed at low temperature, comparable with the effects illustrated in Figure 69. Stress values of monolayer PE film are lower, and strain values are higher in comparison with multilayer film. This is caused by the presence of a thin PET outer layer in the multilayer topfilm. Stress values of 20 and 30 N.mm⁻² correspond respectively with normalized strength values of 1.2 and 1.8 N.mm⁻¹. The average values (not shown) of yield and peak stress at -18, 4 and 23 °C are statistically different at a 95 % confidence level.

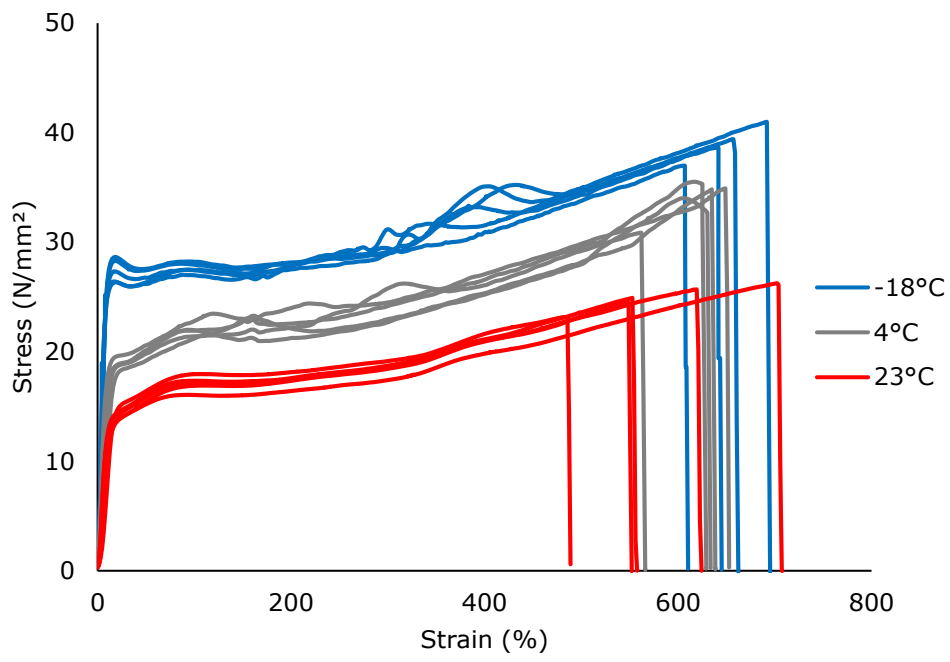


Figure 70: Influence of ambient temperature on tensile stress-strain curves of a 60 µm thick blown extruded monolayer LDPE (LDPE FE8000, Total) film, tested at 300 mm.min⁻¹. on 15 mm wide rectangular shaped samples (n=5).

5.4.4 Evaluation of peel performance during cold storage

This section discusses the impact of temperature on peel strength and peel energy during cold storage.

Figure 71 shows bending movements of the sealed bottomweb that occurs during the peel test. Once a pulling load is exerted on the seal, and peeling initiates, the sealed bottomweb will slightly bend. The bottomweb straightens when the seal is peeled towards the end of the seal. In a previous study on peel films of low-density PE, with minor contents of isotactic poly(1-butene), bending force and bending energy was neglected because the values were 200- and 100-times smaller as peel force and peel energy⁹. In the flexural test of this study flexural stress reached values up to 75 N.mm⁻² around 2% flexural strain, corresponding with respective normalized strength values of 0.2 N.mm⁻¹ at 6 mm. Although different test protocols were used, these values indicate a higher proportion of bending force peel force, which reaches to 0.5-1.2 N.mm⁻¹ in Table 21 as maximum peel strength. This was expected as the bottomweb is a more rigid material because of the presence of a thick PET outer layer of 250 µm.

The bending of the bottomweb causes a change in peel angle during the test. If the bottomweb is fixed a peel angle of 0° would be assumed for the bottomweb and 180° for the topfilm. The bottomweb is not fixed in the peel test of this study causing a change in peel angle partitioning over bottomweb and topfilm during the peel test.

Root rotation, which is described in a previous study⁸, is another important factor that could impact the peel performance. The angle of root rotation (θ_0) is dependent on the peel angle (θ) , with values between 0° and θ . The applied peel energy will be partitioned between the part that bends the peel arms and the part that creates new interfacial area. The previous study also showed the dependency of θ_0 with yield stress. As this material property increases typically at decreased temperature it is likely that decreasing processing temperature will increase θ_0 and more in general impact the peel performance during cold storage.

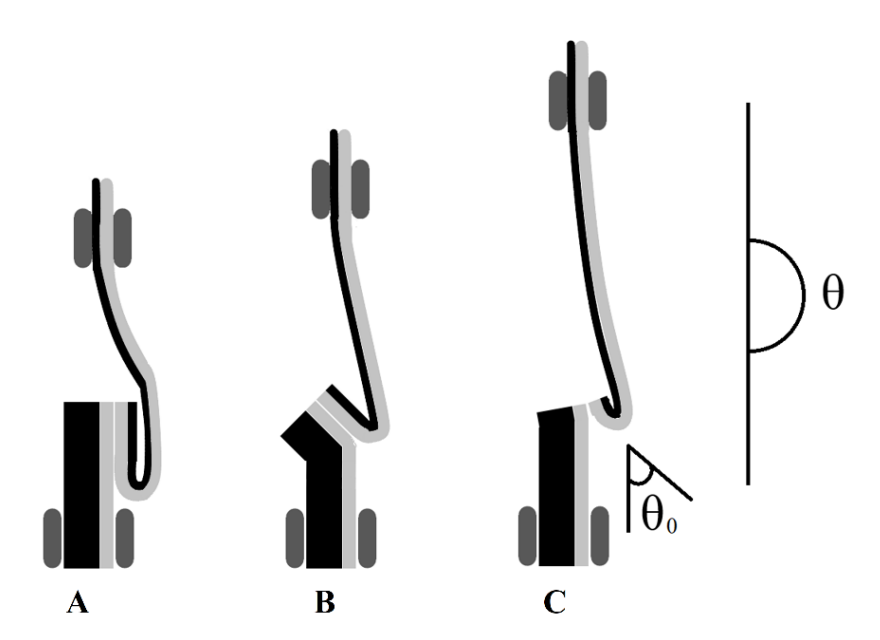


Figure 71: Bending of sealed bottomweb during a peel test. A, B and C represent respectively start situation, peel initiation and peel end (black: outer layer, grey: seal layer).

Figure 72 shows all raw peel strength-position curves, used to calculate the average and maximum peel strengths in Table 21, and compares it with sealed samples with a reinforced bottomweb to eliminate the differences in bending movement of the bottomweb, and the changes in peel angle partitioning as a consequence of this, at considered temperatures -18, 4 and 23 °C.

In all tests sealed samples with regular bottomwebs tend to achieve lower peel strengths than those that are reinforced with a thin metal plate. These results indicate a slightly negative impact of bending movement on peel strength and peel energy (area under the curve).

The total distance or end position of the peel tests at 23 °C is around 20 mm. The end position is the sum of the deformation of the peel arm(s), the peeled distance and the deformation of the peel area.

In the beginning of each curve deformation of the peel arms takes place. This deformation can be differentiated in tensile deformation of the topfilm and bending

deformation of the bottomweb. With the reinforced samples bending deformation is eliminated and a trend of slightly steeper initial slopes can be observed. Initial slopes of regular and reinforced samples are however both very steep and only take a small amount of the total distance. In this regard, the observed higher yield stresses at low temperature in Figure 69 have a zero to minimal impact on total distance, especially with the corresponding normalized strength values that are multiples of the observed peel strength values.

In a T-peel test the peeled distance corresponds to twice the width of the seal area (W). In a fixed arm peel test the peeled distance is $W-W*cos\theta.^9$ In the peel tests of this study, which are carried out at a peel angle of 180° , peel distance values of 20 mm are expected because the seal width is 10 mm. In this test deformation of the peel area is very limited because peeling ends around 20 mm. The impact of the observed higher yield stresses at low temperature with the standard LDPE in Figure 70 has zero to minimal impact on peel distance because of the lack of deformation.

In the curves of the tests during -18 and 4 °C peel strength is not decreasing as sharply when compared to other tests. This can be explained by the seal failure mechanism. With cohesive peel failure the materials will be opened around 20 mm and the strength very sharply drops to zero. With combined failure of cohesive peeling and delamination a small area of the topfilm delaminates during and shortly after cohesive peeling. This results in a less sharp decrease of strength compared to the samples that are fully cohesive peeled. With the regular samples, tested at respectively -18, 4 and 23 during cold storage, full cohesive peel failure is observed at 3, 4 and 5 out of 5 samples. With the reinforced samples it was observed at respectively 1, 4 and 5 out of 5 samples. Other samples were partially delaminated, the occurrence increases at cool temperatures and even more with the use of metal plates as reinforcement for the bottomweb. In a previous study on peelable PE films translaminar crack propagation was observed with 180° fixed arm peel test. It caused peel force to increase compared to samples with interlaminar crack propagation9. As temperature decreases density of PE will increase because of the decrease in free volume of the amorphous regions in the polymer skeleton¹⁴. A decreased chain mobility of the polymers in the seal layer at 4°C and especially at -18 °C is suggested to be the general cause to promote brittle failure in the peel test of this study. The full cohesive peeling is the preferred failure mechanism because of the clean look and absence of delaminated plastic parts. After cold storage, once the samples are tested at 23°C, delamination of the topfilm is rarely observed.

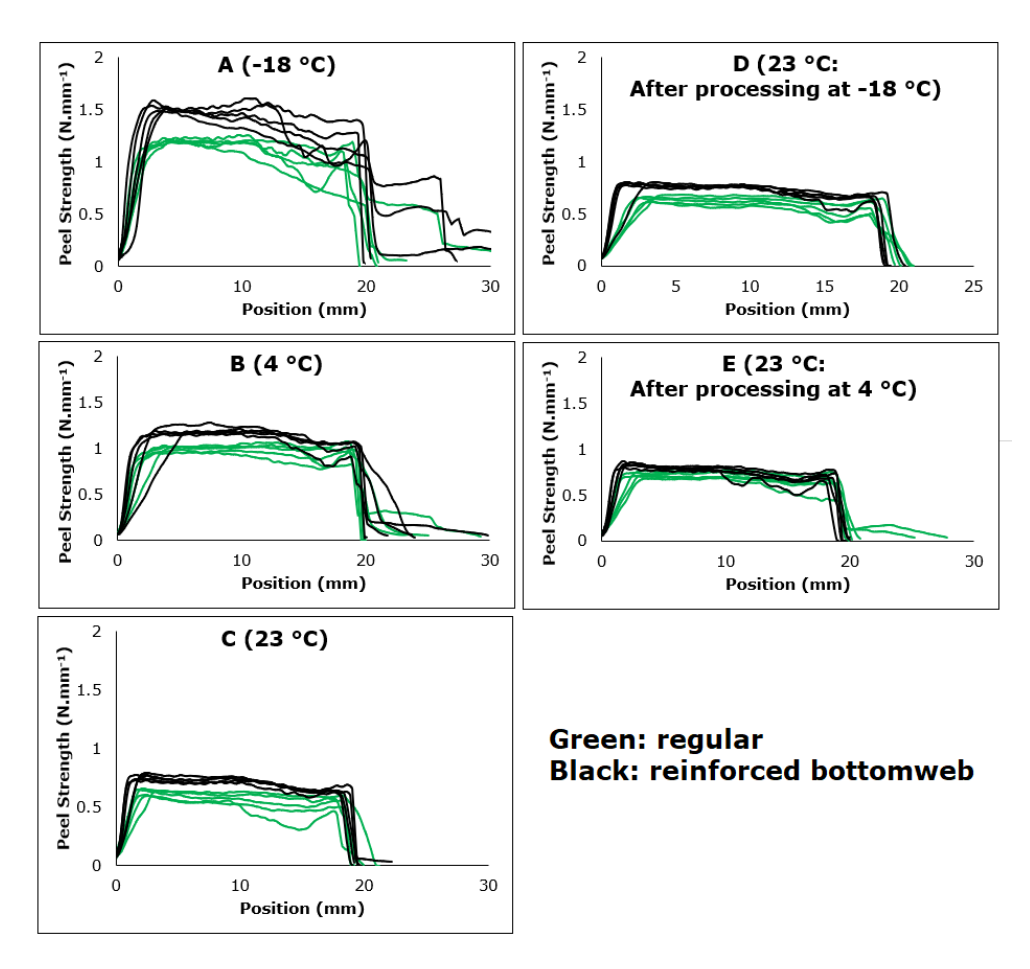


Figure 72: Influence of cold storage on peel performance of regular and reinforced samples, sealed at 170 °C, 1.0 s, 2.0 N.mm⁻², during (A, B and C) and after (D and E) cold storage at -18, 4 and 23 °C (n=5).

Figure 73 and Figure 74 show images of one sealed sample and peeled surfaces of topfilm and bottomweb. At the right side microscopic cross sections are shown to visualise the impact of the peel test during cold storage on the layer distributions of the peeled topfilm and bottomweb. Partially delaminated samples of the tests at -18 and 4 °C are selected to show more detail of the undesired seal failure mechanism. As previously mentioned, full cohesive peeling occurred in the majority of samples. To prevent delamination seals can be optimized towards a specified performance at -18 °C, care must be taken to reach sufficient peel strengths at higher temperature that prevent opening during transportation, storage and/or handling.

A cross section of a sealed sample in Figure 73a shows that the thickness is around 360 μ m, this is a result of sealing a 60 μ m topfilm against a 290 μ m bottomweb. Small deviations can occur because of heterogeneity of the thickness of commercial plastic films. Cross sections of cohesive peeled topfilms are shown in

figures b, d and h. At all considered temperatures thickness is around 50µm. This consistent slight decrease of total thickness can be a result of thin layers that are peeled off because of the cohesive failure. Cross sections of cohesive peeled bottomwebs are shown in figures c, q and j. At all considered temperatures thickness is around 285 um which is very close to the original material thickness. Possible effects of thickness increase because of a sticking layer of the topfilm are not clear. With a thick commercial web with a heterogenous thickness distribution it is harder to observe slight differences in µm range compared to similar differences in the thin topfilm. Cross sections of delaminated topfilms after peel tests at 4 and -18 °C are shown in figures e and f. This cross section is cut out of the transparent part of the topfilm on the left side of the image. The thickness of 12 µm indicate that the 35 µm blown extruded part sticks against the bottomweb and that only one layer remains at the topfilm, PET. This 12 µm part is highly transparent compared to rather hazy elongated seal materials. One cross section (figure i) is made of a stretched out hazy plastic part that remains attached at the bottomweb after peel testing during 4 °C. The resulting thickness of 35 µm indicates that the blown extruded part of the topfilm (PE-EVOH-PE) is delaminated and elongated because of the peel test.

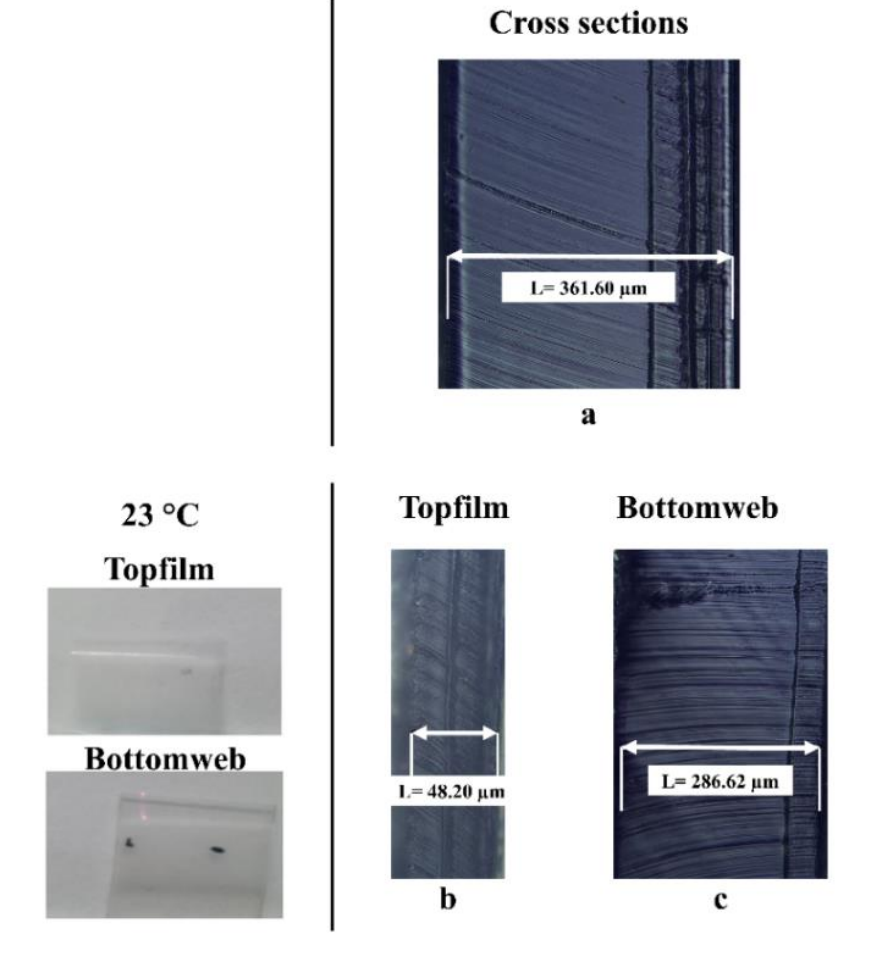


Figure 73: Pictures and cross sections of sealed and peeled samples, that are tested in a peel test at 23 °C.

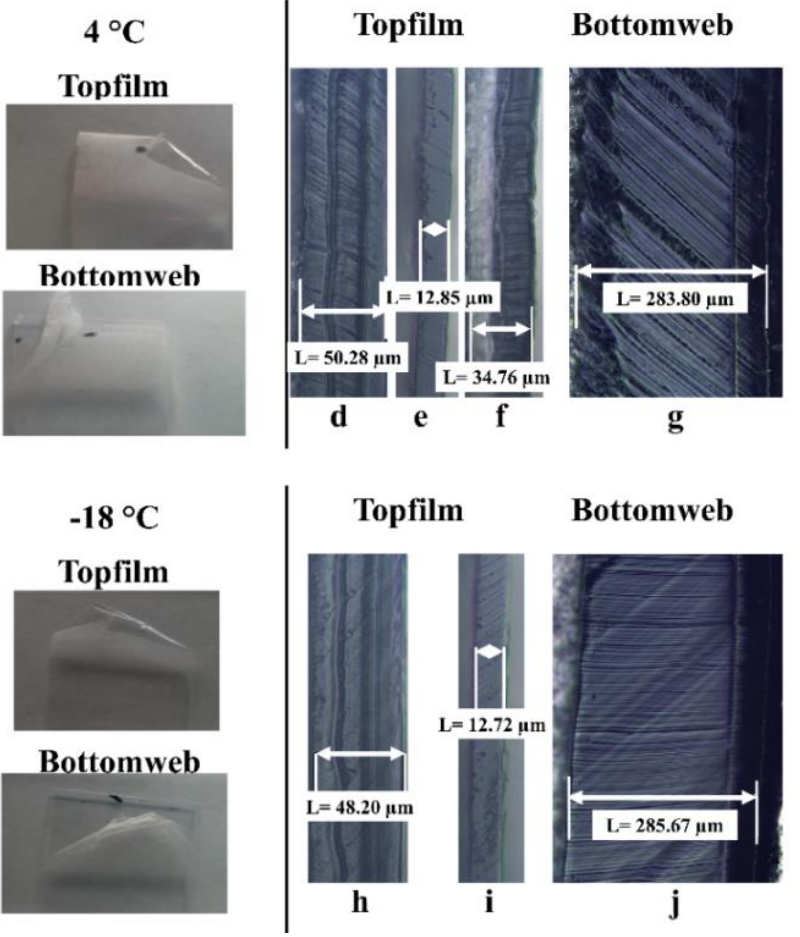


Figure 74: Pictures and cross sections of peeled samples, that are tested in a peel test during cold storage at 4 and -18 °C.

Humidity was neglected during this work, in a next study it can be added as factor. The proposed method can also be applied with different temperatures, such as pasteurization and sterilisation temperatures, relevant for retort packages.

5.5 Conclusions

This work presents a DOE-method to evaluate peel performance of a packaging concept with a peelable topfilm sealed to a bottomweb, during and after cold storage, by comparing optimized peel performances at different processing temperatures. Models are fitted and experimentally validated at optimal settings to match peel strength to 0.5 N.mm⁻¹ at 23 °C and maximize peel energy. During cold storage, at -18 and 4 °C, peel strength increased. After cold storage, there was no impact of processing temperature on peel strength.

Additional seal and mechanical experiments are performed to gain understanding of the impact of low temperatures on peel performance.

Bending stiffness of the bottomweb increased slightly during -18 and 4 °C, suggesting a minor impact of processing temperature on bending of the bottomweb during the peel test.

The impact of rigidity on the peel strength is evaluated by comparing regular samples with reinforced samples. Peel strength increased in a peel test with reinforced bottomweb at all considered processing temperatures.

The increase in peel strength is clearly related with a change in seal failure mechanism. Translaminar crack propagation was previously observed with a 180° fixed arm peel test in another study. The current study shows that this effect is more pronounced during cold storage, illustrated by the difference in seal failure mechanisms at different processing temperatures. Seals peel cohesively, when tested at 23 °C. Partial delamination occurs during 4 and, more often, during -18 °C.

The framework, presented in this chapter, has broad applicability towards different packaging materials, during and after cold storage at other temperatures, desirability functions, etc. The evaluation and optimization of burst and cohesive peel performance, the impact of hot processing on peel performance are potential topics for further research.

5.6 References

- [1] Yam KL. The Wiley Encyclopedia of Packaging Technology, Third Edition. John Wiley & Sons, Inc **2009**, New Jersey, pp. 1222-1228. Print ISBN: 9780470087046.
- [2] Coles R, McDowell D, Kirwan MJ. Food packaging technology. *Blackwell publishing Ltd* **2003**, Oxford, pp. 42-54. ISBN 13: 9780849397882.
- [3] Goldman A, McKay B, Mojet J, Kremer S. Scientific Information Bulletin (SIB). Meeting the food needs of the ageing population– implications for food science and technology. *The International Union of Food Science and Technology (IUFoST)* **2014**.
- [4] Schreib I, Liebmann A. Merkblatt No. 106/2011. Guideline für die Gestaltung von peelbaren Verpackungen unter dem Gesichtspunkt "Easy Opening". Arbeitsgruppe Abfüllen und Verpacken von Lebensmitteln AVL. Fraunhofer Anwendungszentrum für Verarbeitungsmaschinen und Verpackungstechnik, Dresden: Berlin, **2011**.
- [5] Wenk S, Brombach C, Artigas G, Järvenää E, Steinemann N, Ziesemer K, Yildirim S. Evaluation of the Accessibility of selected packaging by comparison of quantitative measurements of the opening forces and qualitative surveys through focus group studies. *Packaging, Technology and Science* **2016**, 29 (11), pp. 559-570, DOI: 10.1002/pts.2237.
- [6] D'huys, K, Bamps B. Peeters R, De Ketelaere B. Multi-criteria evaluation and optimization of the ultrasonic sealing performance based on design of experiments and response surface methodology. *Packaging Technology and Science* **2019**, 32 (4), pp. 165-174, https://doi.org/10.1002/pts.2425.
- [7] Bamps B, D'huys K, Schreib I, Stephan B, De Ketelaere B, Peeters R. Evaluation and optimization of seal behaviour through solid contamination

- of heat sealed films. *Packaging Technology and Science* **2019**, 32 (7), pp. 335-344, https://doi.org/10.1002/pts.2442.
- [8] Kinloch AJ, Lau CC, Williams JG. The peeling of flexible laminates. *International Journal of Fracture* **1994**, 66, pp. 45-70, DOI: 10.1007/BF00012635.
- [9] Nase M, Langer B, Grellmann W. Fracture mechanics on polyethylene/polybutyene-1 peel films. *Polymer testing* 2008, 27 (8), pp. 1017-1025, DOI: 10.1016/j.polymertesting.2008.09.002.
- [10] Morris B. 2017. The science and technology of flexible packaging multilayer films from resin and process to end use. *Elsevier inc* **2016**, Amsterdam, pp. 351-400. ISBN: 978-0-323-24273-8.
- [11] Goos, P., Jones, B. Optimal Design of Experiments: A Case Study Approach. *John Wiley & Sons, Inc* **2011**, New Jersey. ISBN: 9780470744611.
- [12] Antony J. Design of Experiments for Engineers and Scientists. *Elsevier* **2003**, Amsterdam. ISBN: 9780750647090.
- [13] Jensen WA. Confirmation runs in design of experiments. *J Qual Technol* **2016**, 48(2), pp. 162-177, DOI: https://doi.org/10.1080/00224065.2016.11918157.
- [14] Alnaimi S, Elouadi B, Kamal I. Structural, thermal and morphology characteristics of low density polyethylene produced by QAPCO. Paper presented at 'The 8th International Symposium on Inorganic Phosphate Materials', September 13-19, **2015**, Agadir, Morocco. Retrieved December 4 from https://www.researchgate.net/publication/281818492 Structural Therm al and Morphology Characteristics of Low Density Polyethylene Produced by QAPCO.

6. Characterizing mechanical, heat seal and gas barrier performance of biodegradable films to determine food packaging applications

Bamps B, Guimaraes RM, Duijsters G, Hermans D, Vanminsel J, Vervoort E, Buntinx M, Peeters R. Characterizing mechanical, heat seal and gas barrier performance of biodegradable films to determine food packaging ap-plications. *Polymers* **2022**; 14(13); pp. 2569. DOI: https://doi.org/10.3390/polym14132569.

To reduce the accumulation of plastic waste, a transition from a linear to a circular material flow is proposed. The circular economy diagram of the Ellen MacArthur foundation illustrates a continuous flow of technical and biological materials through the value circle ¹. Biodegradation by composting is a strategy that fits in that circular vision. Poly(butylene adipate-co-terephthalate) (PBAT), poly(butylene succinate) (PBS), poly(lactic acid) (PLA), polyhydroxyalkanoates (PHA), starch blends and cellulose films are biodegradable material groups with the largest production capacities in 2021². Packaging functionality is one of the main bottlenecks for their widespread introduction in food packaging.

The DOE-approach of the previous chapters is followed in the seal-throughcontamination study of this chapter. More broadly, this chapter determines application areas in food packaging for biodegradable materials. The scope is broadened to gas permeation and mechanical performance in this study. Specifically, for heat sealing, the performance is screened by performing hot tack and seal strength experiments, following the industrial standards that are described in chapter 2. Besides this screening, additional seal-throughcontamination studies are added, based on the application and statistical methodology of chapter 4. A DOE-method with four factors (hot tool process parameters: temperature, pressure and time + contamination type) and one performance indicator (maximum seal strength), referred to as responses in this publication, is developed, validated and applied to evaluate the seal-throughcontamination performance. Similar to the screening of seal performance, mechanical and gas barrier performances are screened by performing experiments, based on industrial standards. Oxygen and water vapor transmission rates are measured to evaluate the gas barrier performance. Tensile, puncture and tear resistance properties are determined to evaluate the mechanical performance. This study is performed within the TETRA-framework (BIOFUN: "Evaluation of the functionality of new generation compostable bioplastics in food packaging", funded by the Flemish government (Agentschap Innoveren & Ondernemen (VLAIO-TETRA HBC.2020.2096).

6.1 Introduction

Plastic materials are increasingly applied in packaging during the last decades because of their low cost, low weight, and customizable functional properties. In 2019, 368 million tons of plastics are produced globally, from which a staggering amount of around 40% is used in packaging³. To reduce the amount of plastic waste, global and local initiatives, such as the European directive (EU) 2018/852⁴, are taken, that fit in a vision of a circular economy of plastics.

Plastic biodegradation is defined as the microbial conversion of all its organic constituents to carbon dioxide (CO_2), new microbial biomass and mineral salts under aerobic conditions⁵. Composting of biodegradable packaging is described in the DIN EN 13432 standard⁶. Besides composting, anaerobic degradation systems that produce methane gas are emerging. Currently, only a small fraction of globally produced plastics is biodegradable- (1.553 million tons in 2021), but this amount is predicted to rise to 5.297 million tons in 2026.² With a low but increasing availability of biodegradable plastics, this group of materials can become an emerging alternative to mechanical recycling and reuse in a long term organic circular economy. Packaging is already the main application of biodegradable plastics, with 43% and 16% of biodegradable materials being applied as flexible and rigid packaging respectively⁵.

With a projected growth from \$338 billion in 2021 to \$478 billion in 2028, the food packaging market plays an important role in our society⁷. Considering the number of food packages, plastic and paper are the most important materials for food applications8. In food packaging films, different materials are often combined to obtain high performing and cost-effective packages. This can be achieved by blending, coating or laminating. In order to maintain biodegradability by composting, it is important that these composites are made of compostable materials. However, small fractions of non-compostable materials, limited to a maximum content of 10% because of degradation and disintegration criteria, can be allowed for composting if the whole package meets the demands of the DIN EN 13432 standard⁵. Industrial and home compostability can be differentiated, these processes differ in temperature and time. Poly(lactic acid) (PLA), poly(butylene adipate-co-terephthalate) (PBAT), poly(butylene succinate) (PBS) and polyhydroxyalkanoates (PHAs) are biodegradable plastics that were subject of previous studies on packaging functionality in food applications^{9, 10, 11}. These materials are industrial compostable¹². Depending on the properties of the coating, coated paper can be considered as biodegradable packaging. Interest is increasing for its implementation in food packaging, mainly because of the versatile end-of-life options of this material^{13, 14}. Cellulose, the main component of paper, is a natural polymer that can be easily obtained from the cell wall of plants. Processes to extract and modify cellulose are subjects of recent studies, of which the lyocell process is one example¹⁵. Plant waste streams can be valorized by extracting cellulose to make packaging films. A recent study extracted cellulose from cocoa pod husk, a waste stream of the chocolate industry, to develop biodegradable cellulose films¹⁶. Cellulose and its derivatives can be found in food packaging films, such as solution casted cellulose acetate, extruded cellulose nanocrystals, electrospun hydroxymethyl cellulose and many others¹⁷. Starch is another example of a natural abundant polymer that can be used in packaging. This polymer is home compostable, which is a less aggressive process than industrial composting. Also, cellulose is home compostable, if the lignin content does not exceed a threshold value of 5%¹².

In a 2021 survey, amongst 24 European food companies and packaging material providers, functionality of biodegradable materials is indicated, besides high cost, low availability and the end-of-life concerns, as bottleneck for implementation in food packaging. Because of the interest of the food industry in packaging functionality of biodegradable materials, the research project 'BIOFUN' evaluates typical food packaging functionalities, such as mechanical, gas barrier and heat seal performance of commercially available films in 2021 and 2022¹⁸.

The objective of this study is to determine application areas in food packaging of currently commercially available biodegradable films. A pragmatic approach is followed, based on a broad characterization of the mechanical, seal and gas barrier performance. Additionally, opacity and water contact angle are determined for further characterization.

6.2 Materials & methods

6.2.1 Materials

Table 22 lists 10 films that were supplied by companies participating in the BIOFUN project. Results of thickness measurements and the main components of the seal side, identified with attenuated total reflectance Fourier transform infrared (ATR-FTIR) spectroscopy (spectra are not shown), are added to this table to give supporting information of these samples. The identified components with FTIR compensate the lack of commercially available information, which is the result of the high level of secrecy on the chemical composition in the industry. The list includes paper, PLA, PBAT, PBS, poly(butylene succinate-co-butylene adipate) (PBSA), starch, cellulose and poly(3-hydroxybutyrate-co-3-hydroxyvalerate) (PHBV), which are considered for use as food packaging. Coated paper 1, with PE as coating material, is unlikely to be compostable. The materials of Table 22 are differentiated in 4 material groups: coated papers, cellulose films, pilot extrusions and commercial monolayers. Two coated papers, two cellulose films, two rather thick pilot extrusions and four commercial monolayers, subdivided in 2 monolayer monomaterials and 2 monolayer blends, are subject of this study. Results of materials in each group are mutually compared and discussed. Digital photos of the samples in Table 22 are shown in Figure 75.

Table 22: Sample description.

Code: details	Thickness (mm) (n=10)	Identified components of seal surface ¹
1. coated paper 1: commercial coated paper	0.097 ± 0.003	LDPE
2. coated paper 2: commercial coated paper	0.076 ± 0.002	PLA, PBAT
3. cellulose 1: commercial coated cellulose film	0.030 ± 0.000	Cellulose, PVDC
4. cellulose 2: commercial laminated cellulose film	0.087 ± 0.002	PBS
5. pilot extrusion PHBV : monolayer blend of PHBV + PBAT + mineral filler + process additives	0.264 ± 0.005	PHBV, PBAT
6. pilot extrusion PBS : monolayer blend of PBS + PBSA + process additives	0.284 ± 0.002	PBS, PBSA
7. PBS: commercial monolayer	0.047 ± 0.001	PBS
8. PLA: commercial monolayer	0.030 ± 0.001	PLA
9. PLA + PBAT: commercial monolayer blend	0.020 ± 0.001	PBAT, PLA, CaCO₃
10. starch + PBAT: commercial monolayer blend	0.025 ± 0.003	PBAT

¹ Identified with ATR-FTIR.

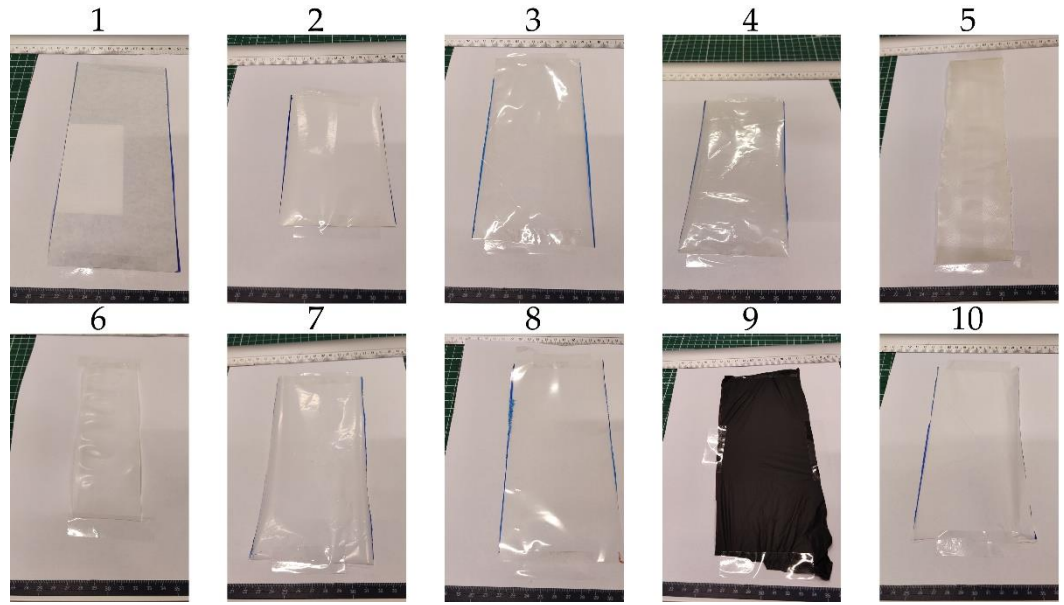


Figure 75: Digital photos of samples on white paper.

6.2.2 Methods

To compare the test materials based on their packaging performance, the mechanical, gas barrier and seal characteristics are determined for all samples. Tests are performed in machine direction in standard climate (23 °C, 50% relative humidity (RH)), unless otherwise stated. Standard deviations are calculated to show the level of scattering of results.

Mechanical performance

Thickness is measured in tenfold according to ISO 4593. Peak stress (N.mm-²) and total strain (%) are determined in fivefold with a tensile tester. Dumbbell shaped samples with 3.18 mm width of the narrow section, described in ASTM

D638¹⁹, are used to prevent the samples from breaking at the clamp. Total strain values are mainly used for mutual comparison. No extensometer is used, so comparisons of total strain values in literature must be made with caution. Slipping is prevented by clamping the wide section in diamond coated jaws. A clamp distance of 20 mm and a separation rate of 100 mm.min⁻¹ are used to perform the test. Additional experiments in a temperature chamber are performed to evaluate the impact of ambient temperature on peak stress and total strain. Relevant temperatures for food processing, ranging from freezing at -18 °C until pasteurization, hot fill and/or microwave at 100 °C and/or melting of the sample, were considered in this test.

Maximum force (N), total displacement (mm) and total energy (mJ) are determined in fivefold with a puncture resistance test. A penetration probe, as described in ASTM F1306 20 , moves towards the outer side of a clamped film with a speed of 25 mm.min $^{-1}$ until the film is penetrated.

Tear resistance (mN) is determined in tenfold with an Elmendorf test, which uses a pendulum to propagate an existing slit, as described in ISO 6383-2²¹.

Gas permeability

Single measurements are performed in standard conditions to screen the oxygen transmission rates (OTR) of all samples at 23 °C and 0% relative humidity, as described in ASTM F1307²². Additional tests on high gas barrier materials are performed at 23 °C and 50% relative humidity, following ASTM F1927²³, at both sides of the film.

Single measurements are performed in extreme test conditions to screen the water vapor transmission rates (WVTR) of all samples in a worst-case scenario. WVTR, according to ASTM F1249 24 , is determined at 38 °C and 100% relative humidity at the outer side of the film, while 0 % relative humidity is maintained at the inner side.

Seal performance

Seal temperature is varied with two hot jaws, at a seal time of 1.0 s and a seal pressure of 1.0 N.mm-². Samples of 30 mm width are sealed while Teflon sheets are used on both sides to prevent the material from sticking against the jaws. At each temperature, 3 samples are sealed. Seal strength, following ASTM F88²5, is evaluated in a timeframe of 4 hours after sealing. 15 mm wide samples are clamped with a distance of 20 mm and separated at a rate of 300 mm.min⁻¹. Three characteristics of the sigmoidal seal curve are determined: an initiation temperature, which is the jaw temperature at which seal strength exceeds a threshold value of 0.05 N.mm⁻¹ ²⁶; a mid-slope temperature, which is the jaw temperature at which half of the maximum seal strength is exceeded; and the maximum seal strength.

Hot tack tests, following ASTM F1921²⁷, are performed on 15 mm wide samples at a test speed of 200 mm.s⁻¹. Seal time and seal pressure are respectively set at 1.0 s and 1.0 N.mm⁻², while seal temperature of two Teflon coated hot jaws is varied. At each temperature, 3 samples are measured. Seals are evaluated 0.1 s after opening of the seal jaws. Four characteristics are determined: seal initiation temperature, which is the jaw temperature at which a threshold value of 0.03 N.mm⁻¹ is exceeded²⁸; the temperature of maximum strength, which is the jaw temperature at which hot tack strength reaches its maximum; the hot tack window, which is the temperature range of the jaws where hot tack strength is higher than 0.1 N.mm⁻¹ ²⁸; and the maximum hot tack strength.

Besides the above described broad seal characterization, additional seal experiments can be performed to check the compatibility with specific food applications. Real food contamination is applied in seal-through-contamination tests. Two case studies, that relate film samples with food applications, are defined, based on gas barrier performance. Low gas barrier samples are evaluated with contamination types that are related with unprocessed fruit and vegetables. In this application, water droplets and solid soil particles are expected. Sand and coffee particles are selected as simulants of soil particles. High gas barrier samples are evaluated as grated cheese packaging. Square samples of approximately 10x10 cm² are cut and attached to a cardboard tool with plastic tape. A rectangle of 20x40 mm² was marked in the center of the sample to ensure that the contamination was distributed over the entire length of the seal. Then, 10 mg of the solid contamination or 30 uL of water was evenly spread into the rectangle to maintain a 12.5 g/m² or 37.5 mL/m² contamination density. Specifically, for grated cheese, three strings were placed vertically and distributed in the middle and the two corners of the rectangle. A second sample was also attached to the cardboard tool to cover the contamination. In a final step, the tool was manually placed between the hot bars, forming the seal. The above described set-up is illustrated in Figure 76.

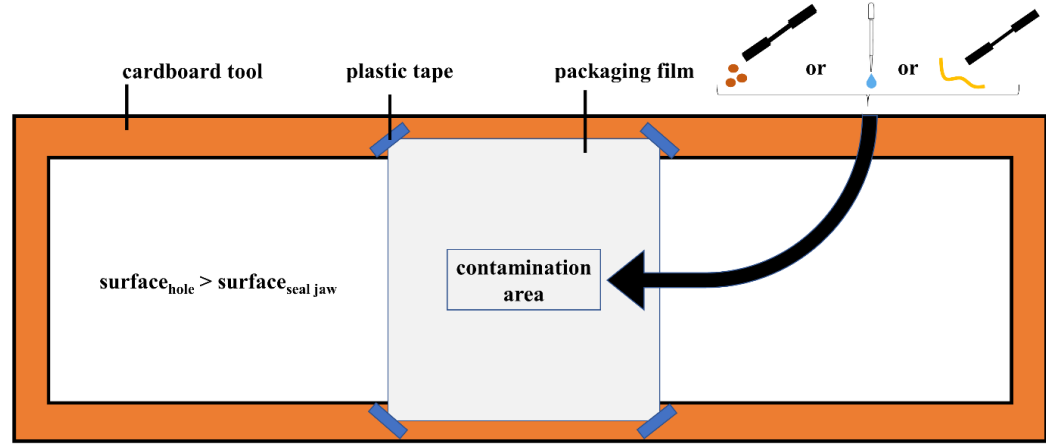


Figure 76: Set-up to contaminate the seal area.

In a previous study, solid contamination was applied in a standardized method and seal-through-contamination performance was evaluated with a design of experiments (DOE) approach²⁸. This approach was followed, with the exception of adding contamination as a categorical parameter in the design space. For the low gas barrier samples, three levels are considered for seal temperature, time and pressure, and contamination was added as a categorical variable with 4 levels: clean, ground coffee, sand and water. Three replicates are carried out for each contamination level in the centre point. Main order, second order and interaction effects are considered with seal strength as response, resulting in a D-optimal designs for coated papers 1 and 2 with respectively 46 and 41 runs. A similar approach is followed for the contamination experiments with the high barrier cellulose samples, with the exception of only two considered levels for contamination: clean and grated cheese, 3 replicates are carried out for grated cheese contamination in the centre point, resulting in a D-optimal design with 24 runs for both films. After experimentation, a standard least square method is followed to fit a model. Second order and interaction terms with a p-value above 0.05 were not used in the model. Seal strength is maximized for clean seals and the predicted values are validated by performing 5 measurements at maximal settings. All contaminations are also validated at equal settings to allow comparison between clean and contaminated seal strength. For more details on this approach, the reader is referred to the previous study²⁸.

Additional characterization

Opacity is measured to show the appearance and decoration potential in food packaging. The Hunter lab method in the reflectance mode is followed. The opacity Y (in %) is calculated by dividing the opacity on a black standard Y_b with the opacity on a white standard Y_w . For each sample, average values of 4 measurements, twice on each side, are calculated.

Water contact angle measurements are carried out to characterize hydrophobic properties of the samples. Samples are cut to fit the sampling area. A 2 μ L MQ water (18.2 MOhm.cm) drop is gently deposited on the seal surface, using a micro-syringe, and digitally photographed immediately. Contact angles are measured at both sides. Average values of contact angles of 15 drops at different spots on the surface of each sample are calculated.

Apparatus

Thickness is measured with a precision thickness gauging model 2010 U (Wolf Messtechnik GmbH, Germany). Tensile, puncture and seal strength tests are performed with a 5ST universal testing machine (Tinius Olsen Ltd, United Kingdom), inside a TH 2700 temperature chamber (Thümler GmbH, Germany). Tear resistance is tested with a tearing tester ED 300 (MTS Adamal Lhomargy, France). Dry and humid oxygen permeation are respectively measured with the OX-TRAN® model 702 and the OX-TRAN® model 2/21 SH (Ametek Mocon, United States). Water vapor permeation is measured with the Permatran-W models 3/33 MG and SW (Ametek Mocon, United States). Seals are prepared with a Labthink HST-H3 heat seal tester (Labthink Instruments Co Ltd, People's Republic of China). Hot tack samples are evaluated with a J&B Hot Tack Tester model 5000 MB (Vived-Management, Belgium). Opacity is measured with a Datacolor Check3 (Datacolor België BVBA, Belgium). Water contact angle is measured with a GBX Digidrop contact angle (GBX Scientific, Republic of Ireland).

6.3 Results and Discussion

6.3.1 Mechanical performance

Table 23 shows the average values and standard deviations of the mechanical characterization of all materials in standard climate (23 °C, 50% RH). Representative stress-strain curves of each of the samples are shown in Figure 77.

Coated paper shows moderate peak stress values in Table 23. As a result, actual tensile forces will be high because of the rather thick materials that are used in food packaging. The strain of coated paper is limited because of the immediate break of the paper substrate in a tensile test, high variations can be caused by delamination of the plastic coating. In a previous study on PLA coated paper, tensile stress and elongations are ranging respectively from 58-75 N.mm-² and 3-4 %.²⁹. However, paper type, coating material and coating thickness impact, amongst others aspects, the mechanical properties of coated papers. The

puncture results show moderate forces, small displacements and moderate energies. Also tear resistance was moderate, compared to other samples.

Cellulose 1 was the strongest material in the tensile test. The decreased peak stress of cellulose 2 is probably caused by the lamination with a weaker but tougher PBS layer. Cellulose films have limited strain because of the almost immediate break of the brittle cellulose layer in a tensile test, high variations of cellulose 2 are caused by the delamination of the tough seal layer. The experimental values of stress and strain of cellulose 1 are equal with values in the datasheet of commercial cellulose film³⁰. Puncture resistance forces and energies of cellulose films are high, displacements are moderate. The tear resistance of cellulose 1 reaches the lowest value of all samples. This property can be dramatically improved by laminating a tough seal layer, as observed in the results of cellulose 2, which has a laminated PBS layer.

The pilot extrusion of PBS is mechanically superior to that of PHBV, with the exception of tear resistance. There is no comparable value found in literature for the PHBV-PBAT blend. In a review on monomaterial PHBV¹¹ a tensile stress range of 18-45 N.mm⁻² is found. The peak stress value of the PHBV film of this study, which is blended with PBAT, mineral filler and process additives, fits within the range of monomaterial PHBV. PBS is strong and tough at the same time, this is reflected in the tensile and puncture results. In the comparison of the puncture and tear resistance results of the pilot extrusions with the commercial films, caution must be taken with puncture and tear resistance, because of the different thickness.

The strong mechanical performance of PBS is also reflected in the results of the commercial monolayer, reaching a moderate peak stress and very high strain in the tensile test. The stress values of the two PBS based films, the pilot extrusion and the commercial monolayer, are relatively high, compared to the stress values, ranging from 20 to 34 N.mm-2, found in a study on poultry meat packaging 10, bread packaging³¹ and a recent review on PBS properties³². The increase in strength of the films in this study indicate a difference in production, which is known of the pilot extrusion film, by blending with PBSA and process additives, but is not known of the commercial monolayer. A previous study on PBS blends showed that mechanical properties were majorly influenced by compatibility between polymers and morphology including microstructures and crystallinity³¹. A moderate puncture force, high displacement and high energy in the puncture test are achieved. Tear resistance of PBS is rather low, compared to other samples. PLA also stands out as a mechanical good performing film, with high peak stress and moderate strain in the tensile test, and high force, displacement and energy in the puncture test. Also, this film is easy-tearable. The two blended films with PBAT are characterized with low strength, high toughness and very high tear resistance. A previous study on the mechanical properties of PLA and PLA-PBAT blended films illustrates a strong but brittle tensile performance of PLA film and a weaker but tougher performance of the PLA-PBAT blended film³³. PBAT is often used in blends to increase flexibility and toughness of brittle biodegradable materials.

Table 23: Results of mechanical characterization.

	Ter	nsile		Puncture		Tear resist.
Samples	Peak stress ¹ (N.mm ⁻²)	Total strain ¹ (%)	Max. force ² (N)	Total displ. ² (mm)	Total energy² (mJ)	Tear resist. ³ (mN)
1. coated paper 1	37.6 ± 6.1	5.28 ± 0.49	12.2 ± 1.5	2.91 ± 0.13	16.4 ± 2.0	663 ± 37
2. coated paper 2	55.1 ± 7.5	56.8 ± 72.8	7.35 ± 0.82	2.95 ± 0.21	11.3 ± 0.7	455 ± 41
3. cellulose 1	125 ± 3.0	20.7 ± 1.5	16.7 ± 1.0	5.03 ± 0.34	36.4 ± 4.3	76 ± 4
4. cellulose 2	46.5 ± 2.4	199 ± 244	17.1 ± 0.9	4.79 ± 0.18	34.4 ± 2.9	680 ± 104
5. pilot extrusion PHBV	37.8 ± 1.8	24.9 ± 2.8	8.62 ± 0.65	3.77 ± 0.07	20.5 ± 1.7	526 ± 40
6. pilot extrusion PBS	106 ± 5.0	165 ± 17	54.6 ± 1.0	7.43 ± 0.29	194 ± 10.0	375 ± 19
7. PBS	56.5 ± 2.6	443 ± 22	10.3 ± 0.6	8.65 ± 0.36	57.2 ± 5.5	127 ± 67
8. PLA	68.8 ± 5.4	147 ± 29	13.4 ± 1.9	7.85 ± 1.07	59.3 ± 16.5	142 ± 4
9. PLA + PBAT	19.7 ± 4.2	272 ± 44	1.28 ± 0.08	6.65 ± 0.34	6.03 ± 0.56	992 ± 189
10. starch + PBAT	16.5 ± 2.4	311 ± 67	2.14 ± 0.25	8.90 ± 0.52	12.7 ± 1.98	5181 ± 1992

¹ n=5; average values and standard deviations are calculated.

³ n=10; average values and standard deviations are calculated.

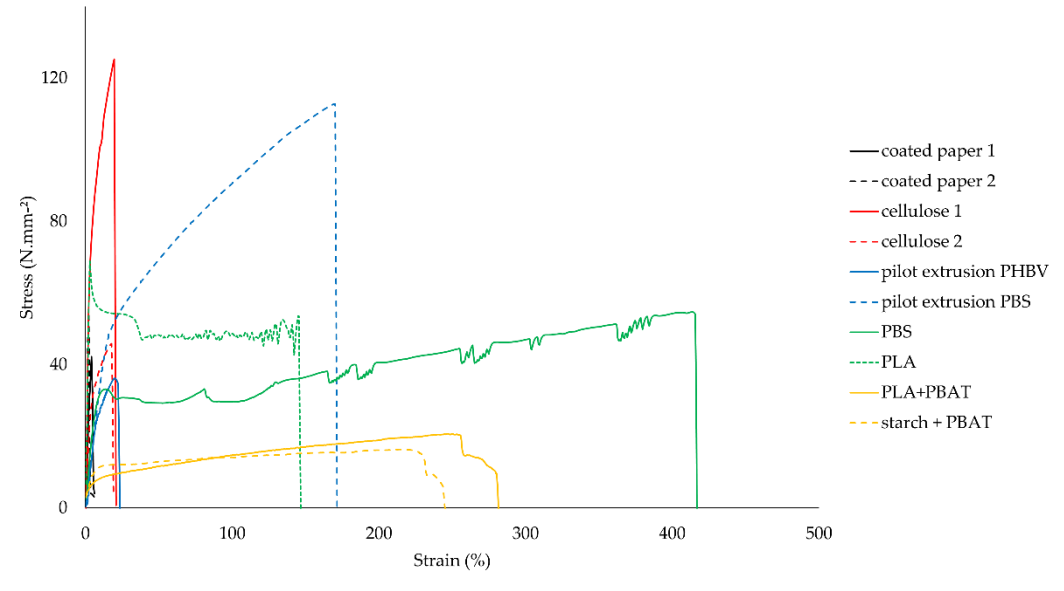


Figure 77: Stress-strain curves.

Because of the high relevance of processing temperatures in the food industry, such as in freezing, cooling, hot filling, microwaving and/or pasteurizing, ambient temperature is varied in tensile tests of a selection of materials. Thin commercial films with no backing layer, with the addition of coated paper 2 and cellulose 1, are evaluated in this test. Samples are tested at -18, 4, 23, 40, 60, 80 and 100 °C. The results of peak stress and total strain are shown in Figure 78 and Figure 79.

 $^{^2}$ n =5; average values and standard deviations are calculated; orientation sample: penetration at outer side.

With the exception of cellulose 1, peak stress tends to decrease at increasing temperatures. The tendency for total strain is less clear. PBS, PLA and the PBAT blends could not be tested at high temperatures because of high stickiness. With respective glass transition and melting temperature values of PBS and PLA of -32 °C and 114; 59 °C and 154 °C, it is clear that the sticky behavior occurs above glass transition temperature³⁴.

The peak stress of coated paper 2 decreased from 51 N.mm $^{-2}$ at -18 °C to 23 N.mm $^{-2}$ at 100 °C while remaining brittle at all ambient temperatures of Figure 78. The deviating results of total strain at 4 and 23 °C were caused by delamination of the plastic coating. Cellulose 1 remains very strong, mostly above 100 N.mm $^{-2}$, and brittle, with strain values ranging from 8 to 22%, at all considered temperatures.

PBS remains strong up to 60 °C. Total strain decreased below 100% at cool temperatures.

PLA showed a bigger temperature depending peak stress behavior, compared to PBS, achieving 89 N.mm $^{-2}$ at -18 °C and 22 N.mm $^{-2}$ at 80 °C. The drop in tensile stress from 20 to 60 °C is previously illustrated in another study on the mechanical performance of PLA tensile specimens, attributed to approaching the glass transition region of PLA 35 . Total strain decreased below 20% at cool temperatures.

PBAT blends have low peak stress values, between 24 and 40 $\rm N.mm^{-2}$ at cool temperatures and 12 $\rm N.mm^{-2}$ at 60 °C, but high total strain values.

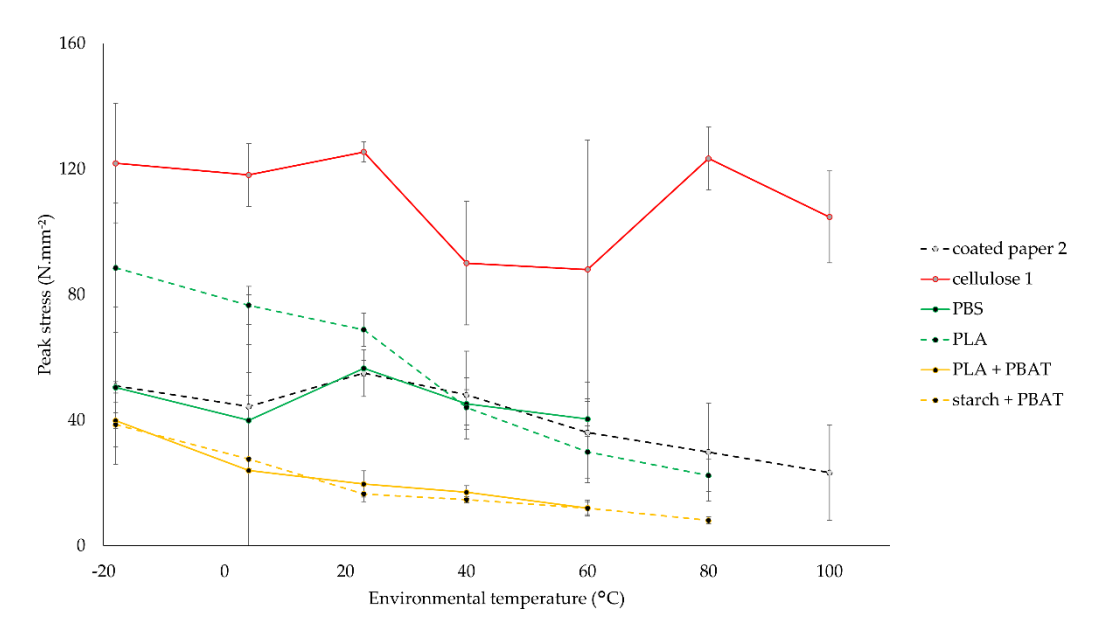


Figure 78: Impact of ambient temperature on average values of peak stress of biodegradable films \pm standard deviations(n=5).

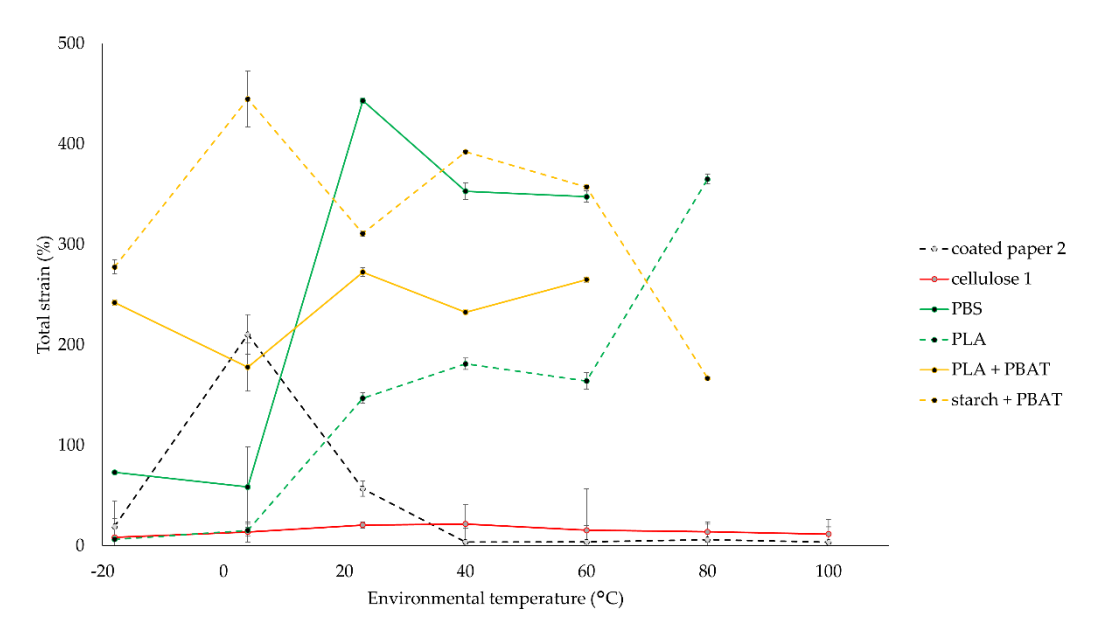


Figure 79: Impact of ambient temperature on average values of total strain of biodegradable films \pm standard deviations (n=5).

In conclusion, the mechanical characterization of coated paper and cellulose based films can be described as strong but very brittle materials. The low strain values, compared to other tougher samples, are illustrated in Figure 77. However, brittleness might be overcome by laminating a tough layer. Both materials can be used over a wide temperature range, from freezing at -18 °C up to 100 °C. The film with PHBV is rather weak and brittle, compared to the other materials. The films with PBS and PLA are strong and tough materials at standard conditions. The toughness, however, decreases at low temperatures. On top of that, stickiness initiates well below 100 °C, what will restrict their use to a narrow temperature range, especially if moderate toughness is required. If brittleness is no big issue, these materials can be used in cold and standard temperatures. The blended PBAT films, with starch or PLA, are rather weak but very tough, even at cool temperatures. Because of the melt initiation well below 100 °C, the use of these blends is restricted to cold and standard temperatures.

6.3.2 Gas permeability

Table 24 shows the transmission rates for oxygen gas and water vapor. Coated paper 1 shows similar barrier properties as polyolefin film, because of its high OTR and rather low WVTR values³⁶. This gas barrier performance can be related with the presence of low-density poly(ethylene) (LDPE) at the seal surface, identified with ATR-FTIR. A 25 μ m pure LDPE reference film has OTR between 6500 and 7800 cc.m⁻².d⁻¹, measured at 23 °C and 0 % RH, and WVTR between 12 and 19 g/m².d, measured at 38 °C and 90 % RH ³⁶. The values of coated paper 1 correspond with TR values of 10-15 μ m LDPE. Coated paper 2 on the other hand is a low gas barrier material for food packaging applications. Specifically, for WVTR

of coated paper, a recent study compared high gas barrier coated papers at 23 $^{\circ}$ C, 85% RH and 38 $^{\circ}$ C, 85% RH and suggested that the integrity of the barrier layer was disrupted at 38 $^{\circ}$ C 37 . The authors of that study suggest to use milder test conditions to simulate more closely the environment of food packages and to prevent disruption of barrier layers.

Because of the low OTR-values of the cellulose films, additional oxygen measurements at 50% RH are performed to check the influence of humidity on oxygen transmission. With respective values of 3.7 and 5.8 cc. m⁻².d⁻¹ it is clear that the OTR increases with increasing RH. These cellulose films have barrier coatings because neat cellulose is a low gas barrier for food applications. Both films achieve similar values than poly(vinylidene dichloride) (PVDC) coated materials. PVDC, which is a high gas barrier for food applications³⁶, is identified in the seal surface with ATR-FTIR in cellulose 1, but not in cellulose 2. Cellulose 2 is, however, laminated with a PBS layer that obstructs identification with ATR-FTIR of parent layers. These films can be used to maintain modified atmosphere in food packages.

Paper and cellulose are low barrier substrates that require a barrier layer, such as in coatings, to improve the barrier properties. This is illustrated in Figure 80. Barrier properties of such coated materials are mostly attributed to thin barrier layer(s) in the coating. Coating thickness, multilayer architecture, individual layer composition and concentration gradient are determining factors in this process³⁶. An example of such a process is the transmission of water vapor in the atmosphere, across a packaging material, in dry headspace of food applications, such as cookies. In some applications, such as yoghurt, the process is reversed. A previous study, that produced biodegradable blown extruded films of blends of thermoplastic starch and PBAT, functionalized with plasticized nitrite, measured a relative low oxygen permeability with a permeability coefficient down to 1.2 cc.mm.m⁻².d⁻¹ for films with 5% nitrite content³⁸. This coefficient corresponds with an OTR-value of 24 cc.m⁻².d⁻¹, considering a film of 50 um thickness. There is still a gap between this moderate value and those that are measured with the commercial cellulose films in this study. More research is needed to obtain biodegradable food packaging with the permeation levels of the cellulose films in this study, without the need of non-biodegradable functional components.

The pilot extrusions and monolayer films are low gas barrier materials for food packaging applications. The application of low gas barrier samples, such as the coated papers, the pilot extrusions and the monolayer films, is restricted to foods with low barrier or high respiration requirements such as unprocessed fruit and vegetables with short shelf lives. With these food applications, high permeation of water vapor and oxygen gas is required to avoid respectively the accumulation of saturated water vapor which leads to fungal growth, and anoxic condition³⁹. If a high gas barrier is required, these films need to be coated and/or laminated with materials that are able to add this property.

Coated paper 1 might be used for applications that need a water vapor barrier, but no oxygen barrier, which can be the case for some dry foods, such as flour, dried pastas, crackers and cookies. The barrier cellulose films can be used for applications with oxygen and water vapor barrier requirements. Typical examples are cheese, meat, high fat products and ready meals³⁶.

Table 24: Results of gas barrier characterization (orientation samples: transmission rates are measured from outside to inside, inside = seal side).

Samples	OTR 0 % RH, 23 °C (cc/m².d) (n=1)	OTR 50 % RH, 23°C (cc/m².d) (n=1)	WVTR 100 % RH, 38°C (g/m².d) (n=1)
1. coated paper 1	3564	NA	29.1
2. coated paper 2	2718	NA	>1000
3. cellulose 1	0.40	3.65	187
4. cellulose 2	0.34	5.78	58.8
5. pilot extrusion PHBV	50.6	NA	36.8
6. pilot extrusion PBS	122	NA	67.9
7. PBS	306	NA	420
8. PLA	519	NA	274
9. PLA + PBAT	2725	NA	1095
10. starch + PBAT	1472	NA	624

coating headspace

low barrier substrate

Figure 80: Permeation of gas and/or vapor, from atmosphere to headspace, through coated low barrier substrates.

6.3.3 Seal performance

atmosphere

Table 25 shows the results of the seal characterization.

Seal strength-, hot tack strength initiation and mid-slope temperatures are, with the exception of the thick pilot extrusion films, below or equal to that of typical polyolefin-based seal layers, such as LDPE, ionomers or metallocene plastomers 40 . Six out of ten films achieve over half of the maximum seal strength at jaw temperatures below 100 °C. These materials can be considered in high speed packaging operations.

Since uncoated paper cannot be heat sealed, heat seal characteristics of coated paper are mainly attributed to the coating material, coating thickness and coating process. Coated paper 2 outperforms coated paper 1, with lower initiation temperatures and higher hot tack strength. It is capable to maintain a minimum hot tack strength threshold value of 0.1 N.mm⁻¹ over a very wide temperature

region of $110\,^{\circ}$ C. The seals of coated paper fail by delamination of paper fibers during seal strength and hot tack tests.

Cellulose 2 has lower initiation temperatures and higher strengths as cellulose 1. The better seal performance of cellulose 2 is attributed to the lamination of a PBS layer with excellent seal properties. The seals of cellulose 1 fail by peeling cohesively, while those of cellulose 2 fail by breaking unsealed material during a seal strength test. The difference in failure mechanism is related with the big difference in maximum seal strength. In the hot tack test, both materials fail by peeling cohesive. The different seal failure mechanism of cellulose 2 in the hot tack test, compared with the seal strength test, is related with the very low cool time. The seal is evaluated 0.1 s after opening of the hot jaws, when it is still hot. The pilot extrusion films show high initiation temperatures, this is typical with heat conductively sealed thick films, where heat is transferred through a thick layer, from the hot jaws to the outer layers and the seal interface so entanglement can occur. The seals of the PHBV blend fail by peeling cohesively, while those of the PBS blend fail by breaking unsealed material during a seal strength test. In the hot tack test, break in the proximity of the seal is observed with both materials. The presence of a weak spot in the remote materials is suggested as hypothesis. The weak spot is still hot, but thinner than the seal area. Both thick pilot extrusion films can be heat sealed, but a thinner commercial structure should be evaluated to determine specific application areas for these materials. The thin PBS and PLA monolayers have low initiation temperatures and rather high strengths for materials without rigid backing layers. The seals of these materials fail by breaking unsealed material during a seal strength test. In the hot tack test, both materials peel cohesively and/or break in proximity of the seal. PLA has the advantage to maintain its hot tack strength over a wide temperature range. The thin monolayers with PBAT also seal at low temperatures but strengths are rather low. Both PBAT blends show similar seal failure mechanisms than those observed with the PLA and PBS monolayers. Low seal strengths are beneficial in easy-peel applications. In a previous study, that evaluated the seal performance of several PLA-PBAT blend ratios, sealed to a PLA container, the blended films were characterized as easy-peel⁹.

It can be concluded that coated paper 2, cellulose 2 and PLA are very well suited for packaging operations where the hot seal is put under pressure, such as in vertical-form-fill-sealing or when spring back forces are induced, immediately after sealing, for example by solid food contaminants in the seal area. The thin PBS monolayer could similarly be used but a stricter temperature control is advised because of the smaller hot tack temperature window. The use of coated paper 1 is restricted to operations where the hot seal is not pressurized. Cellulose 1 and the two thin PBAT blends are heat sealable, but their use is restricted to applications where low strength is required, such as in packaging of low weight foods or easy-peel applications.

Table 25: Results of seal characterization.

Samples	T _{initiat} . 1 (°C)	T _{max} strength/2 1 (°C)	Seal Str. _{max} ¹ (N.mm ⁻¹)	T _{initiat} . 2 (°C)	T _{max} . strength ² (°C)	T _{win.} 2 (°C)	Hot Tack Str. _{max} ² (N.mm ⁻¹)
1. coated paper 1	100	105	0.40 ± 0.05	105	140	0	0.08 ± 0.00
2. coated paper 2	80	85	0.49 ± 0.03	70	100	110	0.41 ± 0.02
3. cellulose 1	115	115	0.11 ± 0.01	95	145	35	0.13 ± 0.01
4. cellulose 2	75	85	2.69 ± 0.80	65	75	115	0.71 ± 0.02
5. pilot extrusion PHBV	185	195	1.08 ± 0.09	115	135	40	0.37 ± 0.08
6. pilot extrusion PBS	185	195	4.43 ± 1.50	125	150	0	0.12 ± 0.02
7. PBS	80	80	1.49 ± 0.06	65	70	20	0.40 ± 0.01
8. PLA	85	95	1.15 ± 0.05	75	140	70	0.33 ± 0.11
9. PLA + PBAT	85	95	0.29 ± 0.02	75	90	5	0.11 ± 0.01
10. starch + PBAT	85	90	0.29 ± 0.01	75	80	5	0.13 ± 0.01

¹ ASTM F88 (n=3, average seal strength values and standard deviations are calculated).

Two cases are studied in additional seal experiments with contamination: coated papers 1 and 2, with relative low gas barriers, for unprocessed fruit and vegetables, and cellulose films, with relative high gas barriers, for grated cheese. Optimal parameters are determined by maximizing seal strength. Optimal parameters are equal for clean and contaminated seals because all interaction terms of contamination with a seal parameter are not significant and are left out in the fitted models. The results of individual runs, coefficients and p-values of terms in fitted models are not shown because of the sole objective on evaluation of the clean and contaminated maximal seal strengths.

Resulting models of clean and contaminated seal strengths of coated papers and cellulose films are visualized with prediction profilers at optimal settings, as shown in Figure 81 and Figure 82. The models of coated papers predict slightly decreased seal strengths with coffee powder and sand contamination, compared to clean seal strengths. There is no influence of water contamination on maximum seal strength. The models of cellulose films predict slightly decreased seal strengths with grated cheese contamination, compared to clean seal strength.

² ASTM F1921 (n=3 average hot tack strength values and standard deviations are calculated).

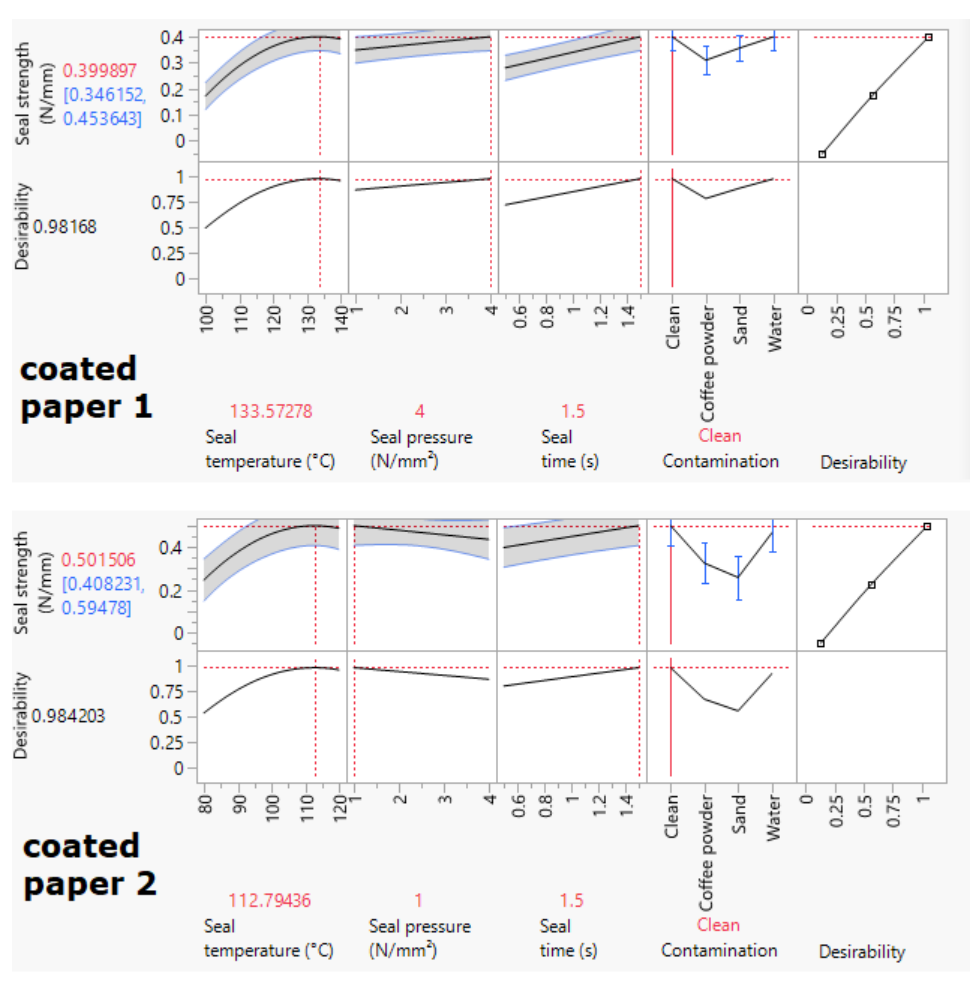
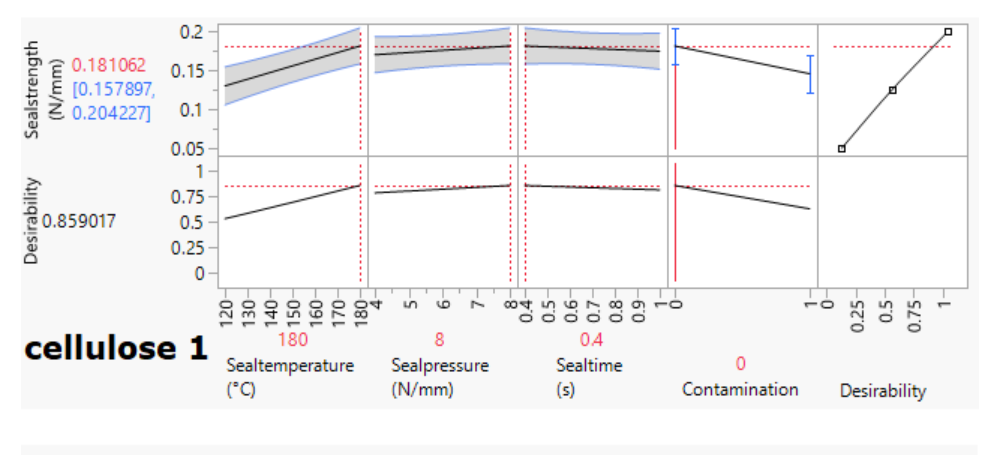


Figure 81: Prediction profilers of models of clean and contaminated seal strengths of coated papers, optimized by maximizing.



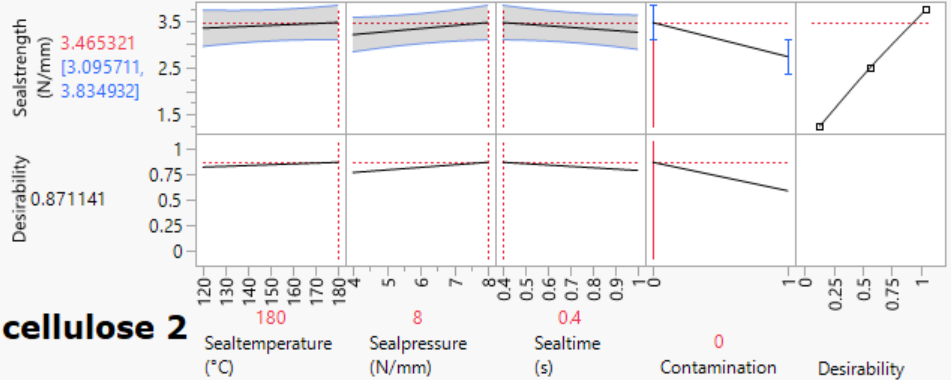


Figure 82: Prediction profilers of models of clean and cheese contaminated seal strengths of cellulose films, optimized by maximizing.

Table 26 shows the numerical values of predicted maximum seal strength values for clean and contaminated seals of all cases at optimal seal parameters.

A 95% confidence interval is calculated, based on 5 experiments at optimal seal parameters. Only with clean coated paper 1, water contaminated coated paper 2 and grated cheese contaminate cellulose 2, predicted values are slightly outside the confidence interval. All other predicted maxima fall in a 95% confidence interval.

All considered materials have overlapping confidence intervals for clean and contaminated seals, so the clean maximal seal strengths can be matched with contamination. Powder contamination densities of 12 g.m⁻² and above are related with aggregate formation and a decrease in maximum seal strength of poly(ethylene) film⁴¹. For the considered coated papers, this threshold value can be exceeded while maximum seal strength is maintained. Further experiments with higher contamination densities can be performed to study the limits for these materials. Both coated papers can be considered to pack fresh foods. Further experiments and/or finite element analysis with target foods and packaging with specified dimensions can be performed to check if the seal strength of these coated papers is sufficient for the food packaging application. The barrier cellulose films can be considered to pack grated cheese. The very low seal strengths of

cellulose 1 makes this material not suited for heavy weight applications. One might think of combining the good seal-through-contamination performance, almost equally strong hot tack, shown in Table 25 and easy-tear features, shown in Table 23, of cellulose 1 in easy-tearable low-weight packages. Cellulose 2 can be used in packages with higher weight in cheese. Besides additional mechanical analysis of the entire food packaging concept, to check if seal strength is sufficient, additional leak tests are advised, because of the importance of good barrier properties of grated cheese packaging.

Table 26: Maximized seal strengths of clean and contaminated seals.

Samples	Contamination	Predicted value (N.mm ⁻¹)	95% Confidence interval (N.mm ⁻¹)	Optimal parameters (seal temperature, time and pressure)	
	Clean	0.40	0.24 - 0.38		
coated paper 1	Coffee powder	0.31	0.22 - 0.40	134 °C, 1.5 s and 4 N.mm ⁻²	
coated paper 1	Sand	0.36	0.28 - 0.36	134 °C, 1.5 S and 4 N.IIIIII -	
	Water	0.40	0.19 - 0.45		
	Clean	0.44	0.31 - 0.49		
coated paper 2	Coffee powder	0.37	0.25 - 0.44	113 °C, 1.5 s and 4 N.mm ⁻²	
coated paper 2	Sand	0.46	0.32 - 0.50	113 °C, 1.5 S and 4 N.IIIII 2	
	Water	0.50	0.31 - 0.48		
cellulose 1	Clean	0.18	0.15 - 0.19	190 9C 0.4 c and 9 N mm ⁻²	
cellulose 1	Grated cheese	0.15	0.12 - 0.18	180 °C, 0.4 s and 8 N.mm ⁻²	
	Clean	3.40	2.90 - 3.60	100 0C 0 4 a and 0 N2	
cellulose 2	Grated cheese	2.70	3.10 - 3.50	180 °C, 0.4 s and 8 N.mm ⁻²	

6.3.4 Additional characterization

Opacity, which is normalized to thickness with homogeneous film structures in previous studies, is correlated with film thickness^{42, 43}. Besides thickness, variations in opacity can be related with the material composition, such as the reflection of light of foreign nanoparticles⁴⁴. There is also an obvious impact of printing and coloration on opacity. The opacity results in Table 27 show big differences between the samples. Non-transparent samples, as shown in in Figure 75, such as the coated papers and the black PLA+PBAT blend, have high opacity values. Food packaging with transparency properties are however preferred by consumers⁴⁵. Samples with low opacity values, such as PLA and cellulose 1 approach full transparency, with respective values of 7.9 and 11.5. These values are in the same range as other biodegradable films that were measured with the same method⁴⁴. Other thin samples have hazier appearances, which is reflected by increased opacity values. The thicker pilot extrusions have moderate opacity values compares to other samples.

Table 27: Average opacities Y (in %) and standard deviations (n=4).

Samples	Y ± SD		
1. coated paper 1	81.9 ± 6.3		
2. coated paper 2	86.0 ± 2.7		
3. cellulose 1	11.5 ± 2.7		
4. cellulose 2	20.6 ± 0.3		
5. pilot extrusion PHBV	46.1 ± 0.9		
6. pilot extrusion PBS	24.8 ± 1.7		
7. PBS	14.0 ± 0.3		
8. PLA	7.9 ± 0.3		
9. PLA + PBAT	98.7 ± 4.6		
10. starch + PBAT	16.1 ± 1.2		

The tendency of food to adhere to the packaging surface determines to a large extent the preservation of food⁴⁶. Hydrophobic properties of the surface are desired to improve the resistance of chemical interactions with food by minimizing the contact area. The values in Table 28 are in a narrow range of 80-105°, between that of smooth cellulose films, which are hydrophilic and have contact angles below 50°, and superhydrophobic surfaces, a property that can also be achieved with biodegradable materials, characterized by contact angles above 150° 47. The standard deviations of the results are rather high, suggesting inhomogeneous surfaces, compared to reported values in literature 48, 49, 50. The water contact angle of coated paper 1 is similar to a value of LDPE, reported in a previous study⁴⁸. Contact angles of PBAT blends, with thermoplastic starch and nano zinc oxide, of a previous study are in between 89 and 104° 50. This range is similar to the ranges of the values of the PBAT blends on the surface of the samples in this study, such as coated paper 2, pilot extrusion PHBV, and the two monolayer blends, PLA+PBAT and starch + PBAT. Another study reports a low value of 57° for PBAT⁴⁸, which highlights the difficulties to compare these values in literature. The same study reports a value of 68° for PLA, while the value for PLA in this study is 80°, which is low compared to the other samples. The two PBS samples of this study are with values of 84° for the thin monolayer and 104° for the pilot extrusion also higher than a value reported in a previous study⁴⁹. Concluding, water contact angle values of the samples in this study are higher or equal, compared to values, found in literature. This is probably related with modifications in commercial food packaging films, in order to decrease the contact area with food.

Table 28: Average water contact angles (WCA) (in $^{\circ}$) and standard deviations (n=15).

Samples	WCA ± SD		
1. coated paper 1	92.7 ± 4.0		
2. coated paper 2	85.1 ± 5.0		
3. cellulose 1	86.9 ± 3.4		
4. cellulose 2	89.6 ± 4.3		
5. pilot extrusion PHBV	95.2 ± 3.5		
6. pilot extrusion PBS	104.6 ± 4.3		
7. PBS	84.2 ± 2.8		
8. PLA	80.0 ± 4.3		
9. PLA + PBAT	102.2 ± 4.3		
10. starch + PBAT	105.0 ± 1.6		

6.4 Conclusions

Coated papers and high barrier cellulose films are brittle materials with a potential use over a wide ambient temperature range. Barrier and/or heat seal properties can be altered with the appropriate plastic coating. The case studies to check the seal-through-contamination performance show that maximal seal strength can be maintained.

In a comparison of two thick pilot extruded films, the PBS blend is stronger and tougher than the PHBV blend at standard ambient temperature. Without the use of additional gas barrier layers, application of these materials is restricted to food with low barrier requirements, such as takeaway meals and unprocessed fruit and vegetables. Both materials can be heat sealed. In order to be able to determine seal application areas, film production need to be optimized to obtain commercial structures, such as thin flexible films or trays.

The application of PBS, PLA, a PLA-PBAT blend and a starch-PBAT blend is restricted to food with low barrier requirements. Additional barrier layers, of which the identified PVDC-layer in high gas barrier cellulose film is an example, are needed to implement these materials for food with high barrier requirements, such as meat, cheese, high fat products and ready meals. Monolayers with PLA and PBS combine high strength and toughness at standard ambient temperature. However, the temperature window of these good mechanical features is narrow. Both materials are able to produce strong seals with low initiation temperatures. Both materials can be applied as strong seal layers in high-speed VFFS applications or as heavy-duty monolayers in standard ambient temperature. The application at cold temperatures can be considered if the low maximum strains are sufficient for the specific food packaging. The PBAT blends are weak but tough from cold to standard ambient temperatures. Application is restricted at temperatures above 60 °C. These materials can be applied as relative weak seal layers, which is of high interest in easy-peel applications, and as light-duty monolayer in cold and standard ambient temperatures.

Depending on the selection of coated and/or laminated materials, the application potential of biodegradable materials in food packaging is very broad, ranging from low barrier packaging of low weight foods at standard temperature, to high barrier packaging, such as modified atmosphere packaging, of high weight foods, extreme temperature processing and/or high-speed applications, such as vertical form fill seal (VFFS). Biodegradable food packaging is emerging. This study fully supports the implementation of commercially available biodegradable materials for the identified food applications.

6.5 References

- [1] Ellen MacArthur Foundation. Circular economy diagram. Available online: https://ellenmacarthurfoundation.org/circular-economy-diagram (accessed on January 28, 2022).
- [2] European bioplastics. Bioplastics facts and figures. Available online: https://docs.european-bioplastics.org/publications/EUBP Facts and figures.pdf (accessed on January 28, 2022).

- [3] PlasticsEurope. Plastics The Facts 2020. Available online: https://plasticseurope.org/wp-content/uploads/2021/09/Plastics the facts-WEB-2020 versionJun21 final.pdf (accessed on January 28, 2022).
- [4] Eur-Lex. Directive (EU) 2018/852 of the European Parliament and of the Council of 30 May 2018 amending Directive 94/62/EC on packaging and packaging waste (Text with EEA relevance). Available online: https://eur-lex.europa.eu/legal-content/EN/ALL/?uri=CELEX:32018L0852 (accessed on January 28, 2022).
- [5] Scientific Advice for Policy by European Academies, SAPEA (2020). Biodegradability of Plastics in the open Environment. Available online: https://www.sapea.info/topics/biodegradability-of-plastics/ (accessed on January 28, 2022).
- [6] DIN EN 13432. Requirements for packaging recoverable through composting and biodegradation Test scheme and evaluation criteria for the final acceptance of packaging. Available online: https://www.enstandard.eu/din-en-13432-requirements-for-packaging-english-version-of-din-en-13432/ (accessed on January 28, 2022).
- [7] Fortune Business Insights. The global food packaging market is projected to grow from \$338.34 billion in 2021 to \$478.18 billion in 2028 at a CAGR of 5.1% in forecast period, 2021-2028. Available online: https://www.fortunebusinessinsights.com/industry-reports/food-packaging-market-101941 (accessed on January 28, 2022).
- [8] Piergiovanni L, Limbo S. *Food Packaging Materials;* Springer:New York, USA, **2016**; Chapter 1, pp. 1-3.
- [9] Liewchirakorn P, Aht-Ong D, Chinsirikul W. Practical approach in developing desirable peel-seal and clear lidding films based on poly(lactic acid) and poly(butylene adipate-co-terephtalate) blends. *Packag. Technol. Sci.* **2017**, *31*(*5*), pp. 269-309, doi: 10.1002/pts.2321.
- [10] Vytejckova S, Vapenka L, Hradecky J, Dobias J, Hajslova J, Loriot C, Vannini L, Poustka J. Testing of polybutylene succinate based films for poultry meat packaging. *Polym. Test.* **2017**, *60*, pp. 357-364, doi: 10.1016/j.polymertesting.2017.04.018.
- [11] Ragaert P, Buntinx M, Maes C, Vanheusden C, Peeters R, Wang S, D'hooge D. Polyhydroxyalkanoates for Food Packaging Applications. *Reference Module in Food Science*, Elsevier: Amsterdam, Netherlands, **2019**; pp. 1-9, doi:10.1016/B978-0-08-100596-5.22502-X.
- [12] Nova institute. Biodegradable Polymers in Various Environments According to Established Standards and Certification Schemes. Available online: https://renewable-carbon.eu/news/new-updated-version-of-the-poster-on-biodegradable-polymers-in-various-environments-according-to-established-standards-and-certification-schemes/ (accessed on June 17, 2022).
- [13] Lahtinen K, Kotkamo S, Koskinen T, Auvinen S, Kuusipalo J. Characterization for water vapour barrier and heat sealability properties of heat-treated paperboard/polylactide structure. *Packag. Technol. Sci.* **2009**, *22*, pp. 451-460. doi: 10.1002/pts.869.

- [14] Müller G, Hanecker E, Blasius K, Seidemann C, Tempel L, Sadocco P, Pozo BF, Boulougouris G, Lozo B, Jamnicki S, Bobu E. End-of-life solutions for fibre and bio-based packaging materials in Europe. *Packag. Technol. Sci.* **2012**, *27*(1), pp. 1-15, doi: 10.1002/pts.2006.
- [15] Jiang X, Bai Y, Chen X, Liu W. A review on materials, commercial production and properties of lyocell fiber. *J.Bioresour.Bioprod.* **2020**, 5(1), pp. 16-25, doi: 10.1016/j.jobab.2020.03.002.
- [16] Azmin SNHM, Hayat NABM, Nor MSM. Development and Characterization of Food Packaging Bioplastic Film from Cocoa Pod Husk Cellulose Incorporated with Sugarcane Bagasse Fibre. *J.Bioresour.Bioprod.* **2020**, 5(4), pp. 259-266, doi: 10.1016/j.jobab.2020.10.003.
- [17] Liu Y, Ahmed S, Sameen DE, Wang Y, Lu R, Dai J, Li S, Qin W. A review of cellulose and its derivatives in biopolymer-based for food packaging application. *Trends Food Sci. Technol.* **2021**, 112, pp. 532-546, doi: 10.1016/j.tifs.2021.04.016.
- [18] VLAIO-TETRA project 'BIOFUN': "Evaluation of the functionality of new generation compostable bioplastics in food packaging", funded by the Flemish Government (Agentschap Innoveren & Ondernemen (VLAIO-TETRA HBC.2020.2096)).
- [19] American Society for Testing and Materials (**2017**). Standard Test Method for Tensile Properties of Plastics (ASTM D638-14). Available online. https://www.astm.org/d0638-14.html (accessed on January 28, 2022).
- [20] American Society for Testing and Materials (**2021**). Standard Test Method for Slow Rate Penetration Resistance of Flexible Barrier Films and Laminates (ASTM F1306). Available online: https://www.astm.org/f1306-21.html (accessed on January 28, 2022).
- [21] International Organization for Standardization (1983). Plastics Film and sheeting Determination of tear resistance Part 2: Elmendorf method (ISO 6383-2:1983). Available online: https://www.iso.org/standard/12716.html (accessed on January 28, 2022).
- [22] American Society for Testing and Materials (**2020**). Standard Test Method for Oxygen Transmission Rate Through Dry Packages Using a Coulometric Sensor (ASTM F1307-20). Available online: https://www.astm.org/f1307-20.html (accessed on January 28, 2022).
- [23] American Society for Testing and Materials (**2020**). Standard Test Method for Determination of Oxygen Gas Transmission Rate, Permeability and Permeance at Controlled Relative Humidity Through Barrier Materials Using a Coulometric Detector (ASTM F1927-14). Available online: https://www.astm.org/f1927-14.html (accessed on January 28, 2022).
- [24] American Society for Testing and Materials (**2020**). Standard Test Method for Water Vapor Transmission Rate Through Plastic Film and Sheeting Using a Modulated Infrared Sensor (ASTM F1249-13). Available online: https://www.astm.org/f1249-13.html (accessed on January 28, 2022).
- [25] American Society for Testing and Materials (**2015**). Standard Test Method for Seal Strength of Flexible Barrier Materials (ASTM F88/F88M-15). Available online: https://www.astm.org/Standards/F88.htm (accessed on January 28, 2022).

- [26] Stehling FC, Meka P. Heat sealing of semicrystalline polymer films. III. Effect of Corona Discharge Treatment of ILDPE. *J. Appl. Polym. Sci.* **1994**, 51(1), pp. 121-131, doi: https://doi.org/10.1002/app.1994.070510113.
- [27] American Society for Testing and Materials (2015). Standard Test Methods for Hot Seal Strength (Hot Tack) of Thermoplastic Polymers and Blends Comprising the Sealing Surfaces of Flexible Webs (ASTM F1921 / F1921M 12). Available online. https://www.astm.org/Standards/F1921.htm ((accessed on January 28, 2022)).
- [28] Bamps B, D'huys K, Schreib I, Stephan B, De Ketelaere B, Peeters R. Evaluation and optimization of seal behaviour through solid contamination of heat sealed films. *Packag. Technol. Sci.* **2019**, *32 (7)*, pp. 335-344, doi: 10.1002/pts.2442.
- [29] Rhim JW, Kim JH. Properties of poly-lactide)-coated paperboard for the use of 1-way paper cup. *J. Food Sci.* **2009**, *74*(2), pp. E105-E111, doi: 10.1111/j.1750-3841.2009.01073.x.
- [30] Futamura Natureflex™ NK Features Transparent High Barrier Heat-Sealable Compostable Film. Available online: https://www.futamuragroup.com/en/divisions/cellulose-films/products/natureflex/barrier/ (accessed on January 28, 2022).
- [31] Bumbudsanpharoke N, Wongphan P, Promhuad K, Leelaphiwat P, Harnkarnsujarit N. Morphology and permeability of bio-based poly(butylene adipate-co-terephthalate) (PBAT), poly(butylene succinate) (PBS) and linear low-density polyethylene (LLDPE) blend films control shelf-life of packaged bread. *Food Control* **2022**, pp. 132, doi: 10.1016/j.foodcont.2021.108541.
- [32] Rafiqah SA, Khalina A, Harmaen AS, Intan, AT, Zaman K. A review on properties and application of bio-based poly(butylene succinate). *Polymers* **2021**, *13*(*9*), pp. 1436, doi: DOI:10.3390/polym13091436.
- [33] Nofar M, Tabatabaei A, Sojoudiasli H, Park CB, Carreau PJ, Heuzey MC, Kamal MR. Mechanical and bead foaming behaviour of PLA-PBAT and PLA-PBSA blends with different morphologies. *Eur. Polym. J.* **2017**, *90*, pp. 231-244, doi: 10.1016/j.eurpolymj.2017.03.031.
- [34] Di Lorenzo ML, Androsch R. *Thermal properties of bio-based polymers*. Springer Nature Switzerland AG: Cham, Switzerland, 2019, pp. 1-36, doi: 10.1007/978-3-030-39962-7.
- [35] Grasso M, Azzouz L, Ruiz-Hincapie P. Effect of temperature on the mechanical properties of 3D-printed PLA tensile specimens. *Rapid Prototyp. J.* **2018**, *24*(*8*), pp. 1337-1346, doi: 10.1108/RPJ-04-2017-0055.
- [36] Morris B. The Science And Technology Of Flexible Packaging: Multilayer Films From Resin And Process To End Use. Elsevier: Amsterdam, Netherlands, **2016**, pp. 259-308.
- [37] Wyser Y, Vishtal A, Giardiello MI, Pelletier C, Deantoni F. Understanding barrier degradation during water vapour transmission rate testing of high barrier metallized paper. *Packag. Technol. Sci.* **2022**, *35*(*3*), pp. 291-299, doi: 10.1002/pts.2626.
- [38] Katekhong W, Wongphan P, Klinmalai P, Harnkarnsujarit N. Thermoplastic starch blown films functionalized by plasticized nitrite blended with PBAT for superior oxygen barrier and active biodegradablemeat packaging. *Food Chem.* **2022**, pp. 374, doi: 10.1016/j.foodchem.2021.131709.

- [39] Phothisarattana D, Harnkarnsujarit N. Characterisations of cassava starch and poly(butylene adipate-co-terephtalate) blow film with silicon dioxide nanocomposities. *Int. J. Food Sci. Technol.* **2022**, Early View, doi: 10.1111/ijfs.15816.
- [40] Morris B. The Science And Technology Of Flexible Packaging: Multilayer Films From Resin And Process To End Use. Elsevier: Amsterdam, Netherlands, **2016**, pp. 181-257.
- [41] Ilhan I, Ten Klooster R, Gibson I. Effects of process parameters and solid particle contaminants on the seal strength of low-density polyethylene-based flexible food packaging films. *Packag. Technol. Sci.* **2021**, *34*, pp. 413-421, doi: 10.1002/pts.2567.
- [42] Riaz A, Lei S, Akhtar HMS, Wan P, Chen D, Jabbar S, Abid M, Hashim MM, Zeng X. Preparation and characterization of chitosand-based antrimicrobial active food packaging film incorporated with apple peel polyphenols. *Int. J. Biol. Macromol.* **2018**, 114, pp. 547-555, doi: 10.1016/j.ijbiomac.2018.03.126.
- [43] Kevij HT, Salami M, Mohammadian M, Khodadadi M, Emam-Djomeh Z. Mechanical, physical, and bio-functional properties of biopolymer flms based on gelatin as afected by enriching with orange peel powder. *Polym. Bull.* **2021**, 78, pp. 4387-4402, doi: 10.1007/s00289-020-03319-9.
- [44] Vandewijngaarden J, Wauters R, Murariu M, Dubois P, Carleer R, Yperman J, D'Haen J, Ruttens B, Schreurs S, Lepot N, Peeters R, Buntinx M. Poly(3-hydroxybutyrate-co-3-hydroxyhexanoate)/Organomodified Montmorillonite Nanocomposites for Potential Food Packaging Applications. *J. Polym. Environ.* **2016**, 24, pp. 104-118, doi: 10.1007/s10924-016-0751-1.
- [45] Sabo B, Becica T, Keles N, Kovacevic D, Brozovic M. The impact of packaging transparency on product attractiveness. *Eng. Des. Graph. J.* **2017**, 8(2), pp. 5-9, doi: 10.24867/JGED-2017-2-005.
- [46] Sablani, S.S.; Bhunia, K.; Rahman, M.S. Food-Packaging Interactions. Handbook of Food Preservation, CRC Press: Boca Raton, USA, **2020**, pp. 923–942.
- [47] Wei DW, Wei H, Gauthier AC, Song J, Jin Y, Xiao H. Superhydrophobic modification of cellulose and cotton textiles: Methodologies and applications. *J.Bioresour.Bioprod.* **2020**, 5(1), pp. 1-15, doi: 10.1016/j.jobab.2020.03.001.
- [48] Rhim JW, Hong SI. Wetting properties of biopolyester films prepared by thermo-compression method. *Food Sci. Biotechnol.* **2007**, 16(2), pp. 234-237.
- [49] Ilsouk M, Raihane M, Rhouta B, Meri RM, Zicans J, Vcstaudza J, Lahcini M. The relationship of structure, thermal and water vapor permeability barrier properties of poly(butylene succinate)/organomodifiedbeidellite clay bionanocomposites prepared by insitu polycondensation. *RSC Adv.* **2020**, 10, pp. 37314, doi: 10.1039/d0ra07521c.
- [50] Yi T, Qi M, Mo Q, Huang L, Zhao H, Liu D, Xu H, Huang C, Wang S, Liu Y. Ecofriendly Preparation and Characterization of a Cassava Starch/Polybutylene Adipate Terephthalate Film. *Process.* **2020**, 8(3), pp. 329, doi: 10.3390/pr8030329.

Conclusions and recommendations

Previous chapters developed and validated the design of experiments (DOE) methods to optimize and evaluate ultrasonic seal performance, heat conductive seal-through-contamination performance and peel performance during and after cold storage. This approach resulted in a better understanding of industrially relevant interactions during heat sealing, including seal materials, process parameters, contamination and further processing. With respect to these aspects, general conclusions and recommendations are formulated.

7.1 General conclusions

The general conclusions, are related with the main objective:

To study and optimise heat seal performance of flexible food packaging by developing and validating innovative design of experiments approaches, including material properties, process parameters, contamination and further processing, for different industrial contexts.

The general conclusions can be categorized in **method development** and in **optimal seal performance, in relation with material properties, process parameters, contamination and further processing.** Seal optimization is discussed below from the perception of each of these aspects. It is, however, not possible to separate these aspects from each other because of the complexity of the industrial sealing process.

Method development

The DOE-methods show an enormous potential, because of their power to predict seal performance with an acceptable accuracy, from a packaging engineering point of view, based on a rather low number of runs, compared to an OFAT-approach.

The designs show that it is very efficient to add performance indicators if they can be evaluated on the same sample. This has no impact on the number of runs. The addition of factors however will increase the number of runs. The number of runs can be increased to improve accuracy of predictions. A decrease of runs of the proposed designs is not recommended because of their optimal character.

Material properties

Films with plastomer-based seal layer outperformed other films with metallocene LLDPE and ionomer-based seal layers, with higher clean and contaminated seal strength, wider process windows and a higher degree of leak tightness. This material is suitable for high-speed applications because of its low melting temperature. The film with metallocene LLDPE seal layer showed a similar behaviour but achieved a lower seal performance. The film with ionomer-based seal layer had a worse clean and contaminated seal performance. This conclusion was surprising, because of the good seal-through-contamination claims in literature. The good caulkability of the plastomer and metallocene LLDPE-based seal layers, that can be visualised with transparent images of the contaminated seals, is suggested to attribute to a high extent to the good seal-through-contamination performance with solid particles. Ionomers are less caulkable, because of the restricted chain mobility, caused by the ion clusters, and the

resulting low melt flow index, but have a high hot tack strength, as a result of the high melt strength, compared to other polyolefins. This feature attributes more to sealing through smaller contaminations, but less to thick particles, as shown in the studies with coffee powder and blood powder. This material is also suited for high speed applications because of its low melting temperature.

For ultrasonic sealing, similar materials can be used, but more attention must be given to the film layer architecture, because it cannot be assumed that entanglement only occurs at the surface of a superficial thin seal layer. Seal thickness is changing rapidly during ultrasonic sealing, up to the point that all seal materials can be expelled, so other parental layers participate in a larger extent, compared to the mechanically gentler heat conductive technology, in the sealing process.

For peel applications, seal layers need to be altered to allow peel failure at a wider process window than what can be achieved with singular control of process parameters. The matrices of the considered materials above can be contaminated with another polymer, in most cases this will be poly(1-butene), to decrease seal strength and thus obtain cohesive peel failure.

Special attention in this dissertation is given to biodegradeable materials. Monomaterial films, composed of PLA and PBS showed low seal initiation temperatures what makes them suitable for high speed applications. Hot tack performance was good, with low initiation temperatures, a moderate maximal hot tack strength and an acceptable hot tack process window. PLA is more suited for applications where the width of the hot tack process window is more relevant, such as vertical-form-fill-sealing, where the hot seal is put under pressure. PBS would also be suitable for VFFS but showed a narrower hot tack process window which makes PBS slightly more sensitive to failure when the seal is still hot. PBS is a much tougher material, compared to PLA. This feature makes PBS more suitable for applications where the cooled down seal, and package as a whole is subject to long term loads, f.e. vibrations during transport cycles. PBAT blends of starch or PLA are very tough materials but achieved low seal and hot tack strengths. These materials could be of interest in easy opening applications. Similar to fossil-based packaging films, multilayer structures with a thermal resistant outer layer can be found on the market for biodegradable packaging materials. The outer layer of these materials must be biodegradable as well, to achieve a biodegradable package. The two current main options in industry are cellulose and paper. With both options good seal performance can be obtained, as shown in chapter 6. Similar remarks can be made for the use of biodegradable seal materials in ultrasonic sealing and peel seal applications as the ones that are described with poly(ethylene)-based seal layers. The peel component, however, should be biodegradable or be present in a very low percentage to allow biodegradability, such as compostability, following the EN 13432 standard.

Process parameters

For ultrasonic sealing, force, amplitude and time were considered as factors. Seal force impacts seal performance mostly and time has the smallest impact, within the considered ranges of the design space. Further studies are needed to understand, chemically and physically, the relation of these process parameters with seal performance.

For heat conductive sealing, temperature, time and pressure were considered as process parameters. The impact on seal performance followed the same sequence, with temperature as most influential on seal performance, and pressure as least influential, within the considered ranges of the design space. The relations of temperature, time and the interaction of both parameters on seal interface temperature and seal performance are well known. Pressure is important to achieve a good contact between the seal layers to form bonds. A further increase in pressure has an almost zero impact on seal performance, until the point that the material is squeezed out. This can occur in profiled bars, in combination with high temperature and time.

Contamination

Coffee powder and blood powder were extensively studied with three different seal materials. Smaller and lighter particles, such as blood powder, covered the seal area to a higher extent than larger and heavier coffee particles, at a fixed contamination density of 25 g. m⁻². In the uncontaminated areas it is possible to form a strong bond. With non-peelable materials that were evaluated, these bonds were strong enough to achieve high seal strength values. Resulting seal strengths were higher with coffee powder than with blood powder.

Results of leak tightness tests were not that straight forward. Each solid particle is surrounded with a void, with a surface that is proportional with the caulkability of the seal material at optimal process parameters. A channel leak can be formed with voids that are in contact with each other. The channel leak is a pathway for liquids, gasses and/or microorganisms to travel through the seal and enter or escape from the inside of a food package. The application method that is described in this dissertation is based on a manual distribution of particles and have an impact on channel formation. This method and the collaborative work in the TETRA-CORNET-project EVOCOSEAL were stepping stones to apply contamination in a standardized way, but contamination type and leak tightness are difficult to correlate.

Further processing

Further processing contains all other temperature related processes, besides heat sealing, before, during and after sealing. Optimized peel seal performance of a packaging concept with PE was evaluated during and after cold storage at -18, 4 and 23 °C. Resulting increased strength during cold storage was related with a difference in seal failure mechanism, which can be explained by decreased chain mobility. PE is the most used seal material in food packages in cold chain because of the high chain mobility at low temperatures. Even with PE, which is a material with a glass transition temperature around -100 °C, seal failure changes already at -18 and 4 °C. This effect is expected to be more pronounced with materials with glass transition temperature around freezing and cooling temperature, such as homopolymer PP. The results showed that expectations, based on general seal layer compositions and general thermal properties, can fall short.

Of all considered biodegradeable polymers, blends with PBAT are a good candidate for seal layers in cold chain packaging because they have the capacity to maintain the mechanical properties in a similar way as PE at freezing and cool temperatures. The brittleness of PLA or PBS at these temperatures is not optimal for cold chain applications.

In the THERMOPEEL project, a similar method was used to evaluate peel performance at temperatures of 95 and 121 °C, to simulate pasteurization and sterilization. In these applications, PP is mostly used because of its high melting point. The general results were in line with this dissertation, seal strength decreases at higher temperature. As suggested at low temperatures, this can be attributed as well to increased chain mobility at high temperatures.

Seal performance

Optimal seal performance represents different performance indicators and different target values, depending on the application.

Seal strength was considered as performance indicator but its target value was dependent on the application. For easy-opening, a low value was matched, while for other applications, seal strength was maximized to obtain optimal seal performance.

Energy consumption was added as performance indicator because of its specific relevance to ultrasonic sealing. The energy of ultrasonic sealing is mainly consumed during sealing, to vibrate the parts. It is dependent on process parameters, such as time, force and amplitude. It is also dependent on seal materials. Materials differ in energy consumption to achieve a state that allows entanglement of polymer chains. Energy consumption is almost zero when the parts are not vibrating, with the exception of running some LED-lights and a computer system. Energy consumption is less relevant to optimize in heat conductive sealing on the level that considers process parameters and seal materials. The tools are constantly heated, so the differences in energy consumption are mainly determined by tool design, f.e. long, wide heat conductive sealing consume more energy to maintain their temperature. The relation of tool design and energy consumption is an interesting subject to optimize heat conductive sealing in a current market with potential energy shortages and high energy costs.

Travel displacement was also added as performance indicator because of its specific relevance to ultrasonic sealing. Ultrasonic sealing is a mechanical invasive process that decreases the thickness of the seal in a narrow window of process parameters, compared to heat conductive sealing. Maximizing seal strength without paying attention to seal thickness leads to maximal process parameters. These parameters produce a cut or a very thin seal, both results are not desirable in most cases. With heat conductive sealing, seals can be cut or become very thin when heat sensitive materials are used, in combination with high values of process parameters. In a standard hot tool process with moderate process parameters and a typical film structure with a thermal resistant outer layer, seal thickness needs less attention, compared to ultrasonic sealing, to optimize seal performance, because of the low mechanical invasivity of the hot tool process.

Average seal strength and seal energy were added as performance indicators because of their specific relevance to peel seal performance. Convenient easy opening by peeling supposes a low seal strength which can be opened at a constant force, after exceeding a specific opening force. This can be achieved by matching maximal and average seal strength to target values and maximizing seal

energy. A sole focus on maximal seal strength is not sufficient to achieve convenient peel performance. It is not relevant to consider average seal strength with seals that do not peel. Seal energy, however, can be a performance indicator of interest with non-peel seals to differentiate tough and brittle breaks.

7.2 Recommendations

New optimization studies are proposed below, that allow optimization of seal performance, with material properties, process parameters, contaminations or further processing levels as variables.

Material properties

Film layer architecture of the multilayer, seal layer thickness and seal layer blend ratio are material factors that can be subjects of further studies on a macro level. Molecular weight, rheology, amorphous fraction, branching, orientation and surface character are examples of material factors on a micro level.

Production of films by extrusion is a labour-intensive process with high cost. A mixture DOE can be used to optimize the blend ratio of the seal layer in an efficient way. Besides seal strength, other performance indicators with no direct relation to the sealing process, such as cost, extrusion efficiency, extrusion energy consumption, etc. can be added to the designs as performance indicators with the objective of selecting a cost-effective blend ratio to seal. A DOE-approach can support chemical companies to react more quickly to new materials that come into the market and/or meet new demands.

Process parameters

Seal bar design and (forced) cool time are examples of other relevant process parameters, that can be included in a DOE. Seal bar design can be added as categorical variable with different levels, f.e. flat, rectangular and triangular shapes. Adding cool time as a variable is also interesting because two performance indicators, seal and hot tack strength, that are assessed today with two different standards, ASTM F88 and ASTM F1921, could be combined in one efficient method if test speeds are matched. Fitting a model to the typical sigmoidal shaped curves of seal strength works well, by combining linear and exponential functions. Fitting a model to the more complex shapes of a hot tack curve, with an exponential increase in the beginning, followed by a long decreasing tail, is a huge challenge with the terms that are considered in the equations in this dissertation. More complex terms have to be added and that will increase the number of runs. A design with an acceptable number of runs would be of great value for the food packaging industry as it would allow faster evaluation and optimization of seal strength and thus contribute to well-sealed food packages.

Contamination

Leak tightness is a very important result of heat sealing, especially in seal-through-contamination studies, besides seal strength. Some test standards to measure leak tightness, for example the dye penetration test, are giving a binary response: leak or tight. It complicates DOE-analysis and needs to be repeated x times to generate a non-binary number, for example an average value out of 10 tests. Other test standards, such as the vacuum and pressure decay test, can deliver quantitative output for each sample, but are time consuming because of

the need to seal a pouch for each run. Especially the vacuum decay test (ASTM F2338) is interesting because it is a very gentle test that would allow seal strength testing on the same sample. This facilitates the set-up of an efficient design. After screening the impact of several contamination types on leak tightness and seal strength, additional experiments can be performed to study the rheological behaviour, surface interactions, amongst other aspects.

Further processing

Besides cold storage experiments, there are other processes with a risk of decreasing the seal performance of food packages and thus decreasing food safety and quality, such as the transportation process. It is a complex example of many combined subprocesses, such as vibrations during transportation, sudden impact by dropping packages, pressure changes in flight transport, humidity changes in sea transport and thermal processing. It is very labour-intensive, and in most cases not feasible and/or not necessary to optimize the seal performance for each of these subprocesses. If, however, seal performance at the end of the transport cycle does not meet the requirements, a DOE approach can help to optimize the performance. Critical subprocesses on seal performance need to be identified first before a DOE can be set up. Seal strength and vacuum decay experiments are carried out on food packages before transportation and after each subprocess. By taking 10 randomly chosen packages after each subprocess, a first comparison can be made with the initial seal performance. When one or more critical subprocesses are identified, a DOE can be set up by applying one or more specific tests to screen the seal performance at difference subprocess factors.

The above described recommendations are specific examples of new studies to improve heat seal performance of food packages. In the **broader perspective** of a rapidly changing market, with sudden changes in packaging materials, seal and processing technologies, and shortages in time and manual labour, a DOE approach is a solution to map the impact of all relevant factors and their interactions, and to optimize the heat sealing process with a realistic number of experiments. This is not restricted to food packaging. The discussed methods are flexible to heat sealing in general. With increasing knowledge in statistical modelling and increasing performance of computer systems, a decreasing number of experiments will be needed to find solutions to industrial problems. Virtual versions of real-life products, often referred to as 'digital twins', are already today an important topic in industrial research. DOE's can be seen as a stepping stone between a one-factor-at-a-time and a digital twin methodology.

Scientific output

A list of the publications can be found in Table 29 and Table 30.

Table 29: Scientific output: published papers.

Publications	Contribution	
Bamps B, D'huys K, De Ketelaere B, Adons D, Peeters R. Evaluation of the Ultrasonic Sealing Performance of Flexible Films with Polyolefin Seal Layer. In: Unlocking the Full Potential of Packaging Across the Value-chain, School of engineering and management Vaud (HEIG-VD); 2017; pp. 477-488. (C1-C2).	Methodology, investigation, writing – original draft preparation, visualization, project administration.	
D'huys, K, Bamps B. Peeters R, De Ketelaere B. Multi-criteria evaluation and optimization of the ultrasonic sealing performance based on design of experiments and response surface methodology. <i>Packaging Technology and Science</i> 2019 ; 32 (4); pp. 165-174. DOI: https://doi.org/10.1002/pts.2425. (A1)	Investigation, writing – review & editing, project administration.	
Bamps B, D'huys K, Schreib I, Stephan B, De Ketelaere B, Peeters R. Evaluation and optimization of seal behaviour through solid contamination of heat sealed films. <i>Packaging Technology and Science</i> 2019 ; 32 (7); pp. 335-344. DOI: https://doi.org/10.1002/pts.2442. (A1)	Methodology, validation, investigation, writing – original draft preparation, visualization, project administration.	
Bamps B, De Ketelaere B, Wolf J, Peeters R. Evaluation and optimization of the peel performance of a heat sealed topfilm and bottomweb undergoing cool processing. <i>Packaging Technology and Science</i> 2021 ; 34(7); pp. 401-411. DOI: http://doi.org/10.1002/pts.2562 . (A1)	Methodology, validation, investigation, writing – original draft preparation, visualization, project administration.	
Bamps B, Guimaraes RM, Duijsters G, Hermans D, Vanminsel J, Vervoort E, Buntinx M, Peeters R. Characterizing mechanical, heat seal and gas barrier performance of biodegradable films to determine food packaging ap-plications. <i>Polymers</i> 2022 ; 14(13); pp. 2569. DOI: https://doi.org/10.3390/polym14132569 . (A1)	Methodology, validation, investigation, writing original draft preparation, visualization, project administration, supervision.	

Table 30: Scientific output: posters and oral presentations.

Symposium, title and author list	Organizing institution	Location	Date(s)
International Symposium on Food Packaging - Study of food preservation in defective pouches: The effect of oxygen permeation through a channel leak, induced in a seal of a package, on preservation of the food product ham sausage (POSTER) - Bamps B, Peelman N, Ragaert P, De Meulenaer B, Devlieghere F, Peeters R.	ILSI Europe	Barcelona, Spain	16- 18/11 2016
28th IAPRI symposium on packaging - Evaluation of the ultrasonic sealing performance of flexible monolayer polyolefin films and paper/polyolefin laminates (POSTER) - Bamps B, D'Huys K, De Ketelaere B, Lepot N, Peeters R.	IAPRI	Lausanne, Switzerland	9-12/05 2017
29th IAPRI Symposium on Packaging - Evaluation and optimization of seal behaviour through solid contamination of heat sealed films (ORAL) - Bamps B, D'Huys K, Shreib I, Stephan B, De Ketelaere B, Peeters R.	IAPRI	Enschede, The Netherlands	13/06 2019
17th biennal TAPPI European PLACE conference - Maximizing seal strength of a commercial PET bottom web and top film with solid and liquid contamination (ORAL) - Bamps B.	TAPPI	Porto, Portugal	21/05 2019
30th IAPRI Symposium on Packaging - Evaluation and optimization of the peel performance of a heat sealed topfilm and bottomweb undergoing cool processing (ORAL) - Bamps B, De Ketelaere B, Wolf J, Peeters R.	IAPRI	Online	15/06 2021